Development and Application of Synthetic Methods That Enable Medicinal Research

by

Mathew Sutherland

B.Sc., Simon Fraser University, 2017

Thesis Submitted in Partial Fulfillment of the
Requirements for the Degree of
Master of Science

in the
Department of Chemistry
Faculty of Science

SIMON FRASER UNIVERSITY
Summer 2019

Approval

Name:	**Mathew Sutherland**
Degree:	**Master of Science**
Title:	**Development and Application of Synthetic Methods That Enable Medicinal Research**
Examining Committee:	**Chair:** Corina Andreoiu Associate Professor
	Robert A. Britton Senior Supervisor Professor
	Robert N. Young Supervisor Professor
	Jeffrey Warren Supervisor Assistant Professor
	Peter D. Wilson Internal Examiner Associate Professor
Date Defended/Approved:	June 14, 2019

Abstract

The development of modern pharmaceuticals relies heavily upon the drug discovery process to uncover new molecular entities able to modulate disease states. Integral to this process is the ability of scientists to quickly synthesize analogues of a hit or lead compound to improve critical qualities. Ease of synthesis is directly related to existing methodologies which facilitate key chemical transformations necessary to assemble potential drug molecules.

In this thesis, a medicinal chemistry program is described that relies on the well-established Suzuki-Miyaura coupling to assemble small molecule inhibitors of protein arginine methyl transferase 4, a potential target for cancer therapy. Significant advances are made towards obtaining a potent, selective, and cell-active pharmacological probe. A concise synthesis of the therapeutic 1-deoxygalactonojirimycin is also described, which utilizes a tandem α-chlorination aldol reaction developed by the Britton group to install several stereocenters in one step. In addition, a novel route to access enantioenriched acid-sensitive α-substituted aldehydes via a bench-stable intermediate was investigated.

Keywords: methodology; medicinal chemistry; epigenetic drug discovery; total synthesis; heterocycles

Dedication

This thesis is dedicated to Danelle Gibson, who helps me to keep my priorities right no matter the circumstances.

Acknowledgements

I would like to begin by thanking Robert Britton for being more than just the senior supervisor for my graduate studies at Simon Fraser University. From the beginning of my undergraduate career, he has been a constant support and mentor, encouraging me with advice and engaging my curiosity with questions. His gentle style of tutelage and guidance has been instrumental in providing a fun, yet highly productive laboratory environment to learn, discover, and explore organic chemistry.

My committee members Robert Young and Jeffrey Warren have been the epitome of the word accommodating. They have provided me with valuable insight, helpful suggestions, instruction, and life advice throughout both my undergraduate and graduate programs at SFU. I will always be grateful for their assistance in making the path through my graduate degree smoother.

To all the members of the Britton group, both current and former, I cannot say thank-you enough. Your constant support, guidance, insight, sense of humor, and attitude towards chemistry have helped me navigate the high and low points in my graduate studies. A special thank you goes out to Michael Meanwell who was my mentor in the lab, Johannes Lehmann who kept me on my toes academically and athletically, Dimitrios Panagopoulos with whom the medicinal chemistry project was initiated, Anissa Kaghad who synthesized several analogues for the medicinal chemistry project, Marjan Mohammed who began the α-chloroaldehyde project, and Matt Nodwell who was an unaware example of the ability to have a work-life balance. Gaelen Fehr was my first line of defence for editing, and I am very grateful for his ability to work with my tight evening and weekend – based schedule.

Many members of the SFU chemistry department and beyond deserve recognition. Regine Greis was a kindly resource for difficult chiral GC separations, Nathalie Fournier guided me along the logistical side of graduate school, and all the remaining professors in both the Chemistry and MBB departments deserve a special round of thanks for the effort they invested in engaging me during classes.

Lastly, I would be remiss if I forgot to thank the friends and family who have been with me over the last two years. I simply could not have done it without your support.

Table of Contents

List of Tables

List of Figures

List of Schemes

List of Acronyms

(*R*)-(+)-MTPA-OH	(*R*)-(+)-Mosher's acid
(*S*)-(+)-MTPA-OH	(*S*)-(+)-Mosher's acid
°C	Degrees Celsius
Ac_2O	Acetic anhydride
AcOH	Acetic acid
ADME	Absorption, distribution, metabolism, excretion
API	Active pharmaceutical ingredient
B_2Pin_2	*bis*(Pinacolato)diboron
Bn	Benzyl
Boc	*tert*-Butyloxycarbonyl
Cbz	Carboxybenzyl
CD_3CN	Deuterated acetonitrile
CD_3OD	Deuterated methanol
$CDCl_3$	Deuterated chloroform
cGMP	Current good manufacturing processes
cLogP	Calculated log of the partition coefficient
CRISPR	Clustered regularly interspaced short palindromic repeats
DFT	Density functional theory
DIPEA	Diisopropylethylamine
DKR	Dynamic kinetic resolution
DMF	Dimethylformamide
DMPU	*N*,*N*′-Dimethylpropyleneurea
DMSO	Dimethylsulfoxide
DNA	Deoxyribonucleic acid
EDG	Electron donating group
ee	Enantiomeric excess
EWG	Electron withdrawing group
Fmoc	Fluorenylmethyloxycarbonyl
GC	Gas chromatography
GSK	GlaxoSmithKline
H[X]R[Y]	Arginine Y of Histone X

H-bond	Hydrogen bond
hERG	Human ether-à-go-go-related gene
HPLC	High performance liquid chromatography
HRMS	High resolution mass spectrometry
HTS	High throughput screening
IBX	2-Iodoxybenzoic acid
IC_{50}	Half maximal inhibitory concentration
IP	Intellectual property
IR	Infrared spectroscopy
KO	Knock-out
KOH	Potassium hydroxide
KOtBu	Potassium *tert*-butoxide
k_R	Rate constant for the specified process
LDA	Lithium diisopropylamide
$LiAlH_4$	Lithium aluminum hydride
LiCl	Lithium chloride
LogP	Log of the partition coefficient
MeCN	Acetonitrile
mg	Milligram
MP	Melting point
MYC	Avian myelocytomatosis viral oncogene homolog
NBS	*N*-Bromosuccinimide
n-BuLi	*n*-Butyllithium
NCS	*N*-Chlorosuccinimide
NFSI	*N*-Fluorobenzenesulfonamide
NIS	*N*-Iodosuccinimide
nM	Nanomolar
nm	Nanometers
NMR	Nuclear Magnetic Resonance
NR	No Reaction
Nu	Nucleophile
OGA	*O*-GlcNAcase
oxone	Potassium peroxymonosulfate
PCC	Pyridinium Chlorochromate

Pd/C	Palladium on activated carbon
PET	Positron emission topography
P-GP	Permeability glycoprotein
Piv	Pivolate (protecting group)
PPTS	Pyridinium *para*-toluenesulfonic acid
PRMT	Protein Arginine Methyl Transferase
P-TsOH	*Para*-toluenesulfonic acid monohydrate
PyBOP	Benzotriazol-1-yl-oxytripyrrolidinophosphonium hexafluorophosphate
r.t.	Room temperature
R_f	Retention factor
RNA	Ribonucleic acid
RNAi	Ribonucleic acid interference
RP-HPLC	Reverse phase high performance liquid chromatography
R_t	Retention time
s	Second
SAM	S-Adenosyl-Methionine
SAR	Structure-Activity Relationship
$SbCl_3$	Antimony trichloride
SGC	Structural Genetics Consortium
S_NAr	Nucleophilic aromatic substitution
SOMO	Singly occupied molecular orbital
TBS	*tert*-Butyldimethylsilyl
Tf	Trifl(ate)(ic)
TFA	Trifluoroacetic Acid
THF	Tetrahydrofuran
TLC	Thin layer chromatography
TS	Transition State
USD	United States dollar
UV	Ultra-violet
WHO	World Health Organization
μM	Micromolar

Chapter 1.

Introduction

1.1. From Disease to Treatment: The Drug Discovery Process

1.1.1. The Development of New Pharmaceuticals

The development of small molecule medicines that modulate natural processes in the human body and in disease-causing organisms has changed the face of disease treatment. Many drugs are now considered essential to humans, most notably those recognized by the World Health Organization (WHO) in their Essential Medicines List.[1] The impacts of these medicines are incalculable and have been treating life-threatening diseases for over a century.

In pursuit of developing novel therapeutics for new and existing diseases, an established process in the pharmaceutical industry known as the “target driven drug discovery process” has become prominent. It consists of several steps that guide the discovery and development of a small-molecule therapeutic for a targeted disease. This is accomplished through the identification of an active pharmaceutical ingredient, or API, which is the “substance used in a finished pharmaceutical product, intended to furnish pharmacological activity or to otherwise have direct effect in the diagnosis, cure, mitigation, treatment or prevention of disease, or to have direct effect in restoring, correcting or modifying physiological functions in human beings," as defined by the WHO.[2] Generally, the API interacts with some key biological factor of the disease, often modulating the activity of an enzyme or receptor, to give rise to a therapeutic effect. The key steps in the drug discovery process are as follows and are applicable both to the development of novel therapeutics, as well as the discovery of chemical probes that can be used to test the therapeutic potential of a biological target.

1.1.2. Target Identification

For a chosen disease, identification of a biological target that is integral to the function of the diseased state is often a first step. This target could be a protein, peptide, or other macromolecule known to be important in the disease pathology. Targets are more desirable if sufficient background information exists regarding their biological relevance to the disease state, information often arising from the use of a robust molecular probe. The following critical factors are often used to identify a target.[3]

1. The target is disease-modifying and/or has a proven function in the pathophysiology of a disease.
2. The target is responsible for an easily observed (and quantifiable) biological transformation to enable high throughput screening.
3. A target/disease-specific biomarker exists to monitor therapeutic efficacy.
4. Modulation of the target's activity is unlikely to cause undesired side effects which can be indicated by the effects of genetic manipulations such as knockout mice or genetic mutation databases.
5. It is beneficial if the target has a favorable intellectual property situation, reducing some time constraints due to competition with competitors.

Once identified, a target must be validated to establish its role in the disease phenotype. Techniques to accomplish this vary in approach, but in general require expression of the target in disease-relevant cells or tissues. Following this, modulation of the target, often through the use of a molecular probe, to show relief of the disease's characteristics establishes the therapeutic potential of the target.[4]

1.1.3. Lead Generation

Having identified a target, a candidate molecule known as a lead compound that exhibits a pharmacological or biological effect likely to be therapeutically useful must be identified. If an NMR or X-ray crystal structure of the target with bound ligands exist, these can often be used to identify key structural elements required in a lead compound. In a similar fashion, analysis of known ligands for the target can be used as a starting point.[5] Understanding the biological function of the target itself can also lend insight, as in the case of Galafold, an iminosugar used to treat Fabry disease.[6] The protonated

piperidine (Figure 1.1) mimics the oxocarbenium ion intermediate in enzyme-catalyzed glycosidic bond cleavage. Galafold is believed to bind to and stabilize misfolded protein, facilitating its transport to its site of action.[7]

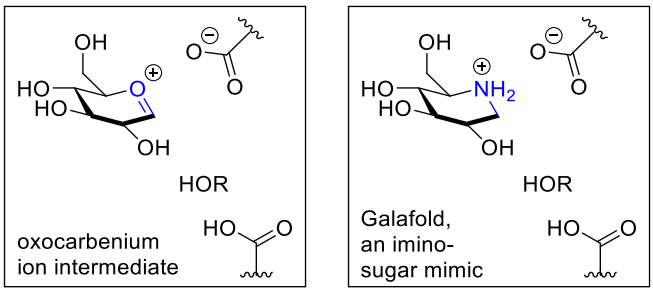

Figure 1.1: Transition state mimicry of Galafold, an iminosugar used to treat Fabry disease.

With the development of technologies that enable compounds to be tested in a high-throughput format, chemical libraries have grown rapidly in response. High-throughput screening (HTS) involves conducting biological assays on large numbers of compounds, at speed, often utilizing automation. Libraries consisting of up to several hundreds of thousands of compounds can be assayed using HTS techniques, enabling the broad examination (random screening) of chemical libraries, or focussed screening to target a subset of the library more likely to contain hits.[8] Once a hit compound has been identified, it must be validated by repetition of the primary assay to obtain a complete dose-response curve to ensure that the response of the target is relative to the concentration of the compound.

1.1.4. Lead Selection

Selecting a lead molecule to advance from a collection of verified hits can be a daunting task. Many physical properties of hit compounds are considered in order to assess whether a compound is amenable to development.[9] These can include both experimental (cell membrane permeability assays, partition coefficients) as well as computational evaluations, such as Lipinski's "Rule of 5" for predicting poor absorption properties for potential lead compounds if two or more of the following conditions are met:[10]

1. There are more than 5 H-bond donors, expressed as the sum of (O-H)'s and (N-H)'s;

2. The molecular weight is over 500;
3. The LogP is over 5
4. There are more than 10 H-bond acceptors (expressed as the sum of N's and O's.

These criteria are easily calculated and provide a rough indication of the polarity and related absorption and permeation profile for the molecule in question. However, compound classes that are actively transported across the membrane often violate many of these criteria, yet still are effectively distributed in the body.[10]

1.1.5. Lead Optimization

Once a lead molecule has been identified, analogues are synthesized to explore the relationship between structure and biological function.[11] This commonly begins with modifications designed to improve potency, while maintaining or also improving other features such as permeability and selectivity. For example, the location and orientation of acidic, basic, polar, and neutral groups all dictate the points at which the lead compound interacts with the target. If modified, some or all these points of contact may become matched or mismatched with the binding site and affect the potency of the compound. The shape of the supporting molecular scaffold is also critical to the overall display of functionality. Hence, stereochemical changes to the core can greatly influence the interactions between compound and target.[12] Hydrogen bonds (H-bonds) are often a critical component of target binding and the addition or removal of H-bond acceptors or donors can have a significant affect on compound potency.[13]

1.2. Synthetic Methodologies Enabling Drug Discovery

1.2.1. The Key to Synthesizing Analogues

Vital to lead selection and optimization is the ability to quickly synthesize analogue molecules in order to generate data about the structure activity relationship (SAR) between lead and target. To accomplish this, a viable synthetic route that relies on robust, functional group tolerant reactions to assemble a range of analogues in a modular fashion is ideal. Medicinal chemistry often relies heavily on synthetic methods developed by academic research groups.[14] For example, a recent focus on synthetic

methods that enable late-stage diversification of lead compounds has transformed the approach to SAR studies carried out by medicinal chemists.[15]

Among the many reactions routinely relied upon in drug discovery efforts, the three most common are amide bond formation, Suzuki-Miyaura coupling, and nucleophilic aromatic substitution reactions.[16] These reactions are desirable as they rely on commercially available reagents, are highly chemoselective, and tolerate a wide substrate scope.[16] Importantly, each of these reactions is highly dependable, easy to operate, and support the modular assembly of unique families of molecules.

1.2.2. Amide Bond Formation

Amide bonds are a reliable point of differentiation and are usually formed via the reaction of an amine and a carboxylic acid moiety that has been activated, two core functional groups in organic chemistry. Many major market drugs contain amide bonds, including the top selling drug worldwide, Atorvastatin **1** (trade name: Lipitor), which blocks the production of cholesterol.[17] Amide bonds are also present in many agricultural chemicals, including the herbicide Metolachlor **2** and fungicide Boscalid **3** (Figure 1.2).

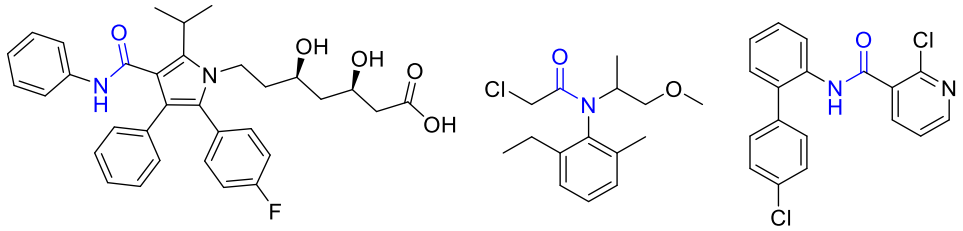

1 Lipitor (Atorvastatin) **2** Metolachlor **3** Boscalid

Figure 1.2: Amide bonds in medicinal and agricultural compounds.

Many methods to form activated carboxylic acids exist, using reagents that result in formation acid chlorides, (mixed) anhydrides, carbonic anhydrides, or active esters. These reactive intermediates then undergo nucleophilic substitution by an amine to form the final amide bond (*e.g.*, **4**), as in Scheme 1.1.[16]

Scheme 1.1: General Procedure for Synthetic Amide Bond Formation

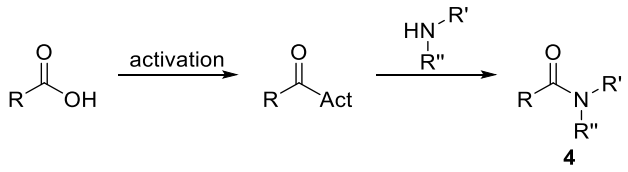

1.2.3. The Suzuki-Miyaura Coupling

Prior to the development of the Suzuki-Miyaura coupling, methods to facilitate biaryl single bond formation were harsh and unselective. The Gomberg–Bachmann–Hey reaction was the first practical synthesis of biaryls, but utilizes sodium nitrite and strong acids to perform a diazotization of an aromatic amine, which greatly reduces the functional group tolerance of this reaction.[18] The Ullman reaction, though effective in the synthesis of simple, symmetric biaryls, cannot be generally applied in the assemblage of unsymmetrical biaryl compounds.[18] With the development of the Suzuki-Miyaura coupling, a mild, general, and selective method of joining two aryl components was realized. Importantly, the precursors for the reaction are often derived from aryl halides, the synthesis of which is well established. The synthetic utility of the Suzuki-Miyaura coupling is well demonstrated in the synthesis of Valsartan **5**, a biaryl drug currently used to treat hypertension. Originally, Novartis employed a 5-step route, assembling the biaryl component via an Ullmann reaction to synthesize the key intermediate **6,** shown in Scheme 1.2. When the Suzuki-Miyaura coupling was discovered, the number of steps to the key intermediate was greatly reduced, and the synthesis improved.[19]

Scheme 1.2: Original and Improved Syntheses of a Key Intermediate of Valsartan

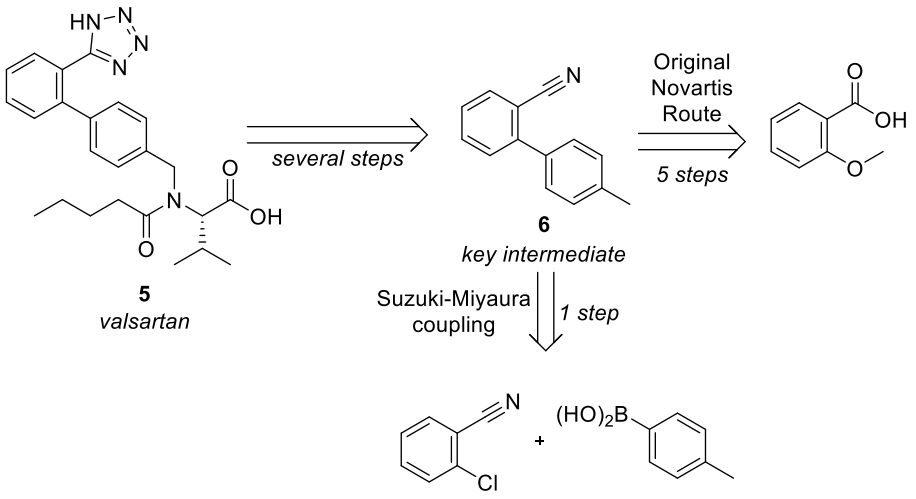

1.2.4. Nucleophilic Aromatic Substitution

The formalization of nucleophilic aromatic substitution (S_NAr) in 1958 by J. F. Bunnett led to wide spread usage of this important process.[20] S_NAr is often preferred over electrophilic aromatic substitution due to the inherent chemoselectivity the comes from reliance on a leaving group.[20]. S_NAr is particularly useful for the synthesis of anilines and their derivatives (*e.g.*, **7**), which can be accessed from the corresponding halides and amines as shown in Scheme 1.3.

Scheme 1.3: Synthesis of Aniline-Type Derivatives Using Nucleophilic Aromatic Substitution

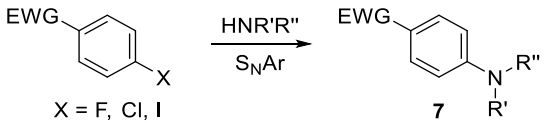

Beyond halogens, sulfides and their oxidized derivatives have also seen use as leaving groups in S_NAr processes. One caveat of S_NAr is the need for an electron withdrawing group (EWG) to be located *ortho*- or *para*- to the leaving group. However, nitro-, cyano-, acyl-, and even metal- substituted aromatics are often acceptable as activating groups.[21] Additionally, S_NAr reactions of heteroaryl halides often proceed even in the absence of an EWG to activate the ring.[22] The range of nucleophiles tolerated includes sulfides, alkoxides, amines and stabilized carbanions, making S_NAr ideal for analogue synthesis.[21] *N*-aryl amines are seen in many natural products and pharmaceutically relevant molecules, notably the kinase inhibitor Gefitinib (**8**, trade

name: Iressa) used to treat metastatic lung cancer.[23] Developed by AstraZeneca, the synthetic route involved S_NAr to install the halogenated aniline **9** to afford intermediate **10**, as in Scheme 1.4.[23] One can easily imagine how S_NAr facilitated the medicinal chemistry effort involved in the discovery of Gefitinib (Scheme 1.4).

Scheme 1.4: The Structure of Gefitinib (8) with the Bond Formed by S_NAr (Blue) Highlighted

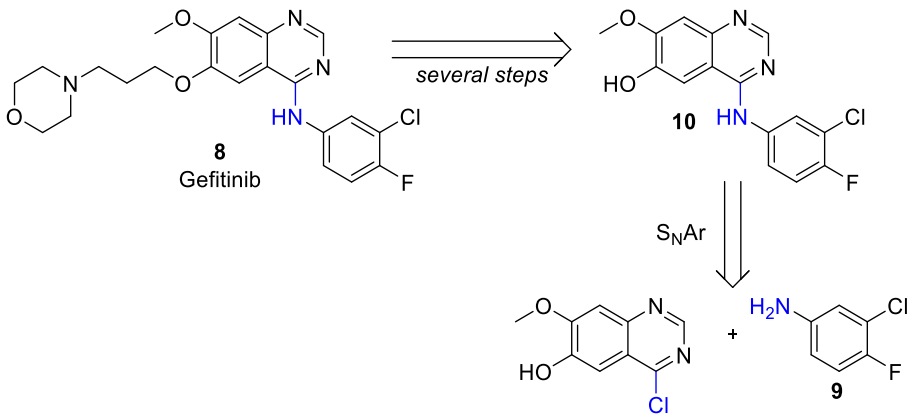

Without question, the development of new synthetic methods has enabled the discovery of many drugs and biological probes. As highlighted above, the development of robust amide bond formation reagents, the Suzuki-Miyaura coupling, and nucleophilic aromatic substitution has greatly impacted the process of drug discovery and the chemical space in which new medicinally relevant molecular entities reside. To further expand accessible chemical space, there is a continual reliance on the development of new synthetic methods.

1.3. The Britton Group Tandem α-Chlorination-Aldol Reaction as an Enabling Methodology

1.3.1. Discovery and Utility of the Tandem α-Chlorination-Aldol Reaction

Recently in the Britton group, a tandem α-chlorination-aldol reaction has been developed between an aldehyde **12** and 2,2-dimethyl-1,3-dioxan-5-one (**11**). This reaction is catalysed by either *(S)*- or *(R)*-proline to afford the *anti*-aldol *syn*-chlorohydrin products (*e.g.*, **13**) in Scheme 1.5, in good yield, enantiomeric excess, and diastereoselectivity, enabling access to chiral building blocks that can be used to synthesize carbohydrates and iminosugars.[24]

Scheme 1.5: Tandem α-Chlorination-Aldol Reaction Recently Developed in the Britton Group

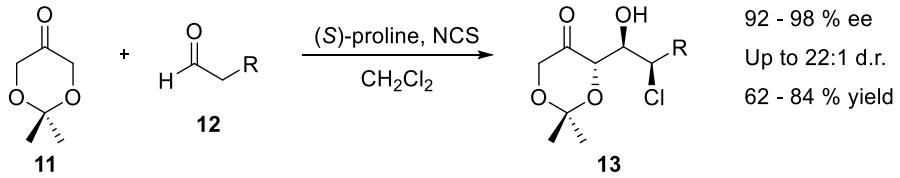

The first step of the reaction is the near racemic α-chlorination of the aldehyde **12** by proline catalyzed enamine attack of the aldehyde on the chlorinating agent, *N*-chlorosuccinimide (NCS). Subsequent proline condensation onto the ketone **11** forms a second enamine (Scheme 1.6, inset, directed to the *si*- face by *L*-Proline) which then undergoes an aldol reaction with either the *R*- or *S*- α-chloroaldehyde, as seen in **TS-1** and **TS-2** (Scheme 1.6).[24]

Scheme 1.6: The Dynamic Kinetic Resolution Driving the Britton Group Tandem α-Chlorination-Aldol Reaction

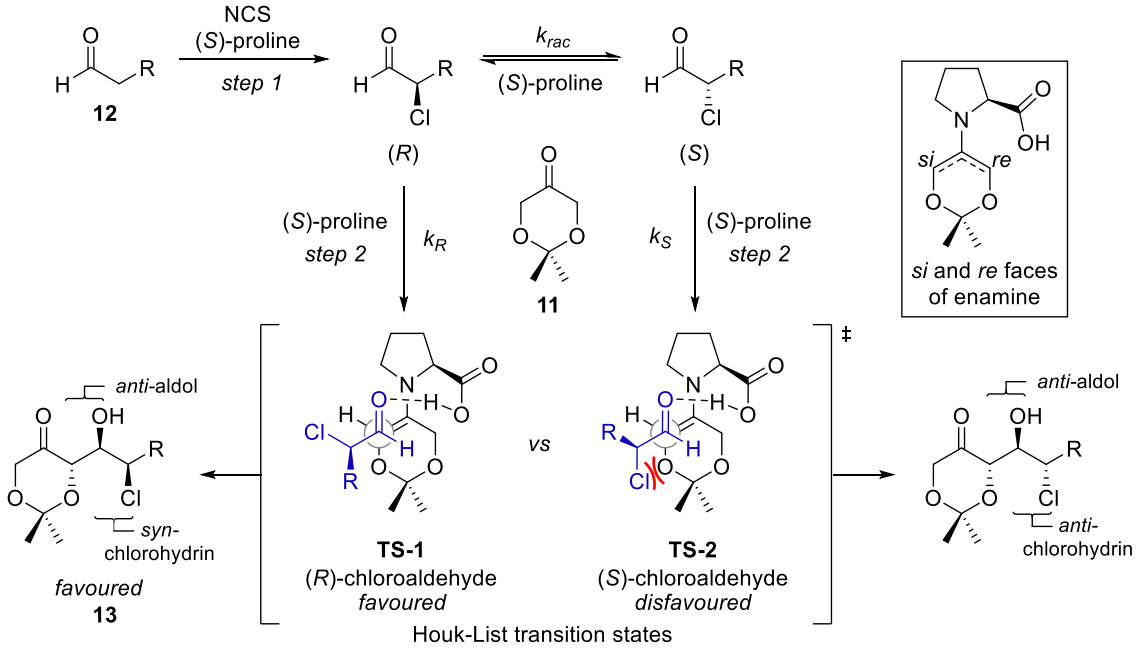

This reaction proceeds through a dynamic kinetic resolution (DKR) of the chloroaldehyde which is controlled by the difference in energy between the two Houk-List transition states (**TS-1** and **TS-2**). The difference in energy between the transition states is proposed to involve electrostatic repulsion between the α-chlorine atom and the endocyclic oxygen of the dioxanone (see)(in **TS-2** of Scheme 1.6) for the *(S)*-chloroaldehyde aldol transition state (when using *(S)*-proline). Formation of the *anti*-aldol

syn-chlorohydrin via **TS-1** is then favoured over the *anti*-aldol *anti*-chlorohydrin via **TS-2** (i.e. $k_R > k_S$). This kinetic resolution is made dynamic by the fast racemization of remaining α-chloroaldehyde by proline (i.e. $k_{rac} >> k_S, k_R$). Enantiocontrol is facilitated by the proline catalyst in the aldol step by directing the aldehyde to the *si*-face instead of the *re*-face of the enamine, as in Scheme 1.6 (inset).

This reaction has proven to be very useful as it establishes three stereogenic centers as well as incorporating much of the exocyclic decoration present in carbohydrates and iminosugars in a single step. The ketochlorohydrins can then undergo diastereoselective *syn*- or *anti*-reduction or reductive amination followed by cyclization to furnish the corresponding carbohydrates **14** or aminosugars **15**, as seen in Scheme 1.7.

Scheme 1.7: Synthetic Utility of the Britton Group Tandem α-Chlorination-Aldol Reaction

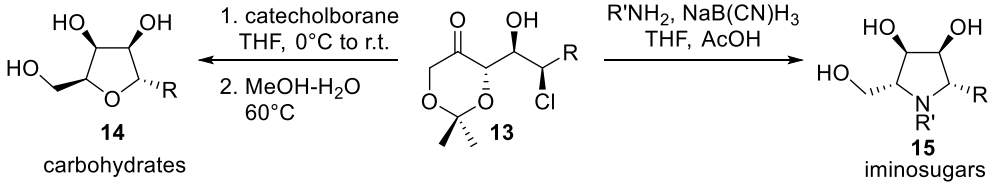

By careful selection of *(S)* or *(R)*-proline, solvent for the tandem reaction, and reductive conditions, many different substituted carbohydrates and iminosugar cores can be accessed. This reaction has seen use in the preparation of several targets of biological relevance, notably in the preparation of piperidine based analogues targeting the glycosidase *O*-GlcNAcase (OGA), a potential therapeutic target of Alzheimer's disease.[25] This methodology has enabled the synthesis of a large (>200 compounds) number of analogues, a process that would have been much longer without the Britton group tandem α-chlorination aldol reaction to provide a short synthetic route to these analogues.

1.3.2. Recent Advances to Diversify the Electrophilic α-Substituting Agent

Currently in the Britton group, generalization of the tandem α-chlorination-aldol reaction to include other electrophiles (other than chlorine) is under way. Specifically, these reactions use electrophilic fluorine (-F), trifluoromethylthio (-SCF_3), and amine (-

NR'R'') sources to produce the corresponding α-substituted aldehydes. Subsequent addition of the dioxanone ketone **11** facilitates the desired aldol reaction, affording substituted compounds analogous to the ketochlorohydrins. The electrophilic sources of substituting groups **16** - **18** are shown in Figure 1.3.

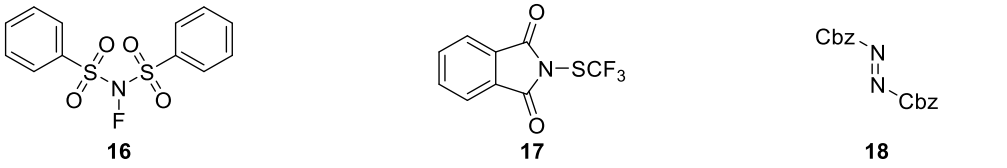

Figure 1.3: Electrophilic α-substitution reagents being explored for use in the Britton group tandem α-substitution-aldol reaction.

Although not all these new reactions proceed through a DKR, they enable the preparation of the substituted hydrins **19** – **21** in Figure 1.4. Two of these substrates are later used as chiral starting materials for the synthesis of α-substituted aldehydes.

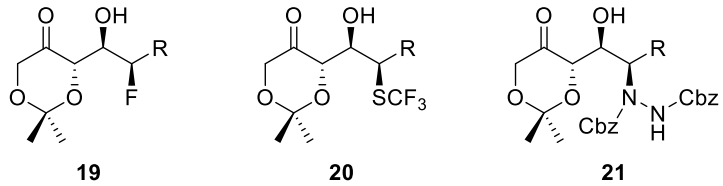

Figure 1.4: New types of α-substituted hydrins prepared using the Britton group tandem α-substitution-aldol reaction.

1.4. Thesis Overview

Chapter 2 describes the development of a novel inhibitor of the epigenetic target protein arginine methyl transferase 4 (PRMT4). To accomplish this, the well-established Suzuki-Miyaura coupling and amide coupling reactions are used as the key methods of assembling analogues for a medicinal chemistry effort to improve the potency, selectivity, and membrane permeability of an initial lead compound. *Chapter 3* establishes the concise synthesis of 1-deoxygalactonojirimycin via the Britton group tandem α-chlorination aldol reaction. The successful development of an improved synthetic route to this marketed pharmaceutical used in the treatment of Fabry disease is presented. *Chapter 4* details a novel synthetic route to enantioenriched α-substituted aldehydes that enables their synthesis via a bench stable intermediate in good yield and purity.

Chapter 2. Development of a Robust Chemical Probe Targeting the Epigenetic Modulator Protein Arginine Methyl Transferase 4

2.1. Epigenetics: A New Approach to Disease Treatment

2.1.1. Epigenetics and Therapeutics

Epigenetics is defined as “the study of heritable changes in gene function that do not involve changes in DNA sequence” by the Merriam-Webster Dictionary.[26] A relatively new field, the study of epigenetics often examines the control exerted by non-coding modifications to the genetic code. These modifications can drastically impact the amount that the affected genes are transcribed. In turn, transcription levels directly influence overall protein expression levels, impacting the characteristics and health of the cell.[27]

Epigenetic markings, including histone modification, DNA methylation, and RNA-associated silencing are well known to play a key role in gene silencing.[28] Mutations of proteins which impart these epigenetic markings can cause inappropriate silencing or activation of genes, in some cases leading to a disease state.[27] Disruption of this balance held by epigenetic networks has been implicated in cancer, syndromes involving chromosomal instabilities, and mental retardation.[27]

Currently, several epigenetic drugs are currently under development that either inhibit direct DNA methylation or target a variety of bromodomains, histone acetylases, protein methyltransferases, and histone deacetylases.[29] These developing drugs have potential applications in the treatment of cardiovascular disease, neurological disorders, metabolic disorders, and cancer.[29]

2.1.2. Validating Epigenetic Targets Using Molecular Probes

Prior to the development of a pharmaceutical compound capable of treating a disease state through modulation of a target, the targets’ therapeutic potential should be confirmed. This can be accomplished using genetic approaches such as RiboNucleic Acid interference (RNAi) or CRIPSR-Cas9 (clustered regularly interspaced short

palindromic repeats – CRISPR-associated protein 9), two techniques that prevent the biological target from being formed in normal levels in the cell by interfering with or inhibiting their synthesis from DNA. However, a second option is to develop a small-molecule modulator of the target, called a pharmacological probe.[30,31] A pharmacological probe effects a change in the activity of a target to varying degrees, enabling the user to explore the mechanistic and phenotypic impact that the target's modulation would have on the disease.[31]

To increase the quality of the chemical probes being developed, groups such as the Structural Genetics Consortium (SGC), a collaboration between academic and industrial medicinal chemists and chemical biologists, have developed criteria to guide their development of new chemical probes in a robust fashion. Each probe produced by the SGC is required to have an *in vitro* potency of <100 nM, possess >30-fold selectivity relative to other isoforms of the same target family, be tested for off-target activity against an industry standard selection of pharmacologically relevant targets, and have proven on-target effects in living cells at concentrations of <1μM.[32] Probes developed without these (or similar) stringent standards are often non-selective or are associated with poor usage characteristics such as reactive groups that have the potential to interfere with common assay features.[31]

Beyond their value in validating therapeutic targets, chemical probes are becoming more common as starting points for drug discovery efforts in industrial settings. For example, the biology and therapeutic potential of the liver X receptor was elucidated with the aid of two structurally distinct agonists GW683965 and T0901317 (Figure 2.1).[33]

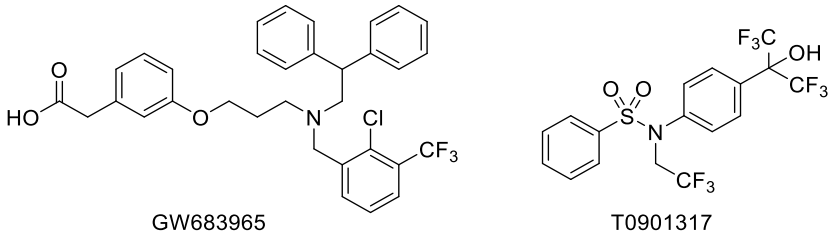

GW683965 T0901317

Figure 2.1: Two structurally distinct liver X receptor chemical probes.

Using these two probes, the liver X receptor family was established as potential therapeutic targets for inflammation, Alzheimer's disease, and atherosclerosis. Since, several liver X receptor agonists have advanced to clinical studies, exemplifying the

ability of well-characterized pharmacological probes to initiate the development of treatments for diseases whose disease pathways are not well-understood.[34]

2.2. The Protein Arginine Methyl Transferase Family

Recently, it has been observed that human cancer cells often bear mutations in proteins that control heritable changes in gene expression, known as epigenetic proteins.[35] These epigenetic proteins can change the expression frequency of factors directly related to cell replication rates.[35] Notably, misregulation of the Protein Arginine Methyl Transferase (PRMT) family of enzymes has been associated with several disease states, one being cancer.[36] PRMT's have many functions, one of which is to transfer a methyl group from *S*-Adenosyl-Methionine (SAM) onto the arginine residues of histone proteins, structures that facilitate DNA packing. Each isoform of PRMT is unique, and functions to methylate select arginine residues (*e.g.*, **22**) at epigenetic sites to varying degrees as in Scheme 2.1.

Scheme 2.1: Methylation Patterns of Different PRMT Isoforms

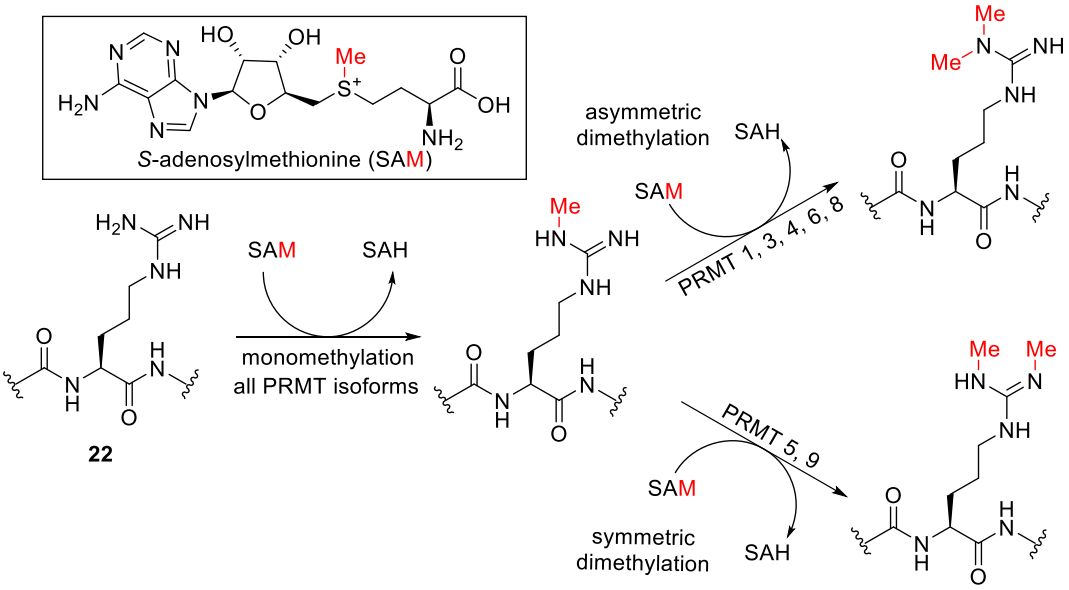

Methylation alters the shape of histone proteins, modulating the extent to which DNA packs around these structures. DNA packing directly impacts the frequency of transcription and thus PRMT's could be responsible for partial epigenetic control over regions of the DNA that produce factors affecting cell replication. In support of this theory, Almeida-Rios *et al.* found PRMT6 to have an oncogenic role in some forms of

cancer.[37] To asses the viability of each PRMT isoform as a therapeutic target for cancer treatment, one or more chemically distinct specific inhibitors could be developed which function in live cells. Like drugs, these probe molecules must be able to pass through the cell membrane and selectively inhibit the desired isoforms of PRMT.

At the start of this project, small molecule molecular probes existed that target multiple PRMT isoforms, in addition to isoform selective probes for PRMT3, PRMT4, and PRMT5.[38] However, even selective probes can often possess unforeseen off-target effects that were not anticipated. The development of orthogonal selective probes is desirable, as it is highly unlikely that two structurally distinct compounds will possess the same off target effects.[31] The parallel use of two orthogonal probes greatly improves the probability that observed effects on the cells are in fact due to the modulation of the targeted biological entity. As of the beginning of this project, a potent and selective chemical probe for PRMT6 had not been developed.

Beyond their epigenetic control, PRMT isoforms 4 and 6 are also key regulators of cell cycle mechanisms, methylating a host of proteins integral to cellular replication. Some of the processes affected by these proteins are summarized in Table 2.1.[39–44]

Table 2.1: Non-Epigenetic Roles of PRMT4 and PRMT 6 in the Cell

	PRMT4	PRMT6
Cell functions regulated by target	RNA splicing and processing Cell cycle control Cellular differentiation	Cell proliferation Cellular senescence DNA repair
Unique histone methylation sites	H3R17 and H3R26	H3R2
Associated cell functions of exclusive histones	Promotes transcriptional activation	Promotes transcriptional silencing of genes such as MYC

The development of a potent, selective small-molecule inhibitor for each isoform of PRMT would facilitate the deconvolution of the relationship between the disease state and its associated aberrant PRMT expression levels. In collaboration with the SGC as well as Bayer Pharmaceuticals, we set out to develop selective small-molecule probes for PRMT's 4 and 6.

2.3. Development of Initial Lead Compound

2.3.1. Starting Point for a PRMT6 Chemical Probe

The SGC, in collaboration with Bayer identified the small molecule **23** via a library screen in search of a novel PRMT 6 inhibitor.

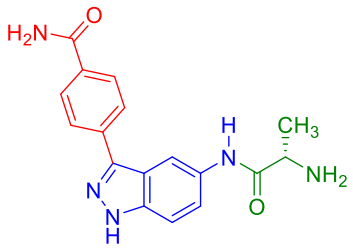

IC_{50} PRMT6: 0.22 μM
IC_{50} PRMT4: 12 μM
23
Initial Hit

Figure 2.2: Initial PRMT6 inhibitor lead compound 23.

Compound **23** inhibits PRMT6 (IC_{50} = 0.22 μM, *n* = 1) and is selective (> 30-fold over other PRMT members) but failed to exhibit in cell effects during *in vivo* studies, a vital requirement for a functional cell-active molecular probe. The lack of *in vivo* efficacy was presumed to be due to low membrane permeability, an assumption later supported by the calculated partition coefficient of **23** residing outside of the ideal range, as well as membrane permeability studies using the Caco-2 assay (*vide infra*). To improve the potency, bioavailability, and selectively of the PRMT 6 inhibitor an efficient and versatile synthesis was necessary to prepare analogues.

In initial studies, the binding geometry of **23** on PRMT6 was unknown, thus a guided approach using Structure Activity Relationship (SAR) generated from an X-ray crystal structure to improve potency was not possible. Furthermore, previously screened molecules showed some modification of the substituted phenyl moiety (red portion, compound **23** in Figure 2.2), but lacked variability in the amino acid moiety (green portion). Thus, the focus for the initial stages of the project was to synthesize analogues which were less polar than **23** to encourage membrane permeability whilst exploring the SAR of the core (blue) and amino acid moiety (green).

2.3.2. Initial Modification to Indole-based Core Analogues

To increase the lipophilicity and reduce the number of hydrogen bond acceptors of **23**, a structure with an indole core rather than an indazole was initially targeted. When designing a synthetic route to produce these analogues, three characteristics were desired: i) a modular route that allows quick access to many compounds; ii) a route that relies on robust, well-precedented reactions; and iii) a divergent synthesis that enables late stage derivatization of the molecule. A retro-synthetic analysis for a series of indole-based analogues identified three key fragments: a substituted aryl group (A, red); a heterocycle (B, blue); and an amino acid (C, green) (Scheme 2.2).

Scheme 2.2: Retrosynthetic Analysis of Initial Indole-Based Analogues

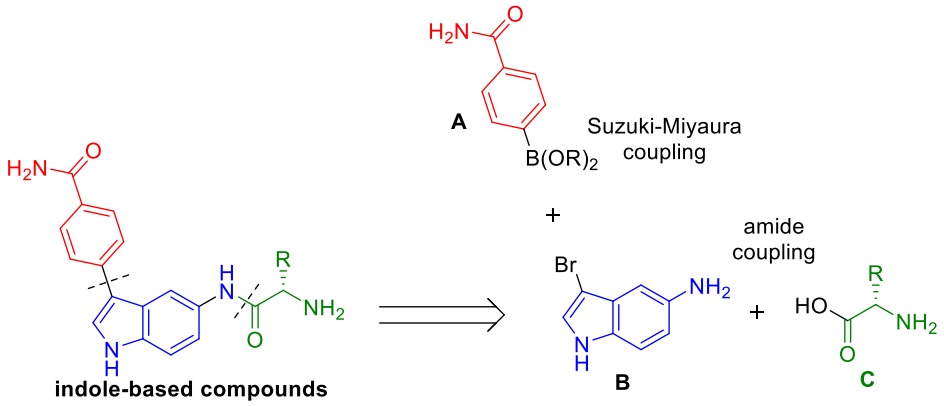

Initially, two different synthetic routes were considered. Route 1 (Scheme 2.3) involved first performing the amide coupling to join fragments **B** and **C**, which would be followed by a Suzuki-Miyaura coupling to attach fragment **A**. Route 2 (Scheme 2.4) reversed the order of these steps, joining fragments **A** and **B** with a Suzuki-Miyaura coupling followed by amide coupling to attach fragment **C**. Unfortunately, route 1 suffered from purification issues with moderate yields (<60 %) for the initial amide coupling of *Boc*-*L*-alanine and 5-aminoindole. This was likely due to the presence of two nucleophilic nitrogens in the starting material (Scheme 2.3, Nu in **24**), for which selective protection of the slightly less nucleophilic endocyclic indole nitrogen would be difficult, as seen in Scheme 2.3.

Scheme 2.3: Attempted Route 1, Showing the Two Nucleophilic Nitrogen's (Nu) Affecting the Amide Coupling, and the Free Indole Nitrogen Complicating the Suzuki-Miyaura Coupling

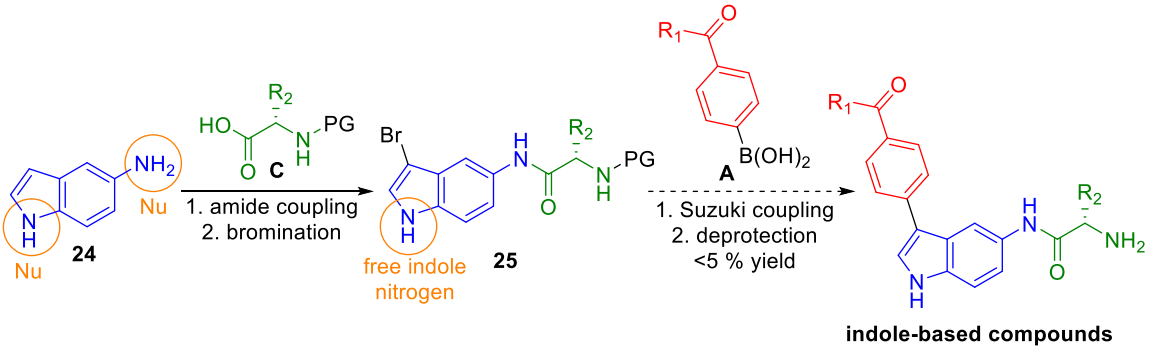

Route 1 also resulted in very poor yields (<5 %) for the Suzuki-Miyaura coupling, likely due to the exposed indole nitrogen (Scheme 2.3, free indole nitrogen of **25**). Thus, route 1 was discontinued. From these efforts, a small amount of methyl ester **26**, seen later in Scheme 2.7 was obtained.

Route 2 was initially designed to produce the key intermediate **29** shown in Scheme 2.4. This intermediate would provide a point in the synthetic sequence to introduce variation in the amide coupling partner. This would enable access to a small library of molecules possessing the desired indole core and provide information regarding the importance and behaviour of fragment **C**.

Scheme 2.4: Synthetic Approach of Route 2 for the Synthesis of Indole-Based Compounds

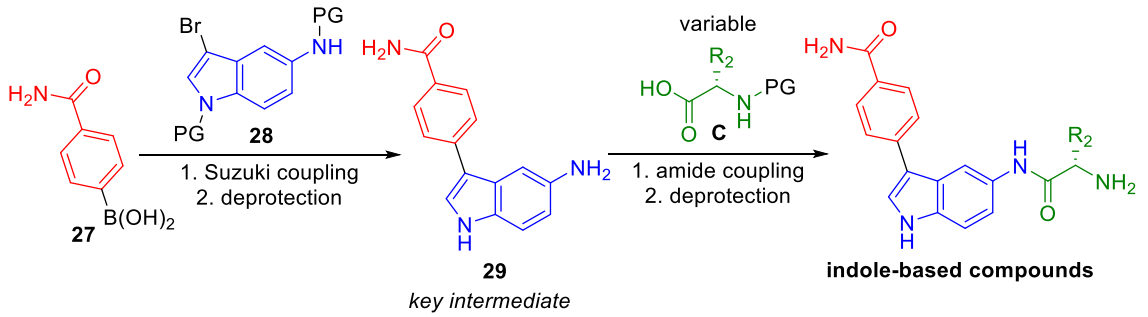

Literature precedent and previous experience for coupling reactions of fragments **27** and **28** suggested that the Suzuki-Miyaura coupling conditions would be more successful when the indole nitrogen of **28** was protected as in Scheme 2.4.[45–47] As such, the first step of the overall synthetic sequence for the synthesis of indole-based analogues was to *bis*-protect the commercially available 5-aminoindole **24** with *tert*-

butyloxycarbonyl (Boc) groups in preparation for the Suzuki-Miyaura coupling, as in Scheme 2.5.[48]

Scheme 2.5: Full Synthetic Route Used to Access Indole-Based Analogues (Yields for the Synthesis of Analogue 33 Shown)

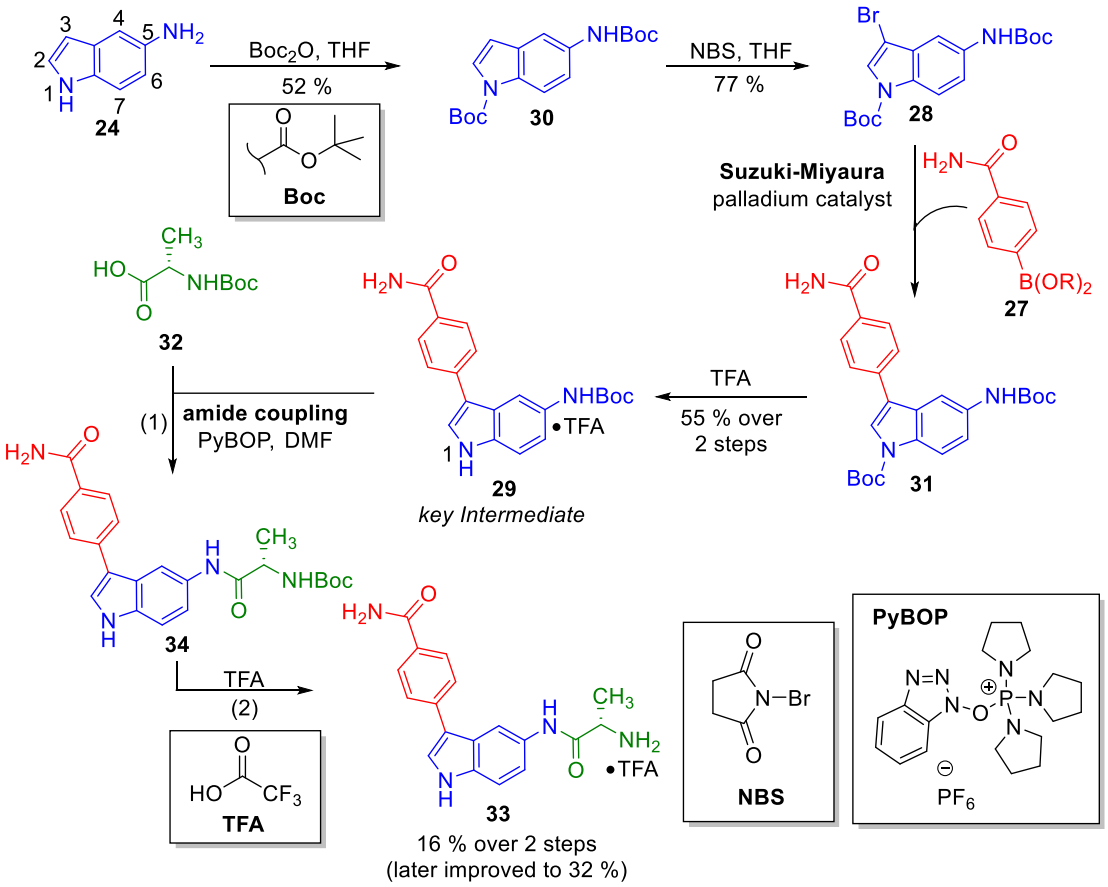

Subsequent electrophilic aromatic substitution at the 3 position of the protected 5-aminoindole **30** with *N*-bromosuccinimide (NBS), an electrophilic source of bromine, afforded the brominated and protected indole **28** in good yield.[49] The Suzuki-Miyaura reaction was then able to proceed between indole **28** and the aryl boronic acid **27** to afford the coupled product **31** in reasonable yield. At first, (1,1'-*bis*(diphenylphosphino)-ferrocene)palladium(II) dichloride dichloromethane adduct ($Pd(dppf)Cl_2 \bullet CH_2Cl_2$) was used as the palladium source for the Suzuki-Miyaura reaction.[50] However, brief optimization studies revealed that tetrakis(triphenylphosphine)palladium ($Pd(PPh_3)_4$) provided slightly better yields. Removal of the Boc protecting groups in neat trifluoroacetic acid (TFA) cleanly afforded the key intermediate **29**, ready to undergo amide coupling on the exposed aniline-type nitrogen. For this step, the amide coupling reagent benzotriazol-1-yl-oxytripyrrolidinophosphonium hexafluorophosphate (PyBOP)

was chosen based on literature precedent of successfully coupling aniline-type amines to amino acids, as well as proceeding without racemization of the amino acid.[51,52]

However, the indole nitrogen (position 1 of **24**) is also sufficiently nucleophilic to undergo coupling with the activated *N*-Boc protected amino acid moiety, leading to a roughly equal mixture of mono- (**34**) and di- (**35**) substituted products (Scheme 2.6) and low isolated yields (<30 %) for the desired amide **34**. This problem was later addressed through reaction optimization including experiments focused on probing the effect of reagent equivalents and reaction conditions.

Scheme 2.6: Reduced Yield of Final Amide Coupling Due to *bis*-Substituted Product

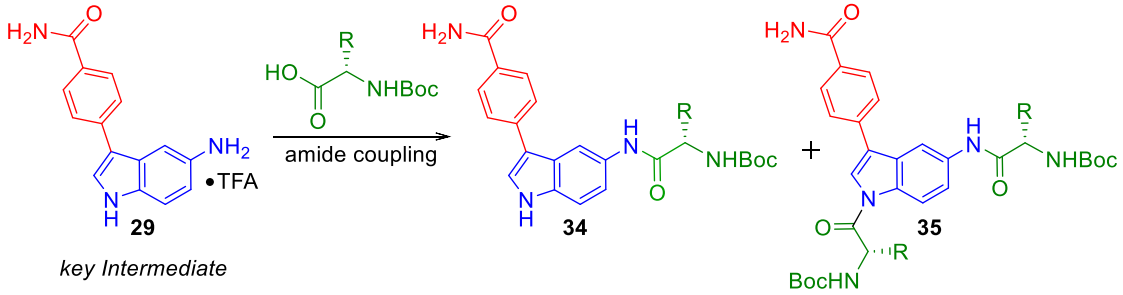

Final deprotection was performed in neat TFA to remove the protecting group on the amino acid moiety in **34** (Scheme 2.5) followed by purification by reverse phase high performance liquid chromatography (RP-HPLC). This sequence afforded the final compound **33** and other analogues as a TFA salt, in high purity, ready for biological testing (Scheme 2.5).

Once the first set of compounds (bearing aliphatic amino acids of increasing steric bulk) was synthesized, biological testing by collaborators at the SGC was performed to generate *in vitro* potency data. A radioactivity based biophysical assay was used to measure the activity of PRMT6 in the presence of PRMT6 substrates, reported via incorporation of tritium (^{3}H) in the methyl group of SAM. When different amounts of inhibitor (be it the control, lead compound, or synthesized analogues) are added, the activity of PRMT6 is inhibited. This reduces the amount of radioactive substrate that is transferred to the histone sub-unit, a change that can be measured and quantified. This generates data known as the half-maximal Inhibitory Concentration (or IC_{50}), the amount of each compound required to inhibit 50% of the maximal PRMT6 activity. These assays were performed once for each analogue unless otherwise indicated (i.e. n = 1). From this

information, qualitative connections between the structural differences of the analogues and their corresponding activity against PRMT6 can be drawn. To investigate the selectivity of the compounds for PRMT6 over other isoforms, each analogue was also tested against the structurally most similar isoform PRMT4. The initial compounds synthesized are shown in Scheme 2.7, with the results of the *in vitro* biological testing of compounds **26**, **36**, **37**, **38**, and **39** summarized in Table 2.2.

Scheme 2.7: Initial Indole Series of Compounds

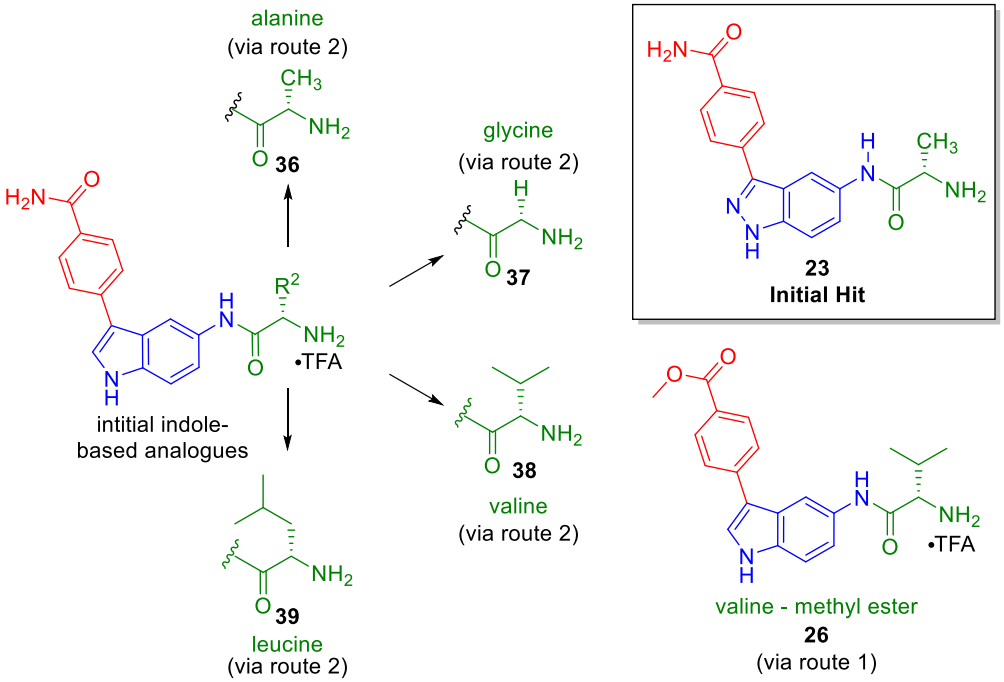

Table 2.2: *In Vitro* Biological Data for Initial Indole Series of Compounds

Compound	Phenyl ring (red)	Core (blue)	Amino acid (green)	IC_{50} PRMT6	IC_{50} PRMT4
23	*para*-amide	indazole	alanine	0.22 μM	12 μM
36	*para*-amide	indole	alanine	0.8 μM	1.1 μM
37	*para*-amide	indole	glycine	19 μM	4.1 μM
38	*para*-amide	indole	valine	22 μM	>100 μM
26	*para*-methyl ester	indole	valine	94 μM	15 μM
39	*para*-amide	indole	leucine	35 μM	>100 μM

The results of the biological data for the initial series of compounds was disappointing. Upon transition from the indazole core (**23,** Table 2.2) to the indole core (**36**), a near four-fold loss in potency for PRMT6 was observed. Furthermore, replacing the alanine moiety (**36**) with any of glycine (**37**), valine (**38**), or leucine (**39**) causes an order of magnitude loss in potency of the compound, as well as loss of selectivity for PRMT6. Also disappointing was the loss of potency upon transition from the amide **38** to

the methyl ester **26**. Furthermore, a large increase in potency for PRMT4 was also observed for this transition, which eliminated the selectivity of the probe for PRMT6. Due to these initial results, we decided to pursue the further development of compounds bearing the indazole core for the PRMT6 selective probe program.

2.3.3. Realization of a PRMT 4 Selective Lead

While examining the data obtained from the first series of indole compounds, as well as newly released data from a small amount of screening Bayer performed prior to our involvement in the project, some key observations were noted (Scheme 2.8). Upon transition from the indazole core **23** to indole core **36**, a loss in potency and selectivity for PRMT6 was observed. Similarly, exchanging the *para*-amide moiety (**23**) for a *meta*-methyl sulfone (**40**) or the *para*-amide (**38)** for a *para*-methyl ester (**26**) also resulted in a decrease in potency and selectivity for PRMT6. However, along with the reduction in potency for PRMT6 came improvements in potency and selectivity for PRMT4. Considering the observed reversal of selectivity observed for two distinct portions of the molecule, we theorized that it might be possible to design a PRMT4 selective probe.

Scheme 2.8: Key Observations of Initial Data (*n* = 1 for biological assays) Reveal the Potential for a PRMT4 Selective Probe

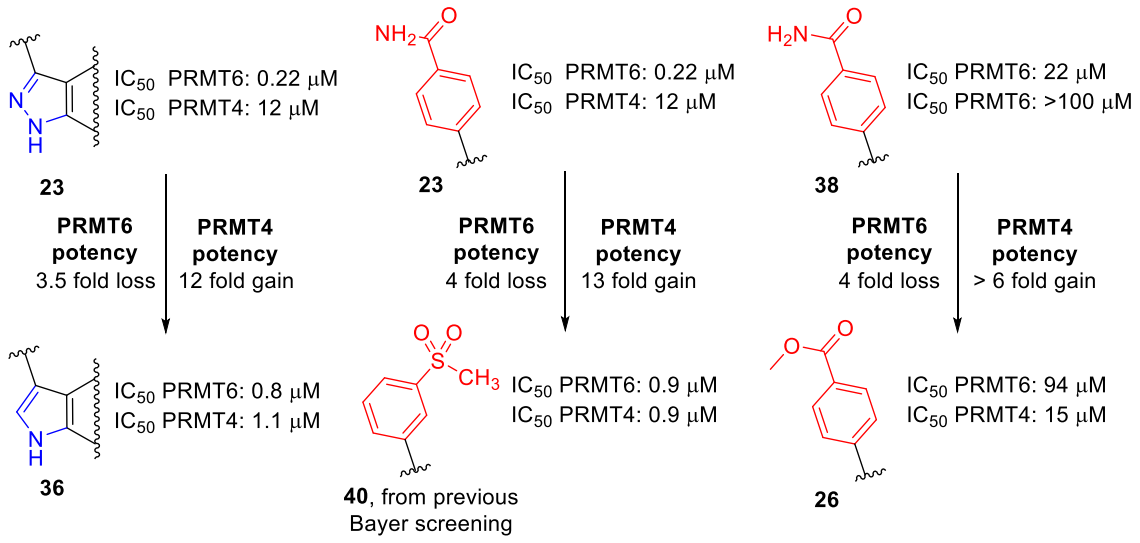

To explore this possibility, two analogues (**43** and **44**) were synthesized from the key intermediates **41** and **42** according to the established synthetic route, bearing the combinations of changes seen in Scheme 2.8 to increase the PRMT4 selectivity. The compounds with their biological data are presented in Figure 2.3. Both compounds **41**

and **42** were selective for PRMT4. Notably, the *meta*-methyl sulfone analogue (**42**) was both potent and selective, inhibiting PRMT4 with an IC_{50} = 21 nM, and a selectivity against PRMT6 of over 400-fold. This exciting discovery met two of the four criteria for molecular probes set out by the SGC (sufficient potency and selectivity). Unfortunately, although having a reduction in H-bonding donors and acceptors relative to the initial hit, it still did not exhibit on-target effects in cells up to concentrations of 30 μM in HEK293 cells, as reported by BAF155 methylation.

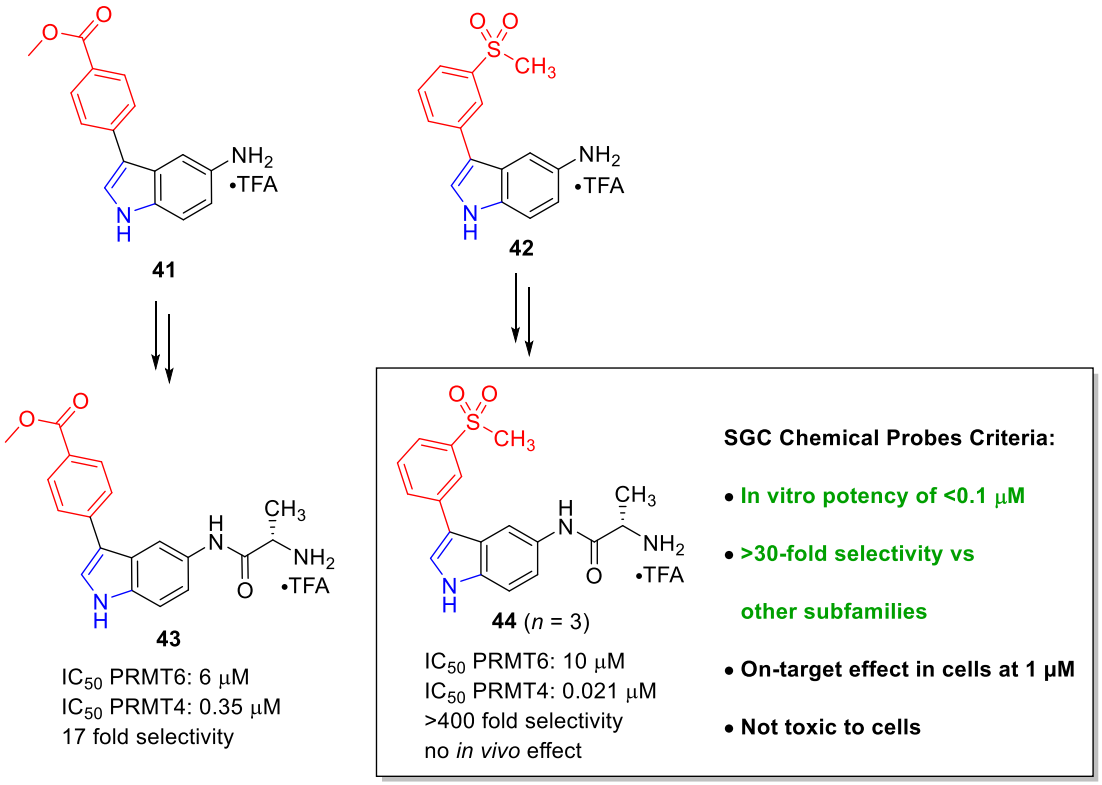

Figure 2.3: Successful realization of a PRMT4 selective probe starting point.

2.4. Lead Optimization to Enhance Membrane Permeability

2.4.1. Analogues Containing an Ethylene Diamine Moiety

With a new aim to develop a PRMT4 selective probe, we noticed that the known PRMT inhibitors seen in Figure 2.4 contain an ethylene-diamine type linkage.[53–55] Although this results in two basic amines in each molecule, these inhibitors are cell permeable. As such, we targeted compounds **45** and **46** bearing a similar ethylene-

diamine linkage in hopes of improving the potency and membrane permeability of the compound.

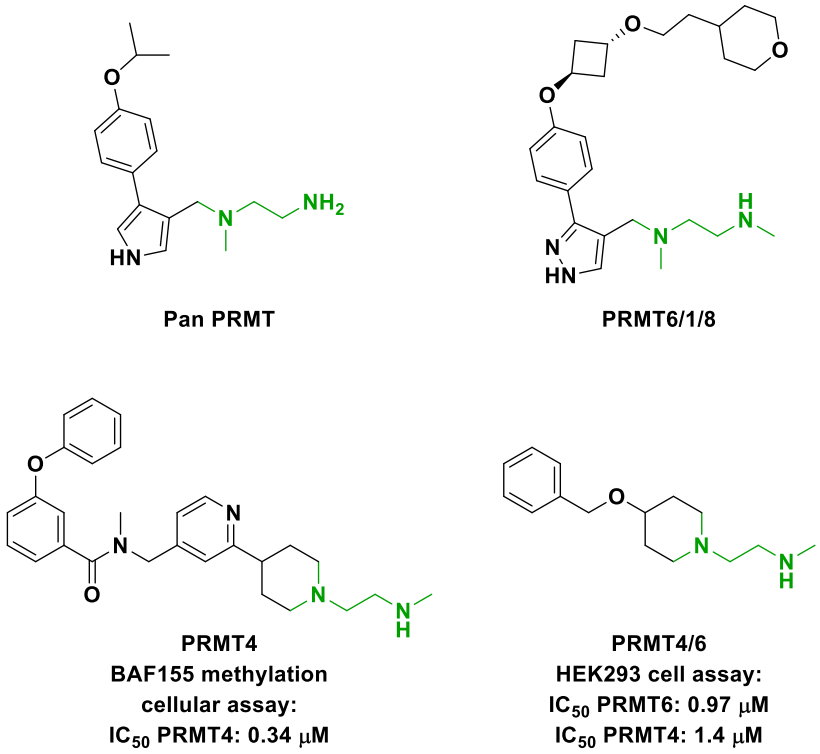

Figure 2.4: Current PRMT probes incorporating an ethylene-diamine linkage (colored green).

The two compounds were synthesized from the free base of the intermediate **42**, via reductive amination of the protected glycine-based aldehyde **47**, or via nucleophilic substitution of the commercially available compound **48**, as shown in Scheme 2.9. Unfortunately, transition to the ethylene-diamine moiety resulted in a loss of *in-vitro* potency from 0.021 to ≥ 27 μM. Coupled with the increased polar surface area and overall charge present with having two basic amines, the exploration of ethylene-diamine type compounds was discontinued.

Scheme 2.9: Exploration of the Ethylene-Diamine Moiety

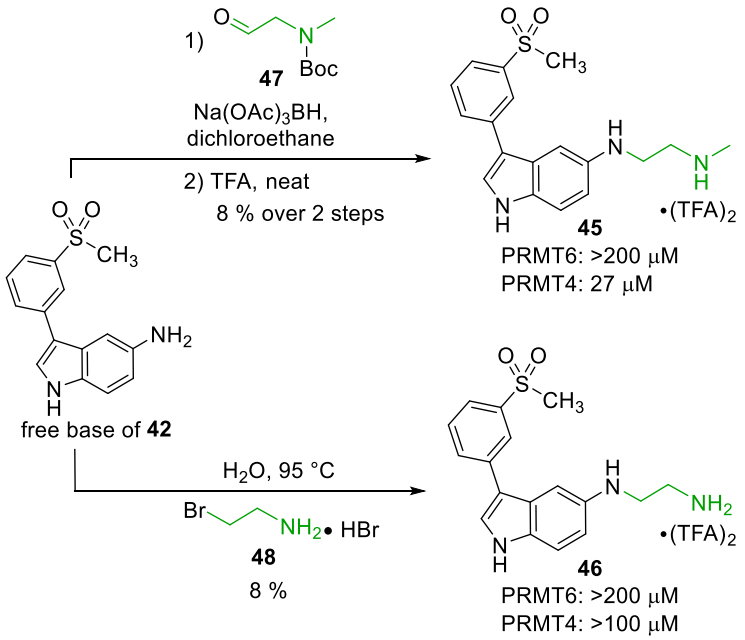

2.4.2. Sulfonamide Exploitation of a Hydrophobic Binding Pocket

At this point, Bayer released a crystal structure of an indazole-core inhibitor **49** bound to PRMT6, obtained from other projects. The inhibitor-bound structure is shown in Figure 2.5 where the amino acid moiety of **49** projects into a channel at the rear.

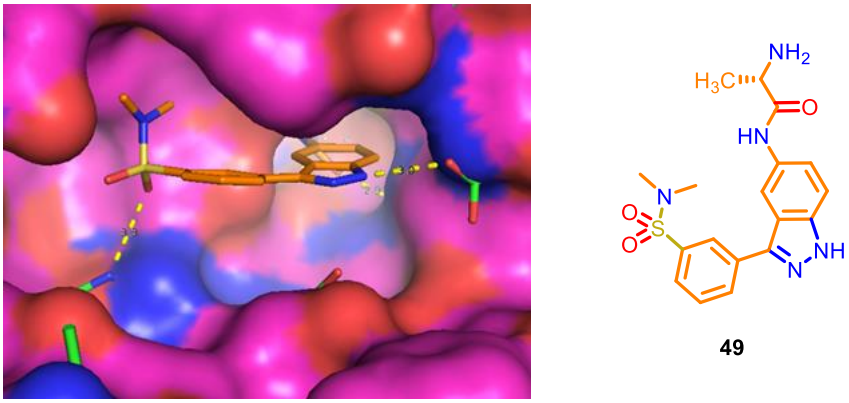

Figure 2.5: Crystal structure of indazole based inhibitor bound to PRMT6, provided by Bayer.

Structurally, PRMT4 and PRMT6 are very similar. One difference however is the depth and hydrophobicity of the pocket that the sulfonamide function in compound **48** projects into (see the left-hand portion of Figure 2.5). In PRMT4, this pocket is more hydrophobic and different in shape than the same pocket in PRMT6. We hypothesized

that exploiting this difference would result in increased selectivity for PRMT4 over PRMT6. Furthermore, replacement of the sulfone in **44** with the dimethyl sulfonamide moiety found in compound **49** would likely improve the membrane permeability due to the increase in lipophilicity, as measured by cLogP value, as explained below.

As part of our goal to improve membrane permeability of these molecular probes, we also considered cLogP values, the calculated log of the partition coefficient of the molecule between *n*-octanol and water. This value is often representative of a molecules ability to cross the cell membrane by passive diffusion. Higher numbers represent increasing lipophilicity, with reasonable membrane permeability generally seen for values of (experimentally determined) LogP from 2-4.[56] In this range, the molecule is still relatively soluble in aqueous and lipophilic environments, allowing it to pass through the membrane effectively. An advantage of the cLogP calculation is that is easily calculated by a variety of software programs such as Chemdraw.

The replacement of the methyl sulfone moiety in compound **44** with a dimethyl sulfonamide moiety would increase the cLogP value for the molecule from 0.9 to 1.7, much nearer to the ideal range. As a result of these findings, we targeted the dimethyl sulfonamide moiety, as well as other alkylated sulfonamides, with the hope that this would improve the membrane permeability of the compound.

To synthesize these sulfonamide analogues, commercially available 3-bromobenzenesulfonyl chloride (**50**) was exposed to several secondary amines of increasing size to afford sulfonamides **51** - **53**. A subsequent Miyaura borylation of the sulfonamides using Pd(dppf)Cl_2•CH_2Cl_2 and bis(pinacolato)diboron yielded the desired 3-pinacolboronate aryl-sulfonamides **54** - **56**, as shown in Scheme 2.10.

Scheme 2.10: Synthetic Route to Access 3-Pinacolboronate Aryl-Sulfonamides *Compound was synthesized by Anissa Kaghad

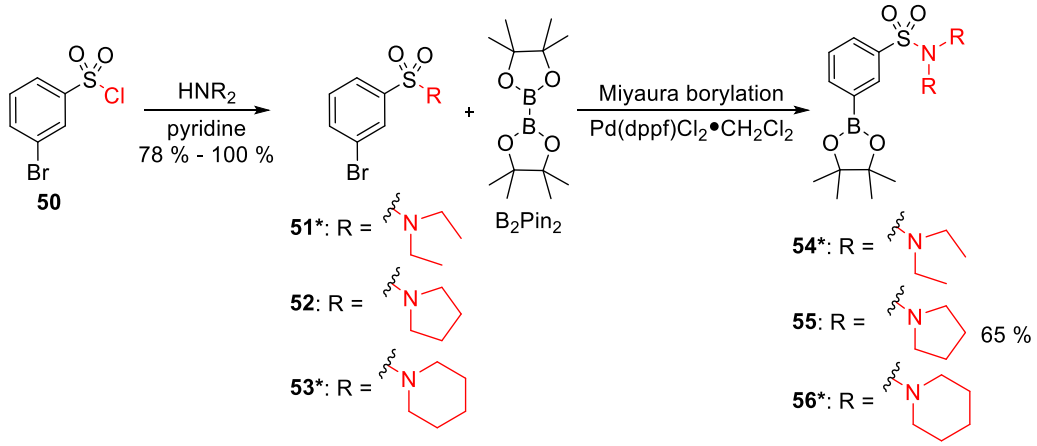

Using these 3-pinacolboronate aryl-sulfonamides **54** – **56** or N,N-dimethyl-3-(4,4,5,5-tetramethyl-1,3,2-dioxaborolan-2-yl)benzenesulfonamide (commercially available), the key intermediates **57** - **60** seen in Figure 2.6 were synthesized via a Suzuki-Miyaura coupling. Subsequent completion of the established sequence for the synthesis of indole-based analogues (Scheme 2.5) afforded the sulfonamide derivatives **61** – **64** found in Scheme 2.11.

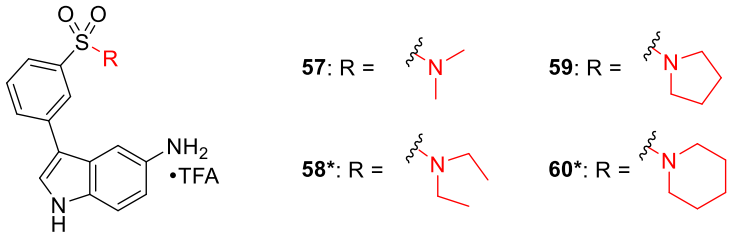

Figure 2.6: Key intermediates synthesized to enable the production of sulfonamide analogues 61 – 64. *Compound was synthesized by Anissa Kaghad.

The resulting derivatives **61** – **64** showed promising biological activity. Although potency was lost upon transition from the methyl sulfone **44** to a bulkier (**62**) or larger cyclic sulfonamide (**63, 64**), it was improved when exchanged for the dimethyl sulfonamide (**61**). Furthermore, while the increase in potency and selectivity (from 0.021 μM, 400 fold selective for methyl-sulfone **44** to 0.007 μM, 1000 fold selective for dimethyl sulfonamide **61**) was beneficial, the fact that it coincided with a dramatic increase in lipophilicity (estimated by cLogP) which had the potential to improve the membrane permeability was very exciting. Unfortunately, when tested in cells, **61** was not found to

be active, suggesting that it still was not able to cross the cell membrane to have an effect on living cells.

Scheme 2.11: Analogues to Probe the SAR of the Amino Acid Moiety and Test the Hypothesis Regarding the Sulfonamide Moiety

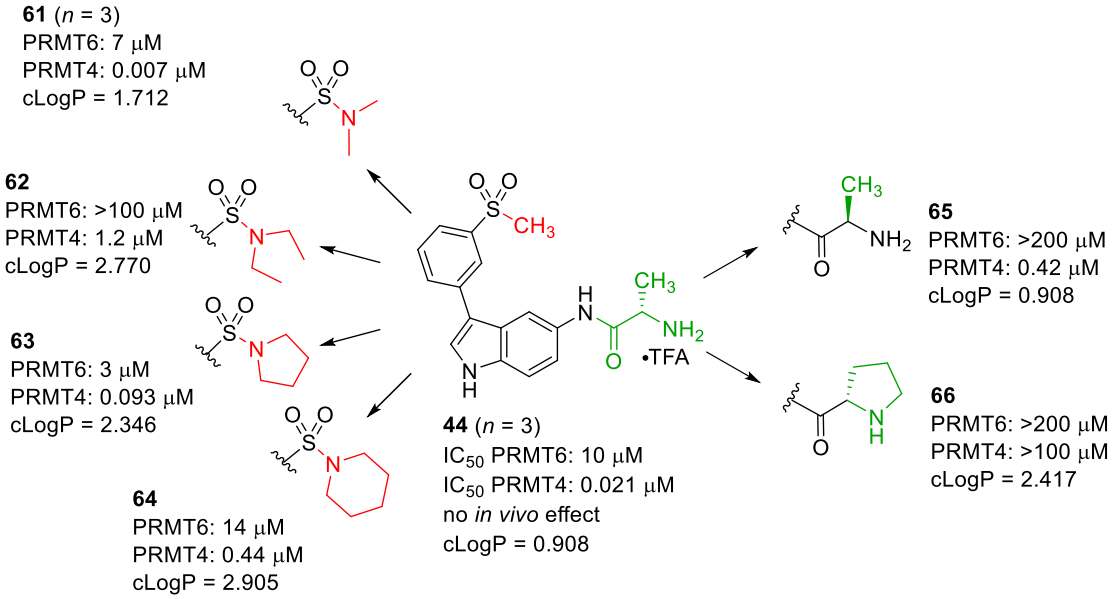

Compounds **65** and **66** in Scheme 2.11 were synthesized to probe the SAR of the amino acid moiety. The *D*-alanine analogue **65** was synthesized to explore the stereochemical constraints of the binding pocket. Since the protein's substrate contains chiral centers, the stereochemistry of the pocket likely influences the binding affinity of two enantiomers. Furthermore, challenges with passing through membranes may arise from efflux, the removal of foreign substances from the cell by active transport proteins such as P-glycoprotein. We hypothesized that if efflux was occurring, it could potentially be avoided by exchanging the *L*-alanine subunit (**44**) for *D*-alanine (**65**), modifying the efflux pump's recognition of and affinity for the analogue. Unfortunately, this transition resulted in a 20-fold loss in potency. The *L*-proline analogue **66** was synthesized to test the effect of increasing size of the amino acid moiety on binding as well as whether two hydrogen bond donors were necessary to maintain potency on the basic amine. Unfortunately, the amino acid analogues **65** and **66** did not maintain sufficient potency to advance.

2.4.3. Transition to Sulfone and Modification of Basic Nitrogen Group

To explore the effect of replacing the sulfonamide with a sulfone, the isopropyl (**67**) and cyclopentyl (**68**) sulfones were set as target compounds. Although having cLogP values similar to their sulfonamide counterparts **61** and **63**, we hoped that these compounds would confirm the trend towards decreased potency with increased size observed in the sulfonamides **61** and **63**.

The sulfone analogues **67** and **68** were synthesized as follows. A two-step alkylation and oxidation of 3-bromothiophenol **69** afford the aryl sulfones **70** and **71**, followed by a Miyaura borylation to afford the 3-pinacolboronate aryl-sulfones **72** and **73** (Scheme 2.12). Coupling to the indole core and TFA deprotection afforded the key intermediates **74** and **75**.

Scheme 2.12: Synthesis of Isopropyl- and Cyclopentyl-Sulfone Analogues

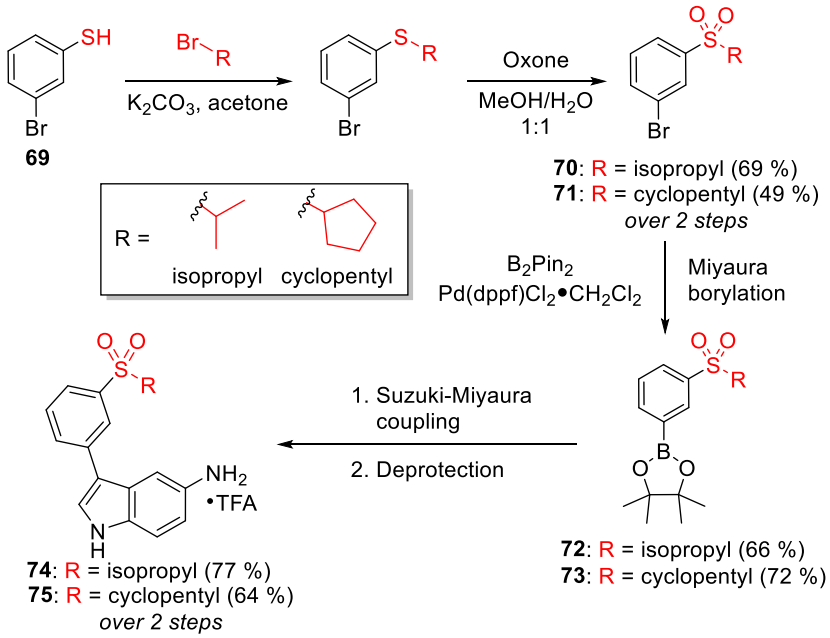

Subsequent final amide coupling and deprotection afforded the sulfone analogues **67** and **68** seen in Scheme 2.14 with their resulting biological data. To determine if the corresponding dimethylamide would be a suitable replacement for the sulfonamide, we also synthesized the key dimethyl amide intermediate **78** via the boronic ester **77**, starting from 3-bromo-*N,N*-dimethylbenzamide **76** as seen in Scheme 2.13.

Scheme 2.13: Synthesis of Dimethyl Amide Key Intermediate 78

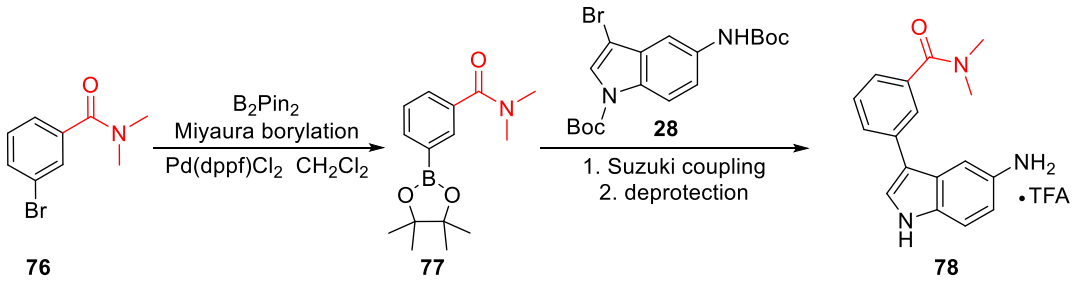

Amide coupling and deprotection of intermediate **78** afforded the dimethyl amide analogue **79**, with its biological data shown in Scheme 2.14. Exchanging the sulfonamide (**61**, IC_{50} = 0.007 μM) for the isopropyl sulfone (**67**, IC_{50} = 0.011 μM) resulted in only a small loss in potency. However, further testing showed that this change was detrimental to the membrane permeability (*vide infra*, Figure 2.9). The cyclopentyl sulfone analogue **68** (IC_{50} = 1 μM), was significantly less potent than the smaller isopropyl sulfone **67** (IC_{50} = 0.011 μM). With the observed 10-fold loss in potency upon transition from the dimethyl sulfonamide (**61**, IC_{50} = 0.011 μM) to pyrrolidine-sulfonamide (**63**, IC_{50} = 0.093 μM), this may suggest that the hydrophobic pocket is not large enough to accommodate five membered rings, though sulfonamides appear better tolerated than their sulfone counterparts. The *in vitro* potency data of dimethyl amide **79** established that this amide moiety is not a suitable substitute for the sulfonamide (**61**), as it resulted in a 43-fold loss in potency for PRMT4.

Scheme 2.14: Exploration of Sulfone Derivatives

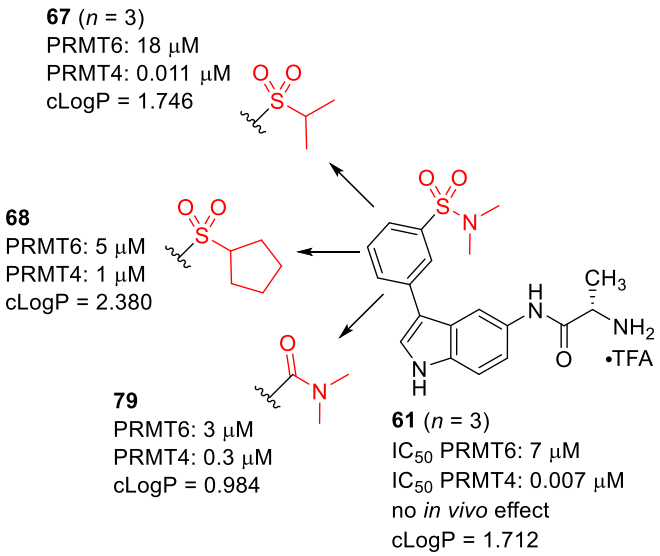

Finally, a variety of commercially available or synthetic amino acid derivatives were targeted bearing the isopropyl sulfone moiety to explore the impact of modulating the basicity of and number of hydrogen bond donors on the basic amine. The *N*-Boc-*mono*-fluoro-*L*-alanine required for synthesis of **80** was prepared by Dimitrios Panagopoulos following an established literature procedure with a different protecting group (Boc instead of fluorenylmethyloxycarbonyl or Fmoc).[57] Compound **81** was prepared via reductive amination of *N*-Boc-*L*-alaninal by the free base of key intermediate **74**, while the corresponding carboxylic acids of the remaining Boc-protected amino acid derivatives used to synthesize **82** and **83** via amide coupling were commercially available. The final compounds can be seen in Scheme 2.15, along with their resulting *in vitro* potency data.

Unfortunately, attempts to modulate the basicity of the terminal amine were unsuccessful, failing in most cases to retain a moderate level of potency (changing from an IC_{50} equal to 0.011 μM for **67** to at least 1.340 μM for compounds **80** - **82** against PRMT4). This observation may be rationalized by disruption of the complex hydrogen bonding network seen in the crystal structure, involving both protons on the amino acid terminal nitrogen as well as the amide carbonyl.

Scheme 2.15: Modification of the Basic Amino Acid Moiety

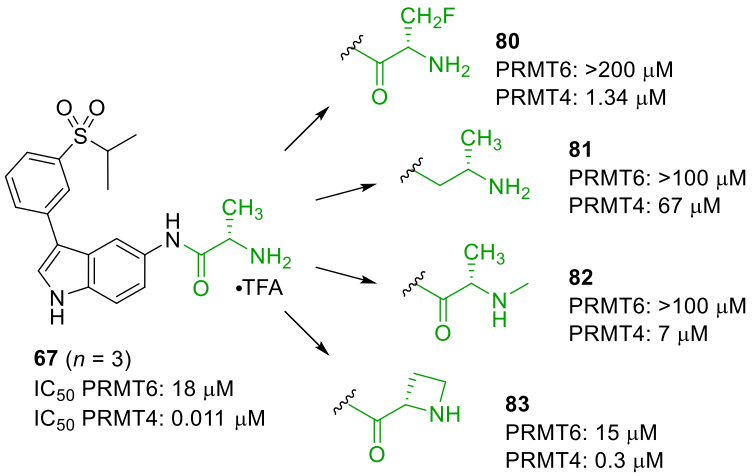

However, azetidine analogue **83** caught our attention for two reasons. Although also likely disrupting the H-bonding network, it retained a potency of 0.3 μM, as well as reduced the number of hydrogen bond donors in the compound, a change which should improve the membrane permeability profile.

2.4.4. Removal of Hydrogen Bonding Donor via Azetidine Moiety

To examine this azetidine scaffold more closely, three more analogues also incorporating the chiral azetidine found in **83** were synthesized, using different synthetic routes. The dimethyl sulfonamide analogue **84** was synthesized as previously described, by addition of dimethyl amine to the sulfonyl chloride (Scheme 2.10). The synthesis of the cyclobutyl sulfone **85** analogue began with the alkylation of 3-bromothiophenol **69** with bromocyclobutane to afford the sulfide, which was then oxidized using oxone® to afford the sulfone **86**, as seen in Scheme 2.16. Miyaura borylation of the sulfone **86** then generated the 3-pinacolboronate aryl-sulfone **87** (Scheme 2.16), which could be used in subsequent Suzuki-Miyaura coupling to the indole core to produce the key intermediate **88** (Figure 2.7).

Scheme 2.16: Synthesis of 3-Pinacolboronate Cyclobutyl Sulfone 87

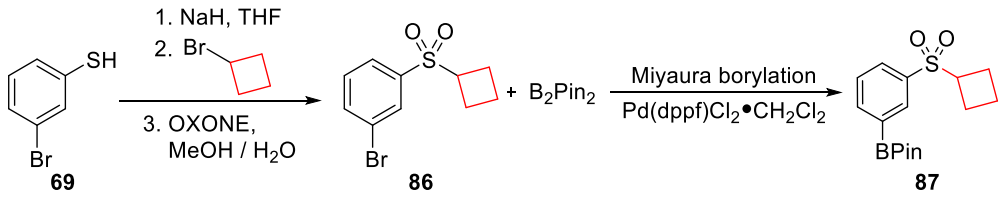

Scheme 2.17: Synthesis of *tert*-Butyl Sulfone Boronic Ester

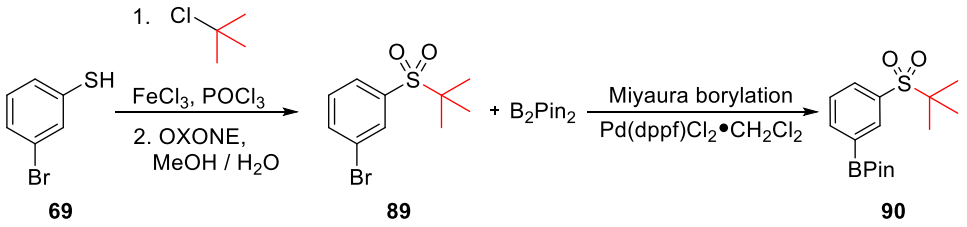

The 3-pinacolboronate *tert*-butyl sulfone **90** was generated through a Lewis-acid catalyzed reaction of *tert*-butyl chloride by 3-bromothiophenol **69** followed by oxidation to the sulfone **89** and Miyaura borylation, as seen in Scheme 2.17. Coupling of **90** to the indole core then provided the key intermediate **91**, shown in Figure 2.7.

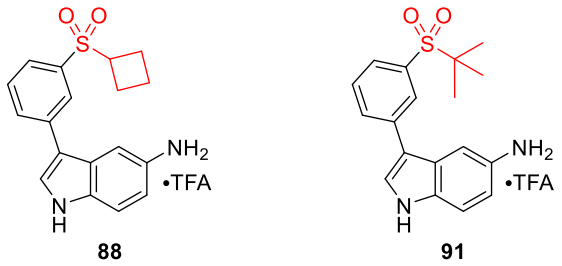

Figure 2.7: Key intermediates for cyclopentyl- and *tert*-butyl-sulfone analogues.

Completion of route 2 (Scheme 2.5) using key intermediates **88** and **91** afforded the final compounds **85** and **92** respectively. Disappointingly, this change to cyclobutyl sulfone **85** or *tert*-butyl sulfone **92** to improve the lipophilicity led to a five-fold loss in potency of the analogues bearing an azetidine moiety (Scheme 2.18) relative to the isopropyl-sulfone **83**. However, transitioning back to the dimethyl sulfonamide **84** from the isopropyl sulfone **83** improved the potency around 3-fold. Unfortunately, the sulfonamide **84** was not found to be active in cells.

Scheme 2.18: Biological Data for Azetidine Containing Analogues

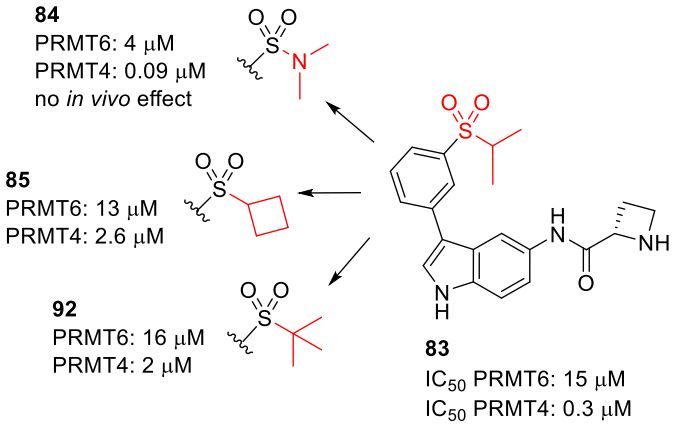

2.4.5. A Need for a Quantitative Analysis Method for Membrane Permeability

Frustrated by our lack of quantitative data regarding membrane permeability, we reached out to collaborators at Bayer and inquired about the possibility of artificial membrane permeability assays to be performed on key compounds. They were very helpful and provided data regarding permeability of these compounds via a Caco-2 assay. The Caco-2 assay is performed on a monolayer of colorectal cells which are polarized, possessing both apical and basolateral sides to give them a direction. Importantly, the Caco-2 assay considers the active removal of compounds by living cells due to the presence of naturally-occurring efflux pumps such as the P-GP efflux pump in the cell membrane. These efflux pumps act in colorectal cells to excrete unwanted compounds from the blood (modeled by the basolateral solution) to the interior of the gut (modelled by the apical solution) for excretion. The basic set-up of the assay can be seen in Figure 2.8.

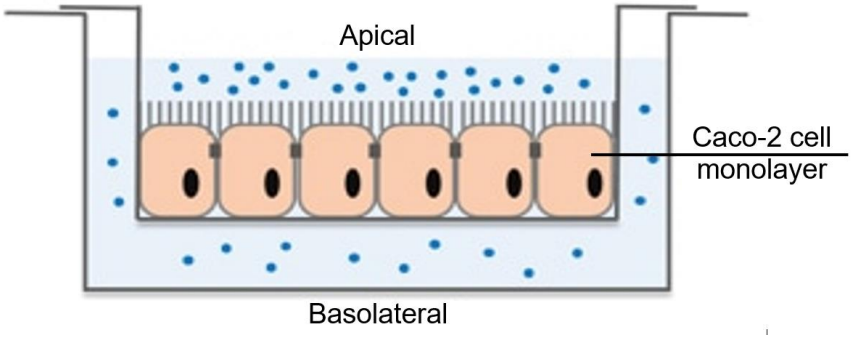

Figure 2.8: Set-up for the Caco-2 assay to assess membrane permeability.

To perform the assay, a solution of the compound of interest is loaded in the apical side. After a set time-period, both apical and basolateral solutions are tested to quantify the amount of compound in each. Molecules that have managed to traverse the polarized cells (Apical (A) → Basolateral (B)) to reach the basolateral side have travelled a set distance through a path similar to that of entering a cell. Based on the time before acquisition, an average rate of travel for the compounds across the cell monolayer can be determined in units of nm/s from the apical (A) to basolateral (B) solutions. This assay can also be performed in the opposite direction (i.e. B → A, indicative of exiting the cell). The ratio between A→ B and B→A permeability rates can be used to determine if active efflux of a compound is occurring. The efflux ratio can be determined according to Formula 1.

$$efflux\ ratio = \frac{B \rightarrow A\ Permeability\ (out)}{A \rightarrow B\ Permeability\ (in)}$$

Formula 1: Calculation for efflux ratio based on the Caco-2 assay results.

In order to expect to see some activity of a compound in living cells, Bayer suggested targeting around 10 nm/s A → B permeability with an efflux ratio <5. Using the Caco-2 assay, several of the key compounds previously synthesized were examined for membrane permeability, with the results shown in Figure 2.9.

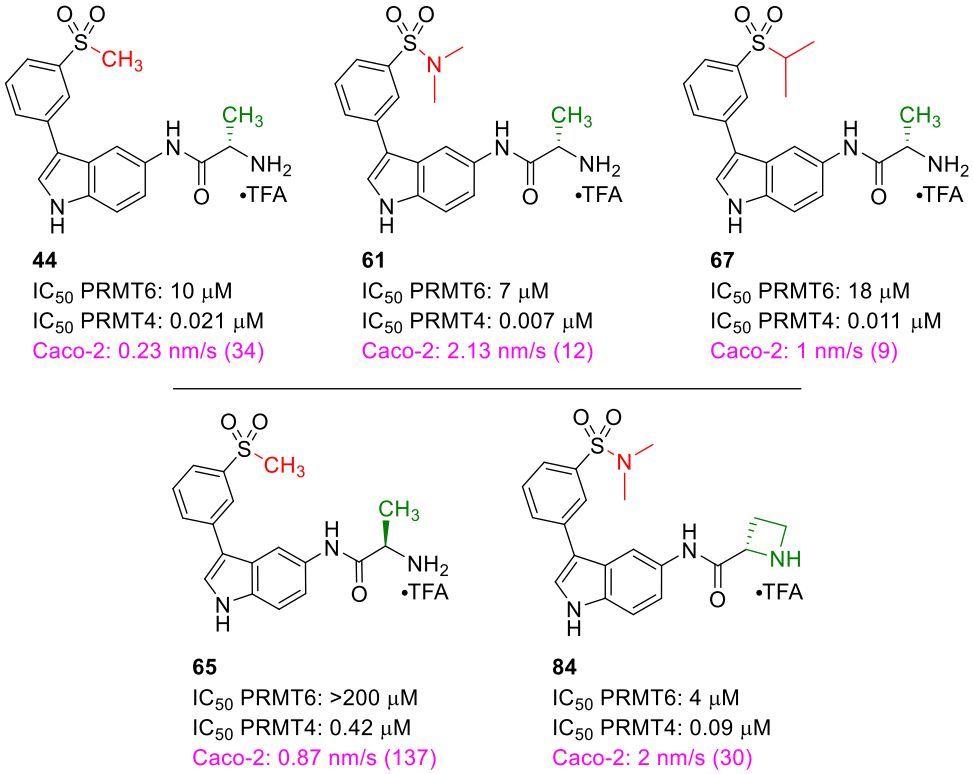

Figure 2.9: Results of Caco-2 data on key compounds. Caco-2 results are expressed as: "Caco-2: [A→ B permeability] nm/s (efflux ratio)"

As can be seen in Figure 2.9, although exchanging *L*-alanine (**44**) for *D*-alanine (**65**) did improve the apical to basolateral permeability, it also drastically increased the level of efflux (efflux ratio increased from 34 for **44** to 137 for **65**). Thus, no subsequent examination of the *D*-alanine analogue was performed, as its incorporation increased efflux.

Excitingly, transitioning from the methyl sulfone **44** to either the dimethyl sulfonamide **61** or the isopropyl sulfone **67** improved membrane permeability. However, the sulfonamide **61** has twice the A → B membrane permeability rate of sulfone **67**, and thus we chose to advance the sulfonamide analogue. Finally, although replacing the alanine moiety (**61**) with the azetidine moiety (**84**) did reduce the number of hydrogen bond donors, it also increased the efflux ratio by nearly a factor of 3 (efflux ratio of 12 for **61** and 30 for **84**). Since introduction of the azetidine moiety decreased potency and membrane permeability while increasing efflux, further analogues bearing this moiety were not targeted.

2.4.6. Further SAR of the Amino Acid Moiety

At this point, the most promising aryl fragment to study was the dimethyl sulfonamide (*e.g.,* **61**) due to its reasonable membrane permeability coupled with good potency and selectivity. We began examining in finer detail the steric limitations on the amino acid moiety. From their corresponding commercially available carboxylic acids and the key intermediate **57**, compounds **93** – **98** were synthesized (Scheme 2.19). Of note is the *D*-alanine derivative **94**, which at this point we knew would not be beneficial for membrane permeability. However, it was synthesized and tested prior to the membrane permeability results, and as such was included to support the observed changes to PRMT4 potency upon stereochemical inversion. The glycine analogue **93** was targeted to examine the effects of reduced bulk, while the *N*-methyl alanine derivative **95** was synthesized to see if the reduction of hydrogen bonding donors on the basic nitrogen could be tolerated in an acyclic system.

Scheme 2.19: Further SAR Development of the Amino Acid Moiety

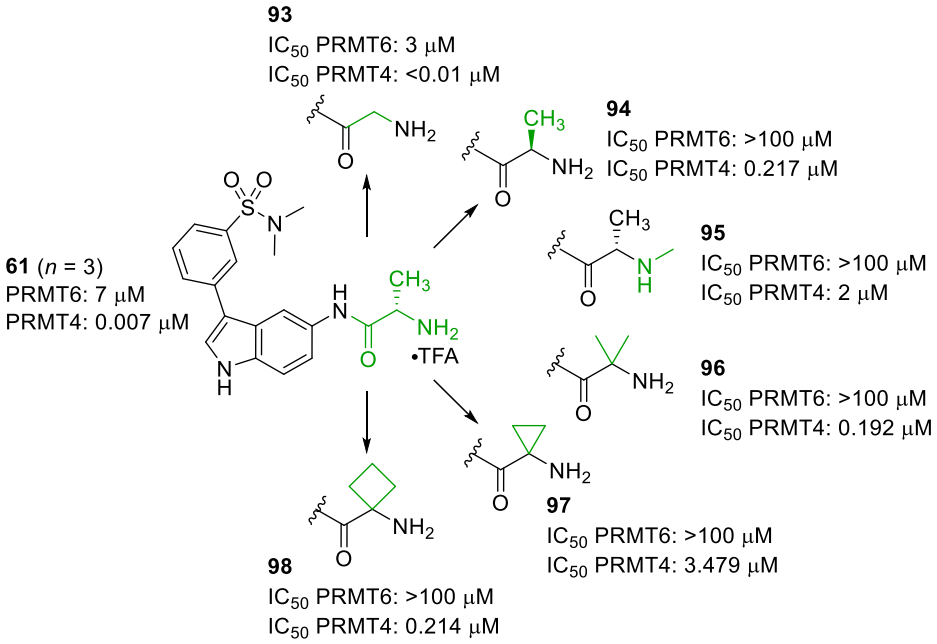

Unfortunately, increasing the size of the alanine's side chain in either a cyclic (**97, 98**) or non-cyclic (**96**) fashion was not tolerated, likely due to steric constraints of the binding pocket. Unfortunately, a similar result was observed when we removed a hydrogen bond donor (**95**), reducing the potency by a factor of >300. As expected, incorporation of the *D*-alanine moiety (**94)** had a detrimental effect on the potency.

Removing the methyl group of the alanine function (i.e. glycine, **93**) retained potency, however, this modification also decreased the selectivity for PRMT4 over PRMT6. In short, none of the changes examined maintained potency whilst improving theoretical membrane permeability as measured by CLogP values.

2.4.7. Modifications to the Substituted Phenyl Ring

With changes to the amino acid moiety providing little in the way of improved potency, selectivity and predicted membrane permeability, we decided to return our attention to the substituted phenyl moiety. Until this point, we had targeted di-substituted benzene moieties. However, the location of the aryl ring in the Bayer crystal structure indicates that it lies near the solvent channel. Thus, modifications to this component may be better tolerated than those made at the amino acid site.

With this in mind, analogues bearing the relatively small methyl and methoxy groups *para* to the indole attachment site of the phenyl ring were investigated. Based on analysis of the crystal structure, we anticipated that a methoxy group in this position would lead to a hydrogen bonding interaction between the methoxy oxygen and a nearby tyrosine residue. To synthesize these pieces, we initially tried to intercept the established route to boronic-ester sulfonamides, as seen in Scheme 2.20. The synthesis of these analogues started with the chlorosulfonation of the corresponding anisole (R = OMe) or toluene (R = Me) derivatives, followed by subsequent amine addition to provide the electron rich aryl bromides **99** and **100** in an analogous fashion to that described previously (Scheme 2.10, first step). However, the Miyaura borylation reactions of the corresponding electron rich aryl-bromides **99** and **100** were unsuccessful, instead providing the corresponding proto-dehalogenated products. Upon examination of the literature, it was determined that electron-rich substrates are often poor substrates in Miyaura borylation reactions.[58]

Instead, electron-rich boronic acids are often prepared via sequential lithium halogen exchange and reaction with trimethylborate followed by an acidic aqueous workup to afford the corresponding boronic acids.[58] This substitution was acceptable, as both boronic esters and acids function well in the subsequent Suzuki-Miyaura coupling to the protected indole core. The second route shown in Scheme 2.20 was successfully performed to provide the key intermediates **101** and **102**.

Scheme 2.20: Synthesis of *para*-Methyl and *para*-Methoxy Key Intermediates 101 and 102

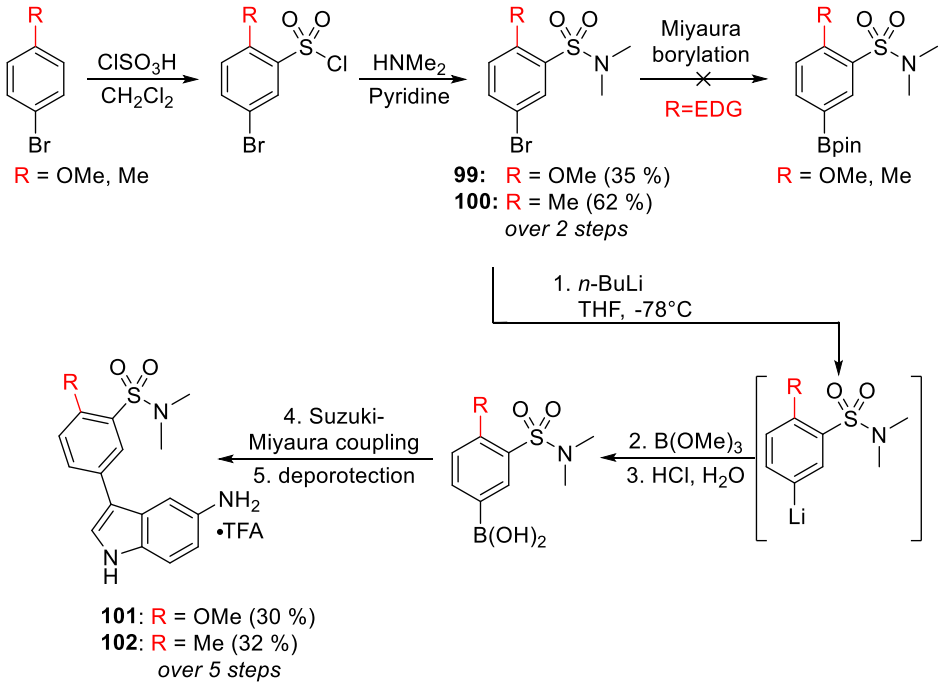

Final amide coupling and deprotection of the key intermediates **101** and **102** provided analogues **103** and **104** shown in Figure 2.10. The *para*-methoxy analogue **103** maintained the potency and selectivity for PRMT4, indicating that the *para*-position of the phenol ring will likely tolerate further derivatization, though the phenolic oxygen may be important in maintaining the potency due to the potential hydrogen bonding interaction.

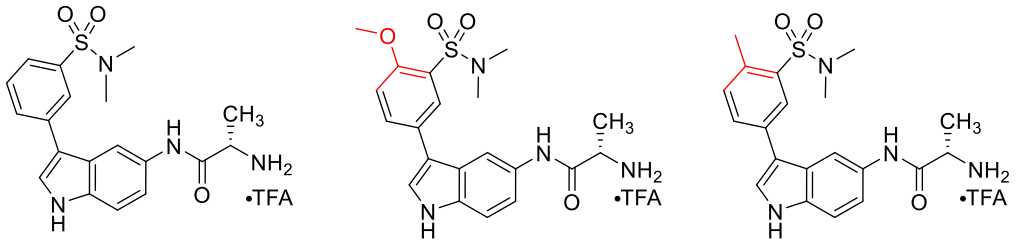

61 (*n* = 3)
IC_{50} PRMT6: 7 μM
IC_{50} PRMT4: 0.007 μM

103
IC_{50} PRMT6: 6 μM
IC_{50} PRMT4: 0.005 μM

104
IC_{50} PRMT6: TBD
IC_{50} PRMT4: TBD

Figure 2.10: Structures and biological data of *para*-methoxy and *para*-methyl analogues.

Although compounds **61** and **103** and have similar cLogP values (**61** = 1.712, **103** = 1.355), we hope that the methoxy derivative may be more membrane permeable, and as such we are waiting on the Caco-2 results to compare. We also anticipate that the *para*-methyl derivative **104** (cLogP = 2.211) may be more permeable than the

methoxy analogue due the absence of the polar oxygen, though it may lack the hydrogen bonding interaction with the nearby tyrosine residue.

2.4.8. Modifications of the Core Component

With a great deal of SAR data being generated for the peripheral components, we felt that data concerning changes to the core was lacking. Until this time, we had focussed solely on indole analogues having a protonated indole nitrogen (N-H). However, this is a hydrogen bond donor and, as such, either removing it or replacing it with a more lipophilic moiety may encourage membrane permeability. To examine the impact that this type of change would have on the potency, selectivity, and membrane permeability of our lead compound, we targeted the *N*-methyl indole and benzofuran analogues seen in Figure 2.11.

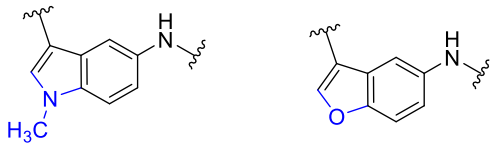

N-methyl indole core benzofuran core

Figure 2.11: Alternate cores to remove indole N-H hydrogen bond donor.

The *N*-methyl indole derivative **105** was synthesized from the intermediate **57** as seen in Scheme 2.21 by Anissa Kaghad. Selective methylation of the indole nitrogen was achieved through phthalate protection of the aniline, followed by deprotonation by sodium hydride and alkylation by methyl iodide. Subsequent deprotection of the phthalate exposed the aniline nitrogen for amide coupling to *N*-Boc-*L*-alanine via a method analogous to the previously synthesized compounds, affording compound **105**. To our delight, the *N*-methyl indole analogue **105** was found to maintain the potency and improve the selectivity compared to the N-H derivative **61**, while removing a hydrogen bond donor. We are currently awaiting the results of the Caco-2 membrane permeability of this compound.

Scheme 2.21: Synthesis of the *N*-methyl Indole Analogue 105 (Performed by Anissa Kaghad)

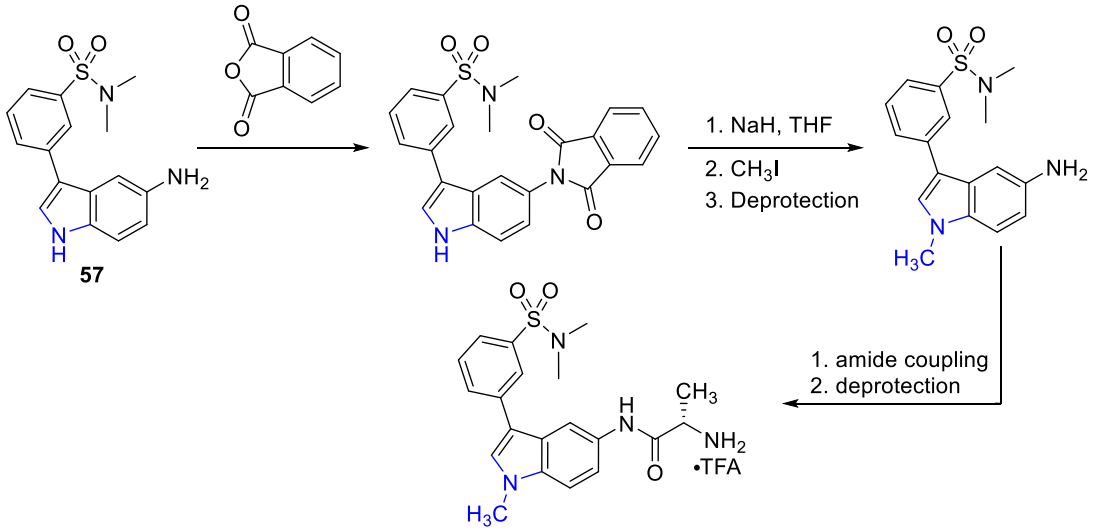

57

105

IC_{50} PRMT6: 44 μM

IC_{50} PRMT4: 0.002 μM

Initially, a synthesis of the benzofuran core was envisioned in a similar fashion to the indole component. Unfortunately, benzofuran, when treated with NBS brominates first at the 2-position.[59,60] Furthermore NBS is not able to brominate the 3-position of benzofuran even when the 2-position is protected of blocked (*vide infra*). However, unsubstituted benzofuran undergoes clean dibromination with Br_2, followed by selective elimination to afford 3-bromobenzofuran **106**, as seen in Scheme 2.22.[61]

Scheme 2.22: Established Method to Synthesize 3-Bromobenzofuran

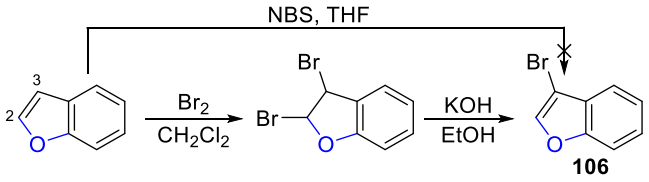

106

With this alternate method of bromination in hand, we were confident that a route initiating with commercially available ethyl 5-nitrobenzofuran-2-carboxylate **107** would be viable, with the necessary reactions to be performed summarized in Scheme 2.23. If the nitro group negatively influenced the bromination, de-carboxylation, or Suzuki-Miyaura coupling, then it could be reduced and protected prior to these steps.

Scheme 2.23: Analysis of the Starting Material 107 for the Synthesis of Benzofuran Analogues

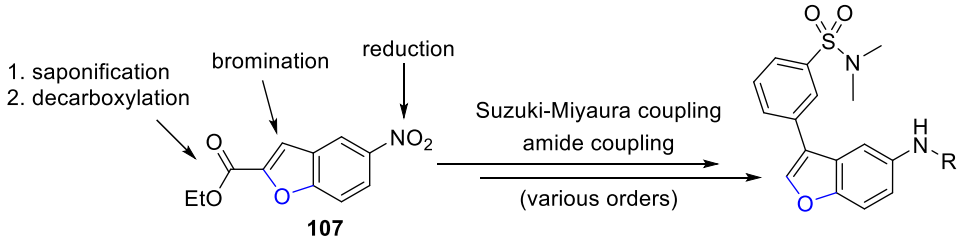

Furthermore, manipulation of the oxidation state of the nitro group would allow the electron density of the heteroaromatic core to be modified at will. Our exploration of different routes to the targeted benzofuran are summarized in Scheme 2.24.

Scheme 2.24: Initial Attempted Routes to Synthesize Benzofuran Analogues (Compounds out of brackets show the desired product of the reaction, while those in brackets show the actual products of the reactions)

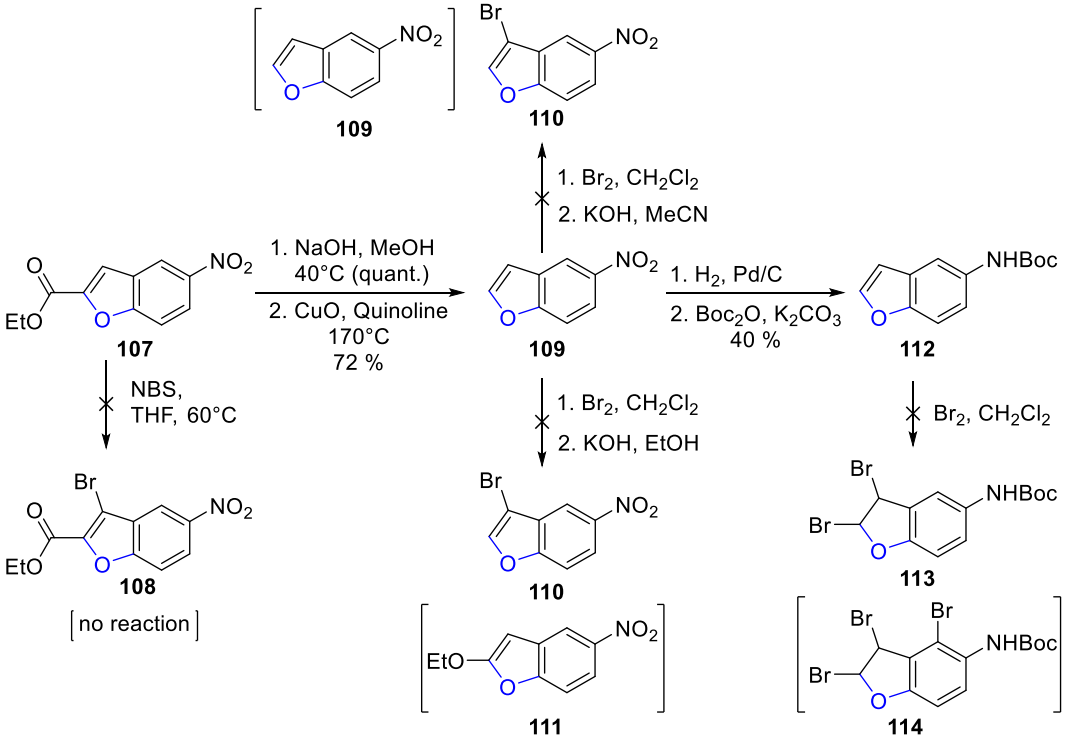

Direct bromination of **107** with NBS to form **108** was unsuccessful. However, saponification of the staring material **107** followed by decarboxylation to yield 5-nitrobenzofuran **109** proceeded smoothly. Unfortunately, different bromination/elimination sequences designed to synthesize **110** (including stepwise sequences not shown) afforded only the 2-ethoxy substituted benzofuran **111** or double

elimination of the intermediate di-bromo compound to regenerate starting material **109**. Hoping to overcome these issues by increasing the electron density in the indole ring, we reduced and protected the nitro group in **109** to afford the *N*-Boc aniline derivative **112**. However, bromination of this compound with elemental bromine to afford the desired di-bromo heterocycle **113** was unsuccessful, instead generating a tri-brominated species (based on HRMS analysis) whose structure is considered to be compound **114**.

Frustrated with this synthetic sequence, we envisioned alternate routes to synthesize the benzofuran. For example, it has been shown that α-phenol ketones (*e.g.,* **115**, Scheme 2.25) can be converted into the corresponding benzofuran analogues (*e.g.,* **116**) through dehydrative cyclization promoted by the Lewis acid boron trichloride.[62] This reaction has been shown to work particularly well on *para*-EDG phenols such as the *para*-methoxy derivative.

Scheme 2.25: Proposed BCl_3 Mediated Synthesis of Benzofuran Core

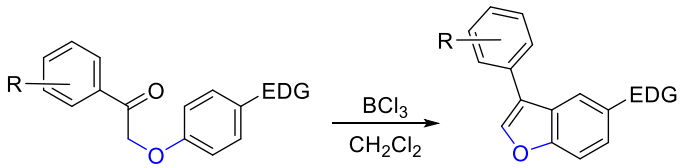

104 **105**

Since our compound would require an *N*-Boc protected aniline in the position of the electron donating group (EDG), we were hopeful that this reaction would work for our substrate. To this end, we started the synthesis of the cyclization precursor from commercially available 3-bromo-*N,N*-dimethylbenzenesulfonamide **117**. Sequential lithium-halogen exchange of aryl-bromide **117** and addition into the corresponding Weinreb amide **118** afforded the substituted acetophenone **119**. The acetophenone **119** was brominated with elemental bromine in acetic acid with close tracking by TLC and NMR to selectively afford the *mono*-brominated compound **120**. Nucleophilic substitution of the installed bromine atom by the *N*-Boc-aminophenol afforded the cyclization precursor **121** in a 4-step, 3-pot sequence.

The cyclization of the precursor **121** was then attempted using boron trichloride (BCl_3) to activate the ketone, in hopes that this reaction would enable a subsequent deprotection, amide coupling, and further deprotection to furnish the benzofuran analogues (*e.g.,* **122**) as seen in Scheme 2.26 (dashed line). Unfortunately, BCl_3 proved

incompatible with the Boc protecting group. Upon addition of BCl_3 (at -78 °C), a major product other than the desired benzofuran was formed. Upon closer examination, we began to suspect that the Boc-group had been cleaved (observed by ^{1}H-NMR and HRMS analysis), and a dimer (possibly in the form of compound **123** shown in Scheme 2.26) formed. We were disappointed that the boron trichloride promoted dehydrative cyclization was not successful on our substrate. To avoid the dimerization in the future, the reaction could be performed under more dilute conditions. Additionally, the use of weaker Lewis acids or an alternative and orthogonal protecting group on the aniline could still afford the desired benzofuran derivatives.

Scheme 2.26: Attempted BCl_3 Promoted Cyclization Route to Benzofuran Analogues

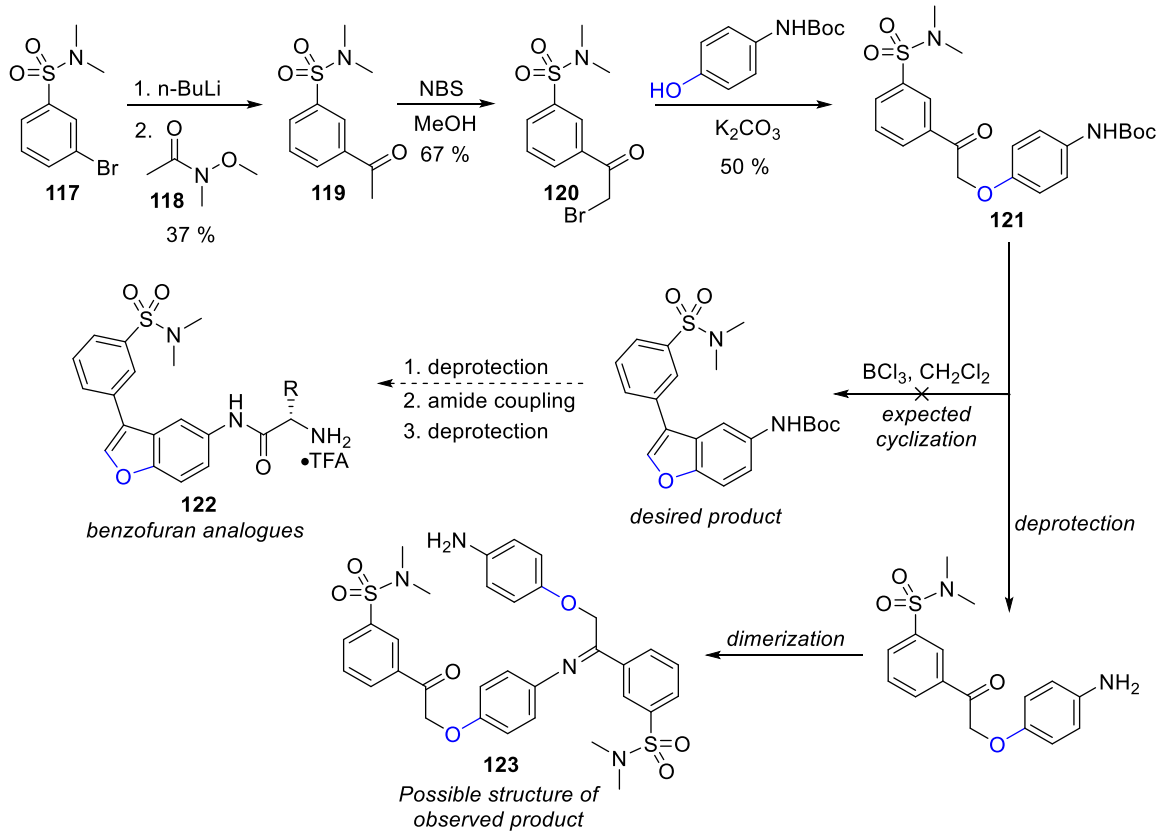

2.4.9. Summary

In collaboration with the SGC and Bayer, we have developed a potent and selective small molecule inhibitor against the epigenetic target PRMT4. A large amount

of SAR has been realized and is summarized in Figure 2.12, displayed on the most potent analogue synthesized to date.

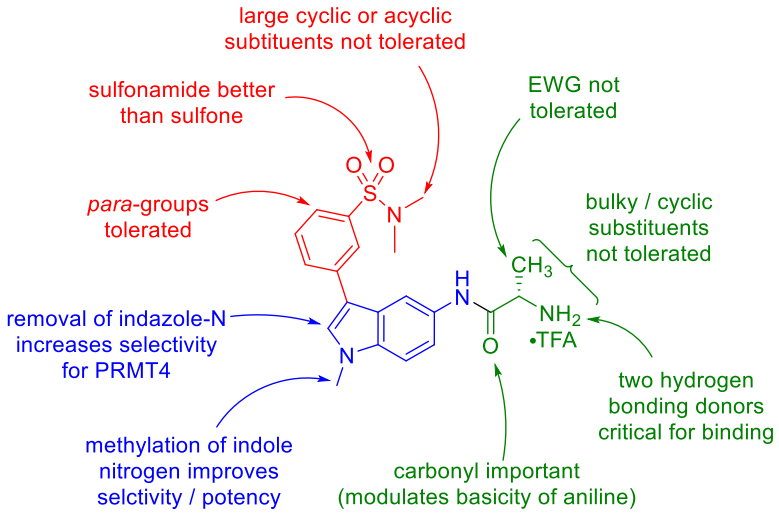

Figure 2.12: Current understanding of SAR for the PRMT4 selective probe.

Improvement of the probes' potency against PRMT4 from IC_{50} = 0.021 μM (**44**) to IC_{50} = 0.002 μM (**105**) was accomplished through the modifications seen in Scheme 2.27. The selectivity (against the structurally most similar isoform PRMT6) was also improved from *ca* 500-fold (**44**) to >20,000-fold (**105**). Though still not active in cells, the membrane permeability was improved from 0.23 nm/s with an efflux ratio of 34 (**44**) to 2.13 nm/s with an efflux ratio of 12 (**61**), as measured by the Caco-2 assay.

Scheme 2.27: Potency, Selectivity, and Membrane Permeability Improvements of the PRMT4 Selective Probe Accomplished Through our Medicinal Chemistry Efforts

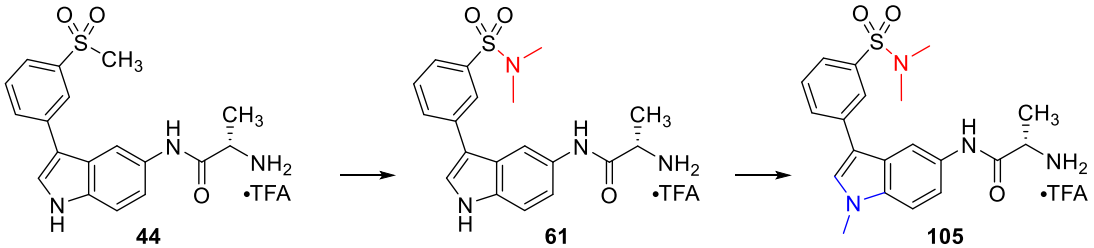

44
IC_{50} PRMT6: 10 μM
IC_{50} PRMT4: 0.021 μM
Caco-2: 0.23 nm/s (34)

61
IC_{50} PRMT6: 7 μM
IC_{50} PRMT4: 0.007 μM
Caco-2: 2.13 nm/s (12)

105
IC_{50} PRMT6: 44 μM
IC_{50} PRMT4: 0.002 μM
Caco-2: TBD

In the future, further analogues centered around the *N*-methyl indole or benzofuran cores should be synthesized to examine if these changes are enough to enable *in vivo* effects of the PRMT4 selective inhibitor, measured by the Caco-2 assay.

Furthermore, compounds bearing the *para*-methoxy phenyl ring seen in **103**, as well as more lipophilic esters should be targeted as this site appears amenable to derivatization. Continued modification of the current lead compound will likely provide a cell-active PRMT4 selective probe that can be used by biologists to help discern the role of PRMT4 in cancer cells, as well as whether PRMT4 is a viable therapeutic target.

2.5. Experimental Information

2.5.1. General Considerations

Flash chromatography was carried out with Geduran® Si60 silica gel (Merck). Concentration and removal of trace solvents was done using a Büchi rotary evaporator equipped with a dry ice/acetone condenser, and vacuum applied from an aspirator or Büchi V-500 pump. All reagents and starting materials were purchased from Sigma Aldrich, Alfa Aesar, TCI America, Carbosynth, and/or Strem, and were used without further purification. All solvents were purchased from Sigma Aldrich, EMD, Anachemia, Caledon, Fisher, or ACP and used without further purification, unless otherwise specified. Nuclear magnetic resonance (NMR) spectra were recorded using acetonitrile-d_3 (CD_3CN), chloroform-*d* ($CDCl_3$), methanol-d_4 (CD_3OD), dimethylsulfoxide-d_6, or D_2O. Signal positions (δ) are given in parts per million from tetramethylsilane (δ = 0) and were measured relative to the signal of the solvent (^{1}H NMR: CD_3CN: δ = 1.94, $CDCl_3$: δ = 7.26, CD_3OD: δ = 3.31, DMSO-d_6: δ = 2.50, D_2O: δ = 4.78; ^{13}C NMR: CD_3CN: δ = 118.26, $CDCl_3$: δ = 77.16, CD_3OD: δ = 49.00, DMSO-d_6: δ = 36.52). Coupling constants (*J* values) are given in Hertz (Hz) and are reported to the nearest 0.1 Hz. ^{1}H NMR spectral data are tabulated in the order: multiplicity (s, singlet; d, doublet; t, triplet; q, quartet; quint, quintet; m, multiplet), coupling constants (Hz), number of protons. NMR spectra were recorded on a Bruker Avance 600 equipped with a QNP or TCI cryoprobe (600 MHz), Bruker 500 (500 MHz), or Bruker 400 (400 MHz). Assignments of ^{1}H and ^{13}C NMR spectra and the connectivity of products are based on analysis of ^{1}H^{1}H COSY, HSQC, HMBC, and NOESY spectra, where applicable. High resolution mass spectra were measured on an Agilent 6210 TOF LC/MS using ESI-MS. Preparative RP-HPLC was performed on an Agilent 1200 series instrument with a SiliCycle SiliaChrom dtC18 semipreparative column (5 µm, 100Å, 10 x 250 mm) with a flow rate of 5 mL/min eluting with solvent (A: 0.1 % TFA in H_2O B: 0.1 % TFA in ACN) on gradients of (0 → 5) %, (2

→ 30) %, (2 → 50) %, or (2 → 100) %) solvent B over 15 minutes as indicated, equipped with a variable UV-Vis wavelength detector. Infrared spectra were recorded neat on a Perkin-Elmer Spectrum Two FTIR ATR spectrometer. Only selected wavenumbers are provided for each compound. Optical rotations were measured on a Perkin-Elmer Polarimeter 341 at 589 nm at 20°C.

2.5.2. General Procedures

General Procedure A: Suzuki-Miyaura Coupling of Aryl-Boronic Acids or Esters to Indole Moiety and Their Subsequent Deprotection

A pressure vial was charged with a stir bar, *bis*-protected bromo-indole **28** (1.0 equiv.), boronic acid or ester (1.0 – 1.6 equiv.), K_2CO_3 (3.0 equiv.), and $Pd(PPh_3)_4$ or $Pd(dppf)Cl_2•CH_2Cl_2$ (0.10 equiv.). The reaction vessel was immediately sealed and placed under vacuum and the vacuum broken with nitrogen. The vacuum – nitrogen purging procedure was repeated twice. A mixture of degassed THF and H_2O (0.09 M THF:H_2O 3:1 unless otherwise indicated based on the *bis*-protected bromo-indole) was added, and the mixture stirred under an atmosphere of nitrogen at 80˚C for 18 hours or until consumption of the starting material was observed by TLC analysis. The reaction mixture was then cooled to room temperature and concentrated under reduced pressure. The residue was then dissolved in EtOAc and washed with saturated aqueous $NaHCO_3$ and brine. The organic layer was then dried with $MgSO_4$ and concentrated to afford the crude aryl-indole product. Purification of the crude product by flash chromatography (silica gel, Et_2O or EtOAc and hexanes) afforded the pure coupled product. The protected aryl-indole product was then dissolved in TFA (neat, 0.1 M) and stirred at room temperature until completion of the deprotection as monitored by TLC. Concentration of the reaction mixture under reduced pressure afforded the deprotected aryl-indole product which was used without further purification unless otherwise indicated.

General Procedure B: Amide Coupling and Deprotection to Provide the Final Compounds

To a stirred room temperature solution of phenyl-indole intermediate (1.0 equiv.) in dry dimethylformamide (DMF) (0.1 M) was added *N,N*-diisopropylethylamine (DIPEA)

(5 equiv.) followed by benzotriazol-1-yl-oxytripyrrolidinophosphonium hexafluorophosphate (PyBOP) (1-2 equiv.) and acid moiety (1-2 equiv.). The resultant solution was stirred at room temperature until completion of the reaction as monitored by TLC. The reaction mixture was then diluted with saturated aqueous $NaHCO_3$ and extracted with EtOAc (3 times). The combined organic layers were washed with aqueous saturated LiCl (3 times), dried with $MgSO_4$, and concentrated to afford the crude coupled product (brown gum), which was used directly in the next step without further purification. The crude coupled product was dissolved in TFA (neat, 0.1 M) and stirred at room temperature until completion as monitored by TLC. Purification of the crude deprotected indole product by RP-HPLC (using a SiliCycle SiliaChrom dtC18 semipreparative column (5 µm, 100Å, 10 x 250 mm) with a flow rate of 5 mL/min eluting with solvent (A: 0.1 % TFA in H_2O B: 0.1 % TFA in ACN) on gradients of (2 → 30) %, or (2 → 100) %) solvent B over 15 minutes as indicated afforded the final compound.

General Procedure C: Synthesis of Sulfonamides from Sulfonyl Chlorides

To a stirred solution of amine (1.05 equiv.) in dry pyridine (0.2 M) at 0°C was added dropwise (liquids) or in small portions (solids) a sulfonyl chloride (1.0 equiv.). The reaction mixture was warmed to room temperature and stirred until completion as monitored by TLC. The reaction mixture was first concentrated under reduced pressure and then dissolved in EtOAc and washed with 0.5 M HCl (2 times). The organic layer was then dried with $MgSO_4$, filtered, and concentrated to afford the sulfonamide. The sulfonamide was used in subsequent reactions without further purification.

General Procedure D: Miyaura Borylation to Install the Boronic Ester

A vial or RBF was charged with a stir bar, aryl bromide (1.0 equiv.), B_2Pin_2 (1.0 equiv.), $NaHCO_3$ (2.50 equiv.), and $Pd(dppf)Cl_2$ (0.05 equiv.). The reaction vessel was immediately sealed and placed under vacuum and the vacuum broken with nitrogen. The vacuum – nitrogen degassing procedure was repeated twice. Degassed DMSO (0.2 M) was added to the reaction vessel via syringe, and the reaction mixture was stirred under an atmosphere of nitrogen at 80˚C for 18 hours or until consumption of starting material was observed by TLC. The reaction mixture was then cooled to room temperature and diluted with equal parts H_2O and EtOAc and then filtered through Celite to remove insoluble by-products. The Celite pad was rinsed with EtOAc and pulled dry.

The filtrate was then washed with H_2O and brine, dried with $MgSO_4$, and concentrated to afford the crude product. Purification of the crude material by flash chromatography (silica gel, Et_2O or EtOAc and hexanes) afforded the aryl-boronic ester.

General Procedure E: Synthesis of Sulfones from Thiophenol Precursors

A stirred solution of substituted thiophenol (1 equiv.), K_2CO_3 (1.4 equiv.), and secondary bromoalkane (1.2 equiv.) in dry acetone (0.3 M), was stirred under nitrogen at reflux until completion of the reaction as monitored by TLC (*ca.* 18 hours). The reaction mixture was cooled to room temperature, diluted with H_2O, and extracted with Et_2O (3 times). The combined organic layers were washed with brine, dried with $MgSO_4$, and concentrated to afford the crude aryl thioether intermediate. To a stirred solution of the crude aryl thioether intermediate (1.0 equiv.) in MeOH (0.16 M) at 0°C was added oxone (potassium peroxymonosulfate) (3.0 equiv.) in H_2O (0.5 M). The resulting white suspension was warmed to room temperature over 2 hours and stirred at room temperature until completion as monitored by TLC. The reaction mixture was then diluted with H_2O, and extracted with EtOAc (2 times). The combined organic layers were washed with brine, dried with $MgSO_4$, and concentrated to afford the aryl sulfone. The aryl sulfone was used in subsequent reactions without further purification.

2.5.3. Preparation and Characterization Data

*NMR spectra for all compounds from Chapter 2 can be found in Appendix A.

Preparation of Indole Analogue **26**

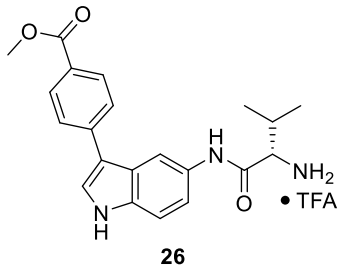

26

The title compound was resynthesized for characterization according to general procedure B using the aryl-indole moiety **41** (40 mg, 0.11 mmol), (*tert*-butoxycarbonyl)-*L*-valine (24 mg, 0.11 mmol), PyBOP (60 mg, 0.12 mmol), DIPEA (0.093 mL, 0.53 mmol),

and dry DMF (1.05 mL). Purification by RP-HPLC (using a SiliCycle SiliaChrom dtC18 semipreparative column (5 µm, 100Å, 10 x 250 mm) with a flow rate of 5 mL/min eluting with solvent (A: 0.1 % TFA in water B: 0.1 % TFA in MeCN) on a gradient of (2 → 100) %) solvent B over 15 minutes, t_R = 6.76 min) of the crude deprotected product afforded the TFA salt **26** as a colorless solid (8 mg, 16%). **^{1}H NMR**: (500 MHz, CD_3OD) δ (ppm) = 8.24 (d, *J* = 2.0 Hz, 1H), 8.06 (d, *J* = 8.4 Hz, 2H), 7.79 (d, *J* = 8.4 Hz, 2H), 7.67 (s, 1H), 7.45 (d, *J* = 8.7 Hz, 1H), 7.34 (dd, *J* = 8.7, 2.0 Hz, 1H), 3.92 (s, 3H), 3.80 (dd, *J* = 6.2, 2.0 Hz, 1H), 2.32 (dqq, *J* = 7.0, 6.8, 6.8 Hz, 1H), 1.16 (d, *J* = 7.0 Hz, 3H), 1.14 (d, *J* = 7.0 Hz, 3H). **^{13}C NMR**: (125 MHz, CD_3OD) δ (ppm) = 168.7, 167.7, 142.7, 136.4, 131.7, 131.1, 127.9, 127.4, 126.5, 126.3, 117.3, 117.2, 113.2, 112.6, 60.6, 52.5, 31.8, 19.0, 18.1. **$[\alpha]_D^{20}$**: +32.4 (c = 8.7 mg/mL, MeOH). **HRMS**: (ESI) *m/z* calculated for $C_{21}H_{23}N_3O_3$ $[M+H]^+$ 366.1812, found 366.1814. **IR (neat):** υ = 3668, 3259, 2975, 1668, 1606, 1435, 1179, 1125 cm^{-1}. **MP**: 143 – 147°C.

Preparation of Protected and Brominated Indole Moiety **28**

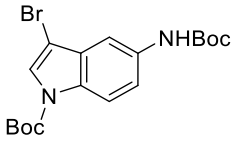

28

To a stirred solution of *bis*-protected indole moiety **30** (1.515 g, 4.56 mmol, 1.0 equiv.) in THF (13.4 mL, 0.34 M) was added NBS (852 mg, 4.79 mmol, 1.05 equiv.). The reaction vessel was wrapped in foil to exclude light and stirred at room temperature for 18 hours, after which it was concentrated under reduced pressure. The reaction residue was then dissolved in Et_2O and filtered to remove the white precipitate (succinimide) which remained. The filtrate was washed with saturated aqueous sodium metabisulfite, saturated aqueous $NaHCO_3$, water, brine, dried with $MgSO_4$, filtered, and concentrated under reduced pressure to afford pure brominated indole moiety **28** (1.456 g, 77 %). **^{1}H NMR**: (500 MHz, $CDCl_3$) δ (ppm) = 8.03 (s, 1H), 7.64 (s, 1H), 7.61 (s, 1H), 7.25 (d, *J* = 8.0 Hz, 1H), 6.60 (s, 1H), 1.65 (s, 9H), 1.54 (s, 9H). **^{13}C NMR**: (125 MHz, $CDCl_3$) δ (ppm) = 153.1, 148.9, 134.5, 131.0, 130.1, 125.6, 117.5, 115.7, 109.2, 98.0, 84.4, 80.7, 28.5, 28.3. **HRMS**: (ESI) *m/z* calculated for $C_{18}H_{23}N_2O_4Br$ $[M+NH_4]^+$ 428.1179, found 428.1204. **IR** (neat): υ = 3330, 2979, 1935, 1693, 1549, 1465, 1362, 1300, 1242, 1150, 1058, 863, 763 cm^{-1}. **MP**: 129 – 132°C.

Preparation of Key Intermediate **29**

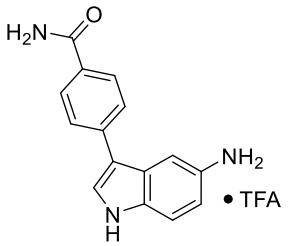

29

The title compound was prepared according to general procedure A using *bis*-protected bromo-indole **28** (454 mg, 1.10 mmol), *para*-carbamoylphenyl-boronic acid (291 mg, 1.76 mmol), K_2CO_3 (457 mg, 3.31 mmol), $Pd(dppf)Cl_2 \bullet CH_2Cl_2$ (90 mg, 0.11 mmol), degassed THF/water (3:1, 20 mL, 0.056 M). Purification by column chromatography afforded the protected coupled product, which was subsequently deprotected in TFA (11 mL) and concentrated under reduced pressure to afford the TFA salt **29** as a brown solid (231 mg, 55%). **^{1}H NMR**: (500 MHz, CD_3OD) δ (ppm) = 7.98 (d, *J* = 8.4 Hz, 2H), 7.92 (d, *J* = 2.1 Hz, 1H), 7.80 – 7.74 (m, 3H), 7.61 (d, *J* = 8.6 Hz, 1H), 7.19 (dd, *J* = 8.6, 2.1 Hz, 1H). **^{13}C NMR**: (125 MHz, CD_3OD) δ (ppm) = 172.2, 140.5, 138.2, 132.0, 129.4, 127.7, 127.3, 127.0, 124.5, 117.6, 117.2, 114.43, 114.39. **HRMS**: (ESI) *m/z* calculated for $C_{15}H_{13}N_3O$ $[M+H]^+$ 252.1131, found 252.1144. **IR (neat):** υ = 2901, 2600, 1724, 1692, 1667, 1435, 1140, 1045, 694 cm^{-1}. **MP**: 189 – 193°C.

Preparation of *Bis*-Protected 5-Aminoindole **30**

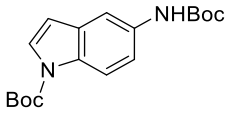

30

To a stirred brown slurry of 5-aminoindole (1.00 g, 7.56 mmol, 1.0 equiv.) in THF (38 mL, 0.2 M) was added triethylamine (1.05 mL, 7.56 mmol, 1.0 equiv.), Boc_2O (3.30 g, 15.1 mmol, 2.0 equiv.), and DMAP (1.39 g, 11.3 mmol, 1.5 equiv.). The resulting slurry was stirred at room temperature under a nitrogen atmosphere (not sealed) for 2 days. The reaction mixture was diluted with *ca.* 60 mL of 1.0 M aqueous HCl and extracted with EtOAc (2 times). The combined organic layers were dried with $MgSO_4$ and concentrated under reduced pressure to afford the crude *bis*-protected aminoindole species. Purification of the crude product (silica gel, Et_2O:Hexanes 1:9) provided the *bis*-

protected aminoindole **30** contaminated with (1.296 g, 52 %). **^{1}H NMR**: (400 MHz, $CDCl_3$) δ (ppm) = 8.02 (d, *J* = 8.8 Hz, 1H), 7.74 (s, 1H), 7.56 (d, *J* = 3.7 Hz, 1H), 7.13 (d, *J* = 9.0 Hz, 1H), 6.65 – 6.54 (m, 1H), 6.49 (d, *J* = 3.6 Hz, 1H), 1.66 (s, 9H), 1.53 (s, 9H). **^{13}C NMR**: (100 MHz, $CDCl_3$) δ (ppm) = 153.3, 149.8, 133.7, 131.6, 131.2, 126.7, 116.4, 115.4, 110.9, 107.5, 83.7, 80.4, 28.5, 28.3. **HRMS**: (ESI) *m/z* calculated for $C_{18}H_{24}N_2O_4$ $[2M+H]^+$ 655.3545, found 655.3574. **IR** (neat): υ = 3677, 3402, 2978, 1709, 1595, 1525, 1474, 1379, 1346, 1291, 1229, 1149, 1132, 1081, 1049, 1024, 764 cm^{-1}. **MP**: 118 – 132°C.

Preparation of Indole Analogue **33**

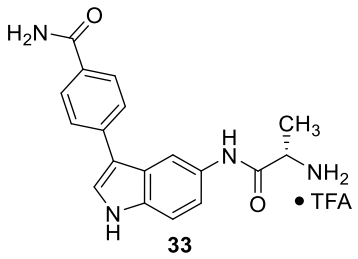

33

The title compound was prepared according to general procedure B using the aryl-indole moiety **29** (25 mg, 0.068 mmol), (*tert*-butoxycarbonyl)-*L*-alanine (17 mg, 0.072 mmol), PyBOP (43 mg, 0.082 mmol), DIPEA (0.06 mL, 0.34 mmol), and dry DMF (0.68 mL). Purification by RP-HPLC (using a SiliCycle SiliaChrom dtC18 semipreparative column (5 µm, 100Å, 10 x 250 mm) with a flow rate of 5 mL/min eluting with solvent (A: 0.1 % TFA in water B: 0.1 % TFA in MeCN) on a gradient of (2 → 100) %) solvent B over 15 min, t_R = 4.52 min) of the crude deprotected product afforded the TFA salt **33** as a colorless solid (9 mg, 32%). **^{1}H NMR**: (500 MHz, CD_3OD) δ (ppm) = 8.23 (d, *J* = 1.7 Hz, 1H), 7.94 (d, *J* = 8.5 Hz, 2H), 7.77 (d, *J* = 8.5 Hz, 2H), 7.64 (s, 1H), 7.43 (d, *J* = 8.7 Hz, 1H), 7.32 (dd, *J* = 8.7, 1.7 Hz, 1H), 4.09 (q, *J* = 7.1 Hz, 1H), 1.64 (d, *J* = 7.1 Hz, 3H). **^{13}C NMR**: (125 MHz, CD_3OD) δ (ppm) = 172.4, 169.0, 141.4, 136.3, 131.8, 131.4, 129.3, 127.5, 126.6, 126.0, 117.3, 117.2, 113.1, 112.5, 50.9, 17.7. **$[\alpha]_D^{20}$**: +3.6 (c = 4.6 mg/mL, MeOH). **HRMS**: (ESI) *m/z* calculated for $C_{18}H_{18}N_4O_2$ $[M+H]^+$ 323.1503, found 323.1477. **IR (neat):** υ = 3681, 3246, 2984, 1667, 1607, 1539, 1201, 1133 cm^{-1}. **MP**: 134 – 139°C.

Preparation of Indole Analogue **37**

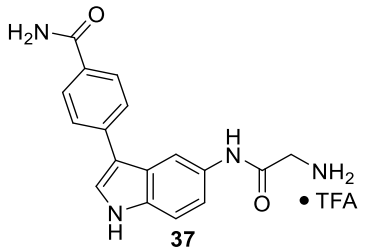

37

The title compound was prepared according to general procedure B using the aryl-indole moiety **29** (23.6 mg, 0.065 mmol), (*tert*-butoxycarbonyl)glycine (22.6 mg, 0.13 mmol), PyBOP (67 mg, 0.13 mmol), DIPEA (0.062 mL, 0.32 mmol), and dry DMF (0.65 mL). RP-HPLC (gradient: 2-100 shortprep, t_R = 5.02 min) of the crude deprotected product afforded the TFA salt **37** as a colorless solid (5 mg, 17%). **^{1}H NMR**: (500 MHz, CD_3OD) δ (ppm) = 8.23 (d, *J* = 2.0 Hz, 1H), 7.94 (d, *J* = 8.4 Hz, 2H), 7.77 (d, *J* = 8.4 Hz, 2H), 7.64 (s, 1H), 7.43 (d, *J* = 8.7 Hz, 1H), 7.31 (dd, *J* = 8.7, 2.0 Hz, 1H), 3.88 (s, 2H). **^{13}C NMR**: (125 MHz, CD_3OD) δ (ppm) = 172.4, 165.2, 141.4, 136.3, 131.9, 131.4, 129.2, 127.5, 126.6, 125.9, 117.3, 117.1, 113.1, 112.3, 42.1. **HRMS**: (ESI) *m/z* calculated for $C_{17}H_{16}N_4O_2$ $[M+H]^+$ 309.1320, found 309.1340. **IR (neat):** υ = 3675, 3241, 2988, 1667, 1606, 1542, 1394, 1201, 1289 cm^{-1}. **MP**: 132 – 139°C.

Preparation of Indole Analogue **38**

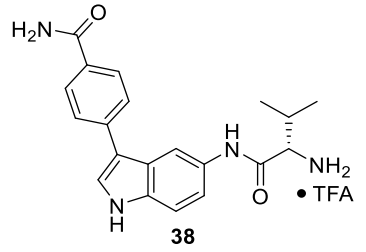

38

The title compound was prepared according to general procedure B using the aryl-indole moiety **29** (19.2 mg, 0.053 mmol), (*tert*-butoxycarbonyl)-*L*-valine (22.8 mg, 0.11 mmol), PyBOP (54.7 mg, 0.11 mmol), DIPEA (0.046 mL, 0.26 mmol), and dry DMF (0.53 mL). Purification by RP-HPLC (using a SiliCycle SiliaChrom dtC18 semipreparative column (5 µm, 100Å, 10 x 250 mm) with a flow rate of 5 mL/min eluting with solvent (A: 0.1 % TFA in water B: 0.1 % TFA in MeCN) on a gradient of (2 → 100) %) solvent B over 15 min, t_R = 5.55 min) of the crude deprotected product afforded the TFA salt **38** as

a colorless solid (4 mg, 17%). **^{1}H NMR**: (500 MHz, CD_3OD) δ (ppm) = 8.23 (d, *J* = 2.0, 1H), 7.94 (d, *J* = 8.5 Hz, 2H), 7.77 (d, *J* = 8.5 Hz, 2H), 7.65 (s, 1H), 7.45 (d, *J* = 8.7, Hz, 1H), 7.33 (dd, *J* = 8.7, 2.0 Hz, 1H), 3.79 (d, *J* = 6.2 Hz, 1H), 2.32 (dqq, *J* = 6.9, 6.2, 6.2 Hz, 1H), 1.16 (d, *J* = 6.9 Hz, 3H), 1.14 (d, *J* = 6.9 Hz, 3H). **^{13}C NMR**: (125 MHz, CD_3OD) δ (ppm) = 172.3, 167.7, 141.4, 136.4, 131.6, 131.5, 129.3, 127.5, 126.6, 126.0, 117.3, 117.2, 113.1, 112.6, 60.6, 31.9, 19.1, 18.1. **$[\alpha]_D^{20}$**: +45.7 (c = 4.1 mg/mL, MeOH). **HRMS**: (ESI) *m/z* calculated for $C_{20}H_{22}N_4O_2$ $[M+H]^+$ 351.1816, found 351.1837. **IR (neat):** υ = 3670, 3232, 2973, 1688, 1607, 1607, 1209, 1139 cm^{-1}. **MP**: 143 – 153°C.

Preparation of Indole Analogue **39**

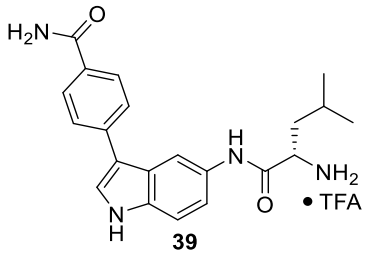

39

The title compound was prepared according to general procedure D using the aryl-indole moiety **29** (20 mg, 0.055 mmol), (*tert*-butoxycarbonyl)-*L*-leucine (24 mg, 0.11 mmol), PyBOP (57 mg, 0.11 mmol), DIPEA (0.048 mL, 0.27 mmol), and dry DMF (0.54 mL). Purification by RP-HPLC (using a SiliCycle SiliaChrom dtC18 semipreparative column (5 µm, 100Å, 10 x 250 mm) with a flow rate of 5 mL/min eluting with solvent (A: 0.1 % TFA in water B: 0.1 % TFA in MeCN) on a gradient of (2 → 100) %) solvent B over 15 min, t_R = 5.88 min) of the crude deprotected product afforded the TFA salt **39** as a colorless solid (5 mg, 19%). **^{1}H NMR**: (500 MHz, CD_3OD) δ (ppm) = 8.23 (d, *J* = 2.0 Hz, 1H), 7.94 (d, *J* = 8.4 Hz, 2H), 7.77 (d, *J* = 8.4, Hz, 2H), 7.64 (d, *J* = 2.9 Hz, 1H), 7.44 (d, *J* = 8.7 Hz, 1H), 7.34 (dd, *J* = 8.7, 2.0 Hz, 1H), 4.07 – 4.01 (m, 1H), 1.94 – 1.74 (m, 3H), 1.07 (d, *J* = 5.8 Hz, 3H), 1.06 (d, *J* = 5.8 Hz, 3H). **^{13}C NMR**: (125 MHz, CD_3OD) δ (ppm) = 172.4, 168.8, 141.4, 136.4, 131.7, 131.4, 129.3, 127.5, 126.6, 126.0, 117.3, 117.3, 113.1, 112.7, 53.8, 41.9, 25.6, 23.2, 22.2. **$[\alpha]_D^{20}$**: +21.2 (c = 1.1 mg/mL, MeOH). **HRMS**: (ESI) *m/z* calculated for $C_{21}H_{24}N_4O_2$ $[M+H]^+$ 365.1972, found 365.1946. **IR (neat):** υ = 3232, 3067, 1963, 1661, 1608, 1480, 1201, 1182, 1135 cm^{-1}. **MP**: 156 – 160°C.

Preparation of Key Intermediate **41**

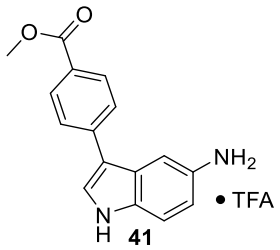

41

The title compound was prepared according to general procedure A using *bis*-protected bromo-indole **28** (152 mg, 0.37 mmol), methyl 4-(4,4,5,5-tetramethyl-1,3,2-dioxaborolan-2-yl)benzoate (99 mg, 0.37 mmol), K_2CO_3 (153 mg, 1.1 mmol), $Pd(dppf)Cl_2 \bullet CH_2Cl_2$ (30 mg, 0.037 mmol), degassed THF/water (3:1, 8.6 mL, 0.056 M). Purification by column chromatography afforded the protected coupled product, which was subsequently deprotected in TFA (4 mL) and concentrated under reduced pressure to afford the TFA salt **41** as a purple solid (40.4 mg, 29%). **^{1}H NMR**: (600 MHz, CD_3OD) δ (ppm) = 8.10 (d, *J* = 8.0 Hz, 2H), 7.91 (s, 1H), 7.82 – 7.78 (m, 3H), 7.60 (d, *J* = 8.6 Hz, 1H), 7.18 (dd, *J* = 8.6, 1.9 Hz, 1H), 3.93 (s, 3H). **^{13}C NMR**: (150 MHz, CD_3OD) δ (ppm) = 167.1, 140.5, 136.6, 129.8, 127.0, 126.2, 126.1, 125.5, 123.8, 116.0, 115.8, 113.0, 112.7, 51.2. **HRMS**: (ESI) *m/z* calculated for $C_{16}H_{14}N_2O_2$ $[M+H]^+$ 267.1128, found 267.1143. **IR (neat):** υ = 2957, 1673, 1606, 1441, 1286, 1201, 1172, 1116, 830, 794, 772 cm^{-1}. **MP**: 209 – 228°C.

Preparation of Key Intermediate **42**

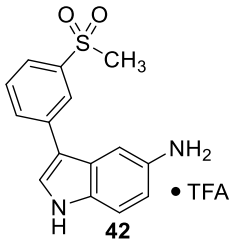

42

The title compound was prepared according to general procedure A using *bis*-protected bromo-indole **28** (583 mg, 1.5 mmol), 4,4,5,5-tetramethyl-2-(3-(methylsulfonyl)phenyl)-1,3,2-dioxaborolane (400 mg, 1.5 mmol), K_2CO_3 (588 mg, 4.3 mmol), $Pd(PPh_3)_4$ (164 mg, 0.15 mmol), degassed THF (12 mL) and degassed water (4 mL). Purification by column chromatography afforded the protected coupled product,

which was subsequently deprotected in TFA (15 mL) and concentrated under reduced pressure to afford the TFA salt **42** as a brown solid (453 mg, 80%). **^{1}H NMR**: (500 MHz, CD_3OD) δ (ppm) = 8.21 (dd, *J* = 1.8, 1.7 Hz, 1H), 8.00 (ddd, *J* = 7.8, 1.8, 1.4 Hz, 1H), 7.91 (d, *J* = 2.1 Hz, 1H), 7.85 (ddd, *J* = 7.9, 1.7, 1.4 Hz, 1H), 7.81 (s, 1H), 7.71 (dd, *J* = 7.9, 7.8 Hz, 1H), 7.63 (d, *J* = 8.6 Hz, 1H), 7.22 (dd, *J* = 8.6, 2.1 Hz, 1H), 3.19 (s, 3H). **^{13}C NMR**: (125 MHz, CD_3OD) δ (ppm) = 142.8, 138.3, 138.2, 133.1, 131.2, 127.5, 126.8, 126.1, 125.5, 124.6, 117.5, 116.8, 114.6, 114.2, 44.4. **HRMS**: (ESI) *m/z* calculated for $C_{15}H_{14}N_2O_2$ $[M+H]^+$ 287.0849, found 287.0857. **IR (neat):** υ = 3682, 3211, 2982, 2900, 1784, 1607, 1751, 1629, 1431, 1167, 1140, 1084, 801, 693 cm^{-1}. **MP**: 195 – 207°C.

Preparation of Indole Analogue **43**

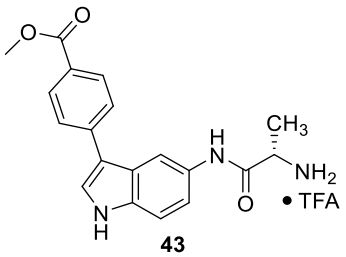

43

The title compound was prepared according to general procedure B using the aryl-indole moiety **41** (26 mg, 0.068 mmol), (*tert*-butoxycarbonyl)-*L*-alanine (15 mg, 0.081 mmol), PyBOP (42 mg, 0.081 mmol), DIPEA (0.09 mL, 0.34 mmol), and dry DMF (0.68 mL). Purification by RP-HPLC (using a SiliCycle SiliaChrom dtC18 semipreparative column (5 µm, 100Å, 10 x 250 mm) with a flow rate of 5 mL/min eluting with solvent (A: 0.1 % TFA in water B: 0.1 % TFA in MeCN) on a gradient of (2 → 100) %) solvent B over 15 min, t_R = 6.23 min) of the crude deprotected product afforded the TFA salt **43** as a colorless solid (7 mg, 24%). **^{1}H NMR**: (600 MHz, CD_3CN) δ (ppm) = 9.70 (s, 1H), 8.81 (s, 1H), 8.17 (s, 1H), 8.06 (d, *J* = 8.3 Hz, 2H), 7.77 (d, *J* = 8.3 Hz, 2H), 7.66 (s, 1H), 7.49 (d, *J* = 8.8 Hz, 1H), 7.34 (d, *J* = 8.7 Hz, 1H), 4.15 (q, *J* = 7.1 Hz, 1H), 1.60 (d, *J* = 7.1 Hz, 3H). **^{13}C NMR**: (150 MHz, CD_3CN) δ (ppm) = 168.0, 167.6, 141.5, 135.5, 131.8, 130.8, 128.2, 127.4, 126.3, 126.0, 117.1, 116.7, 113.3, 111.8, 52.5, 51.3, 17.4. **$[\alpha]_D^{20}$**: -23.8 (c = 3.8 mg/mL, MeOH). **HRMS**: (ESI) *m/z* calculated for $C_{19}H_{19}N_3O_3$ $[M+H]^+$ 338.1499, found 338.1496. **IR (neat):** υ = 3257, 2991, 1668, 1605, 1480, 1290, 1179, 1125, 774 cm^{-1}. **MP**: 148 – 159°C.

Preparation of Indole Analogue **44**

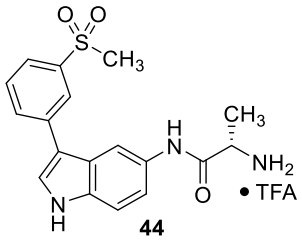

44

The title compound was prepared according to general procedure B using the aryl-indole moiety **42** (63.2 mg, 0.158 mmol), (*tert*-butoxycarbonyl)-*L*-alanine (60 mg, 0.32 mmol), PyBOP (165 mg, 0.32 mmol), DIPEA (0.21 mL, 0.79 mmol), and dry DMF (1.6 mL). Purification by RP-HPLC (using a SiliCycle SiliaChrom dtC18 semipreparative column (5 µm, 100Å, 10 x 250 mm) with a flow rate of 5 mL/min eluting with solvent (A: 0.1 % TFA in water B: 0.1 % TFA in MeCN) on a gradient of (2 → 100) %) solvent B over 15 min, t_R = 5.68 min) of the crude deprotected product afforded the TFA salt **44** as a colorless solid (11 mg, 18%). **^{1}H NMR**: (600 MHz, CD_3OD) δ (ppm) = 8.24 (d, *J* = 1.9 Hz, 1H), 8.22 (s, 1H), 7.99 (d, *J* = 7.7 Hz, 1H), 7.80 (d, *J* = 7.6 Hz, 1H), 7.70 – 7.64 (m, 2H), 7.45 (d, *J* = 8.7 Hz, 1H), 7.33 (dd, *J* = 8.7, 2.0 Hz, 1H), 4.10 (q, *J* = 7.0 Hz, 1H), 3.20 (s, 3H), 1.63 (d, *J* = 7.1 Hz, 3H). **^{13}C NMR**: (150 MHz, CD_3OD) δ (ppm) = 169.1, 142.5, 139.1, 136.2, 132.9, 132.1, 131.0, 126.4, 126.0, 126.0, 124.9, 117.2, 116.4, 113.2, 111.8, 50.9, 44.5, 17.8. **$[\alpha]_D^{20}$**: -5.8 (c = 7.5 mg/mL, MeOH). **HRMS**: (ESI) *m/z* calculated for $C_{18}H_{19}N_3O_3S$ $[M+H]^+$ 358.1220, found 358.1230. **IR (neat):** υ = 3673, 3238, 2987, 1667, 1597, 1289, 1200, 1132, 1092, 782 cm^{-1}. **MP**: 147 – 156°C.

Preparation of Indole Analogue **45**

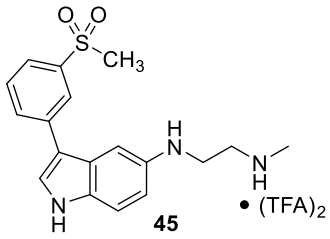

45

To a stirred solution of the free base of the aryl-indole moiety **42** (22 mg, 0.077 mmol, 1.0 equiv.) in 1,2-dichloroethane (0.77 mL, 0.1 M) was added *tert*-butyl methyl(2-oxoethyl)carbamate (13 mg, 0.077 mmol, 1.0 equiv.) at room temperature. The reaction

mixture was then stirred at room temperature for 30 minutes, after which $NaBH(OAc)_3$ (24 mg, 0.12 mmol, 1.5 equiv.) was added. The solution was then stirred for 18 hours, diluted with saturated aqueous $NaHCO_3$ and extracted with CH_2Cl_2 (3 times). The combined organic layers were dried with $MgSO_4$ and concentrated under reduced pressure to afford the crude protected indole moiety (brown gum) which was used in the next step without further purification. The crude protected product was dissolved in TFA (neat, 0.77 mL, 0.1 M) and stirred at room temperature for 30 minutes. The reaction mixture was then concentrated under reduced pressure to afford the crude indole moiety, which was purified by Purification by RP-HPLC (using a SiliCycle SiliaChrom dtC18 semipreparative column (5 µm, 100Å, 10 x 250 mm) with a flow rate of 5 mL/min eluting with solvent (A: 0.1 % TFA in water B: 0.1 % TFA in MeCN) on a gradient of (2 → 30) % solvent B over 15 min, t_R = 8.95 min) to afford the TFA salt **45** as a brown gum (3 mg, 8%). **^{1}H NMR**: (600 MHz, CD_3OD) δ (ppm) = 8.26 (s, 1H), 7.99 (d, *J* = 8.0 Hz, 1H), 7.79 (d, *J* = 7.8 Hz, 1H), 7.68 (dd, *J* = 7.8, 7.8 Hz, 1H), 7.58 (s, 1H), 7.34 (d, *J* = 8.7 Hz, 1H), 7.23 (d, *J* = 2.1 Hz, 0H), 6.80 (dd, *J* = 8.7, 2.1 Hz, 1H), 3.53 (t, *J* = 6.0 Hz, 2H), 3.31 (t, *J* = 6.1 Hz, 2H), 3.19 (s, 3H), 2.78 (s, 3H). **^{13}C NMR**: (15 MHz, CD_3OD) δ (ppm) = 143.0, 142.4, 139.7, 133.6, 132.6, 131.0, 127.1, 125.8, 125.1, 124.5, 115.4, 113.9, 113.8, 102.5, 49.6, 44.4, 42.9, 33.7. **HRMS**: (ESI) *m/z* calculated for $C_{18}H_{21}N_3O_2S$ $[M+H]^+$ 344.1427, found 344.1427. **IR (neat):** υ = 3677, 3365, 2988, 1669, 1600, 1200, 1137, 799, 723 cm^{-1}.

Preparation of Indole Analogue **46**

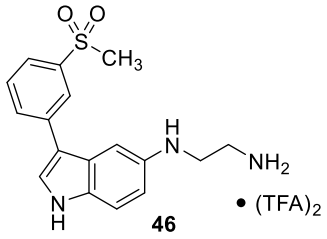

46

To a stirred solution of the free base of the aryl-indole moiety **42** (35 mg, 0.12 mmol, 2.0 equiv.) in water (*ca.* 0.15 mL, 2.0 M) was added 2-bromoethan-1-amine hydrochloride (13 mg, 0.061 mmol, 1.0 equiv.) at room temperature. The reaction mixture was then stirred at 95 °C for 22 hours and cooled to room temperature. The reaction mixture was then diluted with water and extracted with EtOAc (3 times). The remaining aqueous layer was purified by RP-HPLC (gradient: 2-30 shortprep, t_R = 8.33

min) to afford the TFA salt **46** as a brown gum (4 mg, 13%). **^{1}H NMR**: (500 MHz, CD_3CN) δ (ppm) = 9.47 (s, 1H), 8.17 (dd, *J* = 1.9, 1.4 Hz, 1H), 8.01 (ddd, *J* = 7.8, 1.4, 1.1 Hz, 1H), 7.76 (ddd, *J* = 7.8, 1.9, 1.1 Hz, 1H), 7.67 (dd, *J* = 7.8, 7.8 Hz, 1H), 7.57 (d, *J* = 2.6 Hz, 1H), 7.36 (d, *J* = 8.5 Hz, 1H), 7.16 (s, 1H), 6.75 (d, *J* = 8.5 Hz, 1H), 3.49 (t, *J* = 5.9 Hz, 2H), 3.22 (t, *J* = 5.9 Hz, 2H), 3.12 (s, 3H).

Insufficient material was produced for complete characterization. Re-synthesis was attempted but was unsuccessful.

Preparation of Aryl-Sulfonamide **51**

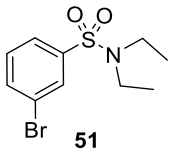

51

Synthesis of the title compound was performed by Anissa Kaghad according to general procedure C.

Preparation of Aryl-Sulfonamide **52**

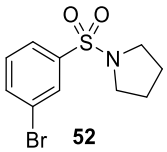

52

The title compound was prepared according to general procedure C, using pyrrolidine (0.27 mL, 3.3 mmol), dry pyridine (16.0 mL), and 3-bromobenzenesulfonyl chloride (800 mg, 3.1 mmol). Workup of the reaction mixture as detailed in general procedure C afforded the aryl-sulfonamide **52** as a colorless oil (710 mg, 78 %). **^{1}H NMR**: (500 MHz, $CDCl_3$) δ (ppm) = 7.97 (dd, *J* = 2.0, 1.7 Hz, 1H), 7.76 (ddd, *J* = 7.8, 1.7, 1.0 Hz, 1H), 7.71 (ddd, *J* = 8.0, 2.0, 1.0 Hz, 1H), 7.41 (dd, *J* = 8.0, 7.8 Hz, 1H), 3.28 – 3.22 (m, 4H), 1.82 – 1.76 (m, 4H). **^{13}C NMR**: (125 MHz, $CDCl_3$) δ (ppm) = 139.2, 135.7, 130.7, 130.4, 126.1, 123.2, 48.1, 25.4. **HRMS**: (ESI) *m/z* calculated for $C_{10}H_{12}BrNO_2S$ $[M+NH_4]^+$ 307.0110, found 307.0112. **IR** (neat): υ = 3084, 2976, 1567, 1459, 1404, 1345, 1159, 1103, 1067, 777, 682, 656, 606, 574 cm^{-1}. **MP**: 77 – 80°C.

Preparation of Aryl-Sulfonamide **53**

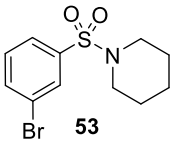

53

Synthesis of the title compound was performed by Anissa Kaghad according to general procedure C.

Preparation of 3-Pinacolboronate Aryl-Sulfonamide **54**

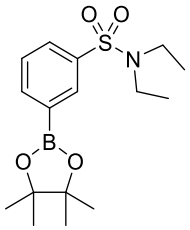

54

Synthesis of the title compound was performed by Anissa Kaghad according to general procedure D.

Preparation of 3-Pinacolboronate Aryl-Sulfonamide **55**

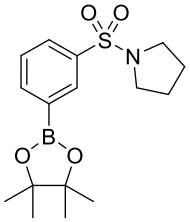

55

The title compound was prepared according to general procedure D, using aryl-sulfonamide **52** (686 mg, 2.4 mmol), B_2Pin_2 (660 mg, 2.60 mmol), NaOAc (485 mg, 5.9 mmol) and Pd(dppf)Cl_2 (97 mg, 0.12 mmol) in degassed DMSO (12 mL). Purification of the crude material by column chromatography (EtOAc:hexanes 16:84) afforded the 3-pinacolboronate aryl-sulfonamide **55** as a colorless solid (493 mg, 65 %). **^{1}H NMR**: (500 MHz, $CDCl_3$) δ (ppm) = 8.25 (dd, *J* = 2.0, 1.4 Hz, 1H), 7.99 (ddd, *J* = 7.4, 1.4, 1.3 Hz, 1H), 7.90 (ddd, *J* = 7.9, 2.0, 1.3 Hz, 1H), 7.51 (dd, *J* = 7.9, 7.4 Hz, 1H), 3.29 – 3.22 (m, 4H), 1.78 – 1.70 (m, 4H), 1.34 (s, 12H). **^{13}C NMR**: (125 MHz, $CDCl_3$) δ (ppm) = 138.8, 136.6, 133.7, 130.1, 128.4, 84.5, 48.1, 25.3, 25.0. *^{13}C-B$(OR)_2$ not observed. **HRMS**:

(ESI) *m/z* calculated for $C_{16}H_{24}BO_4S$ $[M+H]^+$ 338.1529, found 338.1608. **IR** (neat): υ = 3451, 2976, 1597, 1477, 1357, 1344, 1328, 1159, 1139, 1109, 701, 602, 567 cm^{-1}. **MP**: 110 – 114°C.

Preparation of 3-Pinacolboronate Aryl-Sulfonamide **56**

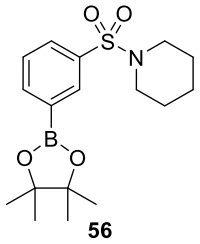

56

Synthesis of the title compound was performed by Anissa Kaghad according to general procedure D.

Preparation of Key Intermediate **57**

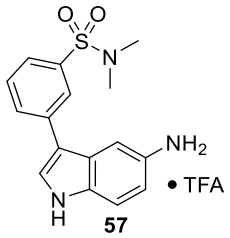

57

The title compound was prepared according to general procedure A using *bis*-protected bromo-indole **28** (400 mg, 0.97 mmol), N,N-dimethyl-3-(4,4,5,5-tetramethyl-1,3,2-dioxaborolan-2-yl)benzenesulfonamide (303 mg, 0.97 mmol), K_2CO_3 (403 mg, 2.9 mmol), $Pd(PPh_3)_4$ (112 mg, 0.097 mmol), degassed THF (8.3 mL) and degassed water (2.8 mL). Purification by column chromatography afforded the protected coupled product, which was subsequently deprotected in TFA (10 mL) and concentrated under reduced pressure to afford the TFA salt **57** as a brown solid (261 mg, 62%). **^{1}H NMR**: (500 MHz, CD_3OD) δ (ppm) = 8.03 (s, 1H), 7.96 (ddd, *J* = 7.2, 1.8 1.7 Hz, 1H), 7.88 (d, *J* = 2.1 Hz, 1H), 7.79 (d, *J* = 1.5 Hz, 1H), 7.72 – 7.66 (m, 2H), 7.63 (d, *J* = 8.6 Hz, 1H), 7.22 (dd, *J* = 8.7, 2.1 Hz, 1H), 2.75 (s, 6H). **^{13}C NMR**: (125 MHz, CD_3OD) δ (ppm) = 138.2, 138.0, 137.2, 132.4, 130.9, 127.4, 126.8, 126.7, 126.0, 124.5, 117.5, 116.8, 114.6, 114.0, 38.4. **HRMS**: (ESI) *m/z* calculated for $C_{16}H_{17}N_3O_2S$ $[M+H]^+$ 316.1114,

found 316.1120. **IR (neat):** υ = 3282, 2922, 1777, 1649, 1598, 1441, 1321, 1168, 1144, 961, 797, 701, 581 cm^{-1}. **MP**: 167 – 181°C.

Preparation of Key Intermediate **58**

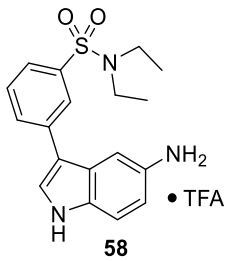

58

Synthesis of the title compound was performed by Anissa Kaghad according to general procedure A.

Preparation of Key Intermediate **59**

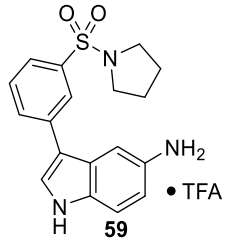

59

The title compound was prepared according to general procedure A using *bis*-protected bromo-indole **28** (100 mg, 0.24 mmol), 3-pinacolboronate aryl-sulfonamide **55** (82 mg, 0.24 mmol), K_2CO_3 (101 mg, 0.75 mmol), $Pd(PPh_3)_4$ (28 mg, 0.024 mmol), degassed THF (2.07 mL) and degassed water (0.7 mL). Purification by column chromatography afforded the protected coupled product, which was subsequently deprotected in TFA (2.4 mL) and concentrated under reduced pressure to afford the TFA salt **59** as a brown solid (40 mg, 36%). **^{1}H NMR**: (500 MHz, CD_3OD) δ (ppm) = 8.09 (s, 1H), 7.95 (d, *J* = 7.6 Hz, 1H), 7.84 (s, 1H), 7.79 (s, 1H), 7.74 (d, *J* = 7.8 Hz, 1H), 7.69 (dd, *J* = 7.8, 7.6 Hz, 1H), 7.61 (d, *J* = 8.6 Hz, 1H), 7.18 (dd, *J* = 8.6, 2.0 Hz, 1H), 3.32 – 3.28 (s, 4H), 1.80 – 1.76 (m, 4H). **^{13}C NMR**: (125 MHz, CD_3OD) δ (ppm) = 138.7, 138.1, 137.9, 132.3, 131.0, 127.3, 126.8, 126.4, 125.7, 125.6, 117.3, 116.8, 114.5, 113.5, 49.3, 26.3. **HRMS**: (ESI) *m/z* calculated for $C_{18}H_{19}N_3O_2S$ $[M+H]^+$ 342.1271, found 342.1276. **IR**

(neat): υ = 2984, 2897, 1673, 1604, 1333, 1200, 1134, 838, 797, 723, 587 cm^{-1}. **MP**: 116 – 124°C.

Preparation of Key Intermediate **60**

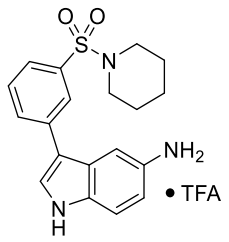

Synthesis of the title compound was performed by Anissa Kaghad according to general procedure A.

Preparation of Indole Analogue **61**

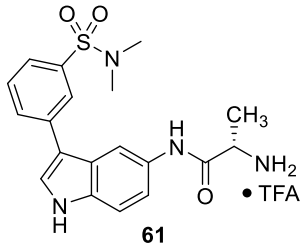

61

Synthesis of the title compound was performed by Anissa Kaghad according to general procedure B.

Preparation of Indole Analogue **62**

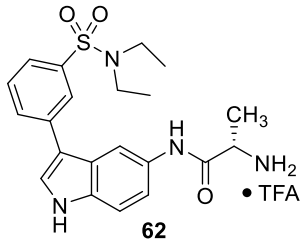

62

Synthesis of the title compound was performed by Anissa Kaghad according to general procedure B.

Preparation of Indole Analogue **63**

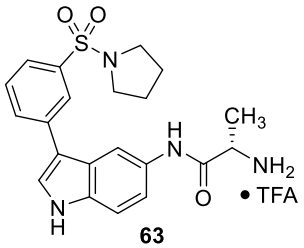

63

The title compound was prepared according to general procedure B using the aryl-indole moiety **59** (27 mg, 0.06 mmol), (*tert*-butoxycarbonyl)-*L*-alanine (11 mg, 0.06 mmol), PyBOP (31 mg, 0.06 mmol), DIPEA (0.08 mL, 0.30 mmol), and dry DMF (0.6 mL). RP-HPLC (gradient: 2-50 shortprep, t_R = 8.99 min) of the crude deprotected product afforded the TFA salt **63** as a colorless solid (11 mg, 34%). **^{1}H NMR**: (500 MHz, CD_3OD) δ (ppm) = 8.29 (s, 1H), 8.10 (s, 1H), 7.94 (d, *J* = 7.6 Hz, 1H), 7.68 (d, *J* = 7.7 Hz, 1H), 7.644 (s, 1H), 7.636 (dd, *J* = 7.7, 7.6 Hz, 1H), 7.45 (d, *J* = 8.7 Hz, 1H), 7.27 (dd, *J* = 8.7 Hz, 1H), 4.09 (q, *J* = 7.0 Hz, 1H), 3.34 – 3.30 (m, 4H), 1.79 – 1.75 (m, 4H), 1.63 (d, *J* = 7.0 Hz, 3H). **^{13}C NMR**: (125 MHz, CD_3OD) δ (ppm) = 169.0, 138.8, 138.3, 136.2, 132.1, 132.0, 130.7, 126.4, 126.3, 125.9, 125.3, 117.3, 116.6, 113.2, 111.9, 50.9, 49.4, 26.2, 17.8. **$[\alpha]_D^{20}$**: +5.8 (c = 8.8 mg/mL, MeOH). **HRMS**: (ESI) *m/z* calculated for $C_{21}H_{24}N_4O_3S$ $[M+H]^+$ 413.1642, found 413.1643. **IR (neat):** υ = 3252, 2973, 1671, 1596, 1201, 1135, 798, 722, 588 cm^{-1}. **MP**: 159 – 167°C.

Preparation of Indole Analogue **64**

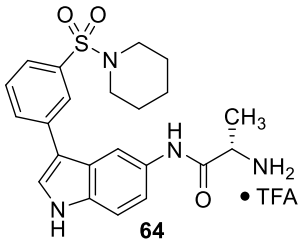

64

Synthesis of the title compound was performed by Anissa Kaghad according to general procedure B.

Preparation of Indole Analogue **65**

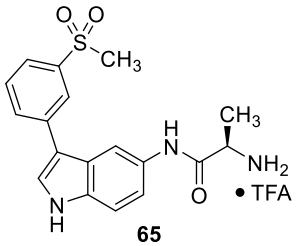

65

The title compound was prepared according to general procedure B using the aryl-indole moiety **42** (100 mg, 0.25 mmol), (*tert*-butoxycarbonyl)-*D*-alanine (57 mg, 0.300 mmol), PyBOP (156 mg, 0.30 mmol), DIPEA (0.33 mL, 1.3 mmol), and dry DMF (2.5 mL). Purification by RP-HPLC (using a SiliCycle SiliaChrom dtC18 semipreparative column (5 µm, 100Å, 10 x 250 mm) with a flow rate of 5 mL/min eluting with solvent (A: 0.1 % TFA in water B: 0.1 % TFA in MeCN) on a gradient of (2 → 100) %) solvent B over 15 min, t_R = 5.66 min) of the crude deprotected product afforded the TFA salt **65** as a colorless solid (31 mg, 26%). **^{1}H NMR**: (600 MHz, CD_3CN) δ (ppm) = 9.75 (s, 1H), 9.26 (s, 1H), 8.16-8.11 (m, 2H), 7.92 (ddd, *J* = 7.8, 1.8, 1.1 Hz, 1H), 7.75 (ddd, *J* = 7.8, 1.9, 1.1 Hz, 1H), 7.66 – 7.60 (m, 2H), 7.43 (d, *J* = 8.7 Hz, 1H), 7.33 (dd, *J* = 8.7, 2.0 Hz, 1H), 4.24 (q, *J* = 7.0 Hz, 1H), 3.11 (s, 3H), 1.58 (d, *J* = 7.0 Hz, 3H). **^{13}C NMR**: (150 MHz, CD_3CN) δ (ppm) = 168.6, 142.3, 138.1, 135.2, 132.5, 132.2, 130.7, 125.9, 125.8, 125.8, 124.8, 117.0, 115.9, 113.1, 111.1, 50.9, 44.4, 17.6. **$[\alpha]_D^{20}$**: -36.4 (c = 22.8 mg/mL, MeOH). **HRMS**: (ESI) *m/z* calculated for $C_{18}H_{19}N_3O_3S$ $[M+H]^+$ 358.1220, found 358.1220. **IR (neat):** υ = 3243, 2982, 1669, 1596, 1289, 1200, 1136, 782, 722 cm^{-1}. **MP**: 143 – 148°C.

Preparation of Indole Analogue **66**

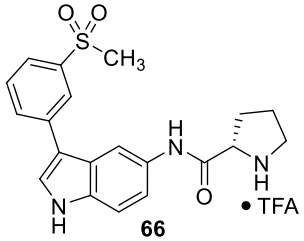

66

The title compound was prepared according to general procedure B using the aryl-indole moiety **42** (100 mg, 0.25 mmol), (*tert*-butoxycarbonyl)-*L*-proline (65 mg, 0.30

mmol), PyBOP (156 mg, 0.30 mmol), DIPEA (0.33 mL, 1.25 mmol), and dry DMF (2.5 mL). Purification by RP-HPLC (using a SiliCycle SiliaChrom dtC18 semipreparative column (5 µm, 100Å, 10 x 250 mm) with a flow rate of 5 mL/min eluting with solvent (A: 0.1 % TFA in water B: 0.1 % TFA in MeCN) on a gradient of (2 → 100) %) solvent B over 15 min, t_R = 5.88 min) of the crude deprotected product afforded the TFA salt **66** as a pale yellow solid (21 mg, 17%). **^{1}H NMR**: (600 MHz, CD_3OD) δ (ppm) = 8.25 (d, *J* = 1.9 Hz, 1H), 8.22 (dd, *J* = 1.9, 1.9 Hz, 1H), 7.99 (ddd, *J* = 7.7, 1.9, 1.8 Hz, 1H), 7.80 (ddd, *J* = 7.6, 1.9 1.8 Hz, 1H), 7.67 (s, 1H), 7.65 (dd, *J* = 7.7, 7.6 Hz, 1H), 7.45 (d, *J* = 8.7 Hz, 1H), 7.34 (dd, *J* = 8.7, 1.9 Hz, 1H), 4.43 (dd, *J* = 7.7, 7.7 Hz, 1H), 3.48 (ddd, *J* = 11.4, 7.1, 7.0 Hz, 1H), 3.39 (ddd, *J* = 11.4, 71, 7.0 Hz, 1H), 3.19 (s, 3H), 2.55 (dddd, *J* = 13.6, 7.1, 7.0, 7.0 Hz, 1H), 2.26 – 2.04 (m, 3H). **^{13}C NMR**: (150 MHz, CD_3OD) δ (ppm) = 167.7, 142.5, 139.1, 136.2, 132.9, 132.1, 131.0, 126.3, 126.0, 126.0, 124.9, 117.2, 116.4, 113.2, 111.8, 61.7, 47.5, 44.5, 31.2, 25.2. **$[\alpha]_D^{20}$**: -14.3 (c = 11.6 mg/mL, MeOH). **HRMS**: (ESI) *m/z* calculated for $C_{20}H_{21}N_3O_3S$ $[M+H]^+$ 384.1376, found 384.1386. **IR (neat):** υ = 3252, 2982, 1668, 1596, 1292, 1200, 1130, 798, 720 cm^{-1}. **MP**: 123 – 128°C.

Preparation of Indole Analogue **67**

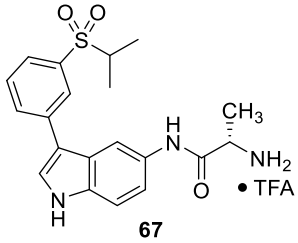

67

The title compound was prepared according to general procedure B using the aryl-indole moiety **74** (56 mg, 0.14 mmol), (*tert*-butoxycarbonyl)-*L*-alanine (30 mg, 0.16 mmol), PyBOP (85 mg, 0.16 mmol), DIPEA (0.18 mL, 0.68 mmol), and dry DMF (1.4 mL). Purification by RP-HPLC (using a SiliCycle SiliaChrom dtC18 semipreparative column (5 µm, 100Å, 10 x 250 mm) with a flow rate of 5 mL/min eluting with solvent (A: 0.1 % TFA in water B: 0.1 % TFA in MeCN) on a gradient of (2 → 100) %) solvent B over 15 min, t_R = 6.11 min) of the crude deprotected product afforded the TFA salt **67** as a colorless solid (10 mg, 15%). **^{1}H NMR**: (600 MHz, CD_3CN) δ (ppm) = 9.71 (s, 1H), 9.31 (s, 1H), 8.19 (d, *J* = 2.0 Hz, 1H), 8.07 (t, *J* = 1.8 Hz, 1H), 7.95 (ddd, *J* = 7.7, 1.5, 1.4 Hz, 1H), 7.71 (ddd, *J* = 7.9, 1.5, 1.4 Hz, 1H), 7.65 (dd, *J* = 7.9, 7.7 Hz, 1H), 7.63 (d, *J* = 2.7 Hz, 1H), 7.44 (d, *J* = 8.7 Hz, 1H), 7.33 (dd, *J* = 8.7, 2.0 Hz, 1H), 4.24 (q, *J* = 7.1 Hz, 1H),

3.35 (septet, *J* = 6.8 Hz, 1H), 1.60 (d, *J* = 7.1 Hz, 3H), 1.26 (d, *J* = 6.8 Hz, 6H). **^{13}C NMR**: (150 MHz, CD_3CN) δ (ppm) = 168.5, 1z38.7, 137.9, 135.2, 132.6, 132.3, 130.6, 127.4, 126.6, 125.9, 125.8, 116.9, 116.0, 113.2, 110.9, 55.9, 50.9, 17.6, 15.88, 15.87. **$[\alpha]_D^{20}$**: +3.5 (c = 4.8 mg/mL, MeOH). **HRMS**: (ESI) *m/z* calculated for $C_{20}H_{23}N_3O_3S$ $[M+H]^+$ 386.1533, found 386.1538. **IR (neat):** υ = 3243, 3092, 2982, 1668, 1596, 1538, 1200, 1132, 798, 695 cm^{-1}. **MP**: 155 – 162°C.

Preparation of Indole Analogue **68**

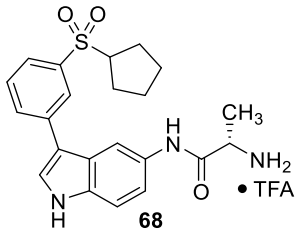

68

The title compound was prepared according to general procedure B using the aryl-indole moiety **75** (45 mg, 0.10 mmol), (*tert*-butoxycarbonyl)-*L*-alanine (19 mg, 0.10 mmol), PyBOP (52 mg, 0.10 mmol), DIPEA (0.14 mL, 0.50 mmol), and dry DMF (1.0 mL). RP-HPLC (gradient: 2-50 shortprep, t_R = 7.52 min) of the crude deprotected product afforded the TFA salt **68** as a colorless solid (27 mg, 50%). **^{1}H NMR**: (500 MHz, CD_3CN) δ (ppm) = 9.74 (s, 1H), 9.18 (s, 1H), 8.17 (d, *J* = 1.9 Hz, 1H), 8.09 (dd, *J* = 1.8, 1.4 Hz, 1H), 7.93 (dd, *J* = 7.8, 1.4, 1.4 Hz, 1H), 7.72 (dd, *J* = 7.9, 1.4, 1.4 Hz, 1H), 7.64 (dd, *J* = 7.9, 7.8 Hz, 1H), 7.62 (d, *J* = 2.6 Hz, 2H), 7.45 (d, *J* = 8.7 Hz, 1H), 7.30 (dd, *J* = 8.8, 2.4 Hz, 1H), 4.23 (q, *J* = 7.0 Hz, 1H), 3.68 (tt, *J* = 8.9, 7.0 Hz, 1H), 2.04 – 1.96 (m, 2H), 1.91 – 1.82 (m, 2H), 1.73 – 1.66 (m, 2H), 1.63 – 1.55 (m, 5H). **^{13}C NMR**: (125 MHz, CD_3CN) δ (ppm) = 168.6, 140.7, 138.1, 135.3, 132.5, 132.2, 130.7, 126.9, 126.1, 126.0, 125.9, 117.1, 116.1, 113.2, 111.2, 64.6, 51.0, 28.0, 27.9, 26.6, 17.6. **$[\alpha]_D^{20}$**: +7.8 (c = 11.5 mg/mL, MeOH). **HRMS**: (ESI) *m/z* calculated for $C_{22}H_{25}N_3O_3S$ $[M+H]^+$ 412.1689, found 412.1706. **IR (neat):** υ = 3266, 2087, 2968, 1670, 1597, 1193, 1200, 1135, 798, 722 cm^{-1}. **MP**: 162 – 168°C.

Preparation of Isopropyl Sulfone **70**

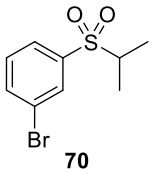

70

The title compound was prepared according to general procedure E, using 3-bromothiophenol (0.66 mL, 6.4 mmol, 1.0 equiv.), K_2CO_3 (1.228 g, 8.89 mmol, 1.4 equiv.), 2-bromopropane (0.72 mL, 7.6 mmol, 1.2 equiv.) in dry acetone (21 mL, 0.3 M). Oxidation was then performed according to general procedure E using MeOH (36 mL, 0.17 M according to the sulfide), oxone (5.593 g, 18 mmol, 3.0 equiv.), and water (36 mL, 0.5 M according to the oxone). Work-up and concentration of the crude reaction mixture afforded the isopropyl sulfone **70** as a yellow oil (1.102 g, 69 % over 2 steps). **^{1}H NMR**: (500 MHz, $CDCl_3$) δ (ppm) = 8.00 (dd, *J* = 1.9, 1.7 Hz, 1H), 7.79 (ddd, *J* = 7.9, 1.7, 1.1 Hz, 1H), 7.76 (ddd, *J* = 8.0, 2.0, 1.0 Hz, 1H), 7.43 (dd, *J* = 8.0, 7.9 Hz, 1H), 3.19 (septet, *J* = 6.9 Hz, 1H), 1.28 (d, *J* = 6.9 Hz, 6H). **^{13}C NMR**: (125 MHz, $CDCl_3$) δ (ppm) = 139.1, 136.8, 131.9, 130.7, 127.7, 123.2, 55.8, 15.7.

Spectral data were in accordance with those in the literature.[63]

Preparation of Cyclopentyl Sulfone **71**

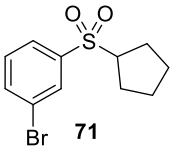

71

The title compound was prepared according to general procedure E, using 3-bromothiophenol (0.44 mL, 4.2 mmol, 1.0 equiv.), Cs_2CO_3 (2.986 g, 8.5 mmol, 2.0 equiv.), bromocyclopentane (0.43 mL, 4.2 mmol, 1.0 equiv.) in dry DMF (21 mL, 0.2 M). Oxidation of the crude sulfide (*ca.* 713 mg, 2.8 mmol, 1.0 equiv.) was then performed according to general procedure E using MeOH (17.0 mL, 0.165 according to the sulfide), and oxone (2.557 g, 8.3 mmol, 3.0 equiv.) in water (17 mL, 0.5 M). Work-up and concentration of the crude reaction mixture afforded the cyclopentyl sulfone **71** as a colorless oil (600 mg, 49 % over 2 steps). **^{1}H NMR**: (500 MHz, $CDCl_3$) δ (ppm) = 8.02 (dd, *J* = 2.0, 1.8 Hz, 1H), 7.81 (ddd, *J* = 7.8, 1.8, 1.1 Hz, 1H), 7.74 (ddd, *J* = 8.0, 2.0, 1.0

Hz, 1H), 7.42 (dd, *J* = 8.0, 7.8 Hz, 1H), 3.47 (tt, *J* = 8.7, 7.1 Hz, 1H), 2.11 – 1.96 (m, 2H), 1.92 – 1.81 (m, 2H), 1.80 – 1.70 (m, 2H), 1.66 – 1.53 (m, 2H). **^{13}C NMR**: (125 MHz, $CDCl_3$) δ (ppm) = 141.2, 136.6, 131.4, 130.8, 127.1, 123.3, 64.4, 27.3, 25.9. **HRMS**: (ESI) *m/z* calculated for $C_{11}H_{13}BrO_2S$ $[M+NH_4]^+$ 306.0158, found 306.0171. **IR** (neat): υ = 3672, 2962, 2869, 1571, 1459, 1405, 1290, 1308, 1146, 1067, 771, 679, 656, 596, 559 cm^{-1}.

Preparation of 3-Pinacolboronate Aryl-Sulfone **72**

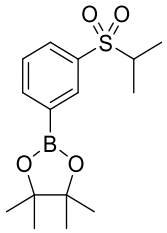

72

The title compound was prepared according to general procedure D, using isopropyl sulfone **70** (1.033 g, 3.92 mmol), B_2Pin_2 (1.096 g, 4.32 mmol), NaOAc (0.8047 g, 9.81 mmol) and $Pd(dppf)Cl_2$ (0.160 g, 0.20 mmol) in degassed DMSO (20 mL). Purification of the crude material by column chromatography (EtOAc:hexanes 1:4) afforded the 3-pinacolboronate aryl-sulfone **72** as a colorless solid (0.805 g, 66 %). **^{1}H NMR**: (500 MHz, $CDCl_3$) δ (ppm) = 8.30 (dd, *J* = 2.0, 1.3 Hz, 1H), 8.05 (ddd, *J* = 7.3, 1.3, 1.3 Hz, 1H), 7.95 (ddd, *J* = 7.9, 2.0, 1.3 Hz, 1H), 7.55 (dd, *J* = 7.9, 7.3 Hz, 1H), 3.21 (septet, *J* = 6.9 Hz, 1H), 1.34 (s, 12H), 1.29 (d, *J* = 6.9 Hz, 6H). **^{13}C NMR**: (125 MHz, $CDCl_3$) δ (ppm) = 139.8, 136.8, 135.1, 131.6, 128.4, 84.6, 55.5, 25.0, 15.8. *^{13}C-$B(OR)_2$ not observed. **HRMS**: (ESI) *m/z* calculated for $C_{15}H_{23}BO_4S$ $[M+NH_4]^+$ 328.1748, found 328.1760. **IR** (neat): υ = 2980, 2938, 1598, 1414, 1353, 1311, 1294, 1135, 1077, 1051, 840, 744, 702, 657, 585 cm^{-1}. **MP**: 75 – 78°C.

Preparation of 3-Pinacolboronate Aryl-Sulfone **73**

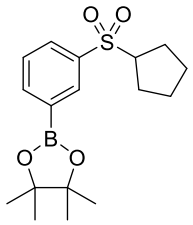

73

The title compound was prepared according to general procedure D, using cyclopentyl sulfone **71** (520 mg, 1.8 mmol), B_2Pin_2 (502 mg, 1.98 mmol), NaOAc (369 mg, 4.5 mmol) and $Pd(dppf)Cl_2$ (73 mg, 0.090 mmol) in degassed DMSO (9.0 mL). Purification of the crude material by column chromatography (EtOAc:hexanes 1:4) afforded the 3-pinacolboronate aryl-sulfone **73** as a yellow solid (438 mg, 72 %). **^{1}H NMR**: (500 MHz, $CDCl_3$) δ (ppm) = 8.32 (dd, *J* = 2.0, 1.4 Hz, 1H), 8.03 (ddd, *J* = 7.4, 1.4, 1.2 Hz, 1H), 7.97 (ddd, *J* = 7.9, 2.0, 1.2 Hz, 1H), 7.54 (dd, *J* = 7.9, 7.4 Hz, 1H), 3.51 (tt, *J* = 8.8, 7.2 Hz, 1H), 2.11 – 2.03 (m, 2H), 1.90 – 1.81 (m, 2H), 1.81 – 1.73 (m, 2H), 1.65 – 1.54 (m, 2H), 1.34 (s, 12H). **^{13}C NMR**: (125 MHz, $CDCl_3$) δ (ppm) = 139.7, 138.7, 134.6, 131.0, 128.5, 84.5, 64.2, 27.3, 26.0, 25.0. *^{13}C-B(OR)$_2$ not observed. **HRMS**: (ESI) *m/z* calculated for $C_{17}H_{25}BO_4S$ $[M+NH_4]^+$ 354.1905, found 354.1933. **IR** (neat): υ = 2979, 1739, 1597, 1411, 1374, 1352, 1328, 1289, 1132, 1079, 962, 838, 702, 555 cm^{-1}. **MP**: 70 – 77°C.

Preparation of Key Intermediate **74**

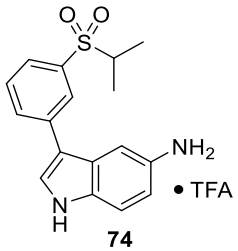

74

The title compound was prepared according to general procedure A using *bis*-protected bromo-indole **28** (597 mg, 1.45 mmol), isopropyl sulfone moiety **72** (450 mg, 1.45 mmol), K_2CO_3 (602 mg, 4.35 mmol), $Pd(PPh_3)_4$ (168 mg, 0.145 mmol), degassed THF (12 mL) and degassed water (4 mL). Purification by column chromatography afforded the protected coupled product, which was subsequently deprotected in TFA (15

mL) and concentrated under reduced pressure to afford the TFA salt **74** as a brown solid (479 mg, 77%). **^{1}H NMR**: (500 MHz, CD_3OD) δ (ppm) = 8.13 (dd, *J* = 1.8, 1.8 Hz, 1H), 8.02 (ddd, *J* = 7.7, 1.8, 1.4 Hz, 1H), 7.89 (d, *J* = 2.1 Hz, 1H), 7.80 (s, 1H), 7.78 (ddd, *J* = 7.9, 1.8, 1.4 Hz, 1H), 7.71 (dd, *J* = 7.9, 7.7 Hz, 1H), 7.63 (d, *J* = 8.6 Hz, 1H), 7.22 (dd, *J* = 8.6, 2.1 Hz, 1H), 3.40 (septet, *J* = 6.8 Hz, 1H), 1.30 (d, *J* = 6.8 Hz, 6H). **^{13}C NMR**: (125 MHz, CD_3OD) δ (ppm) = 139.0, 138.18, 138.16, 133.2, 131.0, 127.7, 127.5, 127.1, 126.7, 124.6, 117.5, 116.6, 114.6, 114.1, 56.5, 15.9. **HRMS**: (ESI) *m/z* calculated for $C_{17}H_{18}N_2O_2S$ $[M+H]^+$ 315.1162, found 315.1170. **IR (neat):** υ = 3673, 2987, 2904, 1761, 1650, 1599, 1167, 1141, 1056, 797, 694, 583 cm^{-1}. **MP**: 184 – 189°C.

Preparation of Key Intermediate **75**

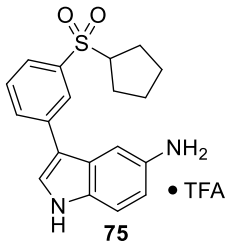

75

The title compound was prepared according to general procedure A using *bis*-protected bromo-indole **28** (200 mg, 0.49 mmol), cyclopentyl sulfone moiety **73** (164 mg, 0.49 mmol), K_2CO_3 (202 mg, 1.46 mmol), $Pd(PPh_3)_4$ (56 mg, 0.049 mmol), degassed THF (4.14 mL) and degassed water (1.4 mL). Purification by column chromatography afforded the protected coupled product, which was subsequently deprotected in TFA (4.8 mL) and concentrated under reduced pressure to afford the TFA salt **75** as a yellow solid (141 mg, 64%). **^{1}H NMR**: (500 MHz, CD_3OD) δ (ppm) = 8.16 (s, 1H), 8.00 (d, *J* = 7.8 Hz, 1H), 7.89 (d, *J* = 2.1 Hz, 1H), 7.90 – 7.88 (m, 2H), 7.71 (dd, *J* = 7.8, 7.6 Hz, 1H), 7.63 (d, *J* = 8.6 Hz, 1H), 7.22 (dd, *J* = 8.6, 2.1 Hz, 1H), 3.76 (ddd, *J* = 15.8, 8.9, 6.9 Hz, 1H), 2.11 – 1.99 (m, 2H), 1.96 – 1.86 (m, 2H), 1.81 – 1.71 (m, 2H), 1.69 – 1.61 (m, 2H). **^{13}C NMR**: (125 MHz, CD_3OD) δ (ppm) = 140.9, 138.23, 138.19, 133.1, 131.1, 127.5, 127.1, 126.8, 126.6, 124.6, 117.5, 116.7, 114.6, 114.1, 65.0, 28.2, 26.9. **HRMS**: (ESI) *m/z* calculated for $C_{19}H_{20}N_2O_2S$ $[M+H]^+$ 341.1318, found 341.1318. **IR (neat):** υ = 3202, 2973, 1752, 1626, 1600, 1428, 1171, 1142, 1086, 798, 695 cm^{-1}. **MP**: 136 – 140°C.

Preparation of 3-Pinacolboronate Aryl-Amide **77**

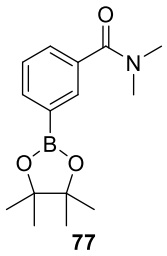

77

The title compound was prepared according to general procedure D, using 3-bromo-*N*,*N*-dimethylbenzamide (517 mg, 2.26 mmol), B_2Pin_2 (604 mg, 2.38 mmol), NaOAc (465 mg, 2.66 mmol) and Pd(dppf)Cl_2 (93 mg, 0.113 mmol) in degassed DMSO (11.3 mL). Purification of the crude material by column chromatography (EtOAc:hexanes 1:3) afforded the 3-pinacolboronate aryl-amide **77** as a brown oil (552 mg, 88 %). **^{1}H NMR**: (600 MHz, $CDCl_3$) δ (ppm) = 7.85 – 7.80 (m, 2H), 7.49 (ddd, *J* = 7.6, 1.7, 1.7 Hz, 1H), 7.39 (dd, *J* = 7.5, 7.5 Hz, 1H), 3.09 (s, 3H), 2.96 (s, 3H), 1.33 (s, 12H). **^{13}C NMR**: (150 MHz, $CDCl_3$) δ (ppm) = 171.8, 135.9, 135.8, 133.2, 129.8, 127.9, 84.1, 39.7, 35.4, 25.0. *^{13}C-B(OR)$_2$ not observed. **HRMS**: (ESI) *m/z* calculated for $C_{15}H_{22}BNO_3$ $[2M+H]^+$ 551.3458, found 551.3503.

Spectral data were in accordance with those in the literature.[64]

Preparation of Key Intermediate **78**

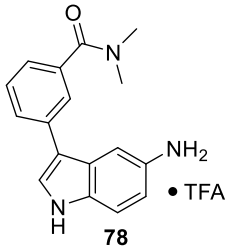

78

The title compound was prepared according to general procedure A using *bis*-protected bromo-indole **28** (200 mg, 0.486 mmol), dimethyl amide **77** (134 mg, 0.486 mmol), K_2CO_3 (202 mg, 1.46 mmol), Pd(PPh_3)$_4$ (57 mg, 0.0486 mmol), degassed THF (4.1 mL) and degassed water (1.4 mL). Purification by column chromatography afforded the protected coupled product, which was subsequently deprotected in TFA (4.8 mL) and concentrated under reduced pressure to afford the TFA salt **78** as a brown solid

(121 mg, 63%). **^{1}H NMR**: (500 MHz, CD_3OD) δ (ppm) = 7.88 (d, *J* = 2.1 Hz, 1H), 7.75 (d, *J* = 7.6 Hz, 1H), 7.71 – 7.68 (m, 2H), 7.60 (d, *J* = 8.6 Hz, 1H), 7.53 (dd, *J* = 7.6, 7.5 Hz, 1H), 7.32 (d, *J* = 7.5 Hz, 1H), 7.19 (dd, *J* = 8.6, 2.0 Hz, 1H), 3.14 (s, 3H), 3.08 (s, 3H). **^{13}C NMR**: (125 MHz, CD_3OD) δ (ppm) = 173.9z, 138.1, 138.0, 137.2, 130.2, 129.5, 127.0, 126.8, 126.4, 125.3, 124.2, 117.7, 117.2, 114.4, 114.3, 40.1, 35.7. **HRMS**: (ESI) *m/z* calculated for $C_{17}H_{17}N_3O$ $[M+H]^+$ 280.1444, found 280.1451. **IR (neat):** υ = 2931, 1673, 1598, 1492, 1401, 1201, 1133, 837, 798, 722 cm^{-1}. **MP**: 136 – 140 °C.

Preparation of Indole Analogue **79**

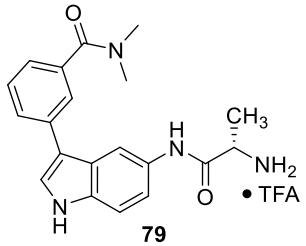

79

The title compound was prepared according to general procedure B using the aryl-indole moiety **78** (42 mg, 0.10 mmol), (*tert*-butoxycarbonyl)-*L*-alanine (19 mg, 0.10 mmol), PyBOP (52 mg, 0.10 mmol), DIPEA (0.14 mL, 0.50 mmol), and dry DMF (1.0 mL). RP-HPLC (gradient: 2-50 shortprep, t_R = 9.03 min) of the crude deprotected product afforded the TFA salt **79** as a colorless solid (20 mg, 44%). **^{1}H NMR**: (600 MHz, CD_3OD) δ (ppm) = 8.20 (d, *J* = 2.0, 0.6 Hz, 1H), 7.75 (ddd, *J* = 7.8, 1.7, 1.5 Hz, 1H), 7.70 (dd, *J* = 1.7, 1.4 Hz, 1H), 7.57 (s, 1H), 7.50 (dd, *J* = 7.8, 7.6 Hz, 1H), 7.42 (dd, *J* = 8.6, 0.6 Hz, 1H), 7.30 (dd, *J* = 8.7, 2.0 Hz, 1H), 7.28 (ddd, *J* = 7.6, 1.5, 1.4 Hz, 1H), 4.09 (q, *J* = 7.0 Hz, 1H), 3.14 (s, 3H), 3.10 (s, 3H), 1.63 (d, *J* = 7.0 Hz, 3H). **^{13}C NMR**: (150 MHz, CD_3OD) δ (ppm) = 174.0, 169.0, 137.9, 137.7, 136.2, 131.7, 130.0, 129.4, 126.6, 126.2, 125.4, 124.9, 117.4, 117.1, 113.0, 112.2, 50.8, 40.2, 35.7, 17.8. **$[\alpha]_D^{20}$**: +9.3 (c = 13.1 mg/mL, MeOH). **HRMS**: (ESI) *m/z* calculated for $C_{20}H_{22}N_4O_2$ $[M+H]^+$ 351.1816, found 351.1825. **IR (neat):** υ = 3668, 3248, 2988, 1668, 1596, 1578, 1400, 1203, 1181, 1130, 799, 722 cm^{-1}. **MP**: 137 – 143°C.

Preparation of Indole Analogue **80**

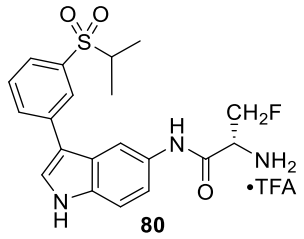

80

Synthesis of the title compound was performed by Dimitrios Panagopoulos.

Preparation of Indole Analogue **81**

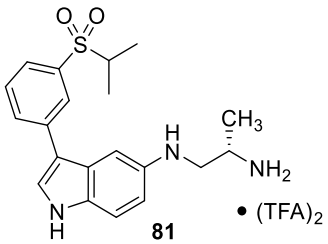

81

To a stirred solution of the free base of the aryl-indole moiety **74** (43 mg, 0.137 mmol, 1.0 equiv.) in 1,2-dichloroethane (1.4 mL, 0.1 M) was added *tert*-butyl (*S*)-(1-oxopropan-2-yl)carbamate (24 mg, 0.137 mmol, 1.0 equiv.) at room temperature. The reaction mixture was then stirred at room temperature for 30 minutes, after which $NaBH(OAc)_3$ (44 mg, 0.205 mmol, 1.5 equiv.) was added. The solution was then stirred for 18 hours, diluted with saturated aqueous $NaHCO_3$ and extracted with CH_2Cl_2 (3 times). The combined organic layers were dried with $MgSO_4$ and concentrated under reduced pressure to afford the crude protected indole moiety (brown gum) which was used in the next step without further purification. The crude protected product was dissolved in TFA (neat, 1.4 mL, 0.1 M) and stirred at room temperature for 30 minutes. The reaction mixture was then concentrated under reduced pressure to afford the crude indole moiety, which was purified by Purification by RP-HPLC (using a SiliCycle SiliaChrom dtC18 semipreparative column (5 µm, 100Å, 10 x 250 mm) with a flow rate of 5 mL/min eluting with solvent (A: 0.1 % TFA in water B: 0.1 % TFA in MeCN) on a gradient of (2 → 30) % solvent B over 15 min, t_R = 10.60 min) to afford the *bis*-TFA salt **81** as a brown gum (25 mg, 38%). **^{1}H NMR**: (600 MHz, CD_3CN) δ (ppm) = 9.73 (s, 1H), 8.08 (dd, *J* = 1.8, 1.7 Hz, 1H), 8.00 (ddd, *J* = 7.6, 1.8, 1.2 Hz, 1H), 7.71 (ddd, *J* = 7.8,

1.7, 1.2 Hz, 1H), 7.66 (dd, *J* = 7.8, 7.6 Hz, 1H), 7.64 (d, *J* = 2.7 Hz, 1H), 7.49 (d, *J* = 2.1 Hz, 1H), 7.46 (d, *J* = 8.7 Hz, 1H), 6.98 (dd, *J* = 8.7, 2.2 Hz, 1H), 3.78 (dqd, *J* = 8.7, 6.7, 4.2 Hz, 1H), 3.55 – 3.43 (m, 2H), 3.34 (*septet*, *J* = 6.8 Hz, 1H), 1.37 (d, *J* = 6.7 Hz, 3H), 1.30 – 1.20 (d, *J* = 6.8 Hz, 6H). **^{13}C NMR**: (150 MHz, CD_3CN) δ (ppm) = 138.7, 137.9, 137.7, 134.5, 132.5, 130.6, 127.3, 126.5, 126.4, 126.1, 115.6, 115.1, 114.1, 106.9, 55.9, 52.1, 47.8, 16.9, 15.8. **$[\alpha]_D^{20}$**: +25.8 (c = 19.4 mg/mL, MeOH). **HRMS**: (ESI) *m/z* calculated for $C_{20}H_{25}N_3O_2S$ $[M+H]^+$ 372.1740, found 372.1752. **IR (neat):** υ = 2978, 2900, 1666, 1598, 1183, 1129, 797, 722 cm^{-1}. **MP**: 110 – 115°C.

Preparation of Indole Analogue **82**

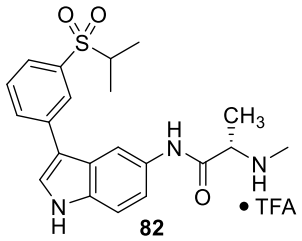

82

The title compound was prepared according to general procedure B using the aryl-indole moiety **74** (50 mg, 0.12 mmol), *N*-(*tert*-butoxycarbonyl)-*N*-methyl-*L*-alanine (25 mg, 0.12 mmol), PyBOP (63 mg, 0.12 mmol), DIPEA (0.16 mL, 0.61 mmol), and dry DMF (1.22 mL). RP-HPLC (gradient: 2-30 shortprep, t_R = 11.84 min) of the crude deprotected product afforded the TFA salt **82** as a colorless solid (19 mg, 30%). **^{1}H NMR**: (600 MHz, CD_3CN) δ (ppm) = 9.86 (s, 1H), 9.39 (s, 1H), 8.19 (s, 1H), 8.07 (d, *J* = 1.8 Hz, 1H), 7.95 (dd, *J* = 7.6, 1.7 Hz, 1H), 7.70 (dd, *J* = 7.8, 1.7 Hz, 1H), 7.65 (dd, *J* = 7.8, 7.6 Hz, 1H), 7.62 (d, *J* = 2.5 Hz, 1H), 7.46 (d, *J* = 8.6 Hz, 1H), 7.32 (d, *J* = 8.7 Hz, 1H), 4.06 (q, *J* = 7.0 Hz, 1H), 3.33 (*septet*, *J* = 6.7 Hz, 1H), 2.68 (s, 3H), 1.59 (d, *J* = 6.8 Hz, 3H), 1.25 (d, *J* = 6.8 Hz, 6H). **^{13}C NMR**: (150 MHz, CD_3CN) δ (ppm) = 167.8, 138.7, 137.9, 135.3, 132.7, 132.0, 130.6, 127.4, 126.6, 126.0, 125.8, 117.1, 116.0, 113.2, 111.3, 58.8, 56.0, 32.1, 16.3, 15.91, 15.90. **$[\alpha]_D^{20}$**: -1.3 (c = 12.8 mg/mL, MeOH). **HRMS**: (ESI) *m/z* calculated for $C_{21}H_{25}N_3O_3S$ $[M+H]^+$ 400.1689, found 400.1703. **IR (neat):** υ = 3270, 2982, 2904, 1667, 1469, 1181, 1200, 1131, 798, 721 cm^{-1}. **MP**: 128 – 133°C.

Preparation of Indole Analogue **83**

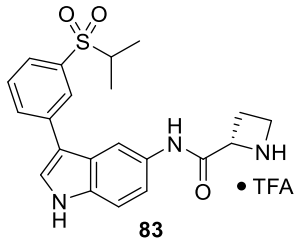

83

The title compound was prepared according to general procedure B using the aryl-indole moiety **74** (50 mg, 0.122 mmol), *N*-Boc-*L*-azetidine-2-carboxylic acid (25 mg, 0.122 mmol), PyBOP (63 mg, 0.122 mmol), DIPEA (0.16 mL, 0.61 mmol), and dry DMF (1.22 mL). Purification by RP-HPLC (using a SiliCycle SiliaChrom dtC18 semipreparative column (5 µm, 100Å, 10 x 250 mm) with a flow rate of 5 mL/min eluting with solvent (A: 0.1 % TFA in water B: 0.1 % TFA in MeCN) on a gradient of (2 → 30) % solvent B over 15 min, t_R = 11.69 min) of the crude deprotected product afforded the TFA salt **83** as a colorless solid (14 mg, 23%). **^{1}H NMR**: (600 MHz, CD_3CN) δ (ppm) = 9.81 (s, 1H), 9.36 (s, 1H), 8.21 (s, 1H), 8.08 (s, 1H), 7.96 (d, *J* = 7.5 Hz, 1H), 7.72 (d, *J* = 7.7 Hz, 1H), 7.66 (dd, *J* = 7.7, 7.5 Hz, 1H), 7.63 (s, 1H), 7.47 (d, *J* = 8.6 Hz, 1H), 7.32 (d, *J* = 8.7 Hz, 1H), 5.23 (dd, *J* = 9.4, 7.7 Hz, 1H), 4.16 (q, *J* = 9.3 Hz, 1H), 3.96 (td, *J* = 10.1, 6.4 Hz, 1H), 3.35 (*septet*, *J* = 6.4 Hz, 1H), 2.82 (qd, *J* = 10.1, 6.5 Hz, 1H), 2.64 (dt, *J* = 18.6, 8.4 Hz, 1H), 1.27 (d, *J* = 6.5 Hz, 6H). **^{13}C NMR**: (150 MHz, CD_3CNz) δ (ppm) = 166.4, 138.8, 138.0, 135.3, 132.7, 132.2, 130.6, 127.4, 126.6, 126.0, 125.9, 116.9, 116.1, 113.3, 111.0, 59.6, 56.0, 44.7, 24.0, 15.9. **$[\alpha]_D^{20}$**: -12.9 (c = 7.8 mg/mL, MeOH). **HRMS**: (ESI) *m/z* calculated for $C_{21}H_{23}N_3O_3S$ $[M+H]^+$ 398.1533, found 398.1564. **IR (neat):** υ = 3233, 2987, 1668, 1596, 1290, 1255, 1199, 1130, 797, 695, 580 cm^{-1}. **MP**: 149 – 156°C.

Preparation of Indole Analogue **84**

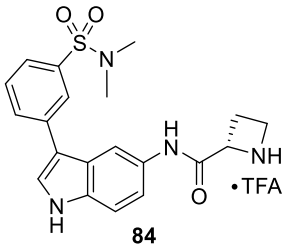

84

Synthesis of the title compound was performed by Dimitrios Panagopoulos according to general procedure B.

Preparation of Indole Analogue **85**

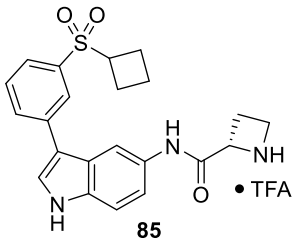

85

The title compound was prepared according to general procedure B using the aryl-indole moiety **88** (44 mg, 0.10 mmol), *N*-Boc-*L*-azetidine-2-carboxylic acid (20.1 mg, 0.10 mmol), PyBOP (52 mg, 0.10 mmol), DIPEA (0.14 mL, 0.50 mmol), and dry DMF (1.0 mL). RP-HPLC (gradient: 2-50 shortprep, t_R = 8.74 min) of the crude deprotected product afforded the TFA salt **85** as a colorless solid (22 mg, 41%). **^{1}H NMR**: (600 MHz, CD_3OD) δ (ppm) = 8.28 (d, *J* = 1.9 Hz, 1H), 8.14 (dd, *J* = 1.8, 1.5 Hz, 1H), 7.98 (ddd, *J* = 7.7, 1.8, 1.3 Hz, 1H), 7.71 (ddd, *J* = 8.0, 1.5, 1.3 Hz, 1H), 7.66 (s, 1H), 7.64 (dd, *J* = 8.0, 7.7 Hz, 1H), 7.45 (d, *J* = 8.7 Hz, 1H), 7.33 (dd, *J* = 8.7, 2.0 Hz, 1H), 5.17 (dd, *J* = 9.6, 7.6 Hz, 1H), 4.18 (q, *J* = 9.5 Hz, 1H), 4.11 – 4.00 (m, 2H), 2.92 (dtd, *J* = 12.1, 9.5, 6.2 Hz, 1H), 2.69 (ddt, *J* = 12.2, 9.7, 7.8 Hz, 1H), 2.58 – 2.50 (m, 2H), 2.26 – 2.18 (m, 2H), 2.08 – 1.94 (m, 2H). **^{13}C NMR**: (125 MHz, CD_3CN) δ (ppm) = 166.7, 139.7, 139.0, 136.2, 132.9, 132.0, 130.9, 126.8, 126.3, 126.0, 125.8, 117.1, 116.3, 113.2, 111.7, 60.5, 57.9, 45.0, 24.9, 23.7, 17.6. **$[\alpha]_D^{20}$**: -29.1 (c = 18.0 mg/mL, MeOH). **HRMS**: (ESI) *m/z* calculated for $C_{22}H_{23}N_3O_3S$ $[M+H]^+$ 410.1533, found 410.1542. **IR (neat):** υ = 3662, 3239, 2986, 1665, 1596, 1189, 1198, 1129, 797, 720 cm^{-1}. **MP**: 126 – 132°C.

Preparation of Cyclobutyl Sulfone **86**

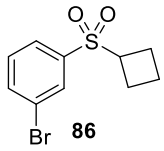

86

To a stirred solution of 3-bromothiophenol (500 mg, 2.64 mmol, 1.2 equiv.) in dry THF (2.2 mL, 1.0 M) under an atmosphere of nitrogen in a pressure vessel at 0 °C was added NaH (196 mg, 8.15 mmol, 3.7 equiv.) in small portions. The mixture was then stirred at 0 °C for 30 minutes, after which bromocyclobutane (0.21 mL, 2.20 mmol, 1.0 equiv.) was added dropwise. The reaction mixture was then stirred at 90 °C for 18 hours, after which the reaction was deemed complete by NMR (measured by consumption of the bromocyclobutane). Water (12 mL) was then added to the reaction mixture, followed by extraction of the intermediate with EtOAc (3 times). The combined organic layers were dried with $MgSO_4$ and concentrated under reduced pressure to afford the crude sulfide, which was used in the next step without purification. To a stirred solution of the crude cyclobutyl sulfide (*ca.* 333 mg, 1.37 mmol, 1.0 equiv.) in MeOH (8.4 mL, 0.165 M) was added oxone (1.264 g, 4.11 mmol, 3.0 equiv.) in water (8.4 mL, 0.5 M according to the oxone). The reaction mixture was stirred at room temperature for 18 hours after which the solution was diluted with water and extracted with EtOAc (3 times). The combined organic layers were washed with brine, dried with $MgSO_4$, filtered, and concentrated under reduced pressure to afford the cyclobutyl sulfone **86** as a colorless oil (289 mg, 40 % over 2 steps). **^{1}H NMR**: (500 MHz, $CDCl_3$) δ (ppm) = 8.01 (t, *J* = 1.8 Hz, 1H), 7.80 (ddd, *J* = 7.8, 1.7, 1.0 Hz, 1H), 7.76 (ddd, *J* = 8.0, 2.0, 1.0 Hz, 1H), 7.43 (t, *J* = 7.9 Hz, 1H), 3.81 (tt, *J* = 8.3, 8.1 Hz, 1H), 2.62 – 2.52 (m, 2H), 2.23 – 2.14 (m, 2H), 2.07 – 1.94 (m, 2H). **^{13}C NMR**: (125 MHz, $CDCl_3$) δ (ppm) = 140.2, 136.8, 131.3, 130.9, 126.9, 123.4, 57.1, 22.9, 17.0. **HRMS**: (ESI) *m/z* calculated for $C_{10}H_{11}BrO_2S$ $[M+NH_4]^+$ 292.0001, found 292.0002. **IR** (neat): υ = 3081, 2997, 1568, 1460, 1405, 1315, 1274, 1143, 1067, 775, 679, 656, 617, 574 cm^{-1}.

Preparation of 3-Pinacolboronate Aryl-Sulfone **87**

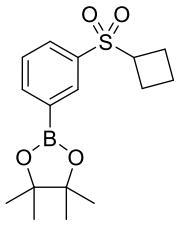

87

The title compound was prepared according to general procedure D, using aryl-sulfone **86** (265 mg, 0.962 mmol), B_2Pin_2 (244 mg, 0.962 mmol), NaOAc (197 mg, 2.41 mmol) and $Pd(dppf)Cl_2$ (39 mg, 0.0481 mmol) in degassed DMSO (4.8 mL). Purification of the crude material by column chromatography (EtOAc:hexanes 1:4) afforded the 3-pinacolboronate aryl-sulfone **87** as a colorless solid (189 mg, 61 %). **^{1}H NMR**: (500 MHz, $CDCl_3$) δ (ppm) = 8.29 (dd, *J* = 1.3, 1.3 Hz, 1H), 8.03 (ddd, *J* = 7.4, 1.3, 1.3 Hz, 1H), 7.94 (ddd, *J* = 7.9, 2.0, 1.3 Hz, 1H), 7.53 (dd, *J* = 7.9, 7.4 Hz, 1H), 3.83 (tt, *J* = 8.3, 8.1 Hz, 1H), 2.63 – 2.52 (m, 2H), 2.19 – 2.11 (m, 2H), 2.03 – 1.90 (m, 2H), 1.34 (s, 12H). **^{13}C NMR**: (125 MHz, $CDCl_3$) δ (ppm) = 139.8, 137.8, 134.5, 130.8, 128.6, 84.6, 57.0, 25.0, 22.9, 16.9. *^{13}C-$B(OR)_2$ not observed. **HRMS**: (ESI) *m/z* calculated for $C_{16}H_{23}BO_4S$ $[M+H]^+$ 340.1748, found 340.1767. **IR** (neat): υ = 3464, 2977, 1598, 1412, 1374, 1352, 1313, 1133, 1076, 838, 703, 613, 574 cm^{-1}. **MP**: 83 – 89°C.

Preparation of Key Intermediate **88**

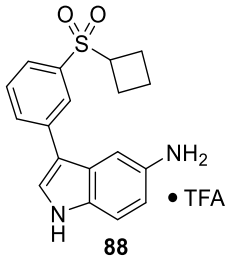

88

The title compound was prepared according to general procedure A using *bis*-protected bromo-indole **28** (200 mg, 0.486 mmol), cyclobutyl sulfone moiety **87** (158 mg, 0.486 mmol), K_2CO_3 (202 mg, 1.46 mmol), $Pd(PPh_3)_4$ (56 mg, 0.049 mmol), degassed THF (4.1 mL) and degassed water (1.4 mL). Purification by column chromatography afforded the protected coupled product, which was subsequently deprotected in TFA (4.8 mL) and concentrated under reduced pressure to afford the TFA salt **88** as a pale

yellow solid (181 mg, 85%). **^{1}H NMR**: (500 MHz, CD_3OD) δ (ppm) = 8.13 (s, 1H), 7.99 (d, *J* = 7.6 Hz, 1H), 7.89 (d, *J* = 2.1 Hz, 1H), 7.80 (s, 1H), 7.77 (d, *J* = 7.7 Hz, 1H), 7.69 (dd, *J* = 7.7, 7.6 Hz, 1H), 7.63 (d, *J* = 8.6 Hz, 1H), 7.22 (dd, *J* = 8.6, 2.1 Hz, 1H), 4.08 (p, *J* = 8.2 Hz, 1H), 2.59 – 2.49 (m, 2H), 2.27 – 2.18 (m, 2H), 2.10 – 1.94 (m, 2H). **^{13}C NMR**: (125 MHz, CD_3OD) δ (ppm) = 140.0, 138.3, 138.2, 133.2, 131.2, 127.5, 126.9, 126.7, 126.4, 124.6, 117.5, 116.7, 114.6, 114.1, 57.9, 23.7, 17.6. **HRMS**: (ESI) *m/z* calculated for $C_{18}H_{18}N_2O_2S$ $[M+H]^+$ 327.1162, found 327.1161. **IR (neat):** υ = 3261, 2959, 1770, 1646, 1600, 1263, 1142, 796, 692, 703, 577 cm^{-1}. **MP**: 177 – 184°C.

Preparation of *tert*-Butyl Sulfone **89**

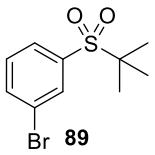

89

To a stirred solution of anhydrous ferric chloride (34 mg, 0.212 mmol, 0.08 equiv.) in $POCl_3$ (1.3 mL, 2.0 M) under a nitrogen atmosphere was added *tert*-butyl chloride (0.29 mL, 2.64 mmol, 1.0 equiv.) followed by 3-bromothiophenol (500 mg, 2.64 mmol, 1.0 equiv.) at room temperature. The reaction was stirred for 18 hours at room temperature, after which it was poured into ice and diluted with Et_2O. The organic layer was then washed with 2.0 M aqueous NaOH, washed with water, dried with $MgSO_4$, filtered, and concentrated under reduced pressure to afford the crude sulfide which was used without further purification. To a stirred solution of the crude sulfide (*ca.* 264 mg, 0.951 mmol, 1.0 equiv.) in MeOH (5.8 mL, 0.165 M) was added oxone (877 mg, 2.85 mmol, 3.0 equiv.) in water (5.7 mL, 0.5 M according to the oxone). The reaction mixture was stirred for 5 hours at room temperature after which the solution was diluted with water and extracted with EtOAc (3 times). The combined organic layers were washed with brine, dried with $MgSO_4$, filtered, and concentrated under reduced pressure to afford the *tert*-butyl sulfone **89** as a yellow oil (288 mg, 39 % over 2 steps). **^{1}H NMR**: (500 MHz, $CDCl_3$) δ (ppm) = 8.03 (dd, *J* = 1.9, 1.7 Hz, 1H), 7.82 (ddd, *J* = 7.8, 1.7, 1.0 Hz, 1H), 7.78 (ddd, *J* = 8.0, 1.9, 1.0 Hz, 1H), 7.44 (dd, *J* = 8.0, 7.8 Hz, 1H), 1.35 (s, 9H). **^{13}C NMR**: (125 MHz, $CDCl_3$) δ (ppm) = 137.6, 136.8, 133.3, 130.3, 129.2, 123.0, 60.4, 23.8. **HRMS**: (ESI) *m/z* calculated for $C_{10}H_{13}BrO_2S$ $[M+NH_4]^+$ 294.0158, found 294.0175. **IR** (neat): υ = 3084, 2975, 1459, 1405, 1306, 1290, 1134, 1078, 770, 686, 663, 570 cm^{-1}.

Preparation of 3-Pinacolboronate Aryl-Sulfone **90**

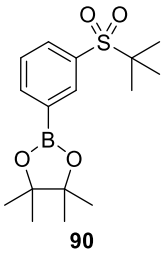

90

The title compound was prepared according to general procedure D, using *tert*-butyl sulfone **89** (280 mg, 1.01 mmol), B_2Pin_2 (269 mg, 1.06 mmol), NaOAc (207 mg, 2.53 mmol) and $Pd(dppf)Cl_2$ (41 mg, 0.051 mmol) in degassed DMSO (5.0 mL). Purification of the crude material by column chromatography (EtOAc:hexanes 1:4) afforded the 3-pinacolboronate aryl-sulfone **90** as a colorless solid (220 mg, 67 %). **^{1}H NMR**: (500 MHz, $CDCl_3$) δ (ppm) = 8.30 (dd, *J* = 2.0, 1.2 Hz, 1H), 8.05 (ddd, *J* = 7.4, 1.3, 1.2 Hz, 1H), 7.95 (ddd, *J* = 7.9, 2.0, 1.3 Hz, 1H), 7.54 (dd, *J* = 7.9, 7.4 Hz, 1H), 1.34 (s, 9H), 1.34 (s, 12H). **^{13}C NMR**: (125 MHz, $CDCl_3$) δ (ppm) = 139.8, 136.6, 135.0, 133.0, 128.2, 84.5, 59.9, 25.0, 23.8. *^{13}C-B(OR)$_2$ not observed. **HRMS**: (ESI) *m/z* calculated for $C_{16}H_{25}BO_4S$ $[M+NH_4]^+$ 342.1905, found 342.1930. **IR** (neat): υ = 2977, 2924, 1597, 1480, 1386, 1350, 1289, 1124, 1074, 837, 703, 637, 570 cm^{-1}. **MP**: 139 – 145°C.

Preparation of Key Intermediate **91**

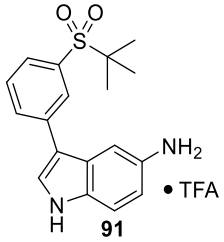

91

The title compound was prepared according to general procedure A using *bis*-protected bromo-indole **28** (200 mg, 0.486 mmol), *tert*-butyl sulfone moiety **90** (158 mg, 0.486 mmol), K_2CO_3 (202 mg, 1.459 mmol), $Pd(PPh_3)_4$ (56 mg, 0.049 mmol), degassed THF (4.1 mL) and degassed water (1.4 mL). Purification by column chromatography afforded the protected coupled product, which was subsequently deprotected in TFA (4.8 mL) and concentrated under reduced pressure to afford the TFA salt **91** as a pale yellow solid (134 mg, 62%). **^{1}H NMR**: (500 MHz, CD_3OD) δ (ppm) = 8.11 (dd, *J* = 1.8,

1.5 Hz, 1H), 8.02 (ddd, *J* = 7.6, 1.5, 1.4 Hz, 1H), 7.87 (d, *J* = 2.1 Hz, 1H), 7.79 (s, 1H), 7.77 (ddd, *J* = 7.8, 1.8, 1.4 Hz, 1H), 7.71 (dd, *J* = 7.8, 7.6 Hz, 1H), 7.63 (d, *J* = 8.7 Hz, 1H), 7.23 (dd, *J* = 8.7, 2.1 Hz, 1H), 1.37 (s, 9H). **^{13}C NMR**: (125 MHz, CD_3OD) δ (ppm) = 138.2, 137.8, 137.0, 133.3, 130.7, 129.2, 128.7, 127.5, 126.7, 124.6, 117.5, 116.6, 114.6, 114.0, 61.1, 23.9. **HRMS**: (ESI) *m/z* calculated for $C_{18}H_{20}N_2O_2S$ $[M+H]^+$ 329.1318, found 329.1331. **IR (neat):** υ = 3668, 3266, 2991, 1756, 1645, 1598, 1427, 1165, 1132, 1079, 796, 694, 568 cm^{-1}. **MP**: 166 – 174°C.

Preparation of Indole Analogue **92**

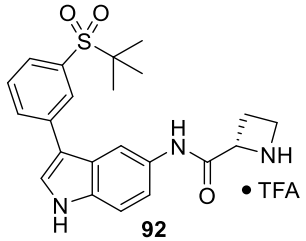

92

The title compound was prepared according to general procedure B using the aryl-indole moiety **91** (44 mg, 0.10 mmol), *N*-Boc-*L*-azetidine-2-carboxylic acid (20 mg, 0.10 mmol), PyBOP (52 mg, 0.10 mmol), DIPEA (0.14 mL, 0.50 mmol), and dry DMF (1.0 mL). RP-HPLC (gradient: 2-50 shortprep, t_R = 8.90 min) of the crude deprotected product afforded the TFA salt **92** as a colorless solid (18 mg, 34%). **^{1}H NMR**: (500 MHz, CD_3CN) δ (ppm) = 9.82 (s, 1H), 9.36 (s, 1H), 8.21 (s, 1H), 8.07 (s, 1H), 7.95 (d, *J* = 7.4 Hz, 1H), 7.71 (d, *J* = 7.5 Hz, 1H), 7.64 (dd, *J* = 7.5, 7.4 Hz, 1H), 7.61 (s, 1H), 7.46 (d, *J* = 7.7 Hz, 1H), 7.28 (d, *J* = 7.6 Hz, 1H), 5.31 – 5.16 (s, 1H), 4.21 – 4.09 (m, 1H), 4.02 - 3.91 (m, 1H), 2.87 – 2.80 (m, 1H), 2.69 – 2.57 (m, 1H), 1.34 (s, 9H). **^{13}C NMR**: (125 MHz, CD_3CN) δ (ppm) = 166.4, 137.7, 136.9, 135.3, 132.7, 132.1, 130.3, 128.9, 128.2, 126.0, 125.9, 117.0, 116.1, 113.3, 111.1, 60.5, 59.7, 44.9, 24.1, 23.9. **$[\alpha]_D^{20}$**: -24.8 (c = 14.2 mg/mL, MeOH). **HRMS**: (ESI) *m/z* calculated for $C_{22}H_{25}N_3O_3S$ $[M+H]^+$ 412.1689, found 412.1695. **IR (neat):** υ = 3256, 3089, 2982, 1668, 1642, 1199, 1184, 1128, 1077, 797, 695 cm^{-1}. **MP**: 167 - 174°C.

Preparation of Indole Analogue **93**

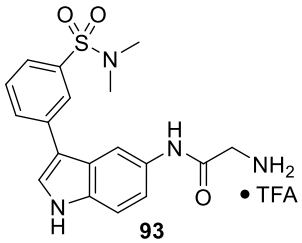

93

The title compound was prepared according to general procedure B using the aryl-indole moiety **57** (45 mg, 0.10 mmol), (*tert*-butoxycarbonyl)glycine (18 mg, 0.10 mmol), PyBOP (54 mg, 0.10 mmol), DIPEA (0.14 mL, 0.52 mmol), and dry DMF (1.0 mL). RP-HPLC (gradient: 2-50 shortprep, t_R = 10.38 min) of the crude deprotected product afforded the TFA salt **93** as a colorless solid (13 mg, 25%). **^{1}H NMR**: (500 MHz, CD_3OD:CD_3CN 1:1, calibrated to CD_3OD) δ (ppm) = 8.32 (d, *J* = 2.0 Hz, 1H), 8.07 (s, 1H), 7.98 (d, *J* = 7.2 Hz, 1H), 7.72 – 7.65 (m, 3H), 7.50 (d, *J* = 8.7 Hz, 1H), 7.29 (dd, *J* = 8.7, 2.0 Hz, 1H), 3.85 (s, 2H), 2.78 (s, 6H). **^{13}C NMR**: (125 MHz, CD_3OD:CD_3CN 1:1, calibrated to CD_3OD) δ (ppm) = 164.9, 138.3, 136.7, 135.6, 132.13, 132.07, 130.7, 126.4, 126.12, 126.08, 125.6, 116.9, 116.2, 113.3, 111.2, 42.0, 38.6. **HRMS**: (ESI) *m/z* calculated for $C_{18}H_{20}N_4O_3S$ $[M+H]^+$ 373.1329, found 373.1343. **IR (neat):** υ = 3252, 3097, 2964, 1673, 1596, 1487, 1330, 1183, 1201, 1157, 1135, 798, 706 cm^{-1}. **MP**: 128 – 134°C.

Preparation of Indole Analogue **94**

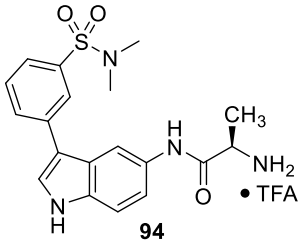

94

The title compound was prepared according to general procedure B using the aryl-indole moiety **57** (44 mg, 0.10 mmol), (*tert*-butoxycarbonyl)-*D*-alanine (20 mg, 0.10 mmol), PyBOP (54 mg, 0.10 mmol), DIPEA (0.14 mL, 0.52 mmol), and dry DMF (1.0 mL). RP-HPLC (gradient: 2-50 shortprep, t_R = 8.61 min) of the crude deprotected product afforded the TFA salt **94** as a colorless solid (13 mg, 26%). **^{1}H NMR**: (500 MHz,

CD_3CN) δ (ppm) = 9.74 (s, 1H), 9.18 (s, 1H), 8.23 (s, 1H), 8.00 (s, 1H), 7.90 (ddd, *J* = 7.3, 3.6, 1.9 Hz, 1H), 7.69 – 7.56 (m, 3H), 7.45 (dd, *J* = 8.4, 3.6 Hz, 1H), 7.26 (d, *J* = 8.6 Hz, 1H), 4.22 (q, *J* = 7.0 Hz, 1H), 2.72 (s, 6H), 1.58 (d, *J* = 6.9 Hz, 3H). **^{13}C NMR**: (125 MHz, CD_3CN) δ (ppm) = 168.6, 137.9, 136.6, 135.3, 132.2, 131.9, 130.6, 126.3, 125.9, 125.6, 117.0, 116.2, 113.2, 111.2, 51.0, 38.6, 17.6. **$[\alpha]_D^{20}$**: -11.4 (c = 9.3 mg/mL, MeOH). **HRMS**: (ESI) *m/z* calculated for $C_{19}H_{22}N_4O_3S$ $[M+H]^+$ 387.1485, found 387.1499. **IR (neat):** υ = 3668, 2982, 1672, 1597, 1487, 1184, 1201, 1157, 1139, 798, 708, 580 cm^{-1}. **MP**: 136 – 142°C.

Preparation of Indole Analogue **95**

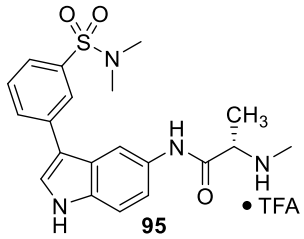

95

The title compound was prepared according to general procedure B using the aryl-indole moiety **57** (50 mg, 0.116 mmol), *N*-(*tert*-butoxycarbonyl)-*N*-methyl-*L*-alanine (24 mg, 0.116 mmol), PyBOP (61 mg, 0.116 mmol), DIPEA (0.15 mL, 0.58 mmol), and dry DMF (1.2 mL). Purification by RP-HPLC (using a SiliCycle SiliaChrom dtC18 semipreparative column (5 µm, 100Å, 10 x 250 mm) with a flow rate of 5 mL/min eluting with solvent (A: 0.1 % TFA in water B: 0.1 % TFA in MeCN) on a gradient of (2 → 30) % solvent B over 15 min, t_R = 11.84 min) of the crude deprotected product afforded the TFA salt **95** as a colorless solid (20 mg, 34%). **^{1}H NMR**: (500 MHz, CD_3OD) δ (ppm) = 8.31 (d, *J* = 2.0 Hz, 1H), 8.06 (dd, *J* = 1.8 Hz, 1H), 7.96 (ddd, *J* = 7.2, 1.8, 1.7 Hz, 1H), 7.70 – 7.61 (m, 3H), 7.45 (d, *J* = 8.7 Hz, 1H), 7.27 (dd, *J* = 8.7, 2.0 Hz, 1H), 3.87 (q, *J* = 7.0 Hz, 1H), 2.77 (s, 6H), 2.70 (s, 3H), 1.60 (d, *J* = 7.0 Hz, 3H). **^{13}C NMR**: (150 MHz, CD_3OD) δ (ppm) = 169.14, 138.8, 136.8, 136.2, 132.2, 132.0, 130.7, 126.6, 126.4, 125.9, 125.6, 117.1, 116.5, 113.2, 111.8, 59.3, 38.6, 32.2, 16.9. **$[\alpha]_D^{20}$**: -1.3 (c = 4.4 mg/mL, MeOH). **HRMS**: (ESI) *m/z* calculated for $C_{20}H_{24}N_4O_3S$ $[M+H]^+$ 401.1642, found 401.1655. **IR (neat):** υ = 3252, 2978, 1667, 1596, 1470, 1200, 1182, 1131, 797, 721, 579 cm^{-1}. **MP**: 120 – 124°C.

Preparation of Indole Analogue **96**

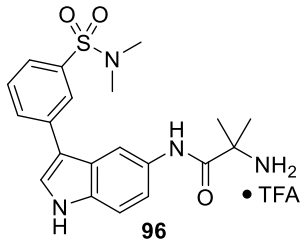

96

The title compound was prepared according to general procedure B using the aryl-indole moiety **57** (50 mg, 0.116 mmol), N-Boc-α–methyl alanine (24 mg, 0.116 mmol), PyBOP (601 mg, 0.116 mmol), DIPEA (0.15 mL, 0.58 mmol), and dry DMF (1.2 mL). RP-HPLC (gradient: 2-50 shortprep, t_R = 8.50 min) of the crude deprotected product afforded the TFA salt **96** as a colorless solid (17 mg, 28%). **^{1}H NMR**: (500 MHz, CD_3CN) δ (ppm) = 9.75 (s, 1H), 8.75 (s, 1H), 8.20 (d, *J* = 1.9 Hz, 1H), 8.01 (dd, *J* = 1.7, 1.6 Hz, 1H), 7.95 (ddd, *J* = 7.3, 1.7, 1.6 Hz, 1H), 7.71 – 7.60 (m, 3H), 7.50 (d, *J* = 8.7 Hz, 1H), 7.34 (dd, *J* = 8.7, 1.9 Hz, 1H), 2.73 (s, 6H), 1.72 (s, 6H). **^{13}C NMR**: (125 MHz, CD_3CN) δ (ppm) = 170.6, 137.8, 136.5, 135.4, 131.9, 131.8, 130.6, 126.3, 125.9, 125.8, 125.6, 117.9, 116.2, 113.1, 112.2, 59.2, 38.6, 24.1. **HRMS**: (ESI) *m/z* calculated for $C_{20}H_{24}N_4O_3S$ $[M+H]^+$ 401.1642, found 401.1652. **IR (neat):** υ = 3248, 2978, 1669, 1538, 1330, 1180, 1156, 1137, 798, 708, 580 cm^{-1}. **MP**: 146 – 153°C.

Preparation of Indole Analogue **97**

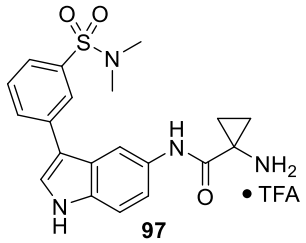

97

The title compound was prepared according to general procedure B using the aryl-indole moiety **57** (50 mg, 0.116 mmol), 1-((*tert*-butoxycarbonyl)amino)-cyclopropane-1-carboxylic acid (23 mg, 0.116 mmol), PyBOP (61 mg, 0.116 mmol), DIPEA (0.15 mL, 0.58 mmol), and dry DMF (1.16 mL). RP-HPLC (gradient: 2-50 shortprep, t_R = 8.43 min) of the crude deprotected product afforded the TFA salt **97** as a colorless solid (16 mg, 27%). **^{1}H NMR**: (500 MHz, CD_3CN) δ (ppm) = 9.68 (s, 1H), 8.12

(d, *J* = 1.9 Hz, 1H), 8.01 (dd, *J* = 1.7, 1.7 Hz, 1H), 7.93 (ddd, *J* = 7.2, 1.8, 1.7 Hz, 1H), 7.89 (s, 1H), 7.70 – 7.62 (m, 3H), 7.49 (d, *J* = 8.7 Hz, 1H), 7.26 (dd, *J* = 8.8, 2.0 Hz, 1H), 2.74 (s, 6H), 1.74 – 1.68 (m, 2H), 1.60 – 1.54 (m, 2H). **^{13}C NMR**: (125 MHz, CD_3CN) δ (ppm) = 167.1, 136.9, 135.8, 134.6, 131.0, 130.3, 129.7, 125.4, 125.0, 124.9, 124.7, 118.2, 115.3, 112.2, 111.7, 37.6, 36.6, 12.4. **HRMS**: (ESI) *m/z* calculated for $C_{20}H_{22}N_4O_3S$ $[M+H]^+$ 399.1485, found 399.1495. **IR (neat):** υ = 3275, 3087, 2914, 1668, 1538, 1184, 1156, 1135, 798, 722, 407, 580 cm^{-1}. **MP**: 128 – 135°C.

Preparation of Indole Analogue **98**

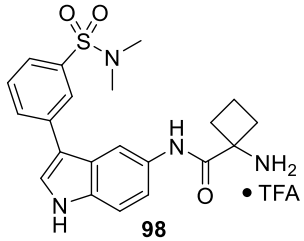

98

The title compound was prepared according to general procedure B using the aryl-indole moiety **57** (50 mg, 0.116 mmol), 1-((*tert*-butoxycarbonyl)amino)cyclobutane-1-carboxylic acid (25 mg, 0.116 mmol), PyBOP (61 mg, 0.116 mmol), DIPEA (0.15 mL, 0.58 mmol), and dry DMF (1.2 mL). RP-HPLC (gradient: 2-50 shortprep, t_R = 8.65 min) of the crude deprotected product afforded the TFA salt **98** as a colorless solid (19 mg, 31%). **^{1}H NMR**: (500 MHz, CD_3OD) δ (ppm) = 8.20 (d, *J* = 1.9 Hz, 1H), 8.05 (d, *J* = 2.3 Hz, 1H), 7.95 (d, *J* = 7.2 Hz, 1H), 7.71 – 7.58 (m, 3H), 7.47 (d, *J* = 8.7 Hz, 1H), 7.33 (dd, *J* = 8.7, 2.0 Hz, 1H), 2.97 – 2.89 (m, 2H), 2.75 (s, 6H), 2.51 – 2.43 (m, 2H), 2.40 – 2.32 (m, 1H), 2.32 – 2.22 (m, 1H). **^{13}C NMR**: (125 MHz, CD_3OD) δ (ppm) = 170.3, 138.7, 136.9, 136.6, 132.2, 131.5, 130.7, 126.6, 126.4, 125.9, 125.5, 118.9, 116.6, 113.8, 113.1, 60.7, 38.5, 31.1, 15.2. **HRMS**: (ESI) *m/z* calculated for $C_{21}H_{24}N_4O_3S$ $[M+H]^+$ 413.1642, found 413.1611. **IR (neat):** υ = 3238, 2973, 1670, 1537, 1471, 1184, 1201, 1161, 1143, 707, 580 cm^{-1}. **MP**: 132 – 140°C.

Preparation of Aryl-Sulfonamide **99**

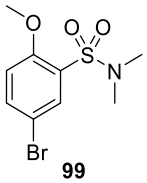

99

To a stirred solution of 4-bromoanisole (0.72 mL, 5.69 mmol, 1.0 equiv.) in CH_2Cl_2 (4.7 mL, 1.2 M) at 0 °C was added chlorosulfonic acid (1.42 mL, 4.0 M) dropwise. Once the addition was complete, the reaction mixture was warmed to room temperature over 1.5 hours. The reaction mixture was then cooled to 0 °C, diluted with CH_2Cl_2, and water (5 mL) was slowly added with vigorous stirring. The reaction mixture was then extracted with EtOAc (3 times), and the combined organic layers were dried with $MgSO_4$ and concentrated under reduced pressure to afford the crude sulfonyl chloride (*ca.* 1.11 g, 3.88 mmol) which was used without further purification. To a stirred solution of dimethylamine (2.0 mL of 2.0 M solution in THF, 4.00 mmol, 1.05 equiv.) in dry pyridine (19 mL, 0.2 M) at 0°C was added in small portions the sulfonyl chloride (1.11 g, 1.0 equiv.). The reaction mixture was warmed to room temperature and then stirred for 1 hour at room temperature, after which the reaction mixture was concentrated under reduced pressure. The crude residue was then dissolved in EtOAc and washed with 0.5 M HCl (2 times). The organic layer was then dried with $MgSO_4$, filtered, and concentrated to afford the aryl-sulfonamide **99** as a yellow solid (593 mg, 35 % over 2 steps). **^{1}H NMR**: (500 MHz, $CDCl_3$) δ (ppm) = 8.02 (d, *J* = 2.5 Hz, 1H), 7.59 (dd, *J* = 8.8, 2.5 Hz, 1H), 6.90 (d, *J* = 8.8 Hz, 1H), 3.91 (s, 3H), 2.84 (s, 6H). **^{13}C NMR**: (125 MHz, $CDCl_3$) δ (ppm) = 156.1, 137.0, 134.3, 128.4, 114.1, 112.6, 56.4, 37.7. **HRMS**: (ESI) *m/z* calculated for $C_9H_{12}BrNO_3S$ $[M+H]^+$ 293.9794, found 293.9803. **IR** (neat): υ = 3675, 3104, 2972, 1483, 1468, 1436, 1382, 1328, 1273, 1145, 1059, 960, 817, 739, 582, 505 cm^{-1}. **MP**: 165 – 169°C.

Preparation of Aryl-Sulfonamide **100**

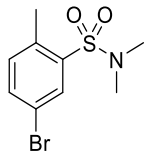

100

To a stirred solution of 4-bromotoluene (0.42 mL, 3.45 mmol, 1.0 equiv.) in dry CH_2Cl_2 (2.2 mL, 1.6 M) at (-5) °C was added chlorosulfonic acid (0.85 mL, 12.7 mmol, 3.7 equiv.) dropwise. Once the addition was complete, the reaction mixture was warmed to room temperature over 18 hours. The reaction mixture was then poured into ice water (9 mL), and the resulting biphasic mixture extracted with CH_2Cl_2 (3 times). The combined organic layers were washed with brine, dried with $MgSO_4$ and concentrated under reduced pressure to afford the crude sulfonyl chloride (*ca.* 841 mg, 3.12 mmol) which was used without further purification. To a stirred solution of dimethylamine (1.64 mL of 2.0 M solution in THF, 3.28 mmol, 1.05 equiv.) in dry pyridine (16 mL, 0.2 M) at 0°C was added in small portions the sulfonyl chloride (841 mg, 1.0 equiv.). The reaction mixture was warmed to room temperature and then stirred for 1 hour at room temperature, after which the reaction mixture was concentrated under reduced pressure. The crude residue was then dissolved in EtOAc and washed with 0.5 M HCl (2 times). The organic layer was then dried with $MgSO_4$, filtered, and concentrated to afford the aryl-sulfonamide **100** as a yellow solid (619 mg, 62 % over 2 steps) with a *ca.* 16 % impurity of the corresponding regioisomer found below that was unable to be removed by column chromatography (silica gel, Et_2O or EtOAc and Hexanes).

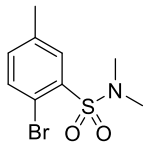

Regioisomer observed for the sulfonamidation of 4-bromotoluene.

Data for desired compound **100**: **^{1}H NMR**: (500 MHz, $CDCl_3$) δ (ppm) = 8.01 (d, *J* = 2.2 Hz, 1H), 7.56 (dd, *J* = 8.1, 2.2 Hz, 1H), 7.19 (d, *J* = 8.1 Hz, 1H), 2.82 (s, 6H), 2.56 (s, 3H). **^{13}C NMR**: (125 MHz, $CDCl_3$) δ (ppm) = 138.0, 137.0, 135.7, 134.5, 132.6, 119.6, 37.2, 20.3. **HRMS**: (ESI) *m/z* calculated for $C_9H_{12}BrNO_2S$ $[M+H]^+$ 277.9845, found

277.9856. **IR** (neat): υ = 2966, 1473, 1456, 1374, 1331, 1270, 1159, 1061, 957, 725, 584 cm^{-1}. **MP**: 47 – 49°C.

Preparation of Key Intermediate **101**

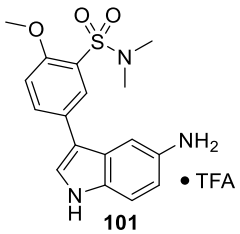

101

To a flame-dried round bottom flask containing the aryl-bromide **99** (250 mg, 0.850 mmol, 1.0 equiv.), dry THF (1.7 mL, 0.5 M) and a stir bar under a nitrogen atmosphere was added *n*-BuLi (0.43 mL of 2.0 M solution in hexanes, 0.850 mmol, 1.0 equiv.) dropwise. The resulting mixture was then stirred at -78 °C for 30 minutes, after which time trimethylborate (79 μL, 0.850 mmol, 1.0 equiv.) was added dropwise. Once the addition was complete, the reaction was warmed to room temperature over 3 hours. The reaction mixture was then cooled to -20 °C, acidified to pH 2 - 3 with 1.0 M aqueous HCl, warmed to room temperature, and extracted with EtOAc (3 times). The combined organic layers were then washed with brine, dried with $MgSO_4$, and concentrated under reduced pressure to afford the crude boronic acid. The crude boronic acid was then coupled to the indole core according to general procedure A using *bis*-protected bromo-indole **28** (480 mg, 1.167 mmol, 1.4 equiv.), K_2CO_3 (484 mg, 3.50 mmol, 4.1 equiv.), $Pd(PPh_3)_4$ (135 mg, 0.117 mmol, 0.14 equiv.), degassed THF/water (3:1) (13 mL, 0.064 M). Purification of the crude reaction mixture by column chromatography afforded the protected coupled product, which was subsequently deprotected in TFA (8.5 mL) and concentrated under reduced pressure to afford the TFA salt **101** as a brown solid (197 mg, 51%). **^{1}H NMR**: (500 MHz, CD_3OD) δ (ppm) = 8.11 (d, *J* = 2.3 Hz, 1H), 7.85 (dd, *J* = 8.5, 2.4 Hz, 1H), 7.82 (d, *J* = 2.1 Hz, 1H), 7.65 (s, 1H), 7.60 (d, *J* = 8.6 Hz, 1H), 7.31 (d, *J* = 8.6 Hz, 1H), 7.19 (dd, *J* = 8.6, 2.1 Hz, 1H), 3.98 (s, 3H), 2.86 (s, 6H). **^{13}C NMR**: (125 MHz, CD_3OD) δ (ppm) = 156.7, 138.0, 134.4, 130.7, 129.2, 127.3, 127.0, 126.3, 124.2, 117.2, 116.8, 114.6, 114.4, 114.0, 56.7, 38.0. **HRMS**: (ESI) *m/z* calculated for $C_{17}H_{19}N_3O_3S$ $[M+H]^+$ 346.1220, found 346.1234. **IR (neat):** υ = 3078, 2927, 1788, 1678, 1582, 1465, 1320, 1180, 1138, 1066, 720 cm^{-1}. **MP**: 121 – 143 °C.

Preparation of Key Intermediate **102**

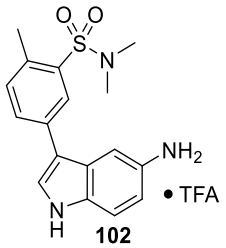

102

To a flame-dried round bottom flask containing the aryl-bromide **100** (400 mg, 1.44 mmol, 1.05 equiv.), dry THF (2.9 mL, 0.5 M according the aryl-bromide) and a stir bar under a nitrogen atmosphere was added *n*-BuLi (0.72 mL of 2.0 M solution in hexanes, 1.44 mmol, 1.05 equiv.) dropwise. The resulting orange mixture was then stirred at -78 °C for 30 minutes, after which time trimethylborate (79 μL, 1.44 mmol, 1.05 equiv.) was added dropwise. Once the addition was complete, the reaction was warmed to room temperature over 3 hours. The reaction mixture was then cooled to -20 °C, acidified to pH 2 - 3 with 1.0 M aqueous HCl, warmed to room temperature, and extracted with EtOAc (3 times). The combined organic layers were then washed with brine, dried with $MgSO_4$, and concentrated under reduced pressure to afford the crude boronic acid. The crude boronic acid was then coupled to the indole core according to general procedure A using *bis*-protected bromo-indole **28** (563 mg, 1.37 mmol, 1.0 equiv.), K_2CO_3 (568 mg, 4.12 mmol, 3.0 equiv.), $Pd(PPh_3)_4$ (158 mg, 0.137 mmol, 0.10 equiv.), degassed THF/water (3:1, 16 mL, 0.09 M). Purification of the crude reaction mixture by column chromatography afforded the protected coupled product, which was subsequently deprotected in TFA (14 mL) and concentrated under reduced pressure to afford the TFA salt **102** as a brown solid (399 mg, 66%) which was used in subsequent reactions without further purification. The crude product was contaminated with a small amount (*ca.* 15 %) of the regioisomer seen below, and this mixture was used in subsequent reactions. A small amount was purified by RP-HLPC (gradient: 2-100 shortprep, t_R = 6.17 min) to remove the regioisomer for characterization purposes only.

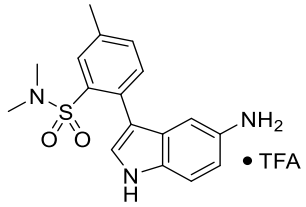

Regioisomer of **102**

Data for desired compound **102**: **^{1}H NMR**: (500 MHz, CD_3OD) δ (ppm) = 8.14 (s, 1H), 7.86 (d, *J* = 2.1 Hz, 1H), 7.80 (d, *J* = 7.9 Hz, 1H), 7.73 (m, 1H), 7.61 (d, *J* = 8.7 Hz, 1H), 7.49 (d, *J* = 7.8 Hz, 1H), 7.21 (dd, *J* = 8.6, 2.1 Hz, 1H), 2.82 (s, 6H), 2.64 (s, 3H). **^{13}C NMR**: (125 MHz, CD_3OD) δ (ppm) = 138.1, 137.3, 136.5, 135.0, 134.7, 132.4, 129.2, 126.92, 126.87, 124.4, 117.3, 116.8, 114.5, 114.1, 37.4, 20.5. **HRMS**: (ESI) *m/z* calculated for $C_{17}H_{19}N_3O_2S$ $[M+H]^+$ 330.1248, found 330.1271. **IR (neat):** υ = 2906, 1672, 1487, 1312, 1205, 1186, 1134, 838, 798, 723, 581, 499 cm^{-1}. **MP**: 115 - 123 °C.

Preparation of Indole Analogue **103**

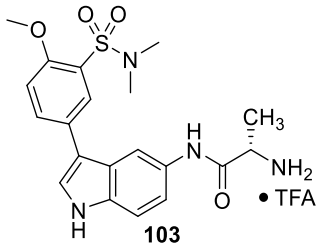

103

The title compound was prepared according to general procedure B using the aryl-indole moiety **101** (50 mg, 0.11 mmol), (*tert*-butoxycarbonyl)-*L*-alanine (21 mg, 0.11 mmol), PyBOP (57 mg, 0.11 mmol), DIPEA (0.14 mL, 0.54 mmol), and dry DMF (1.1 mL). RP-HPLC (gradient: 2-50 shortprep, t_R = 8.30 min) of the crude deprotected product afforded the TFA salt **103** as a colorless solid (18 mg, 30%). **^{1}H NMR**: (500 MHz, CD_3CN) δ (ppm) = 9.63 (s, 1H), 9.15 (s, 1H), 8.13 (s, 1H), 8.06 (d, *J* = 2.3 Hz, 1H), 7.81 (dd, *J* = 8.5, 2.3 Hz, 1H), 7.52 (d, *J* = 2.6 Hz, 1H), 7.45 (d, *J* = 8.7 Hz, 1H), 7.30 (dd, *J* = 8.7, 1.9 Hz, 1H), 7.22 (d, *J* = 8.6 Hz, 1H), 4.24 (q, *J* = 7.0 Hz, 1H), 3.94 (s, 3H), 2.83 (s, 6H), 1.60 (d, *J* = 7.0 Hz, 3H). **^{13}C NMR**: (125 MHz, CD_3CN) δ (ppm) = 167.6, 155.2, 134.2, 132.8, 130.9, 129.5, 128.0, 125.9, 125.1, 123.9, 116.0, 115.3, 113.4, 112.1, 110.2, 55.8, 50.0, 37.2, 16.7. **$[\alpha]_D^{20}$**: +10.7 (c = 12.8 mg/mL, MeOH). **HRMS**: (ESI) *m/z*

calculated for $C_{20}H_{24}N_4O_4S$ $[M+H]^+$ 417.1591, found 417.1591. **IR (neat):** υ = 3248, 2941, 1673, 1491, 1276, 1201, 1139, 800, 741, 722, 576 cm^{-1}. **MP**: 149 – 162°C.

Preparation of Indole Analogue **104**

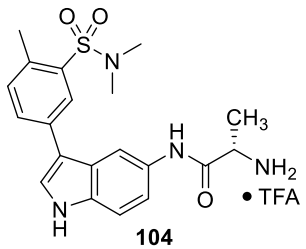

104

The title compound was prepared according to general procedure B using the aryl-indole moiety **102** (120 mg, 0.271 mmol), (*tert*-butoxycarbonyl)-*L*-alanine (54 mg, 0.28 mmol), PyBOP (155 mg, 0.298 mmol), DIPEA (0.24 mL, 1.35 mmol), and dry DMF (2.7 mL). Purification by RP-HPLC (using a SiliCycle SiliaChrom dtC18 semipreparative column (5 µm, 100Å, 10 x 250 mm) with a flow rate of 5 mL/min eluting with solvent (A: 0.1 % TFA in water B: 0.1 % TFA in MeCN) on a gradient of (2 → 100) %) solvent B over 15 min, t_R = 6.45 min) of the crude deprotected product afforded the TFA salt **104** as a colorless solid (45 mg, 32%). **^{1}H NMR**: (500 MHz, CD_3OD) δ (ppm) = 8.24 (s, 1H), 8.14 (s, 1H), 7.78 (d, *J* = 7.9 Hz, 1H), 7.58 (s, 1H), 7.45 – 7.41 (m, 2H), 7.26 (dd, *J* = 8.7, 2.0 Hz, 1H), 4.10 (q, *J* = 7.1, Hz, 1H), 2.84 (s, 6H), 2.63 (s, 3H), 1.63 (d, *J* = 7.0 Hz, 3H). **^{13}C NMR**: (125 MHz, CD_3OD) δ (ppm) = 169.0, 137.0, 136.2, 135.80, 135.78, 134.5, 132.2, 131.8, 128.8, 126.4, 125.4, 117.2, 116.5, 113.1, 112.1, 50.9, 37.6, 20.6, 17.8. **$[\alpha]_D^{20}$**: +14.9 (c = 8.3 mg/mL, MeOH). **HRMS**: (ESI) *m/z* calculated for $C_{20}H_{24}N_4O_3S$ $[M+H]^+$ 401.1642, found 401.1646. **IR (neat):** υ = 3255, 2984, 1669, 1478, 1201, 1134, 800, 734, 722, 583 cm^{-1}. **MP**: 138 – 142°C.

Preparation of *N*-Methyl Indole Moiety **105**

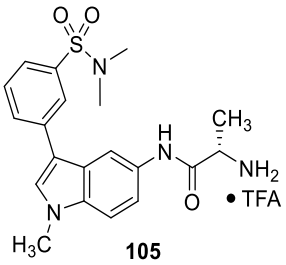

105

Synthesis of the title compound was performed by Anissa Kaghad.

Preparation of Acetophenone **119**

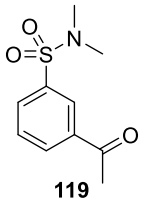

119

To a flame-dried round bottom flask containing 3-bromo-*N,N*-dimethylbenzenesulfonamide (996 mg, 3.77 mmol, 1.03 equiv.), dry THF (8.4 mL, 0.45 M) and a stir bar under a nitrogen atmosphere was added *n*-BuLi (1.5 mL of 2.0 M solution in hexanes, 3.66 mmol, 1.0 equiv.) dropwise. The resulting yellow mixture was stirred at -78 °C for 15 minutes, after which time *N*-methoxy-*N*-methylacetamide (378 mg, 3.66 mmol, 1.0 equiv.) in dry THF (1.4 mL, 2.6 M according to the acetamide) was added dropwise. Once the addition was complete, the reaction was stirred at -78 °C for 2.5 hours. The reaction mixture was quenched with the slow addition of NH_4Cl and diluted with Et_2O. The organic layer was dried with $MgSO_4$, filtered, and concentrated under reduced pressure. The crude residue was purified by column chromatography (silica gel, EtOAc:hexanes 36:64) to afford acetophenone **119** as a colorless solid (313 mg, 37 %). **^{1}H NMR**: (500 MHz, $CDCl_3$) δ (ppm) = 8.31 (dd, *J* = 1.8, 1.4 Hz, 1H), 8.17 (ddd, *J* = 7.8, 1.4, 1.1 Hz, 1H), 7.96 (ddd, *J* = 7.8, 1.8, 1.1 Hz, 1H), 7.67 (dd, *J* = 7.8, 7.8 Hz, 1H), 2.74 (s, 6H), 2.65 (s, 3H). **^{13}C NMR**: (125 MHz, $CDCl_3$) δ (ppm) = 196.5, 137.9, 136.9, 132.2, 131.8, 129.7, 127.4, 38.0, 26.8. **HRMS**: (ESI) *m/z* calculated for $C_{10}H_{13}NO_3S$ $[M+NH_4]^+$ 245.0954, found 245.0952. **IR** (neat): υ = 3672, 2980, 1685, 1428, 1337, 1257, 1158, 951, 799, 711, 673, 577, 528 cm^{-1}. **MP**: 69 - 72 °C.

Preparation of Bromo-Acetophenone **120**

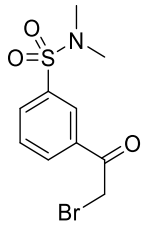

120

To a stirred solution of acetophenone **119** (237 mg, 1.04 mmol, 1.0 equiv.) in glacial acetic acid (1.1 mL, 0.95 M) was added Br_2 (0.52 mL of a 2.0 M bromine in AcOH solution, 1.04 mmol, 1.0 equiv.) dropwise. The reaction mixture was then stirred at room temperature for 85 minutes with close monitoring by TLC to avoid overreaction to the di-bromoketone. The reaction mixture was then diluted with CH_2Cl_2, washed with saturated aqueous $NaHCO_3$, and extracted with CH_2Cl_2 (3 times). The combined organic phases were dried with $MgSO_4$, filtered, and concentrated under reduced pressure to afford the crude residue of the reaction mixture. Purification of the crude residue by column chromatography afforded the bromoketone **120** as a colorless solid (215 mg, 67 %). **^{1}H NMR**: (500 MHz, $CDCl_3$) δ (ppm) = 8.35 (dd, *J* = 1.8, 1.5 Hz, 1H), 8.22 (ddd, *J* = 7.8, 1.8, 1.2 Hz, 1H), 8.01 (dt, *J* = 7.8, 1.4, 1.2 Hz, 1H), 7.71 (dd, *J* = 7.8, 7.8 Hz, 1H), 4.45 (s, 2H), 2.76 (s, 6H). **^{13}C NMR**: (125 MHz, $CDCl_3$) δ (ppm) = 190.1, 137.2, 134.7, 132.9, 132.6, 130.0, 128.2, 38.1, 30.2. **HRMS**: (ESI) *m/z* calculated for $C_{10}H_{12}BrNO_3S$ $[M+NH_4]^+$ 323.0060, found 323.0050. **IR** (neat): υ = 3672, 1708, 1337, 1156, 945, 804, 742, 578, 512 cm^{-1}. **MP**: 103 - 110 °C.

Preparation of α-Phenol Ketone **121**

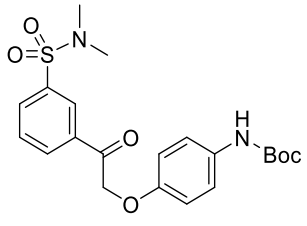

121

To a stirred solution of *tert*-butyl (4-hydroxyphenyl)carbamate (32 mg, 0.15 mmol, 1.1 equiv.) and K_2CO_3 (29 mg, 0.206 mmol, 1.5 equiv.) in acetone (1.4 mL, 0.1 M according to the bromoketone) was added bromoketone **120** (42 mg, 0.137 mmol, 1.0

equiv.) in acetone (1.4 mL, 0.1 M). The reaction mixture was then refluxed at 56 °C for 4 hours, after which the mixture was filtered and then concentrated under reduced pressure. Purification of the α-phenol ketone by column chromatography (silica gel, Et_2O:hexanes 7:3) afforded the α-phenol ketone **121** as a colorless solid (30 mg, 50 %). **^{1}H NMR**: (500 MHz, $CDCl_3$) δ (ppm) = 8.39 (dd, *J* = 1.8, 1.8 Hz, 1H), 8.22 (ddd, *J* = 7.9, 1.4, 1.4 Hz, 1H), 8.00 (dt, *J* = 7.8, 1.3 Hz, 1H), 7.69 (dd, *J* = 7.9, 7.8 Hz, 1H), 7.2 (d, *J* = 9.0 Hz, 1H), 6.87 (d, *J* = 9.0 Hz, 2H), 6.35 (s, 1H), 5.19 (s, 2H), 2.74 (s, 6H), 1.50 (s, 9H). **^{13}C NMR**: (125 MHz, $CDCl_3$) δ (ppm) = 194.3, 153.8, 153.z1, 137.1, 135.5, 132.9, 132.4, 132.4, 129.9, 127.7, 120.6, 115.5, 80.6, 72.0, 38.0, 28.5. **HRMS**: (ESI) *m/z* calculated for $C_{21}H_{26}N_2O_6S$ $[M+NH_4]^+$ 452.1850, found 452.1844. **IR** (neat): υ = 3677, 3374, 2980, 1718, 1700, 1522, 1341, 1231, 1155, 1053, 726, 694, 581, 520 cm^{-1}. **MP**: 150 – 156 °C.

Chapter 3. Application of Sequential Proline Catalyzed α-Chlorination and Aldol Reactions in the Total Synthesis of 1-Deoxygalactonojirimycin

Adapted from the Canadian Journal of Chemistry, 2018, volume 4, pages 144-147 (Michael Meanwell,[†] Mathew Sutherland,[†] and Robert Britton). [†]These authors contributed equally. Used with permission.

3.1. Iminosugars in Medicine

Polyhydroxylated piperidines or iminosugars have received much attention as biological tools and drug leads with potential applications in the treatment of cancer, viral infections, diabetes, and lysosomal storage disorders.[65–67] Perhaps most notably, these iminosugars have proven to be excellent inhibitors of glycosidases and glycosyltransferases[65,67] as they bear the peripheral functionality of the parent sugar and the nitrogen atom is protonated under physiological conditions. Thus, piperidine iminosugars generate an oxycarbenium ion surrogate that mimics the transition state of the enzyme-catalyzed hydrolysis of carbohydrates (see inset, Figure 3.1).[66]

For example, the polyhydroxypiperidines *N*-butyl-deoxynojirimycin (miglustat: **124**)[68] and *N*-hydroxyethyldeoxynojirimycin (miglitol: **125**)[69] have been approved for the treatment of type I Gaucher's disease and non-insulin-dependant diabetes, respectively.[65] Additionally, 1-deoxygalactonojirimycin (migalastat: **126**),[70] a pharmacological chaperone for α-galactosidase A mutants,[71] has been approved for the treatment of Fabry disease.[65] Unfortunately, despite their potentially broad use in medicine,[65,67] a general reliance on carbohydrate- or amino acid-derived starting materials, and low yielding, lengthy synthetic sequences with multiple protecting group or oxidation state manipulations, present challenges to incorporating iminosugars in medicinal chemistry campaigns.[72]

To address these challenges, we have recently developed several convenient strategies for the synthesis of hydroxypyrrolidines and piperidines that exploit readily available α-chloroaldehydes[73–78] or oxazoles[79] as versatile iminosugar building blocks. Here, we describe a short enantioselective synthesis of (+)-1-deoxygalactonojirimycin

(**126**) that relies on a convenient one-pot proline-catalyzed α-chlorination and aldol reaction[24] of aldehydes to rapidly construct the carbohydrate scaffold of **126** from readily available, achiral materials. To the best of our knowledge, this synthesis constitutes the first enantioselective synthesis of 1-deoxygalactonojirimycin that does not rely on chiral pool starting materials or biocatalysis.

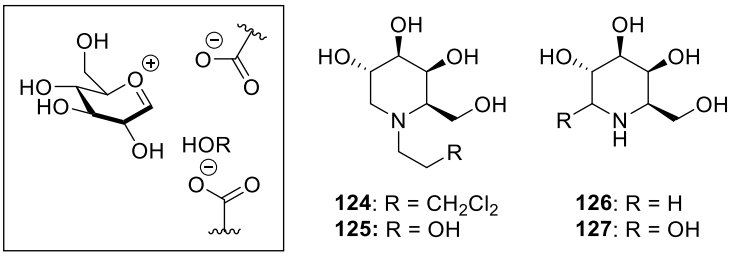

Figure 3.1: Iminosugar inhibitors of carbohydrate processing enzymes and the oxocarbenium ion intermediate in enzyme catalyzed glycosidic bond cleavage (see inset).

3.2. Previous Synthetic Routes Used to Access 1-Deoxygalactonojirimycin

1-Deoxygalactonojirimycin (**126**) is the reduced form of the naturally occurring iminosugar galactostatin (**127**) (Figure 3.1),[80] and was originally reported as a synthetic product by Paulsen in 1980.[70] Owing to its potentially useful biological activities, more than 30 total syntheses of **126** have been reported that range in length from 5 to more than 15 steps. [81,82,91–100,83,101–108,84–90] Many of these syntheses are related by their reliance on chiral starting materials that include various carbohydrates, amino acids, and tartaric acid, or their use of biocatalysis to introduce key stereogenic centers. Of particular note, Stubbs has reported a highly efficient 5-step synthesis of 1-deoxygalactonojirimycin that involves a reductive amination of tetrol **128**.[92] Likewise, Kato and Fleet have reported a short synthesis of **126** that relies on the reductive amination of *L*-tagatose-derived azide **130**.[95] An early synthesis by Wong involved an enzyme-promoted aldol reaction that produced the azide **129**, which subsequently underwent phosphate cleavage and reductive amination to afford **126**.[104] Recently, in an effort to avoid costly carbohydrate-based approaches and potentially hazardous azidation reactions, researchers at GlaxoSmithKline have also reported a microbial synthesis of 1-deoxygalactonojirimycin.[109]

Scheme 3.1: Efficient Synthetic Strategies Used for the Synthesis of 1-Deoxygalactonojirimycin

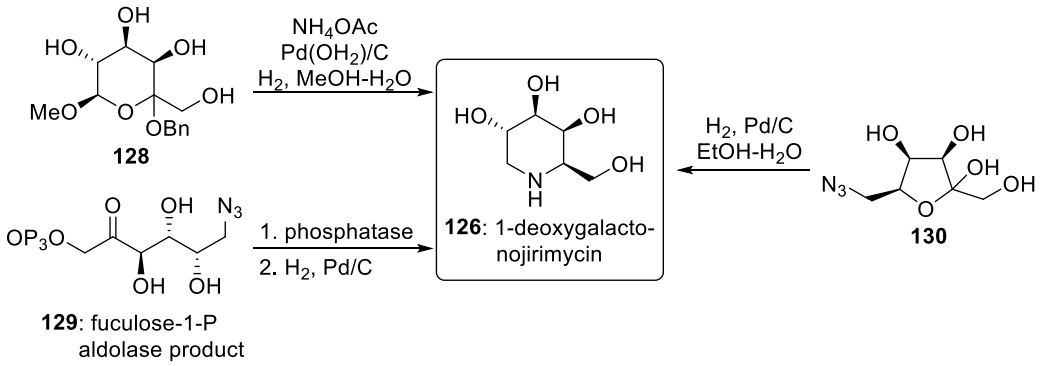

3.3. Synthetic Strategy

The Britton group has previously reported the tandem α-chlorination-aldol reaction that delivers *syn*-chlorohydrins **13** (Scheme 1.5) in good yield, diastereoselectivity and enantioselectivity. Exploiting this advance, we envisaged that a short synthesis of 1-deoxygalactonojirimycin could be realized that relies on a similar reaction involving the suitably protected β-aminopropanal derivative **131** followed by a subsequent reductive amination/annulation event.

As depicted in Scheme 3.2, we were delighted to find that the (*R*)-proline-catalyzed α-chlorination of commercially available aldehyde **131** and subsequent aldol reaction with dioxanone **11** afforded the chlorohydrin **132** in good yield and enantiomeric excess (93 % ee). Analysis of the ^{1}H NMR spectrum recorded on chlorohydrin **132** ($CDCl_3$, 600 MHz) revealed that this material exists as an interconverting mixture of the ketochlorohydrin **132** and two diastereomeric cyclic hemiaminals. As such, when a purified mixture of these materials was hydrogenated in methanol, the piperidine **133** was produced in good yield (54 %), with the expected diastereoselectivity (d.r. = 3:1) favouring the galactose-configured iminosugar **133**. Removal of the acetonide protecting group under acidic conditions gave access to the previously undescribed 2-chloro-1,2-dideoxygalactonojirimycin (**137**, see Scheme 3.2, inset) in 85 % yield.

Alternatively, treatment of the chloropiperidine with sodium hydroxide in ethanol afforded epoxide **134**. While we had anticipated that the regioselective opening of the epoxide with water would be a facile process based on similar reactions of *N*-protected derivatives of **134**,[99] under a variety of reaction conditions we were unable to transform

the epoxide **134** directly into 1-deoxygalactonojirimycin (**126**). Thus, to remedy this situation, epoxide **134** was first converted into the *N*-Boc derivative **135**, a known precursor to **126** previously prepared from Garner's aldehyde by Takahata.[99] Heating the epoxide **135** with H_2SO_4 in a mixture of 1,4-dioxane and water[99] then cleanly afforded the iminosugar **126** in excellent yield. The spectral data (^{1}H NMR, ^{13}C NMR) derived from our synthetic (+)-1-deoxygalactonojirimycin were consistent with that reported previously for this material. [81,82,91–100,83,101–108,84–90] Notably, the propensity for the *N*-Boc epoxide **135** to undergo clean, regioselective epoxide opening while the *N*-H epoxide **134** failed to do so under identical reaction conditions suggests that the carbamate function may play a key role in this reaction (*e.g.*, **136**). Alternatively, protonation of the unprotected epoxy amine **134** may preclude acid promoted epoxide opening.

Scheme 3.2: Enantioselective Synthesis of 1-Deoxygalactonojirimycin (126) and 2-Chloro-1,2-dideoxygalactonojirimycin (137)

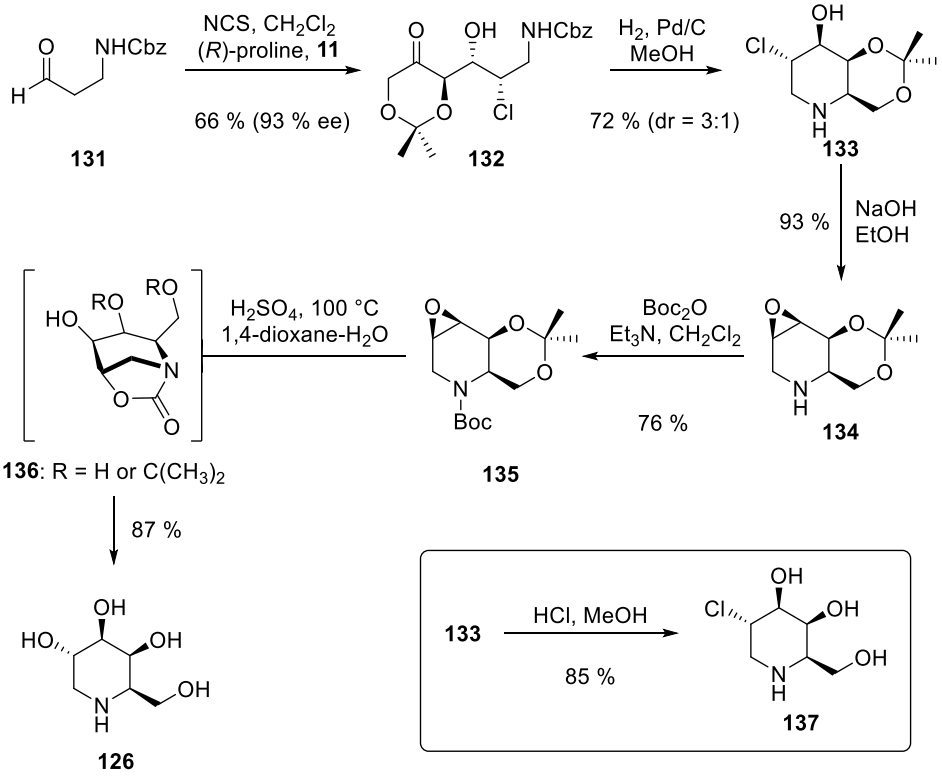

3.4. Summary

By exploiting a proline-catalyzed aldehyde α-chlorination and aldol reaction we have realized a concise and convenient enantioselective synthesis of 1-

deoxygalactonojirimycin that does not rely on chiral pool starting materials or biocatalysis. Notably, this new route delivers **126** in only 5 steps from commercially available, achiral materials in a 22 % yield. The use of inexpensive and readily available reagents makes this a particularly appealing process for the synthesis of 1-deoxygalactonojirimycin and may be adapted for the rapid preparation of analogues through alternative epoxide opening reactions.

3.5. Experimental Information

3.5.1. General Considerations

Please see **General Considerations**, section 2.5.1.

3.5.2. Preparation and Characterization Data

*NMR spectra for all compounds from Chapter 3 can be found in Appendix B.

Preparation of Piperidine **133**

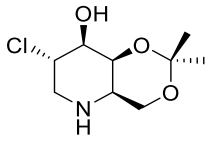

133

A sample of benzyl (3-oxypropyl)carbamate (0.50 g, 2.42 mmol) was added to a stirred suspension of NCS (0.34 g, 2.4 mmol, 1.05 equiv.), (*R*)-proline (0.22 g, 1.9 mmol, 0.80 equiv.), and 2,2-dimethyl-1,3-dioxan-5-one (0.30 mL, 2.53 mmol, 1.05 equiv.) in 16 mL of CH_2Cl_2 at room temperature. After 24 h the mixture was diluted with CH_2Cl_2 (20 mL) and washed twice with H_2O and once with brine. The organic layer was then dried over $MgSO_4$, concentrated under reduced pressure, and the crude product was purified by flash chromatography (EtOAc:pentanes 25:75) to afford a mixture of the chlorohydrin **132** along with the corresponding diastereomeric hemiacetals as a yellow oil (0.59 g, 66 % yield). Through a solution of this purified mixture (0.34 g, 0.93 mmol) and Pd/C (50 % by weight) in MeOH (0.10 M) was bubbled H_2 gas for 1 hr. The reaction vial was then sealed and left for 12 h. The reaction mixture was then filtered, concentrated under reduced pressure, and the crude product was purified by flash chromatography (MeOH-

CH_2Cl_2 5:95) to afford the piperidine **133** as a yellow oil (0.15 g, 72 % yield, dr = 3:1). **^{1}H-NMR** (600 MHz, CD_3OD): δ 4.25 (d, *J* = 3.0 Hz, 1H), 4.16 (dd, *J* = 12.2, 2.2 Hz, 1H), 4.01 (ddd, *J* = 10.8, 10.8, 4.8 Hz, 1H), 3.65 (dd, *J* = 12.2, 0.9 Hz, 1H), 3.51 (dd, *J* = 10.2, 3.2, Hz, 1H), 3.33 (dd, *J* = 13.7, 5.0 Hz, 1H), 2.66 (d, *J* = 13.3 Hz, 1H), 2.56 (br s, 1H), 1.47 (s, 3H), 1.41 (s, 3H); **^{13}C-NMR** (150 MHz, CD_3OD): δ 100.6, 75.8, 72.3, 64.5, 59.8, 52.6, 52.4, 29.7, 18.5; **$[\alpha]_D^{20}$** = -97 (1.4 mg/mL, $CHCl_3$); **HRMS** (EI^+) *m/z* calculated for $C_9H_{16}ClNO_3$ $[M+H]^+$ expected 222.0891 found 222.0842 **IR:** (neat) υ = 3674, 3317, 2990, 1380, 1198, 1105, 1061, 819 cm^{-1}.

Determination of enantiomeric excess of **133:**

Using a 1:1 mixture of (S):(R) proline, a racemic sample of the chlorohydrin **132** was prepared. The optically enriched and racemic samples of chlorohydrin **132** were converted into their corresponding cyclized products **133**. These were then monoacylated with (*R*)-(+)-MTPA-OH (3 equiv.), DIC (6 equiv.), pyridine (3 equiv.), and 4-dimethylaminopyridine (cat.) in CH_2Cl_2 (0.10 M). By analysis of ^{19}F-NMR it was determined that the enantiomeric excess was 93 %. Note: Following the same procedure, the optically enriched cyclized product **132** was also monoacylated with (*S*)-(+)-MTPA-OH whereby analysis of ^{19}F-NMR also revealed an enantiomeric excess of 93 %.

Preparation of Epoxide **134**

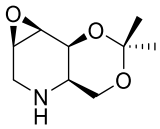

134

The piperidine **133** (21.2 mg, 0.096 mmol) was dissolved in 0.48 mL of EtOH and NaOH (2.0 M aq., 1.2 equiv) was added. The reaction mixture was stirred for 72 hours then concentrated under reduced pressure. The crude product was purified by flash chromatography (MeOH-CH_2Cl_2 5:95) to afford epoxide **134** as a colourless oil (16.4 mg, 93 % yield). **^{1}H-NMR** (500 MHz, $CDCl_3$): δ 4.17 (dd, *J* = 4.5 Hz, 1H), 4.01 (dd, *J* = 12.1, 5.7 Hz, 1H), 3.53 (dd, *J* = 12.1, 5.1 Hz, 1H), 3.39 (dd, *J* = 4.4 Hz, 1H), 3.31 (dd, *J* = 15.3 Hz, 1H), 3.13 (d, *J* = 4.3 Hz, 1H), 3.00 (d, *J* = 15.3 Hz, 1H), 2.53 (m, 1H), 1.46 (s, 3H),

1.45 (s, 3H). **[α]$_D^{20}$** = -19.4 (1.3 mg/mL, $CHCl_3$); **IR:** (neat) υ = 2921, 1461, 1379, 1223, 1101 cm^{-1}. **HRMS** (EI^+) calculated for $C_9H_{15}NO_3$ $[M+H]^+$ 186.1125, found 186.1098.

Preparation of *N*-Boc-Piperidine **135**

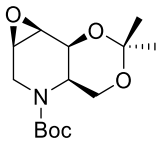

135

To a solution of epoxide **134** (18.3 mg, 0.0989 mmol) and triethylamine (0.035 mL, 0.248 mmol, 2.5 equiv.) in 0.41 mL CH_2Cl_2 was added Boc anhydride (28.9 mg, 0.132 mmol, 1.3 equiv.). The reaction mixture was then stirred for 12 h at room temperature, then diluted with 1 mL of CH_2Cl_2. The organic layer was separated and washed sequentially with 0.5 mL $NaHCO_3$, 0.5 mL H_2O, and 0.5 mL brine. The organic layer was then dried over $MgSO_4$, filtered, and concentrated under reduced pressure. The crude product was purified by flash chromatography (EtOAc-pentanes 30:70) to afford **135** as a yellow oil (21.3 mg, 76% yield). The spectroscopic data recorded on **135** was consistent with that reported previously.[99] **^{1}H-NMR** (500 MHz, $CDCl_3$): δ 4.43 (d, *J* = 6.7 Hz, 1H), 4.22 (br s, 1H), 4.14 (dd, *J* = 10.6 Hz, 1H), 3.71 (m, 3H), 3.53 (m, 2H), 1.67 (s, 3H), 1.47 (s, 9H), 1.44 (s, 3H); **^{13}C-NMR** (125 MHz, $CDCl_3$): δ 155.0, 97.8, 80.9, 68.2, 59.8, 53.6, 53.0, 47.2, 40.4, 30.0, 28.5, 23.2; **[α]$_D^{20}$** = -10.3 (1.2 mg/mL, $CHCl_3$); **HRMS** (EI^+) *m/z* calculated for $C_{14}H_{23}NO_5$ $[M+H]^+$ 286.1649; found 286.1649.

Determination of relative and absolute stereochemistry for **135:**

Comparison of **135** with that of previously reported ^{1}H and ^{13}C NMR confirmed relative stereochemistry.[65] Additionally, comparison of $[\alpha]_D$ with that of previously reported **135** confirmed absolute stereochemistry.[65]

Preparation of 1-Deoxygalactonojirimycin **126**

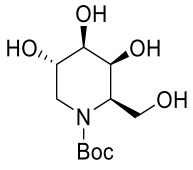

126

To a solution of epoxide **135** (7.9 mg, 0.0277 mmol) in a 2:3 mixture of H_2O-1,4-dioxane (1.15 mL) was added H_2SO_4 (0.075 mL) and the resulting mixture was heated to 100 °C and stirred at this temperature for 3 h. The reaction mixture was then treated with Dowex monosphere 550A (hydroxide form), filtered, and concentrated under reduced pressure to afford crude **126**. The crude reaction product was purified by semi-preparative HPLC eluting with solvent (A: 0.1 % TFA in H_2O B: 0.1 % TFA in ACN) on a gradient of 0 % → 5 % solvent B over 15 minutes to yield purified **126** (6.6 mg, 87 %) as a white solid. The spectroscopic data recorded on 1-deoxygalactonojirimycin•TFA (**126**) were consistent with that reported previously. [81,82,91–100,83,101–108,84–90] **^{1}H-NMR** (600 MHz, D_2O): δ 4.17 (m, 1H), 4.09 (m, 1H), 3.81 (m, 1H), 3.65 (dd, *J* = 9.6, 2.8 Hz, 1H), 3.52 (dd, *J* = 12.3, 5.3 Hz, 1H), 3.42 (m, 1H), 2.88 (dd, J 12.0 Hz, 1H); **^{13}C-NMR** (150 MHz, D_2O): δ 72.9, 66.9, 64.6, 60.1, 59.1, 46.1. **$[\alpha]_D^{20}$** = + 43.7 (0.4 mg/mL, H_2O); **HRMS** (EI^+) *m/z* calculated for $C_6H_{13}NO_4$ $[M+H]^+$ 164.0917, found 164.0751.

Preparation of 2-Chloro-1,2-dideoxygalactonojirimycin **137**

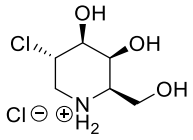

137

A sample of the piperidine **133** (0.031 g, 0.139 mmol) was dissolved in MeOH (0.70 mL) and 1 M HCl (0.14 mL) was added. The reaction mixture was heated to 35 °C and stirred at this temperature for 24 h. The solvent was then removed under reduced pressure to give pure **137** (0.022 g, 85%), which required no additional purification. **^{1}H-NMR** (500 MHz, CD_3OD): δ 4.25 (ddd, *J* = 12.3, 10.0, 5.3 Hz, 1H), 4.03 (br s, 1H), 3.80 (d, *J* = 6.9 Hz, 1H), 3.66 (dd, *J* = 10.0, 2.7 Hz, 1H), 3.58 (dd, *J* = 12.7, 5.2, Hz, 1H), 3.40

(dd, *J* = 6.8 Hz, 1H), 3.18 (dd, *J* = 12.6 Hz, 1H); **^{13}C NMR** (125 MHz, CD_3OD): δ 75.0, 68.8, 62.2, 60.6, 55.3, 48.7; **$[\alpha]_D^{20}$** = + 9.8 (*c* 1.0 in MeOH). **HRMS** (EI^+) m/c calculated for $C_6H_{12}ClNO_3$ $[M+H]^+$ 182.0578, found 182.0540. **IR** (neat): υ = 3290, 2929, 2799, 1589, 1405, 1106, 1059, cm^{-1}.

Chapter 4. Development of a Tandem Cleavage Route to Produce Enantioenriched α-Substituted Aldehydes

4.1. Existing Synthetic Routes to α-Haloaldehydes

The synthesis of an α-haloaldehyde was first reported in 1871 when Schroder formed racemic α-chloro-3-methylbutanal **138** in a reaction between chlorine gas and the corresponding aldehyde, as seen in Scheme 4.1.[110]

Scheme 4.1: Schroder's First Synthesis of an α-Chloroaldehyde

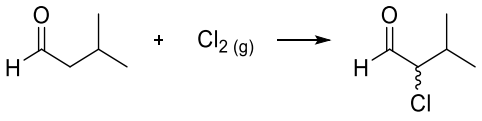

138

Much later in 1964, enantioenriched α-haloaldehydes made an appearance as precursors of 2-deoxy-2-halogen-substituted carbohydrates (e.g., **139**). At the time, fluorine-containing carbohydrates such as **139** were used as Positron Emission Topography (PET) imaging agents. A robust method of synthesizing these 2-deoxy-2-fluoro carbohydrates involves the ^{18}F substitution of terminal epoxides (*e.g.*, **140**) and *in situ* oxidation to install the α-fluoroaldehyde (**141**). Subsequent deprotection and cyclization to form the ring yields the desired carbohydrate analogue **126**, as seen in Scheme 4.2.[111]

Scheme 4.2: Synthesis of ^{18}F PET Imaging Agents via α-Fluoroaldehydes

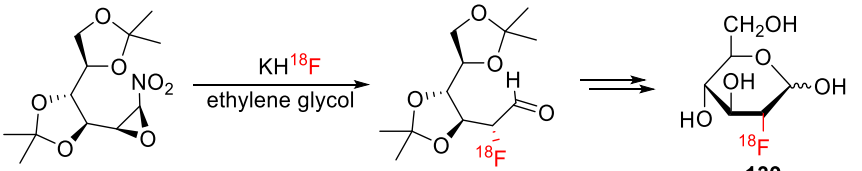

140 **141** **139**

PET imaging agent

This early example of α-haloaldehydes in medicinally relevant syntheses sparked interest in the enantioselective synthesis of α-fluoroaldehydes that could then be used to access PET imaging agents. From these studies and others, the ability to transform both terminal epoxides and epoxy-alcohols such as **142** into α-haloaldehydes attracted

attention. The epoxy-alcohols can be transformed into α-bromo (**144**), α-chloro (**145**), or α-iodo (**146**) aldehydes through stereospecific nucleophilic opening of the epoxide by halides, followed by oxidative cleavage of the resultant 1,3-diol system (**143**), as seen in Scheme 4.3.[112]

Scheme 4.3: Epoxide Opening by Halogen Anions Followed by Oxidative Cleavage to Afford Enantioenriched α-Haloaldehydes

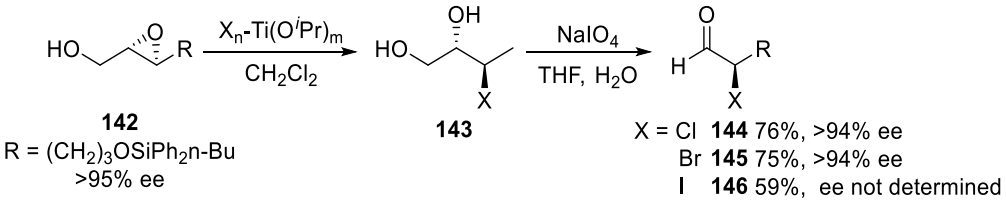

One of the first examples of the synthesis of enantioenriched α-halogenated aldehydes from achiral starting materials was reported not long after by Duhamel and Plaquevent. These chemists produced optically enriched 2-chloro-3,3-dimethylbutanal **148** from the corresponding enamine **147** using a chiral proton source, albeit with moderate enantioselectivity (33 % ee).[113]

Scheme 4.4: Early Example of the Stereoselective Synthesis of α-Chloroaldehydes

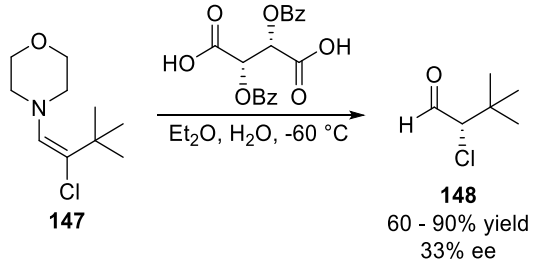

Beyond these examples, the synthesis of α-haloaldehydes in good enantiomeric excess tended to rely heavily upon chiral pool starting materials. Notably, Schurig developed a two-step procedure starting from amino acids to synthesize enantioenriched chlorohydrins[114] which De König then oxidized to afford the corresponding α-chloroaldehydes (*e.g.*, **149**) with high enantiomeric excess, as seen in Scheme 4.5.[48] Unfortunately, this method is limited to substrates accessible from amino acids, which restricts the scope of aldehydes that can be accessed.

Scheme 4.5: Schurig and De Koning's Sequential Synthesis of α-Chloroaldehydes from Amino Acid Starting Materials

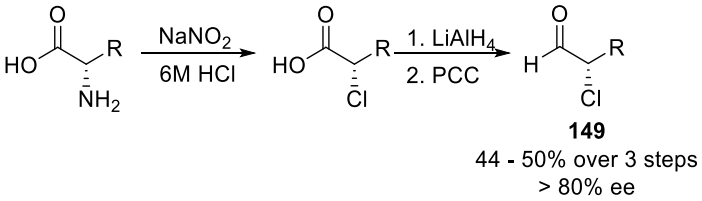

In the last two decades, numerous groups have begun to develop general methods for synthesizing α-haloaldehydes in a more direct fashion. Most methods rely on the use of chiral secondary amine catalysts, capable of forming an enamine on the aldehyde of choice. This enamine (*e.g.*, **150**) then reacts in a stereoselective manner with an electrophilic source of a halogen, as seen in Scheme 4.6.

Scheme 4.6: General Organocatalytic Cycle for the Direct Enantioselective α-Halogenation of Aldehydes

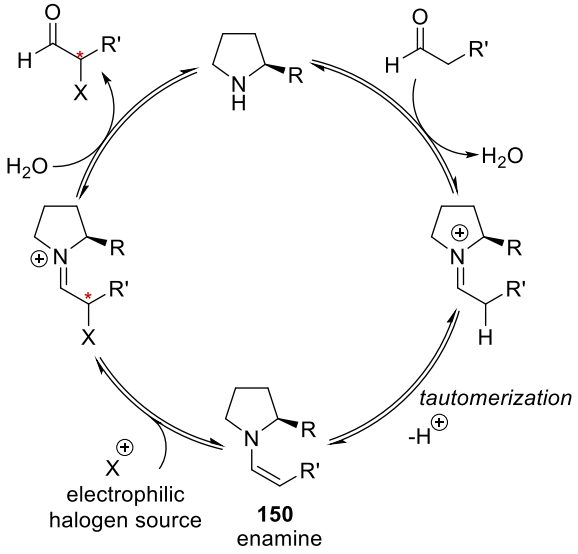

This reactivity mode has been utilized extensively by the groups of Jørgensen,[115,116] MacMillan,[117,118] Enders,[119] and Barbas III[120] in the synthesis of α-chloro, α-bromo, and α-fluoroaldehydes. These methods utilize proline- or pyrrolidine-based organocatalysts **151** - **153** (Figure 4.1) and a variety of electrophilic sources of chlorine and fluorine such as **154, 155**, and **16** (Figure 4.2) to facilitate the α-halogenation of aldehydes.

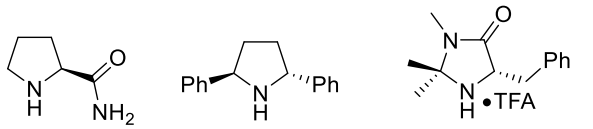

Figure 4.1: Organocatalysts used to perform stereoselective α-halogenation of aldehydes.

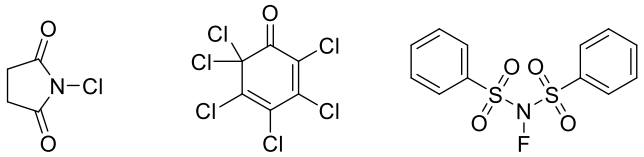

Figure 4.2: Electrophilic halogen sources used for organocatalyzed α-halogenation of aldehydes.

Using these catalysts and electrophilic halogen sources, a variety of α-chloro and α-fluoroaldehydes can be synthesized in good yields and good to excellent enantiomeric excess. Although a facile reaction, subsequent *in situ* racemization of the products leads to decreased enantiomeric excess for certain products, particularly the fluorinated derivatives. Another issue is the lack of generality of these reactions. Most organocatalytic methods struggle to perform well on substrates other than simple aliphatic aldehydes, leading to decreased yields and optical purity in more elaborate scenarios.

Recently, MacMillan has developed a novel α-chlorination of aldehydes which relies on their activation to a Singly Occupied Molecular Orbital (SOMO) state when coupled with the imidazolidinone catalyst **156**.[121] Notably, this method has the advantage of utilizing inexpensive and readily available nucleophilic sources of chlorine such as LiCl or NaCl. The chloride ion is incorporated through nucleophilic attack on the terminal enamine position, as in Scheme 4.7.

Scheme 4.7: Proposed SOMO-Catalyzed Mechanism for the α-Halogenation of Aldehydes by Macmillan

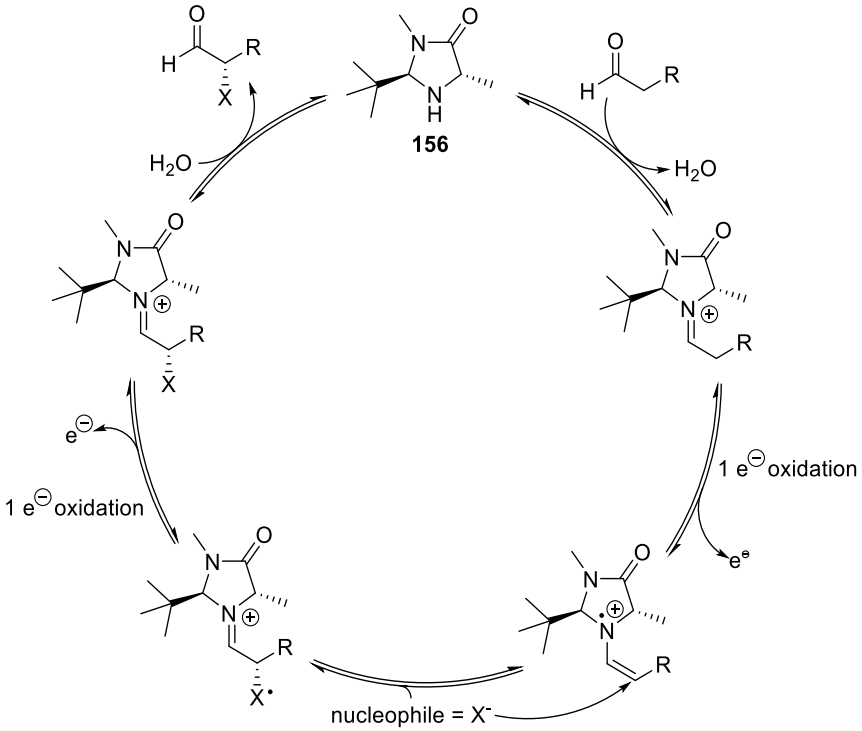

Density Functional Theory (DFT) calculations (later supported by experimental evidence) also suggested that the imidazolidinone catalyst **156** would be unable to condense on the produced α-chloroaldehydes due to occlusion of the nitrogen lone pair by the neighboring *tert*-butyl group. This theory held in practice, eliminating post-product racemization by enamine formation, and enabled the synthesis of α-chloroaldehydes bearing mostly aliphatic functional groups in good yields (75 – 95%) and enantiomeric excess (91 – 96% ee).[121]

Significantly less work has been performed to explore catalytic α-bromination and α-iodination of aldehydes through organocatalysis. Jørgensen reported use of the chiral diphenyl pyrrolidine catalyst **152** in combination with *N*-bromosuccinimide (NBS) and *N*-iodosuccinimide (NIS). However, other more complex halogen donors were required due to initial low yields and enantioselectivity. Even at -24 °C, the reaction between an aldehyde and NBS facilitated by **152** gave a moderate 45 % ee (the equivalent chlorination reaction occurred with 90 % yield and 94 % ee). Optimization of the bromine source to dibromodienone **157** and addition of benzoic acid as an additive increased the utility greatly, affording aliphatic α-bromoaldehydes (*e.g.*, **158**) in good yields and enantiopurity, as seen in Table 4.1.

Table 4.1: Enantioenriched α-Bromoaldehydes Synthesized by Jørgensen

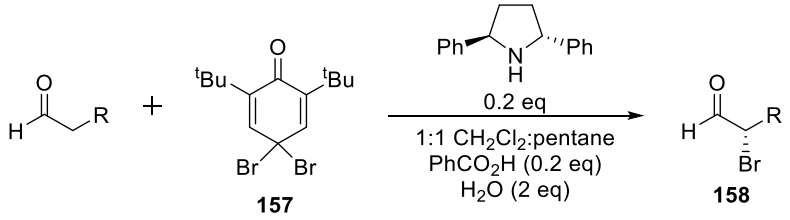

Entry	R	Isolated yield (%)	ee (%)
1		87	96
2		94	89
3		72	77
4	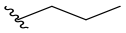	82	85
5	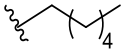	95	68
6	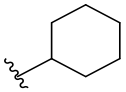	92	73
7		76	76

Maruoka has recently shown that a variety of α-bromo[122] and α-iodoaldehydes[123] (*e.g.,* **159**) can be produced in good yields and enantioselectivities by using the amine catalyst **160** and either the dibromodienone **157** or NIS **161** as the halogen donor, as seen in Scheme 4.8.

Scheme 4.8: Catalytic α-Bromo and α-Iodination of Aldehydes Developed by Maruoka. Iodination Yields are of the Corresponding Methyl Esters

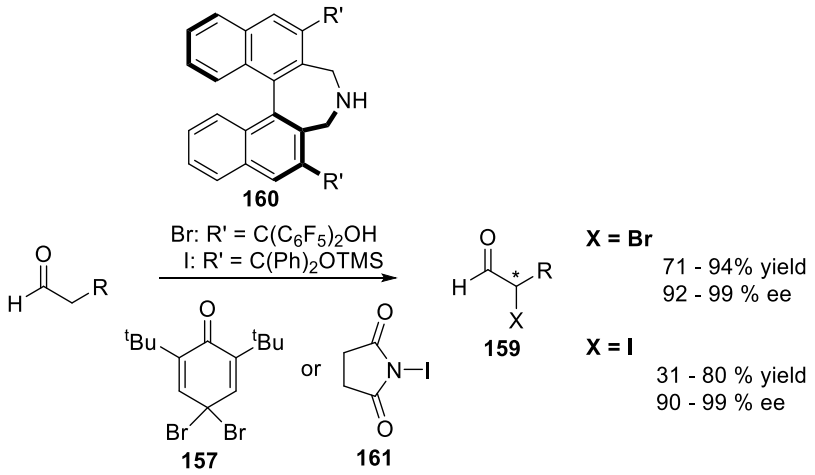

Although many routes to synthesize α-haloaldehydes exist, most suffer from practical issues. Catalysts cost can often be prohibitive if a large-scale process is desired (Jørgenson's biphenyl pyrrolidine is $543 USD / 100 mg). For most organocatalytic routes, the conditions are also not sufficiently robust to tolerate a wide variety of functional groups, though they show good yields and enantioselectivities for simple aliphatic substrates. Finally, approaches utilizing chiral pool starting materials are hindered by the availability of the required enantioenriched substrates.

4.2. Utility of Enantioenriched α-Haloaldehydes

4.2.1. General Reactivity of α-Haloaldehydes

Aldehydes bearing a halogen at the alpha position have become important intermediates and starting materials in modern organic synthesis. Due to their bifunctional nature, they can often be used to facilitate the synthesis of complex compounds in short order. Furthermore, the proximity of the α-halogenated to the electrophilic aldehyde often imparts diastereoselectivity to reactions at the carbonyl.

α-Chloroaldehydes first received attention as electrophiles in diastereoselective organometallic reactions in 1959 when Cornforth reported the addition of Grignard reagents into α-chloroaldehydes.[124] The resulting stereoselectivity was unexpected, and from these studies Cornforth proposed his now widely accepted model for diastereoselective addition of nucleophiles into α-haloaldehydes, as seen in Scheme 4.9.

Scheme 4.9: Source of Diastereoselectivity Predicted by the Cornforth Model

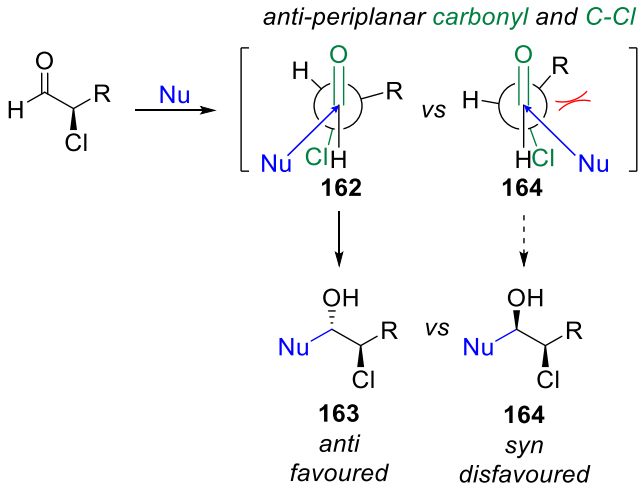

The Cornforth model suggests that the determining factor in the pre-addition aldehyde structure is the anti-periplanar arrangement of the carbonyl and halogen substituent, which reduces energy by minimizing electrostatic dipole effects.[124] The incoming nucleophile ("Nu") approaches the carbonyl carbon along the Burgi-Dunitz angle from either the side of the carbonyl having the α-hydrogen atom (**162**, favoured), or the α-R group (**164**, disfavoured due to steric hindrance, see)(in Scheme 4.9). The difference in energy between the two transition states leads to a bias for the *anti*-chlorohydrin **163** over the *syn*-chlorohydrin **165**.

4.2.2. Synthesis of Heterocycles

α-Haloaldehydes can also be used for the synthesis of heterocycles of different sizes. Reduction of α-chloroaldehydes affords a terminal chlorohydrin of the form **166**, which under basic conditions can be reliably transformed into a chiral terminal epoxide such as **167** in Scheme 4.10. Terminal epoxide formation is one example reported by Amatore *et. al.* in support of their development of α-chloroaldehydes as enantioenriched linchpin intermediates for the preparation of a variety of useful synthons.[121] Winter *et. al.* exploited terminal epoxide formation as a method for derivatizing readily available terpene-derived aldehydes into useful intermediates.[125] Opening of these chiral epoxides (**168** or **169**) by a *tert*-butyllithium-mediated cyclization afforded vinylcylopropanes, while opening via carbon-based nucleophiles formed several compounds responsible for pleasant fragrances such as the aerengic lactone in short order, as seen in Scheme 4.10.[125] Furthermore, Olugbeminiyi *et. al.* developed a general method of synthesizing

enantioenriched terminal aziridines in good yield and enantiomeric excess, accessed via reductive amination and base-induced cyclization of α-chloroaldehydes, as seen in Scheme 4.10.

Scheme 4.10: Use of α-Chloroaldehydes to Form 3-Membered Heterocycles and Valuable Derivatives

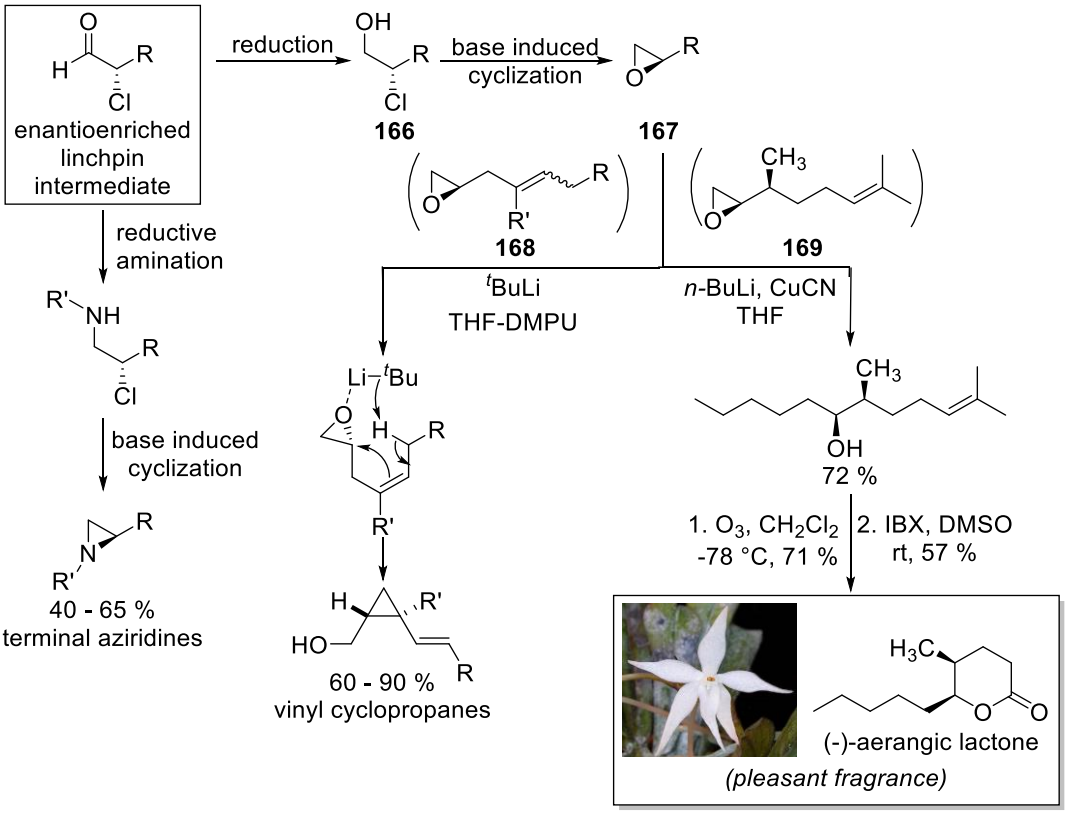

A three step sequence to synthesize chiral morpholines or piperazines (*e.g.*, **171**) from α-chloroaldehydes has been developed by O'Reilly and Lindsley that uses the corresponding triflate derivatives (*e.g.*, **170**) of chlorohydrins in a dual substitution reaction to afford the desired heterocycles in moderate yields and good optical purity, (Scheme 4.11).[126] Notably, the chiral morpholine **172**, a specific dopamine subtype 4 (D_4) antagonist with anti-psychotic behaviour, was synthesized in an optically pure fashion in 98 % ee, with an improved overall yield (Scheme 4.11, inset).

Scheme 4.11: Synthesis of Chiral Morpholines, Piperazine, and Azetidines from α-Chloroaldehydes

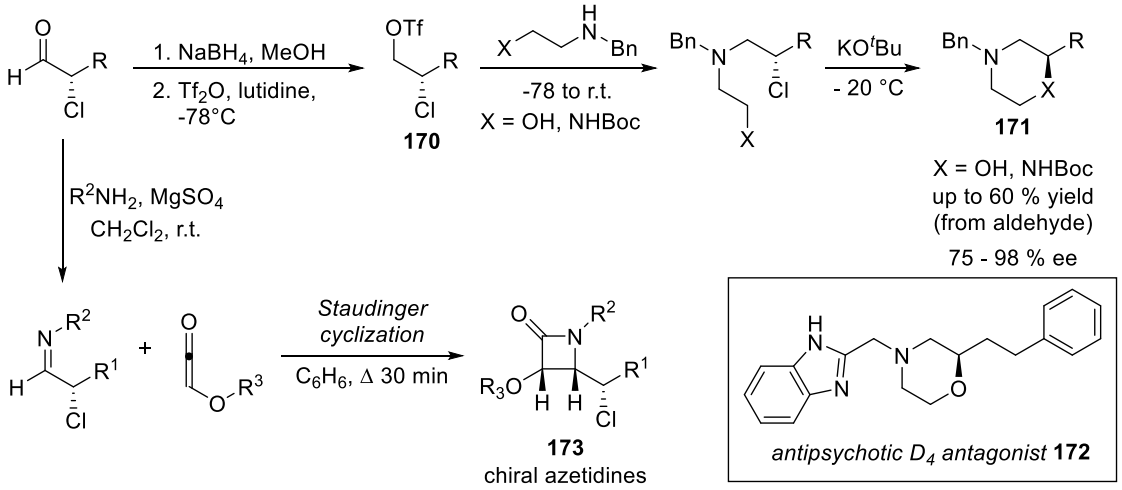

Staudinger cycloadditions of imines generated from chiral α-chloroaldehydes have been utilized by De Kimpe in the construction of chiral azetidines (*e.g.*, **173**) and pyrrolidines, as seen in Scheme 4.11. This reaction required exquisitely pure α-chloroaldehydes and would not perform with those produced using organocatalytic methods.[127] However, De Koning's sequence beginning with amino acids produced α-chloroaldehydes of sufficient purity for the reaction, though it limited the available substrate scope.[48,127]

4.2.3. Ongoing Applications in Total Synthesis in the Britton Group

α-Chloroaldehydes have found use in several total synthesis projects in the Britton group, including the syntheses of biselide A (**174**) and ongoing synthesis of eribulin (**175**), depicted in Figure 4.3.

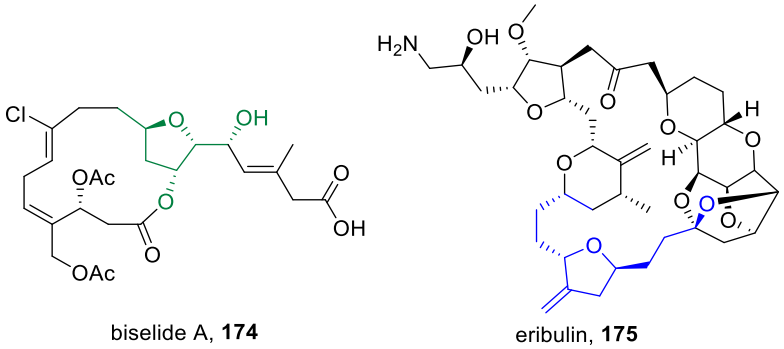

Figure 4.3: Britton group total synthesis projects using enantioenriched α-chloroaldehydes.

Scheme 4.12: Synthetic Routes to Total Synthesis Targets Biselide A and Eribulin via Optically Enriched α-Chloroaldehydes

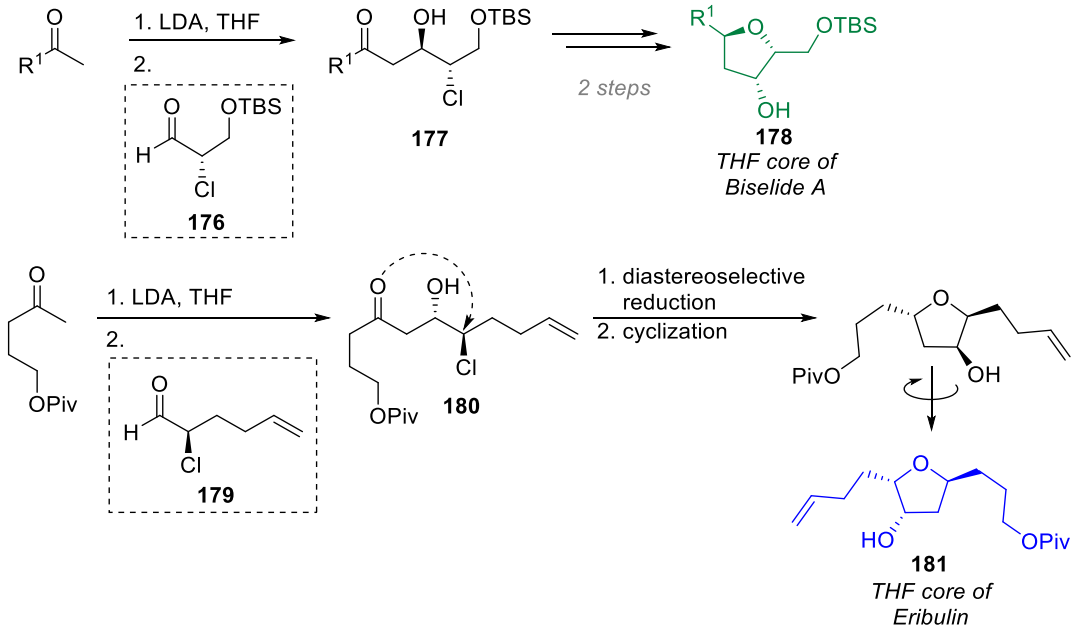

The core heterocyclic rings found in biselide A (**178**) and eribulin (**181**) can be synthesized by performing the aldol reactions with α-chloroaldehydes **176** or **179** shown in Scheme 4.12. However, attempts to synthesize intermediates **177** or **180** via the aldol reactions shown in Scheme 4.12 method were unsuccessful when using α-chloroaldehydes produced by existing organocatalytic methods. The source of problems here was multiple: i) impurities remaining from the organocatalytic α-chlorination reaction (*e.g.*, di-chlorinated aldehyde) complicated further reactions, ii) dichlorination, and iii) elimination of the beta-alkoxyl/silyloxy/acyloxy group predominated under virtually all organocatalytic reaction conditions except proline catalysis, which unfortunately delivers racemic α-chloroaldehyde. At this point, a new method of synthesizing enantio-enriched and highly pure α-chloroaldehydes was required.

4.3. Initial Cleavage Conditions

Prior to joining this project, a previous member of the Britton group (Marjan Mohammed) had begun to examine the possibility of generating α-chloroaldehydes from the chlorohydrins such as **13**. These chlorohydrin moieties have been well characterized by the Britton group and are available in excellent enantiomeric excess (92 – 98 % ee) and purity through a simple and inexpensive proline-catalyzed reaction. From this result,

we proposed a one-pot, two-step reaction shown in Scheme 4.13, which proceeds via sequential acetonide and diol cleavages, to afford the desired α-chloroaldehydes.

Scheme 4.13: Envisioned Synthetic Route to Access α-Chloroaldehydes

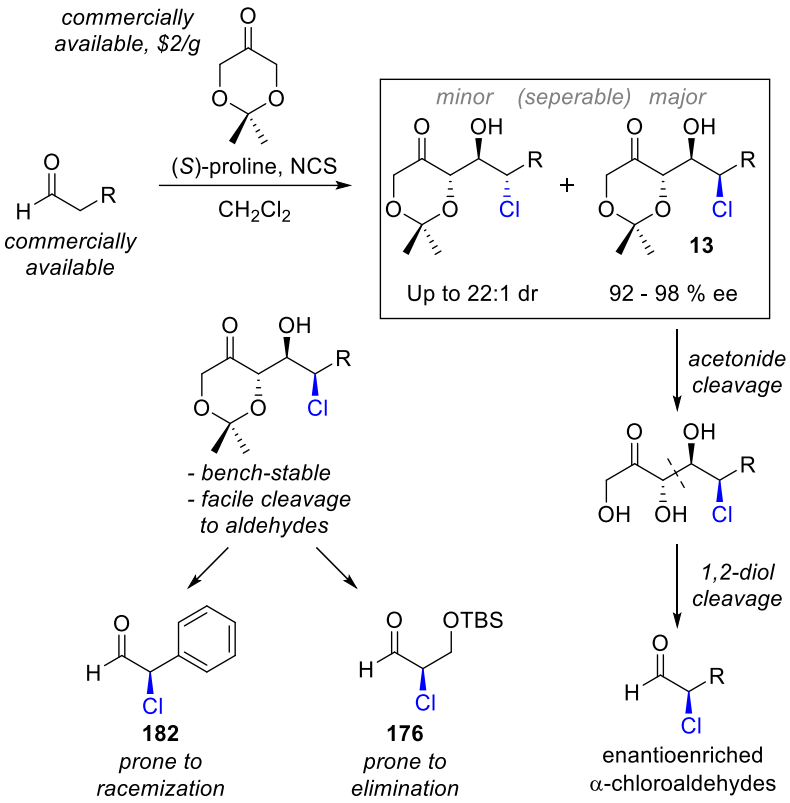

If realized in practice, this synthesis of α-chloroaldehydes could provide access to virtually any α-chloroaldehyde (if stable under oxidative cleavage conditions) that performed well in the Britton group tandem α-chlorination aldol reaction. Notably, this would include aldehydes that readily undergo racemization at the halogenated site such as α-aryl aldehydes (*e.g.*, **182**), and other substrates that had previously been problematic, such as **176**. Furthermore, the enantiomeric excess of the enantioenriched aldehydes should be high, due to the physical separation of the two diastereomers (which would become the distinct enantiomers) resulting from the tandem α-chlorination aldol reaction, as seen in Scheme 4.13.

A one pot route to α-chloroaldehydes from their corresponding chlorohydrins was initially developed by Marjan Mohammed. He determined that an acidic methanol solution was sufficient to cleave the acetonide protecting group, and an oxidative 1,2-diol

cleavage by sodium periodate performed well in forming aldehydes **183** - **188** in reasonable yields, as seen in Figure 4.4.

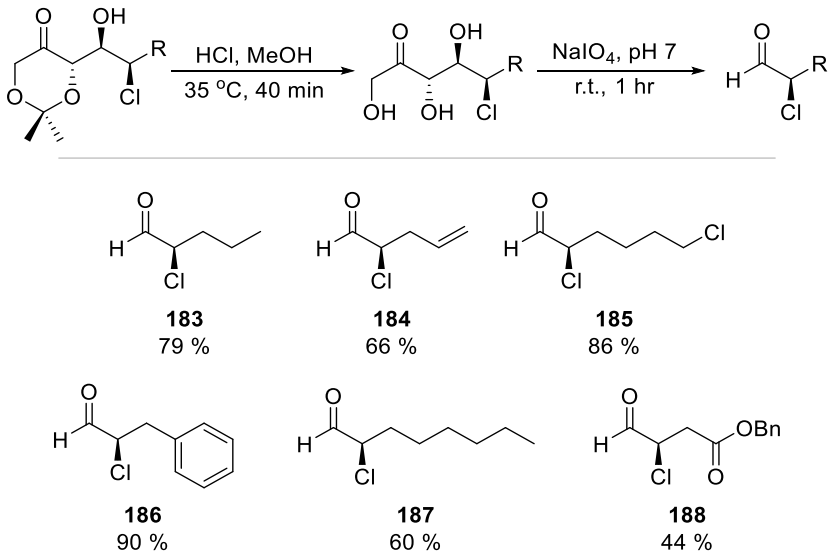

Figure 4.4: Initial results for tandem cleavage route to access α-chloroaldehydes. Compounds isolated as alcohols following reduction by $NaBH_4$.

Although promising, no data regarding the optical purity of the resulting α-chloroaldehydes had been determined. Furthermore, this route unfortunately did not allow us access to the O-TBS protected aldehyde **182**, due to the nature of the acid labile protecting group which was also cleaved under these conditions. At this point, we elected to explore alternative acetonide cleavage protocols that would not impact the O-TBS group, as well as other potentially acid-sensitive substrates.

4.4. Optimization for Acid-sensitive Substrates

4.4.1. The Search for Selective Acetonide Deprotection Conditions

Despite the acid sensitivity of both the O-TBS and acetonide protecting groups on **189**, we were hopeful that a milder acid might facilitate the selective deprotection of the acetonide. Upon investigation of more mild acids for this step (Table 4.2), we discovered several side products were formed that we suspected to be compounds **B** and **C** shown in Table 4.2, determined by TLC, HRMS, and ^{1}H NMR analysis.

Table 4.2: Results of Brönsted Acid Screen for the Selective Acetonide Cleavage of O-TBS Protected Chlorohydrin 189

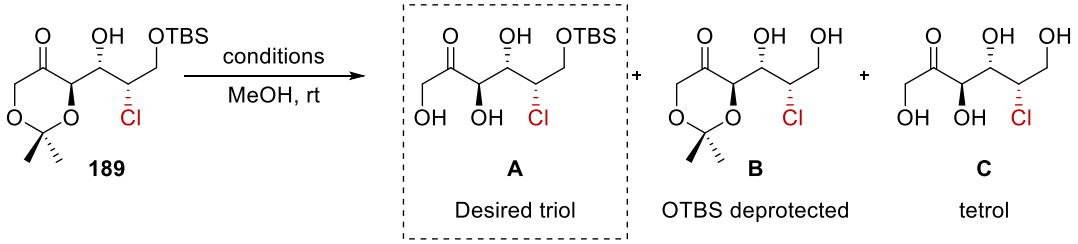

Entry	Acid	Equivalents (1.0 M in H_2O)	Reaction Time	Result[a]
1	HCl	1.0	5 min	**B** + C
2	HCl	0.4	5 min	**B** + C
3	HCl	0.1	30 min	**B** + C
4	*P*-TsOH	1.0	5 min	B + **C**
5	PPTS	1.0	18 hours	**B** + C
6	TFA	1.0	18 hours	**B** + SM
7	$NaHSO_4$	1.0	3 days	**B** + SM
8	AcOH	1.0	3 days	**B** only

[a]Products in bold are major products based on qualitative TLC analysis.

The results of Table 4.2 showed that milder acids resulted only in selective cleavage of the O-TBS group (forming product **B**), and not the acetonide (to produce desired triol **A**). This was a disappointing result, as it showed that with regard to Brönsted acids, the O-TBS group is more susceptible to cleavage.

Several publications describe the use of Lewis acids to perform acetonide cleavages.[128–130] Notably, the use of either indium trichloride or antimony trichloride was reported to facilitate the selective cleavage of an acetonide in the presence of other acid-sensitive functionalities.[131,132] To explore the possibility of using a Lewis acid to facilitate acetonide removal, we screened a selection of Lewis acids. The protected chlorohydrin **189** was treated with one equivalent of each of the Lewis acids shown in Table 4.3.

Table 4.3: Results of Lewis Acid Screen for the Selective Acetonide Cleavage of Chlorohydrin 189

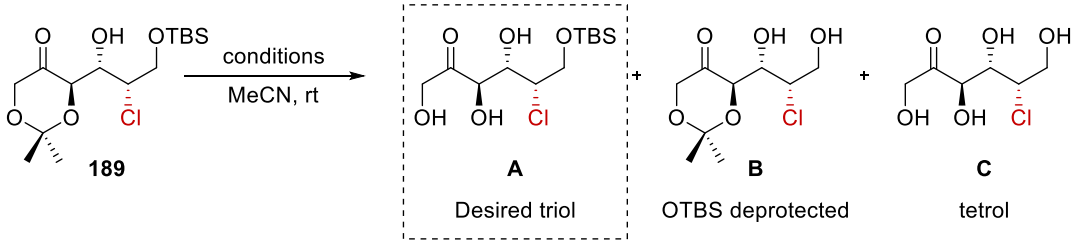

Entry	Lewis Acid	Stop Time	Result[a]
1	$FeCl_3$	1 day	NR
2	$YCl_3•6H_2O$	1 day	NR
3	$SnCl_4•5H_2O$	1 hour	**B** + **C**
4	$Yb(OTf)_3$	2 hours	B + **C**
5	$SnCl_4$	1 day	**B** + C
6	$TiCl_4$	1 day	**B** + C
7	$Sc(OTf)_3$	1 day	**B** + SM
8	$AlCl_3$	1 day	**B** + SM
9	$BF_3•OEt_2$	2 hours	**B**
10	$InCl_3$	1 day	A + **B** + C
11	$SbCl_3$	1 day	**A** + B + C

[a]Products in bold are major products based on qualitative TLC analysis.

Although we primarily observed removal of the TBS protecting group for many Lewis acids (Table 4.3, entries 3 – 9), two were able to accomplish selective cleavage of the acetonide (Table 4.3, entries 10 and 11). This observation suggested that through further optimization a reasonable amount of selectivity could likely be achieved. At this point, we moved forward with the antimony trichloride as reactions with this Lewis acid were found to be cleaner than with indium trichloride and provided better yields of the desired triol **A**.

4.4.2. Optimization of Antimony Trichloride Route for Acid-sensitive Substrates

With a catalytic amount of antimony having afforded some selectivity in promoting acetonide cleavage, we examined this reaction in more detail. Likely, the reaction proceeds through the reaction mechanism depicted in Scheme 4.14.[131] The first step involves activation of the acetonide through donation of the endocyclic oxygen lone pair to the Lewis acid (**190**). Once partially cleaved, the resulting oxocarbenium ion in

191 could be attacked by either water (red arrows, leading to the desired acetonide cleavage product **A**), or the nearby secondary alcohol (blue arrows, leading to a more stable protected 1,2 diol system **D**).[131]

Scheme 4.14: Suggested Mechanism for the Antimony Trichloride Mediated Deprotection of Acetonides

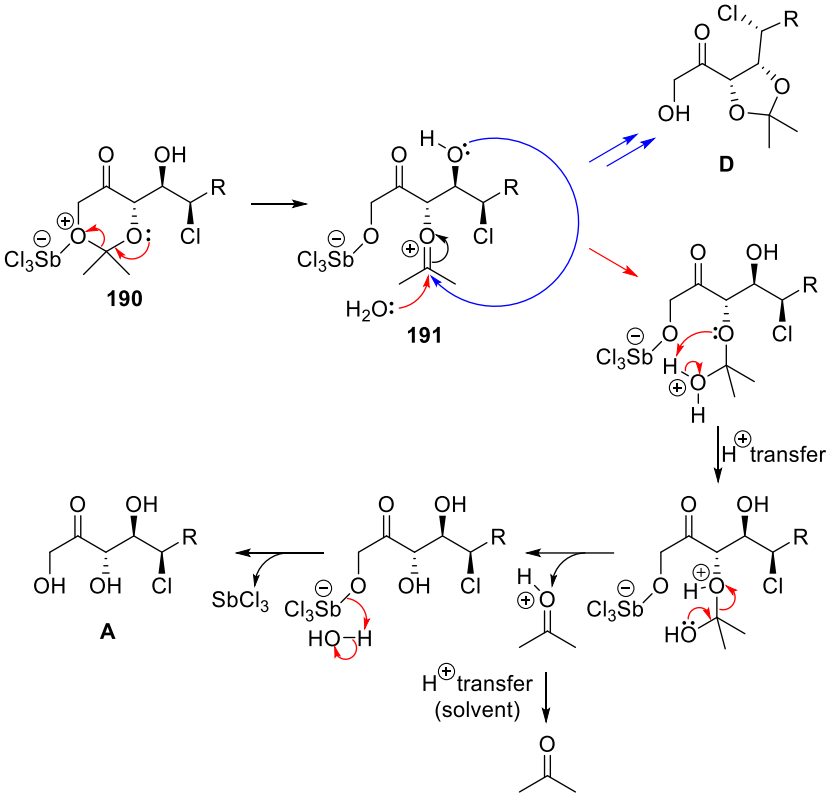

With these mechanistic insights in mind, we began to screen reaction conditions and solvents, some of which are summarized in Table 4.4. Attempting the reaction in solvents other than acetonitrile resulted in lower amounts of the desired product being formed (Table 4.4, entries 1 – 6). As such, all subsequent reactions were performed in acetonitrile. Unfortunately, when using a stoichiometric amount of water as an additive (Table 4.4, entries 7 – 10) the yield of the desired triol **A** decreased and instead the reaction favoured O-TBS cleavage to provide **B**. Here, addition of water to the Lewis acid likely generated excess HCl. This free acid, like the Brönsted acids screened previously, would favour the deprotection of the O-TBS instead of the acetonide protecting group.

With this in mind, we performed the reaction under rigorously dry conditions (Table 4.4, entry 11). Unsurprisingly, we then observed larger amounts of the migrated acetonide **D** rather than the desired triol **A**. However, we also noticed that in the absence of water the formation of tetrol **C** was slower. Inspired by this observation, we examined alternative acetonide scavengers (other than water) to stop the acetonide migration from occurring whilst avoiding the formation of free acid. To our delight, this strategy was successful, increasing the yield of the desired product appreciably (Table 4.4, entries 12 - 14). Increasing the temperature from room temperature to 60 °C while shortening the reaction time (Table 4.4, entry 15) was also positive.

Table 4.4: Optimization of Acetonide Cleavage for Acid-Sensitive O-TBS Substrate

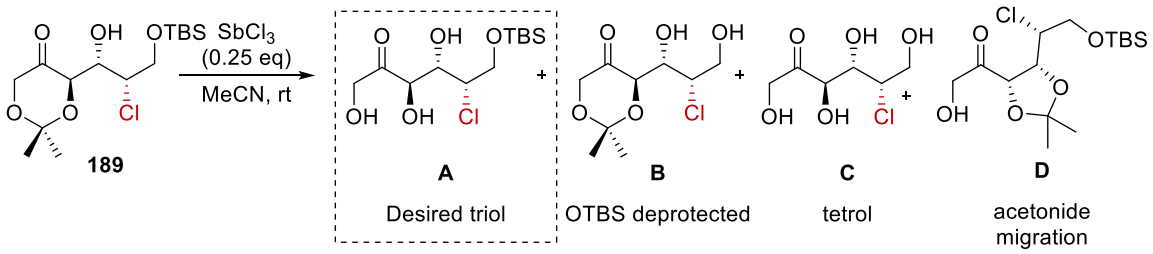

Entry	Solvent	Additive	Temperature	Products[b]
1	MeOH	-	r.t.	**B** + **C**
2	$CHCl_3$	-	r.t.	(B + C)
3	THF	-	r.t.	(B)
4	Toluene	-	r.t.	(B)
5	DMPU	-	r.t.	NR
6	MeCN	-	r.t.	A + **B** + **C**
7	MeCN	H_2O (1 equiv.)	r.t.	A + B + **C**
8	MeCN	H_2O (2 equiv.)	r.t.	A + B + **C**
9	MeCN	H_2O (5 equiv.)	r.t.	(A) + B + **C**
10	MeCN	H_2O (10 equiv.)	r.t.	B + **C**
11	MeCN, dry	-	r.t.	(A) + B + **C** + **D**
12	MeCN, dry	2,2-dimethylpropan-1,3-diol (1 equiv.)	35 °C	**A**: 29 % (NMR)
13	MeCN, dry	ethylene glycol (1 equiv.)	35 °C	**A**: 44 % (NMR)
14	MeCN, dry	ethylene glycol (5 equiv.)	35 °C	**A**: 51 % (NMR)
15	MeCN, dry	ethylene glycol (5 equiv.)	60 °C, 10 min	**A**: 66 % (NMR)

[b]Products in bold are major products; products in brackets are trace amounts; yields are based on qualitative TLC analysis or measured via NMR using the internal standard of 0.5 or 1 molar equivalent of cyclohexene.

With these conditions for selective acetonide cleavage in hand, we then added the diol cleavage to give the two-step procedure shown in Scheme 4.15. When no purification is performed prior to the diol cleavage, the yields are slightly reduced (53%

with intermediate purification, 35% with no intermediate purification). However, purification of the intermediate triol **A** results in pure aldehyde through simple extraction with diethyl ether from the diol cleavage solution. Using these conditions, we were able to synthesize the O-TBS protected α-chloroaldehyde **176** in moderate yield, as seen in Scheme 4.15.

Scheme 4.15: Result of Optimization Strategy to Synthesize Acid-Sensitive O-TBS Protected α-Chloroaldehyde 163

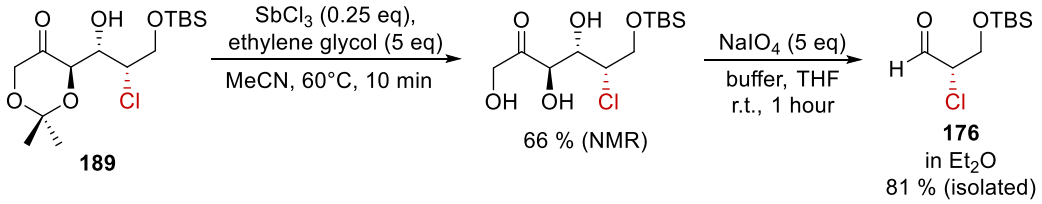

Encouraged by this result, we contemplated the general utility of this route to access other enantioenriched α-chloroaldehydes. To examine this, we performed the two-step sequence on both undecylic aldehyde and hydrocinnamaldehyde derived chlorohydrins **192** and **194**, with improved yields of the corresponding α-chloroaldehydes **193** and **195** as compared to the O-TBS protected substrate (Scheme 4.16).

Scheme 4.16: Expansion of the Two-Step Dual Cleavage Methodology to Synthesize Other α-Chloroaldehydes

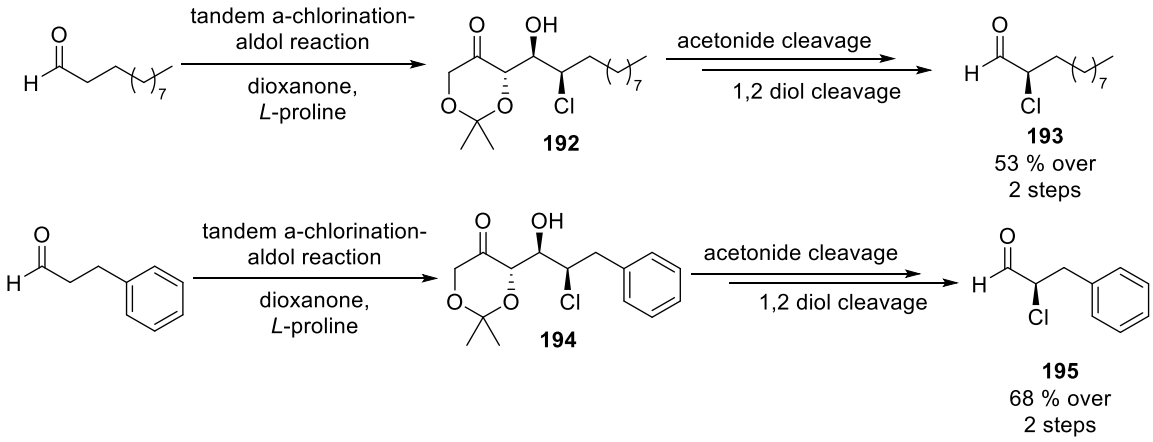

4.5. Determination of Enantiomeric Excess of Resultant α-Chloroaldehydes

To determine the enantiomeric excess of α-chloroaldehydes we examined a variety of derivatization methods to provide compounds that were both UV active and

separable by chiral HPLC. These methods included epoxidation or esterification of the corresponding alcohol, as well as Grignard addition to the aldehyde. The chromophores shown in Scheme 4.17 were installed in an attempt to enable detection and separation of enantiomers on an HPLC system utilizing a UV detector. Unfortunately, the chiral HPLC columns that we had access to were unable to separate any of the enantiomers shown in Scheme 4.17.

Scheme 4.17: Attempts to Enable the Chiral Separation of α-Chloroaldehydes by Derivatization and Chiral HPLC Analysis

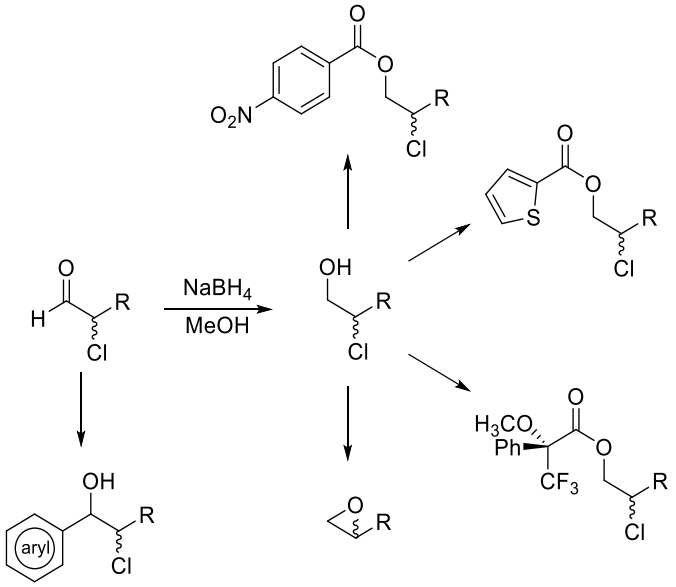

In order to avoid chiral HPLC, we next explored derivatization using Mosher's acids to generate a pair of diastereomers. Though their separation on HPLC was unsuccessful, the two diastereomers did give distinct signals in their ^{19}F NMR spectra which we could integrate to obtain the % ee. To increase the resolution, we turned to chiral GC analysis to facilitate the separation of the α-chloroaldehydes or derivatives thereof. Fortunately, we were able to establish a chiral GC method that separates the reduced, and acylated α-chloroaldehydes **176**, **193**, and **195** found in Scheme 4.18. Excited by the small but diverse scope tolerated by this new route to synthesize α-chloroaldehydes, we questioned whether this methodology could be utilized to afford other chiral α-substituted-aldehydes.

Scheme 4.18: α-Chloroaldehydes Synthesized via the Antimony Trichloride Route and Their Derivatization to Determine Their Optical Purity

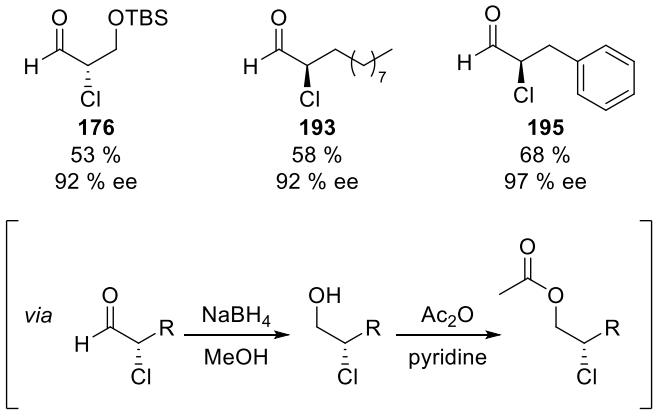

Excited by the small but diverse scope tolerated by this new route to synthesize α-chloroaldehydes, we questioned whether this methodology could be utilized to afford other chiral α-substituted-aldehydes.

4.6. Expansion to Include α-F- and α-SCF_3-Aldehydes

As many substrates are not acid-sensitive (i.e. do not possess an O-TBS group), we chose at this point to develop a procedure that could be followed by using either the acid-based cleavage or the antimony-based cleavage, with the parallel conditions shown in Scheme 4.19.

Scheme 4.19: Parallel Cleavage Routes to Produce Enantioenriched α-Chloroaldehydes

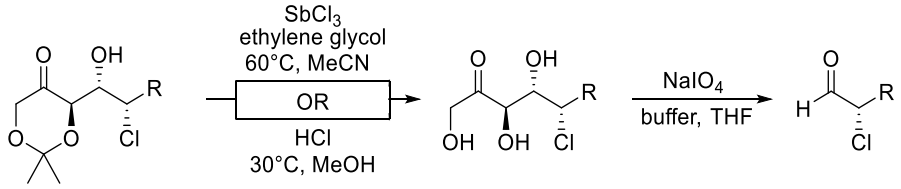

Recently in the Britton group, the methodology developed for tandem α-chlorination-aldol reaction of aldehydes has been expanded to include electrophiles equivalent to "F^+" and "SCF_3^+". This has enabled the synthesis of fluorohydrins and trifluromethylthiohydrins of the forms **196** and **198**, seen in Scheme 4.20. When these new processes were developed, we recognized the opportunity to explore their cleavage to provide optically enriched α-substituted aldehydes of the form **197** and **199**.

Scheme 4.20: Novel fluorohydrins and Trifluromethylthiohydrins Produced in the Britton Group, and Their Potential to be Precursors for α-Substituted Aldehydes

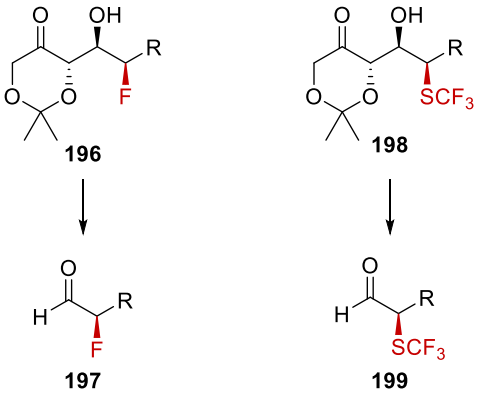

With the goal to begin the exploration of alternative α-substituted aldehydes from their corresponding fluorohydrins (*e.g.*, **200**) and trifluoromethylthiohydrins (*e.g.*, **202**), we synthesized the α-substituted aldehydes **201** and **203** seen in Scheme 4.21, in moderate yields, with the optical purities still to be determined.

Scheme 4.21: Initial Results for Proof of Concept Supporting the Generalization of the Cleavage Route to Produce Enantioenriched α-Substituted Aldehydes.

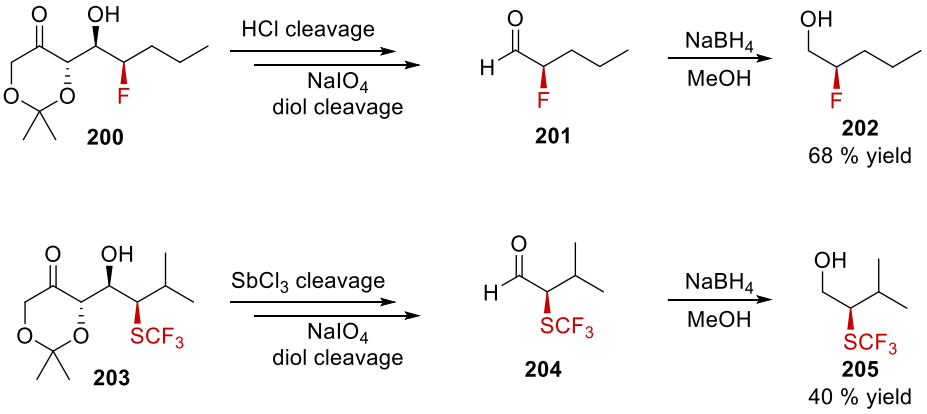

From these initial studies, a full analysis of the breadth of utility of this route was initiated and is currently ongoing in the Britton group. This analysis involves exploration of the functional group tolerance of the reaction, as well as determination of the optical purity of the synthesized α-substituted aldehydes.

4.7. Summary

Utilizing the previously developed tandem α-chlorination aldol reaction by the Britton group we have developed a stereoselective route to enantioenriched α-substituted aldehydes relying on either Brönsted or Lewis acids and an oxidative cleavage reaction. Initial studies show good optical purity, and moderate yields for a variety of both aliphatic and acid-sensitive α-chloroaldehyde products, with promise for expansion to produce α-chloro-, α-fluoro-, and α-trifluoromethylthio-aldehydes. The stability of the precursors and their ease of cleavage to afford highly pure α-substituted aldehydes that result in good-yielding subsequent reaction has resulted in the adoption of the route into total synthesis projects in the Britton group. The use of inexpensive proline to afford the α-chloroaldehydes makes this process scalable and has been conducted on a >10 g scale in support of the total synthesis of the natural product eribulin.

The scalability, stability of precursors, purity of products, and the use of inexpensive proline to synthesize the α-substituted aldehydes make this route desirable on scale. Further development to include α-aryl- α-substituted aldehydes could enable the synthesis of very sensitive α-substituted aldehydes from stable precursors in good yields and optical purity. This methodology likely will be used to install initial stereochemistry in total synthesis projects within the Britton group as well as beyond.

4.8. Experimental Information

4.8.1. General Considerations

Please see **General Considerations,** section 2.5.1.

4.8.2. General Procedures

General Procedure F: $SbCl_3$ Based Tandem Cleavage Route to Produce α-Substituted Aldehydes

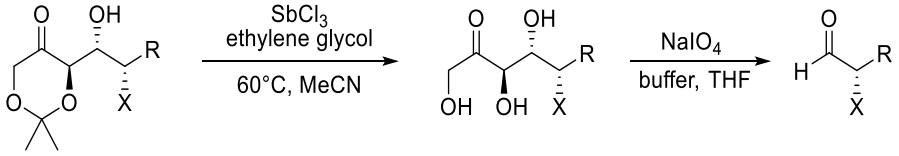

To a stirred solution of substituted-hydrin in (1.0 equiv.) in dry MeCN (0.1 M) was added dry ethylene glycol (5.0 equiv.) followed by $SbCl_3$ (0.25 equiv.). The reaction was immediately heated to 60 °C and monitored closely by TLC for the disappearance of starting material. Once the starting material was consumed as measured by TLC (*ca.* 10 - 2 hours), the reaction was cooled and then immediately filtered through a plug of silica (1 cm of silica, eluent EtOAc:hexanes 50:50 – 80:20) until all triol had been eluded (R_f *ca.* 0.14 in EtOAc:hexanes 35:65). The filtrate was then concentrated under reduced pressure and purified by column chromatography (EtOAc:hexanes) to afford the intermediate triol. To a stirred solution of the intermediate triol (1.0 equiv.) in THF:buffer (aq. phosphate, pH = 7) (1:1, 0.1 M) was added $NaIO_4$ (5.0 equiv.) at room temperature. The reaction mixture was then stirred at room temperature until disappearance of the intermediate triol was observed by TLC (*ca.* 1 hour), at which point the mixture was extracted with CH_2Cl_2 or Et_2O(2 times). The combined organic layers were dried with $MgSO_4$, filtered, and either **1:** concentrated under reduced pressure to afford the α-substituted aldehyde; **or 2:** added to a solution of MeOH (0.2 M according to the triol) with stirring. To this stirred MeOH/Et_2O or MeOH/CH_2Cl_2 solution was added $NaBH_4$ (1.5 equiv.) in small portions at 0 °C. The resulting mixture was warmed to room temperature and stirred until the reaction was complete as monitored by TLC. Once complete, a saturated aqueous solution of NH_4Cl was added to the reaction mixture, followed by extraction with CH_2Cl_2 (5 times). The combined organic layers were dried over $MgSO_4$, filtered, and concentrated under reduced pressure to afford the α-substituted alcohol.

4.8.3. Preparation and Characterization Data

Preparation of O-TBS Protected α-Chloroaldehyde **176**

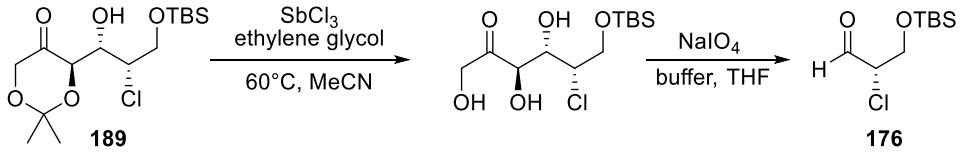

Following general procedure F:

To a stirred solution of chlorohydrin **189** (synthesized according to established literature procedure)[24] (100 mg, 0.283 mmol, 1.0 equiv.) in dry MeCN (2.8 mL, 0.1 M) was added dry ethylene glycol (80 μL,1.4 mmol, 5.0 equiv.) followed by $SbCl_3$ (16 mg, 0.071 mmol, 0.25 equiv.). The reaction was immediately heated to 60 °C for 10 minutes after which it was cooled in an ice bath and immediately filtered through a plug of silica (1 cm of silica, eluent EtOAc:hexanes 50:50) until all triol had been eluded (R_f *ca.* 0.16 in EtOAc:hexanes 35:65). The filtrate was then concentrated under reduced pressure and purified by column chromatography (EtOAc:hexanes 35:65) to afford the intermediate triol (40 mg, 45 % isolated yield, 66 % NMR yield based on internal standard observed for other trials of the same reaction). To a stirred solution of the intermediate triol (40 mg, 0.13 mmol, 1.0 equiv.) in THF:buffer (aq. phosphate, pH = 7) (1:1, 1.3 mL, 0.1 M) was added $NaIO_4$ (136 mg, 0.64 mmol, 5.0 equiv.) at room temperature. The reaction mixture was then stirred at room temperature for 70 minutes at which point the mixture was extracted with Et_2O (2 times). The combined organic layers were dried with $MgSO_4$, filtered, and concentrated under reduced pressure to afford the α-substituted aldehyde **176** as a colorless oil (55 mg, 36 % isolated yield over 2 steps). **^{1}H NMR**: (500 MHz, $CDCl_3$) δ (ppm) = 9.52 (d, *J* = 2.5 Hz, 1H), 4.19 (ddd, *J* = 6.1, 4.9, 2.5 Hz, 1H), 4.08 (dd, *J* = 11.0, 4.9 Hz, 1H), 4.02 (dd, *J* = 11.0, 6.1 Hz, 1H), 0.88 (s, 9H), 0.08 (s, 3H), 0.08 (s, 4H).

Spectral data were in accordance with those in the literature.[133]

Determination of the enantiomeric excess of **176**:

A racemic sample of α-chloroaldehyde **176** was prepared by stirring 3-((*tert*-butyldimethylsilyl)oxy)propanal (1.0 equiv.) with NCS (1.05 equiv.) and 1:1 *D*/*L*-proline

(0.1 equiv.) in CH_2Cl_2 (0.35 M) for 5 hours, followed by aqueous workup. The crude racemic α-chloroaldehyde was then dissolved in MeOH (0.2 M) and reduced by addition of $NaBH_4$ (5 equiv.) to afford the corresponding racemic α-chloroalcohol, which was isolated upon workup. The alcohol was then acylated in a 1:1 mixture (1.5 M total) of acetic anhydride and pyridine and partitioned between Et_2O and water. The organic layer was washed with 1.0 M HCl, dried with $MgSO_4$, and concentrated to afford the racemic α-chloro acetylated alcohol which was separated by chiral GC (CDX-3 column, ran with an isothermal temperature of 120 °C, at 10 psi to afford the two enantiomer peaks at R_t = 50.54 and 51.55 minutes). Reduction and acylation of the enriched α-chloroaldehyde **176** by an analogous procedure afforded the enriched α-chloro acetylated alcohol (R_t = 50.44) which was found to have 92 % ee by the same GC method.

Preparation of α-Chloroaldehyde **193**

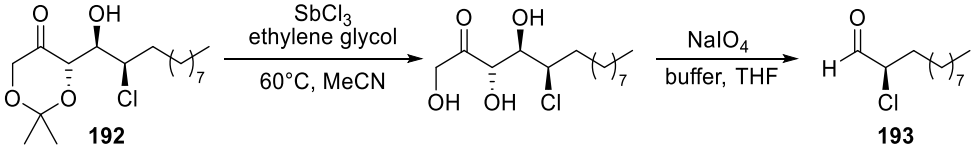

Following general procedure F:

To a stirred solution of chlorohydrin **192** (synthesized according to established literature procedure)[24] (100 mg, 0.30 mmol, 1.0 equiv.) in dry MeCN (3.0 mL, 0.1 M) was added dry ethylene glycol (83 μL, 1.5 mmol, 5.0 equiv.) followed by $SbCl_3$ (17 mg, 0.075 mmol, 0.25 equiv.). The mixture was immediately heated to 60 °C for 10 minutes, after which it was cooled in an ice bath and immediately filtered through a plug of silica (1 cm of silica, eluent EtOAc:hexanes 50:50) until all triol had been eluded (R_f *ca.* 0.21 in EtOAc:hexanes 50:50). The filtrate was then concentrated under reduced pressure and purified by column chromatography (EtOAc:hexanes 50:50) to afford the intermediate triol as a colorless oil (51 mg, 58 % isolated yield). To a stirred solution of the intermediate triol (43 mg, 0.145 mmol, 1.0 equiv.) in THF:buffer (aq. phosphate, pH = 7) (1:1, 1.5 mL, 0.1 M) was added $NaIO_4$ (155 mg, 0.73 mmol, 5.0 equiv.) at room temperature. The reaction mixture was then stirred at room temperature for 70 minutes at which point the mixture was extracted with Et_2O (2 times). The combined organic layers were dried with $MgSO_4$, filtered, and concentrated under reduced pressure to afford the α-chloroaldehyde **193** as a colorless oil (35 mg, 53 % over 2 steps). **^{1}H NMR**:

(400 MHz, $CDCl_3$) δ (ppm) = 9.48 (d, *J* = 2.4 Hz, 1H), 4.15 (ddd, *J* = 8.2, 5.5, 2.5 Hz, 1H), 1.97 (ddd, *J* = 14.2, 9.8, 5.8, 5.8 Hz, 1H), 1.90 – 1.75 (m, 1H), 1.57 – 1.39 (m, 2H), 1.39 – 1.23 (m, 12H), 0.88 (t, *J* = 6.7 Hz, 3H).

Spectral data were in accordance with those in the literature.[134]

Determination of the enantiomeric excess of **193**:

A racemic sample of α-chloroaldehyde **193** was prepared by stirring undecanal (1.0 equiv.) with NCS (1.05 equiv.) and 1:1 *D*/*L*-proline (0.1 equiv.) in CH_2Cl_2 (0.35 M) for 23 hours, followed by aqueous workup. The crude racemic α-chloro-undecanal was then dissolved in MeOH (0.2 M) and reduced by addition of $NaBH_4$ (5 equiv.) to afford the corresponding racemic α-chloroalcohol which was isolated upon work-up. The alcohol was then acylated in a 1:1 mixture of acetic anhydride and pyridine (1.5 M total) for 18 hours and then partitioned between Et_2O and water. The organic layer was washed with 1.0 M HCl, dried with $MgSO_4$, filtered, and concentrated to afford the racemic α-chloro acetylated alcohol, which was separated by chiral GC analysis (Chiral column containing a 1:1 mixture of heptakis-(2,6-di-*O*-methyl-3-*O*-pentyl-ß-cyclodextrin and OV-1701,[135] ran with an isothermal temperature of 125 °C, at 10 psi with a split ratio of 10:1 to afford the two enantiomer peaks at R_t = 49.28 and 50.64 minutes). Reduction and acylation of the enriched α-chloroaldehyde **193** by an analogous procedure afforded the enriched α-chloro acetylated alcohol (R_t = 50.64 minutes) which was found to have 92 % ee by the same GC method.

Preparation of α-Chlorohydrocinnamaldehyde **195**

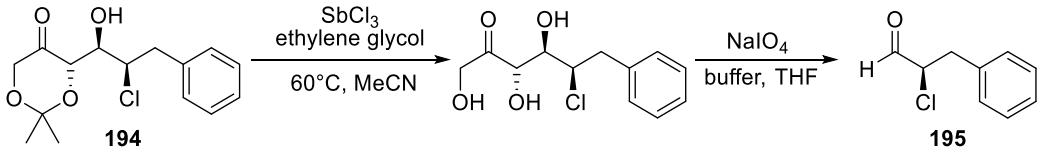

Following general procedure F:

To a stirred solution of chlorohydrin **194** (100 mg, 0.34 mmol, 1.0 equiv.) in dry MeCN (3.4 mL, 0.1 M) was added dry ethylene glycol (93 μL, 1.7 mmol, 5.0 equiv.) followed by $SbCl_3$ (19 mg, 0.084 mmol, 0.25 equiv.). The mixture was immediately heated to 60 °C for 10 minutes, after which it was cooled in an ice bath and immediately

filtered through a plug of silica (1 cm of silica, eluent EtOAc:hexanes 70:30) until all triol had been eluded (R_f *ca.* 0.16 in EtOAc:hexanes 60:40). The filtrate was then concentrated under reduced pressure and purified by column chromatography (EtOAc:hexanes 60:40) to afford the intermediate triol as a colorless oil (59 mg, 68 % isolated yield). To a stirred solution of the intermediate triol (51 mg, 0.20 mmol, 1.0 equiv.) in THF:buffer (aq. phosphate, pH = 7) (1:1, 2.0 mL, 0.1 M) was added $NaIO_4$ (209 mg, 0.976 mmol, 5.0 equiv.) at room temperature. The reaction mixture was then stirred at room temperature for 70 minutes at which point the mixture was extracted with Et_2O (2 times). The combined organic layers were dried with $MgSO_4$, filtered, and concentrated under reduced pressure to afford the α-chloroaldehyde as a colorless solid (32.5 mg, 67 % isolated yield over 2 steps). **^{1}H NMR**: (500 MHz, $CDCl_3$) δ (ppm) = 9.55 (d, *J* = 2.2 Hz, 1H), 7.37 – 7.21 (m, 5H), 4.39 (ddd, *J* = 8.1, 5.7, 2.2 Hz, 1H), 3.38 (dd, *J* = 14.5, 5.7 Hz, 1H), 3.09 (dd, *J* = 14.5, 8.3 Hz, 1H).

Spectral data were in accordance with those in the literature.[121]

Determination of the enantiomeric excess of **195:**

A racemic sample of α-chloroaldehyde **195** was prepared by stirring hydrocinnamaldehyde (1.0 equiv.) with NCS (1.05 equiv.) and 1:1 *D*/*L*-proline (0.1 equiv.) in CH_2Cl_2 (0.35 M) for 5 hours, followed by aqueous workup. The crude racemic α-chlorohydrocinnamaldehyde was then dissolved in MeOH (0.2 M) and reduced by addition of $NaBH_4$ (5 equiv.) to afford the corresponding racemic α-chloroalcohol which was isolated upon work-up. The alcohol was then acylated in a 1:1 mixture (1.5 M total) of acetic anhydride and pyridine for 18 hours and then partitioned between Et_2O and water. The organic layer was washed with 1.0 M HCl, dried with $MgSO_4$, filtered, and concentrated to afford the racemic α-chloro acetylated alcohol, which was separated by chiral GC (CDX-3 column, ran with an isothermal temperature of 115 °C, at 10 psi with a split ratio of 10:1 to afford the two enantiomer peaks at R_t = 153.79 and 156.43 minutes). Reduction and acylation of the enriched α-chloroaldehyde **195** by an analogous procedure afforded the enriched α-chloro acetylated alcohol (R_t = 156.53 minutes) which was found to have 97 % ee by the same GC method.

Preparation of α-Fluoroaldehyde **201** (isolated as the α-fluoroalcohol)

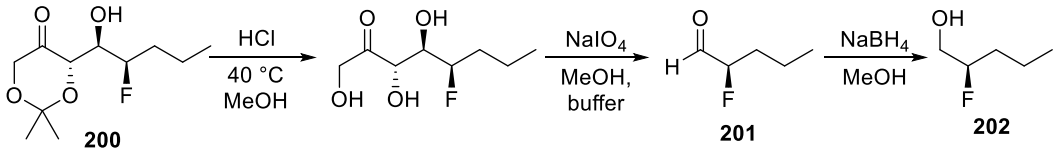

To a stirred solution of chlorohydrin **200** (100 mg, 0.428 mmol, 1.0 equiv.) in MeOH (2.1 mL, 0.1 M) was added HCl (0.43 mL of a 1.0 M aqueous solution, 0.43 mmol, 1.0 equiv.). The reaction mixture was then heated with stirring to 40 °C and monitored by TLC for consumption of starting material. After 30 minutes, the acetonide deprotection was complete, and following cooling to room temperature pH 7 buffer (phosphate buffer, 2.1 mL, 0.1 M) was added with stirring. To this clear colorless solution at room temperature was added $NaIO_4$ (137 mg, 0.64 mmol, 1.5 equiv.), and the resulting white slurry was stirred for 60 minutes, after which the mixture was extracted CH_2Cl_2 (2 times) which contained the α-chloroaldehyde **201**. The combined organic layers were dried over $MgSO_4$, cooled to 0 °C, and $NaBH_4$ (24 mg, 0.64 mmol, 1.5 equiv.) was added and the resulting mixture was stirred for 35 minutes at room temperature. A saturated aqueous solution of NH_4Cl was then added, and the resulting biphasic mixture was extracted with CH_2Cl_2 (2 times). The combined organic layers were dried over $MgSO_4$, filtered, and concentrated under reduced pressure (carefully) to afford the (volatile) crude α-fluoro alcohol **202** as a colorless oil (31 mg, 68 % over 3 steps). **^{1}H NMR** (for the alcohol **202**): (500 MHz, $CDCl_3$) δ (ppm) = 4.64 (ddddd, *J* = 49.7, 8.4, 7.0, 4.3, 2.9 Hz, 1H), 3.78 – 3.62 (m, 2H), 1.89 – 1.17 (m, 4H), 0.96 (t, *J* = 7.1 Hz, 3H).

Spectral data were in accordance with those in the literature.[136]

Determination of optical purity of the α-fluoroalcohol **202** is ongoing in the Britton group.

Preparation of the α-Trifluoromethylthio-Aldehyde **204** (isolated as the α-SCF_3 alcohol)

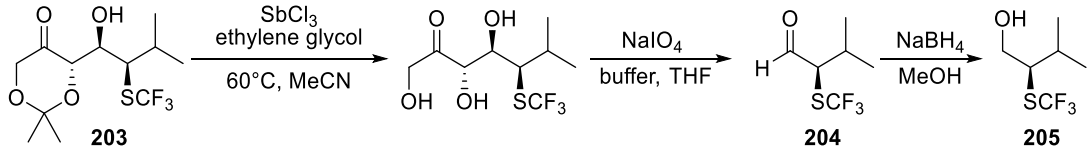

Following general procedure F:

To a stirred solution of chlorohydrin **204** (55 mg, 0.17 mmol, 1.0 equiv.) in dry MeCN (1.7 mL, 0.1 M) was added dry ethylene glycol (48 μL, 0.86 mmol, 5.0 equiv.) followed by $SbCl_3$ (10 mg, 0.043 mmol, 0.25 equiv.). The mixture was heated to 60 °C for 130 minutes, after which the mixture was cooled in an ice bath and immediately filtered through a plug of silica (1 cm of silica, eluent EtOAc:hexanes 80:20) until all triol had been eluded (R_f *ca.* 0.44 in EtOAc:hexanes 80:20). The filtrate was then concentrated under reduced pressure and purified by column chromatography (EtOAc:hexanes 50:50) to afford the intermediate triol as a colorless solid (30 mg, 64 % isolated yield). To a stirred solution of the intermediate triol (20 mg, 0.071 mmol, 1.0 equiv.) in THF:buffer (aq. phosphate, pH = 7) (1:1, 0.70 mL, 0.1 M) was added $NaIO_4$ (76 mg, 0.35 mmol, 5.0 equiv.) at room temperature. The reaction mixture was then stirred at room temperature for 60 minutes at which point the mixture was extracted with Et_2O (2 times) to obtain pure α-chloroaldehyde **204**. The combined organic layers containing **204** were dried with $MgSO_4$, filtered, and added to a solution of MeOH (0.35 mL, 0.2 M according to the triol) with stirring. To this stirred MeOH/Et_2O solution was added $NaBH_4$ (11 mg, 0.28 mmol, 4 equiv.) in small portions at 0 °C. The resulting mixture was warmed to room temperature and stirred for 25 minutes. A saturated aqueous solution of NH_4Cl was then added to the reaction mixture, followed by extraction with CH_2Cl_2 (5 times). The combined organic layers were dried over $MgSO_4$, filtered, and concentrated under reduced pressure to afford the α-substituted alcohol **205** as a colorless oil (8.2 mg, 62 % over 2 steps). **^{1}H NMR** (for the alcohol **205**): (500 MHz, $CDCl_3$) δ (ppm) = 3.87 – 3.76 (m, 2H), 3.15 (ddd, *J* = 5.8, 5.8, 5.8 Hz, 1H), 2.16 (dqq, *J* = 6.8, 6.4, 6.4 Hz, 1H), 1.82 (dd, *J* = 7.2, 5.7 Hz, 1H), 1.09 (d, *J* = 6.8 Hz, 3H), 0.98 (d, *J* = 6.8 Hz, 3H).

Full characterization including determination of optical purity of the α-SCF_3-alcohol **205** is ongoing in the Britton group.

References

(1) World Health Organization. *Model List of Essential Medicines*; 2017.

(2) World Health Organization. *Definition of Active Pharmaceutical Ingredient*; 2011.

(3) Gashaw, I.; Ellinghaus, P.; Sommer, A.; Asadullah, K. *Drug Discov. Today* **2011**, *17*, S24–S30.

(4) Lindsay, M. A. *Nat. Rev. Drug Discov.* **2003**, *2* (10), 831–838.

(5) Wang, L.-H.; Evers, A.; Monecke, P.; Naumann, T. *J. Cheminform.* **2012**, *4*, 20.

(6) Lillelund, V. H.; Jensen, H. H.; Liang, X.; Bols, M. *Chem. Rev.* **2002**, *102* (2), 515–554.

(7) Meanwell, M.; Sutherland, M.; Britton, R. *Can. J. Chem.* **2017**, *96* (2), 144–147.

(8) Entzeroth, M.; Flotow, H.; Condron, P. *Curr. Protoc. Pharmacol.* **2009**, No. SUPPL. 44, 1–27.

(9) *The Process of New Drug Discovery and Development*, Second Ed.; Smith, C., O'Donnell, J., Eds.; CRC Press, 2006.

(10) Lipinski, C. A.; Lombardo, F.; Dominy, B. W.; Feeney, P. J. *Adv. Drug Deliv. Rev.* **2012**, *64*, 4–17.

(11) Crum Brown, A.; Fraser, T. R. *Trans. R. Soc. Edinburgh* **1868**, *25*, 151–203.

(12) Maxwell, R. A.; Keenan, P. D.; Chaplin, E.; Roth, B.; Batmanglidj Eckhardt, S. *J. Pharmacol. Exp. Ther.* **1969**, *166* (2), 320–329.

(13) Du, X.; Li, Y.; Xia, Y.-L.; Ai, S.-M.; Liang, J.; Sang, P.; Ji, X.-L.; Liu, S.-Q. *Int. J. Mol. Sci.* **2016**, *17*, 144–178.

(14) Palmer, M.; Chaguturu, R. *Expert Opin. Drug Discov.* **2017**, *12* (6), 537–540.

(15) Cernak, T.; Dykstra, K. D.; Tyagarajan, S.; Vachal, P.; Krska, S. W. *Chem. Soc. Rev.* **2016**, *45* (3), 546–576.

(16) Dean, M.; Brown, G.; Boström, J. *J. Med. Chem.* **2015**, *59*, 4443–4458.

(17) Graul, A.; Castaner, J. *Drugs Future* **1997**, *22*, 956–968.

(18) Cepanec, I. *Synthesis of Biaryls*; Elsevier Science Ltd, 2004.

(19) King, A. O.; Yasuda, N. **2004**, *6*, 205–245.

(20) Bunnett, J. F. *Q. Rev. Chem. Soc.* **1958**, *12*, 1–16.

(21) Goldstein, S. W.; Bill, A.; Dhuguru, J.; Ghoneim, O. *J. Chem. Educ.* **2017**, *94*, 1388–1390.

(22) Walsh, K.; Sneddon, H. F.; Moody, C. J. *ChemSusChem* **2013**, *6*, 1455–1460.

(23) Maskrey, T. S.; Kristufek, T.; Laporte, M. G.; Nyalapatla, P. R.; Wipf, P. *Synlett* **2019**, *30*, 471–476.

(24) Bergeron-Brlek, M.; Teoh, T.; Britton, R. *Org. Lett.* **2013**, *15* (14), 3554–3557.

(25) Abdel-Magid, A. F. *ACS Med. Chem. Lett.* **2014**, *5*, 1270–1271.

(26) Merriam-Webster. Definition of Epigenetics https://www.merriam-webster.com/dictionary/epigenetics (accessed Mar 26, 2019).

(27) Egger, G.; Liang, G.; Aparicio, A.; Jones, P. A. *Nature* **2004**, *429* (6990), 457–463.

(28) Holliday, R.; Pugh, J. E. *Science.* **1975**, *187* (4173), 226–232.

(29) Heerboth, S.; Lapinska, K.; Snyder, N.; Leary, M.; Rollinson, S.; Sarkar, S. *Genet. Epigenet.* **2014**, *6*, 9–19.

(30) Weiss, W. A.; Taylor, S. S.; Shokat, K. M. *Nat. Chem. Biol.* **2007**, *3* (12), 739–744.

(31) Arrowsmith, C. H.; Audia, J. E.; Austin, C.; Baell, J.; Bennett, J.; Blagg, J.; Bountra, C.; Brennan, P. E.; Brown, P. J.; Bunnage, M. E.; Buser-Doepner, C.; Campbell, R. M.; Carter, A. J.; Cohen, P.; Copeland, R. A.; Cravatt, B.; Dahlin, J. L.; Dhanak, D.; Edwards, A. M.; Frederiksen, M.; Frye, S. V; Gray, N.; Grimshaw,

C. E.; Hepworth, D.; Howe, T.; M Huber, K. V; Jin, J.; Knapp, S.; Kotz, J. D.; Kruger, R. G.; Lowe, D.; Mader, M. M.; Marsden, B.; Mueller-Fahrnow, A.; Müller, S.; O, R. C.; Overington, J. P.; Owen, D. R.; Rosenberg, S. H.; Roth, B.; Ross, R.; Schapira, M.; Schreiber, S. L.; Shoichet, B.; Sundström, M.; Superti-Furga, G.; Taunton, J.; Toledo-Sherman, L.; Walpole, C.; Walters, M. A.; Willson, T. M.; Workman, P.; Young, R. N.; Zuercher, W. J. *Nat. Chem. Biol.* **2015**, *11*, 536–541.

(32) The Structural Genetics Consortium. Chemical Probes: Criteria https://www.thesgc.org/chemical-probes (accessed Mar 28, 2019).

(33) Collins, J. L.; Fivush, A. M.; Watson, M. A.; Galardi, C. M.; Lewis, M. C.; Moore, L. B.; Parks, D. J.; Wilson, J. G.; Tippin, T. K.; Binz, J. G.; Plunket, K. D.; Morgan, D. G.; Beaudet, E. J.; Whitney, K. D.; Kliewer, S. A.; Willson, T. M. *J. Med. Chem.* **2002**, *45* (10), 1963–1966.

(34) Hong, C.; Tontonoz, P. *Nat. Publ. Gr.* **2014**, *13*, 433–444.

(35) Jahan, S.; Davie, J. R. *Adv. Biol. Regul.* **2015**, *57*, 173–184.

(36) Fuhrmann, J.; Clancy, K. W.; Thompson, P. R. *Chem. Rev.* **2015**, *115* (11), 5413–5461.

(37) Almeida-Rios, D.; Graça, I.; Vieira, F. Q.; Ramalho-Carvalho, J.; Pereira-Silva, E.; Martins, A. T.; Oliveira, J.; Gonçalves, C. S.; Costa, B. M.; Henrique, R.; Jerónimo, C. *Oncotarget* **2016**, *7* (33), 53018–53028.

(38) Hu, H.; Qian, K.; Ho, M.-C.; Zheng, Y. G. *Expert Opin. Investig. Drugs* **2016**, *25* (3), 335–358.

(39) Shishkova, E.; Zeng, H.; Liu, F.; Kwiecien, N. W.; Hebert, A. S.; Coon, J. J.; Xu, W. *Nat. Commun.* **2017**, *8*, 15571–15584.

(40) Schurter, B. T.; Koh, S. S.; Chen, D.; Bunick, G. J.; Harp, J. M.; Hanson, B. L.; Henschen-Edman, A.; Mackay, D. R.; Stallcup, M. R.; Aswad, D. W. *Biochemistry* **2001**, *40* (19), 5747–5756.

(41) Shaaban, S.; Bedford, M. T. *Mol. Cell* **2007**, *25*, 71–83.

(42) El-andaloussi, N.; Valovka, T.; Toueille, M.; Steinacher, R.; Focke, F.; Gehrig, P.; Covic, M.; Hassa, P. O.; Hu, U. *Mol. Cell* **2006**, *22*, 51–62.

(43) Neault, M.; Mallette, F. A.; Vogel, G.; Michaud-Levesque, J.; Richard, S. *Nucleic Acids Res.* **2012**, *40* (19), 9513–9521.

(44) Stein, C.; Rüthnick, D.; Nötzold, R. R.; Riedl, S.; Bauer, U.-M. *Nucleic Acids Res.* **2012**, *40* (19), 9522–9533.

(45) Kaila, N.; Follows, B.; Leung, L.; Thomason, J.; Huang, A.; Moretto, A.; Janz, K.; Lowe, M.; Mansour, T. S.; Hubeau, C.; Page, K.; Morgan, P.; Fish, S.; Xu, X.; Williams, C.; Saiah, E. *J. Med. Chem.* **2014**, *57* (4), 1299–1322.

(46) Zou, Y.; Yue, G.; Xu, J.; Zhou, J. S. *European J. Org. Chem.* **2014**, *2014* (27), 5901–5905.

(47) Frischmuth, A.; Knochel, P. *Angew. Chemie Int. Ed.* **2013**, *52* (38), 10084–10088.

(48) de Koning, C. B.; Michael, J. P.; Rousseau, A. L. *J. Chem. Soc. Perkin Trans. 1* **2000**, *0* (11), 1705–1713.

(49) Blough, B. E.; Landavazo, A.; Partilla, J. S.; Decker, A. M.; Page, K. M.; Baumann, M. H.; Rothman, R. B. *Bioorg. Med. Chem. Lett.* **2014**, *24* (19), 4754–4758.

(50) Livendahl, M.; Jamroskovic, J.; Ivanova, S.; Demirel, P.; Sabouri, N.; Chorell, E. *Chem. - A Eur. J.* **2016**, *22* (37), 13004–13009.

(51) Taddei, M.; Cini, E.; Giannotti, L.; Giannini, G.; Battistuzzi, G.; Vignola, D.; Vesci, L.; Cabri, W. *Bioorg. Med. Chem. Lett.* **2014**, *24* (1), 61–64.

(52) Valeur, E.; Bradley, M. *Chem. Soc. Rev.* **2008**, *38*, 606–631.

(53) Shen, Y.; Szewczyk, M. M.; Eram, M. S.; Smil, D.; Kaniskan, H. Ü.; Ferreira de Freitas, R.; Senisterra, G.; Li, F.; Schapira, M.; Brown, P. J.; Arrowsmith, C. H.; Barsyte-Lovejoy, D.; Liu, J.; Vedadi, M.; Jin, J. *J. Med. Chem.* **2016**, *59* (19), 9124–9139.

(54) Eram, M. S.; Shen, Y.; Szewczyk, M. M.; Wu, H.; Senisterra, G.; Li, F.; Butler, K. V; Kaniskan, H. Ü.; Speed, B. A.; dela Seña, C.; Dong, A.; Zeng, H.; Schapira, M.; Brown, P. J.; Arrowsmith, C. H.; Barsyte-Lovejoy, D.; Liu, J.; Vedadi, M.; Jin, J. *ACS Chem. Biol.* **2016**, *11* (3), 772–781.

(55) Mitchell, L. H.; Drew, A. E.; Ribich, S. A.; Rioux, N.; Swinger, K. K.; Jacques, S. L.; Lingaraj, T.; Boriack-Sjodin, P. A.; Waters, N. J.; Wigle, T. J.; Moradei, O.; Jin, L.; Riera, T.; Porter-Scott, M.; Moyer, M. P.; Smith, J. J.; Chesworth, R.; Copeland, R. A. *ACS Med. Chem. Lett.* **2015**, *6* (6), 655–659.

(56) Hann, M. M.; Keserü, G. M. *Nat. Rev. Drug Discov.* **2012**, *11*, 355–365.

(57) Carpentier, C.; Godbout, R.; Otis, F.; Voyer, N. *Tetrahedron Lett.* **2015**, *56* (10), 1244–1246.

(58) Lennox, A. J. J.; Lloyd-Jones, G. C. *Chem. Soc. Rev.* **2014**, *43* (1), 412–443.

(59) Lu, B.; Shen, X.; Zhang, L.; Liu, D.; Zhang, C.; Cao, J.; Shen, R.; Zhang, J.; Wang, D.; Wan, H.; Xu, Z.; Ho, M.-H.; Zhang, M.; Zhang, L.; He, F.; Tao, W. *ACS Med. Chem. Lett.* **2018**, *9* (2), 98–102.

(60) Liu, J.; Do, T. J.; Simmons, C. J.; Lynch, J. C.; Gu, W.; Ma, Z.-X.; Xu, W.; Tang, W. *Org. Biomol. Chem.* **2016**, *14* (38), 8927–8930.

(61) Fredrich, S.; Bonasera, A.; Valderrey, V.; Hecht, S. *J. Am. Chem. Soc.* **2018**, *140* (20), 6432–6440.

(62) Kim, I.; Lee, S.-H.; Lee, S. *Tetrahedron Lett.* **2008**, *49* (46), 6579–6584.

(63) Cogolli, P.; Maiolo, F.; Testaferri, L.; Tingoli, M.; Tiecco, M. *J. Org. Chem.* **1979**, *44* (15), 2642–2646.

(64) Bisht, R.; Hoque, M. E.; Chattopadhyay, B. *Angew. Chemie Int. Ed.* **2018**, *57* (48), 15762–15766.

(65) *Iminosugars : From Synthesis to Therapeutic Applications*; Compain, P., Martin, O. R., Eds.; John Wiley and Sons, 2007.

(66) Lillelund, V. H.; Jensen, H. H.; Liang, X.; Bols, M. *Chem. Rev.* **2002**, *102* (2), 515–554.

(67) Asano, N. *Curr. Top. Med. Chem.* **2003**, *3* (5), 471–484.

(68) Platt, F. M.; Neises, G. R.; Dwek, R. A.; Butters, T. D. *J. Biol. Chem.* **1994**, *269* (11), 8362–8365.

(69) Joubert, P. H.; Venter, C. P.; Joubert, H. F.; Hillebrand, I. *Eur. J. Clin. Pharmacol.* **1985**, *28* (6), 705–708.

(70) Paulsen, H.; Hayauchi, Y.; Sinnwell, V. *Chem. Ber.* **1980**, *113* (8), 2601–2608.

(71) Yam, G. H.-F.; Bosshard, N.; Zuber, C.; Steinmann, B.; Roth, J. *Am. J. Physiol. Physiol.* **2006**, *290* (4), 1076–1082.

(72) Hong, Z.; Liu, L.; Sugiyama, M.; Fu, Y.; Wong, C.-H. *J. Am. Chem. Soc.* **2009**, *131* (24), 8352–8353.

(73) Britton, R.; Kang, B. *Nat. Prod. Rep.* **2013**, *30*, 227–236.

(74) Draper, J. A.; Britton, R. *Org. Lett.* **2010**, *12* (18), 4034–4037.

(75) Dhand, V.; Draper, J. A.; Moore, J.; Britton, R. *Org. Lett.* **2013**, *15* (8), 1914–1917.

(76) Bergeron-Brlek, M.; Meanwell, M.; Britton, R. *Nat. Commun.* **2015**, *6*, 6903–6909.

(77) Bergeron-Brlek, M.; Goodwin-Tindall, J.; Cekic, N.; Roth, C.; Zandberg, W. F.; Shan, X.; Varghese, V.; Chan, S.; Davies, G. J.; Vocadlo, D. J.; Britton, R. *Angew. Chemie Int. Ed.* **2015**, *54* (51), 15429–15433.

(78) Roth, C.; Chan, S.; Offen, W. A.; Hemsworth, G. R.; Willems, L. I.; King, D. T.; Varghese, V.; Britton, R.; Vocadlo, D. J.; Davies, G. J. *Nat. Chem. Biol.* **2017**, *13*, 610.

(79) Qadoumi, Z.; Senior, J.; Bergeron-Brlek, M.; Britton, R. *Synlett* **2013**, *24* (18), 2427–2430.

(80) Miyake, Y.; Ebata, M. *Agric. Biol. Chem.* **1988**, *52* (3), 661–666.

(81) Bernotas, R. C.; Pezzone, M. A.; Ganem, B. *Carbohydr. Res.* **1987**, *167*, 305–311.

(82) Furneaux, R. H.; Tyler, P. C.; Whitehouse, L. A. *Tetrahedron Lett.* **1993**, *34* (22), 3609–3612.

(83) Chida, N.; Tanikawa, T.; Tobe, T.; Ogawa, S. *J. Chem. Soc. Chem. Commun.* **1994**, *0* (10), 1247–1248.

(84) Heightman, T. D.; Ermert, P.; Klein, D.; Vasella, A. *Helv. Chim. Acta* **1995**, *78* (2), 514–532.

(85) Barili, P. L.; Berti, G.; Catelani, G.; D'andrea, F.; De Rensis, F.; Puccioni, L. *Tetrahedron* **1997**, *53* (9), 3407–3416.

(86) Shilvock, J. P.; Fleet, G. W. J. *Synlett* **1998**, No. 5, 554–556.

(87) Takahashi, S.; Kuzuhara, H. *J. Carbohydr. Chem.* **1998**, *17* (1), 117–128.

(88) Uriel, C.; Santoyo-González, F. *Synlett* **1999**, No. 5, 593–595.

(89) Kiguchi, T.; Tajiri, K.; Ninomiya, I.; Naito, T. *Tetrahedron* **2000**, *56* (32), 5819–5833.

(90) McDonnell, C.; Cronin, L.; O'Brie, J. L.; Murphy, P. V. *J. Org. Chem.* **2004**, *69* (10), 3565–3568.

(91) Schitter, G.; Scheucher, E.; Steiner, A. J.; Stütz, A. E.; Thonhofer, M.; Tarling, C. A.; Withers, S. G.; Wicki, J.; Fantur, K.; Paschke, E.; Mahuran, D. J.; Rigat, B. A.; Tropak, M.; Wrodnigg, T. M. *Beilstein J. Org. Chem.* **2010**, *6*, 21–28.

(92) Gandy, M. N.; Piggott, M. J.; Stubbs, K. A. *Aust. J. Chem.* **2010**, *63* (10), 1409–1412.

(93) Chan, T.-H.; Chang, Y.-F.; Hsu, J.-J.; Cheng, W.-C. *European J. Org. Chem.* **2010**, *2010* (29), 5555–5559.

(94) Wennekes, T.; Meijer, A. J.; Groen, A. K.; Boot, R. G.; Groener, J. E.; van Eijk, M.; Ottenhoff, R.; Bijl, N.; Ghauharali, K.; Song, H.; O'Shea, T. J.; Liu, H.; Yew, N.;

Copeland, D.; van den Berg, R. J.; van der Marel, G. A.; Overkleeft, H. S.; Aerts, J. M. *J. Med. Chem.* **2010**, *53* (2), 689–698.

(95) Jenkinson, S. F.; Fleet, G. W. J.; Nash, R. J.; Koike, Y.; Adachi, I.; Yoshihara, A.; Morimoto, K.; Izumori, K.; Kato, A. *Org. Lett.* **2011**, *13* (15), 4064–4067.

(96) Corkran, H. M.; Munneke, S.; Dangerfield, E. M.; Stocker, B. L.; Timmer, M. S. M. *J. Org. Chem.* **2013**, *78* (19), 9791–9802.

(97) Asano, K.; Hakogi, T.; Iwama, S.; Katsumura, S. *Chem. Commun.* **1999**, *0* (1), 41–42.

(98) Kim, J.-S.; Lee, Y.-T.; Lee, K.-H.; Myeong, I.-S.; Kang, J.-C.; Jung, C.; Park, S.-H.; Ham, W.-H. *J. Org. Chem.* **2016**, *81* (17), 7432–7438.

(99) Takahata, H.; Banba, Y.; Ouchi, H.; Nemoto, H. *Org. Lett.* **2003**, *5* (14), 2527–2529.

(100) Chacko, S.; Ramapanicker, R. *J. Org. Chem.* **2015**, *80* (9), 4776–4782.

(101) Aoyagi, S.; Fujimaki, S.; Yamazaki, N.; Kibayashi, C. *J. Org. Chem.* **1991**, *56* (2), 815–819.

(102) Ruiz, M.; Ruanova, T. M.; Blanco, O.; Núñez, F.; Pato, C.; Ojea, V. *J. Org. Chem.* **2008**, *73* (6), 2240–2255.

(103) Ruiz, M.; Ruanova, T. M.; Ojea, V.; Quintela, J. *Tetrahedron Lett.* **1999**, *40* (10), 2021–2024.

(104) Kajimoto, T.; Chen, L.; Liu, K. K. C.; Wong, C. H. *J. Am. Chem. Soc.* **1991**, *113* (17), 6678–6680.

(105) Liu, K. K. C.; Kajimoto, T.; Chen, L.; Zhong, Z.; Ichikawa, Y.; Wong, C. H. *J. Org. Chem.* **1991**, *56* (22), 6280–6289.

(106) Johnson, C. R.; Golebiowski, A.; Sundram, H.; Miller, M. W.; Dwaihy, R. L. *Tetrahedron Lett.* **1995**, *36* (5), 653–654.

(107) van den Nieuwendijk, A. M. C. H.; Ruben, M.; Engelsma, S. E.; Risseeuw, M. D.

P.; van den Berg, R. J. B. H. N.; Boot, R. G.; Aerts, J. M.; Brussee, J.; van der Marel, G. A.; Overkleeft, H. S. *Org. Lett.* **2010**, *12* (17), 3957–3959.

(108) Sethi, M. K.; Kumar, A.; Maddur, N.; Shukla, R.; Vemula, L. N. *J. Mol. Catal. B Enzym.* **2015**, *112*, 54–58.

(109) Alvarez-Ruiz, E.; Collis, A. J.; Dann, A. S.; Fosberry, A. P.; Ready, S. J.; Vazquez, M. J. (GlaxoSmitheKline plc). WO 2015121488 A1, 2015.

(110) Schroder, A. *Berichte der Dtsch. Chem. Gesellschaft* **1871**, *4*, 400–404.

(111) Szarek, W. A.; Hay, G. W.; Doboszewski, B.; Perlmutter, M. M. *Carbohydr. Res.* **1986**, *155*, 107–118.

(112) Martin, V. S.; Palazon, J. M. *Tetrahedron Lett.* **1992**, *33* (11), 2399–2402.

(113) Duhamel, L.; Plaquevent, J.-C. *Bull. Soc. Chim. Fr.* **1982**, *2*, 69.

(114) Koppenhoefer, B.; Weber, R.; Schurig, V. *Synthesis.* **1982**, *1982* (04), 316–318.

(115) Halland, N.; Braunton, A.; Bachmann, S.; Marigo, M.; Jørgensen, K. A. *J. Am. Chem. Soc.* **2004**, *126* (15), 4790–4791.

(116) Franzén, J.; Marigo, M.; Fielenbach, D.; Wabnitz, T. C.; Kjærsgaard, A.; Jørgensen, K. A. *J. Am. Chem. Soc.* **2005**, *127* (51), 18296–18304.

(117) Beeson, T. D.; MacMillan, D. W. C. *J. Am. Chem. Soc.* **2005**, *127* (24), 8826–8828.

(118) Brochu, M. P.; Brown, S. P.; MacMillan, D. W. C. *J. Am. Chem. Soc.* **2004**, *126* (13), 4108–4109.

(119) Enders, D.; Hüttl, M. R. M. *Synlett* **2005**, *2005* (06), 991–993.

(120) Steiner, D. D.; Mase, N.; Barbas III, C. F. *Angew. Chemie Int. Ed.* **2005**, *44* (24), 3706–3710.

(121) Amatore, M.; Beeson, T. D.; Brown, S. P.; MacMillan, D. W. C. *Angew. Chemie Int. Ed.* **2009**, *48* (28), 5121–5124.

(122) Kano, T.; Shirozu, F.; Maruoka, K. *Chem. Commun.* **2010**, *46* (40), 7590–7592.

(123) Kano, T.; Ueda, M.; Maruoka, K. *J. Am. Chem. Soc.* **2008**, *130*, 3728–3729.

(124) Cornforth, J. W.; Cornforth, R. H.; Mathew, K. K. *J. Chem. Soc.* **1959**, *0*, 112–127.

(125) Winter, P.; Swatschek, J.; Willot, M.; Radtke, L.; Olbrisch, T.; Schafer, A.; Christmann, M. *Chem. Commun.* **2011**, *47*, 12200–12202.

(126) Fadeyi, O. O.; Lindsley, C. W.; Schulte, M. L. *Org. Lett.* **2012**, *14* (11), 3276–3278.

(127) Dekeukeleire, S.; D'hooghe, M.; T€ Ornroos, K. W.; De Kimpe, N. *J. Org. Chem.* **2010**, *75*, 5934–5940.

(128) Fox, R. J.; Lalic, G.; Bergman, R. G. *J. Am. Chem. Soc.* **2007**, 14144–14145.

(129) Desvergnes, S.; Vallée, Y.; Py, S. *Org. Lett.* **2008**, *10* (14), 2967–2970.

(130) Kim, K. S.; Song, Y. H.; Lee, B. H.; Hahn, C. S. *J. Org. Chem.* **1986**, *51* (3), 404–407.

(131) Zhang, Q.; Qu, Y.; Chen, W.; Wang, Y.; Wu, Q. *Lett. Org. Chem.* **2006**, *3* (4), 271–274.

(132) Pfrengle, F.; Dekaris, V.; Schefzig, L.; Zimmer, R.; Reissig, H. U. *Synlett* **2008**, No. 19, 2965–2968.

(133) Halperin, S. D.; Kang, B.; Britton, R. *Synthesis.* **2011**, *2011* (12), 1946–1953.

(134) Kang, B.; Britton, R. *Org. Lett.* **2007**, *9* (24), 5083–5086.

(135) König, W. A.; Gehrcke, B.; Icheln, D.; Evers, P.; Dönnecke, J.; Wang, W. *J. High Resolut. Chromatogr.* **1992**, *15* (6), 367–372.

(136) Marigo, M.; Fielenbach, D.; Braunton, A.; Kjærsgaard, A.; Jørgensen, K. A. *Angew. Chemie Int. Ed.* **2005**, *44* (24), 3703–3706.

Appendix A

NMR Spectra of Compounds Synthesized in Chapter 2

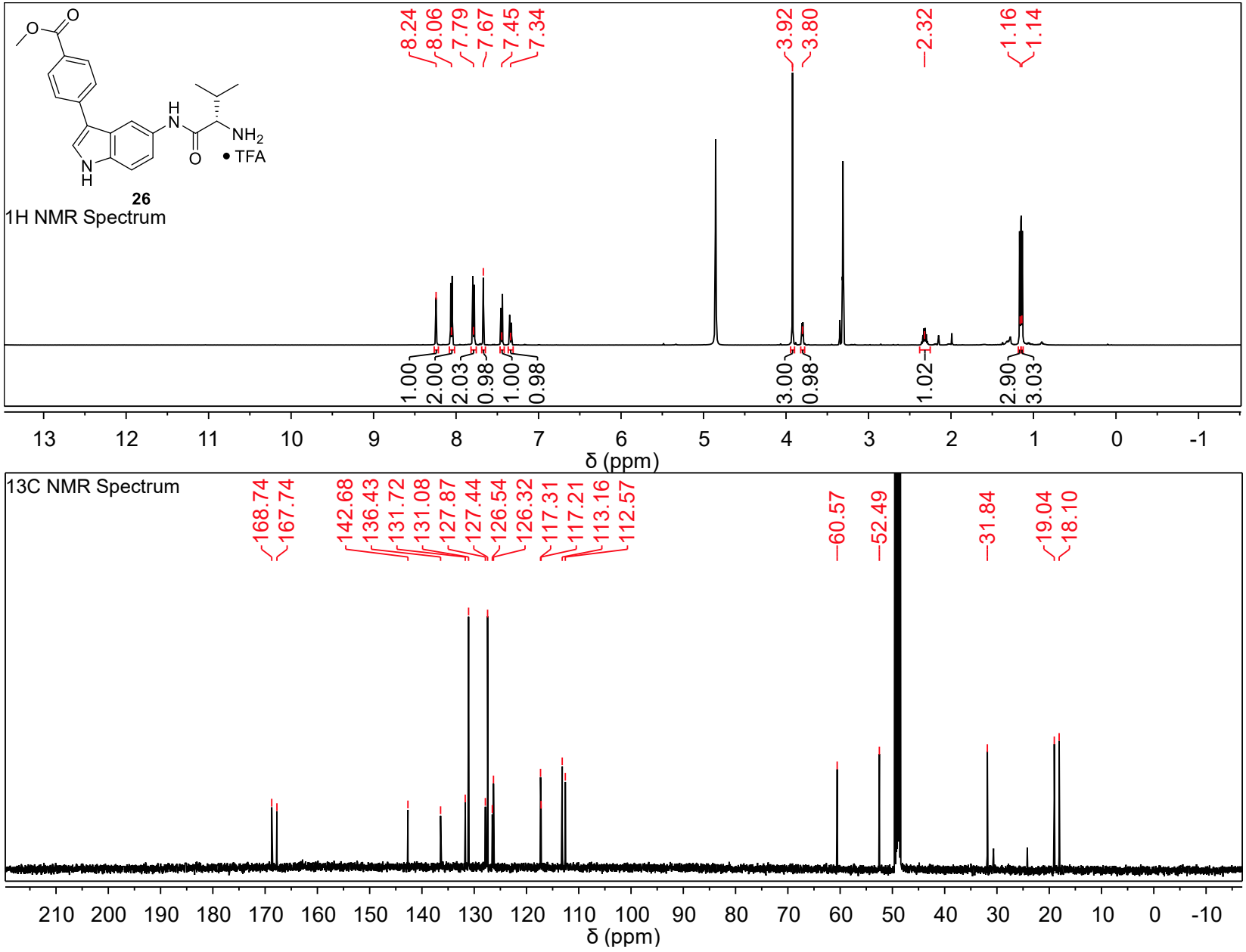
26
1H NMR Spectrum
8.24
8.06
7.79
7.67
7.45
7.34
3.92
3.80
2.32
1.16
1.14
1.00
2.00
2.03
0.98
1.00
0.98
3.00
0.98
1.02
2.90
3.03
δ (ppm)
13C NMR Spectrum
168.74
167.74
142.68
136.43
131.72
131.08
127.87
127.44
126.54
126.32
117.31
117.21
113.16
112.57
60.57
52.49
31.84
19.04
18.10
δ (ppm)

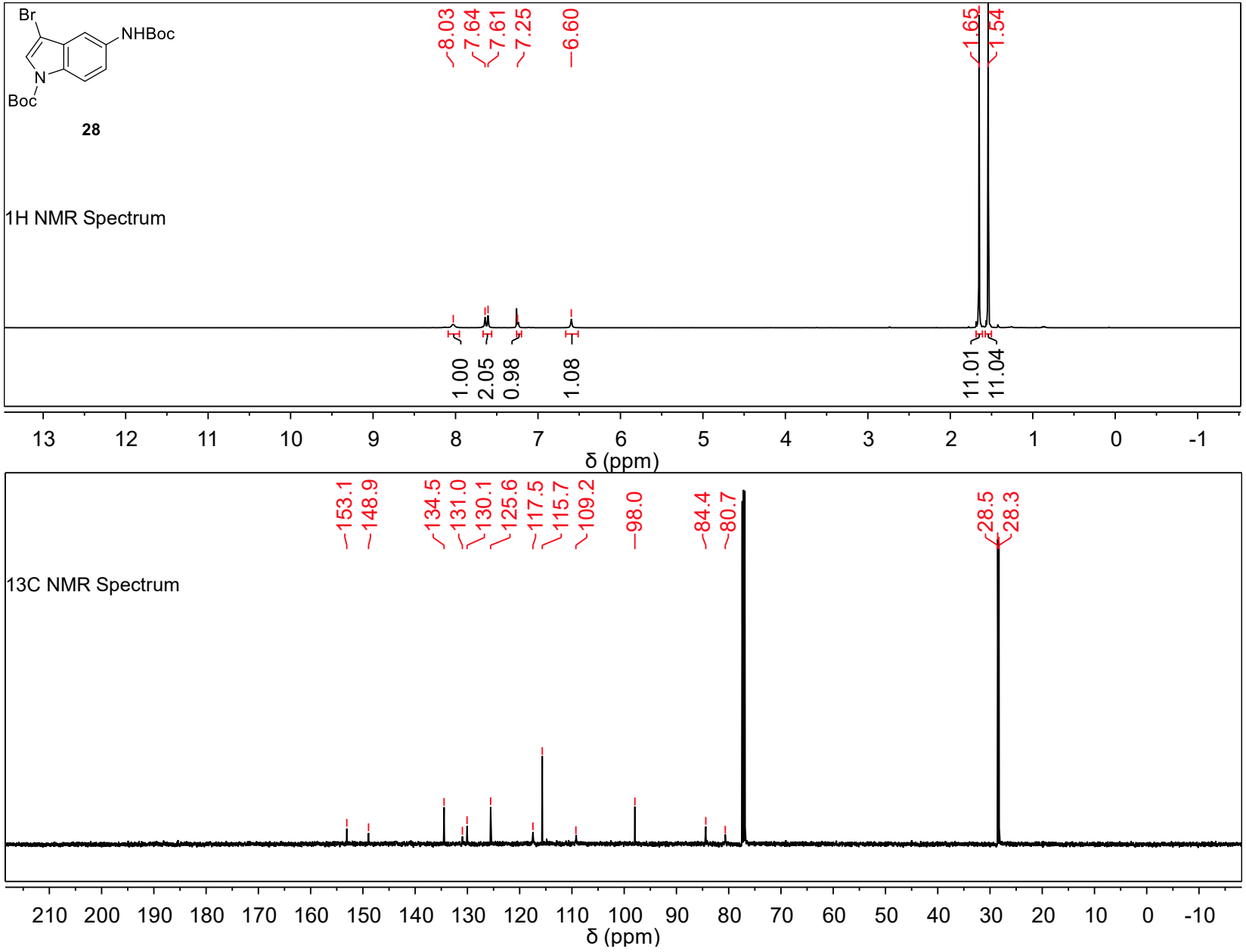
Br
NHBoc
N
Boc
28
1H NMR Spectrum
8.03
7.64
7.61
7.25
6.60
1.65
1.54
1.00
2.05
0.98
1.08
11.01
11.04
δ (ppm)
13C NMR Spectrum
153.1
148.9
134.5
131.0
130.1
125.6
117.5
115.7
109.2
98.0
84.4
80.7
28.5
28.3
δ (ppm)

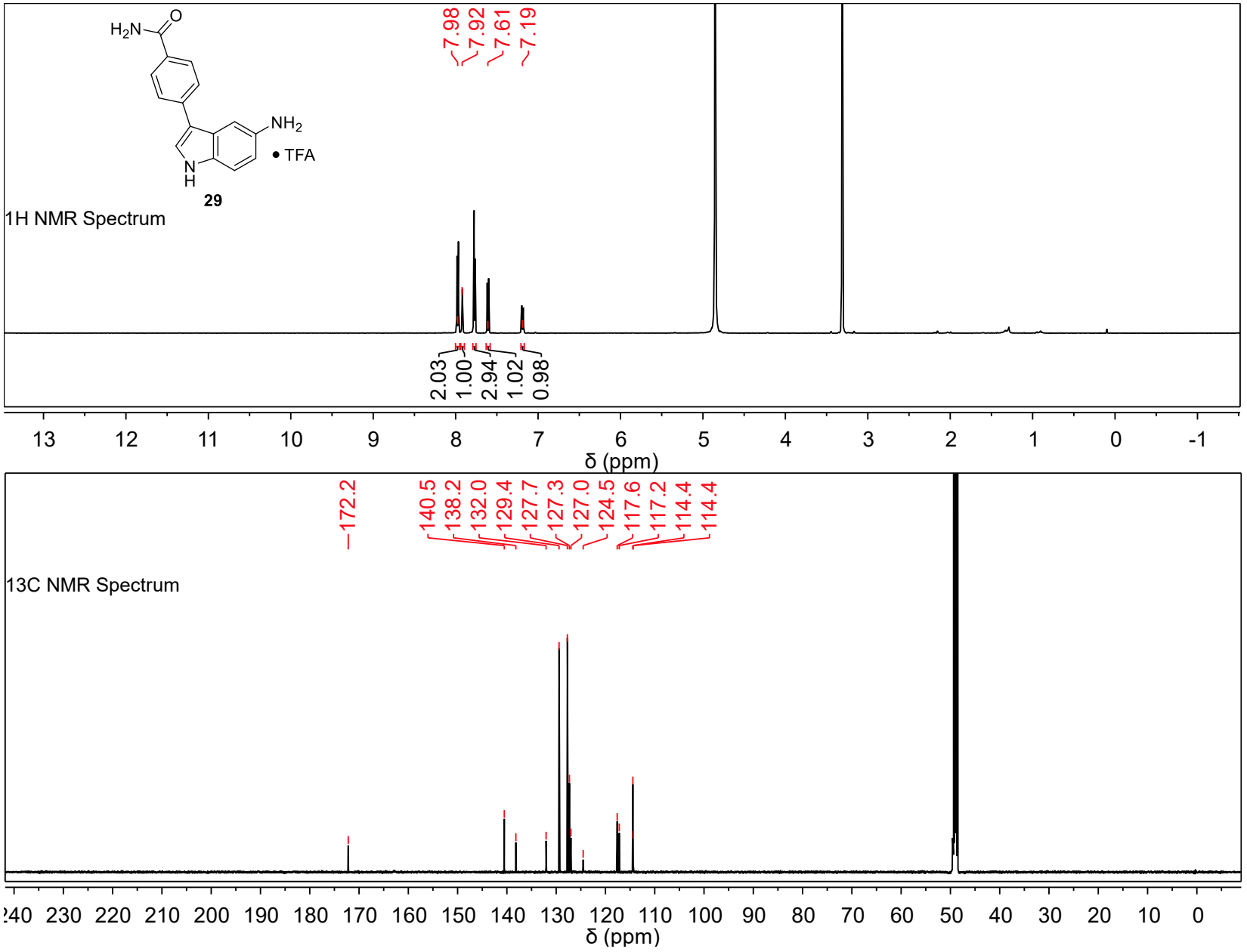
H2N
O
NH2
• TFA
N
H
29
1H NMR Spectrum
7.98
7.92
7.61
7.19
2.03
1.00
2.94
1.02
0.98
13 12 11 10 9 8 7 6 5 4 3 2 1 0 -1
δ (ppm)
13C NMR Spectrum
172.2
140.5
138.2
132.0
129.4
127.7
127.3
127.0
124.5
117.6
117.2
114.4
114.4
240 230 220 210 200 190 180 170 160 150 140 130 120 110 100 90 80 70 60 50 40 30 20 10 0
δ (ppm)

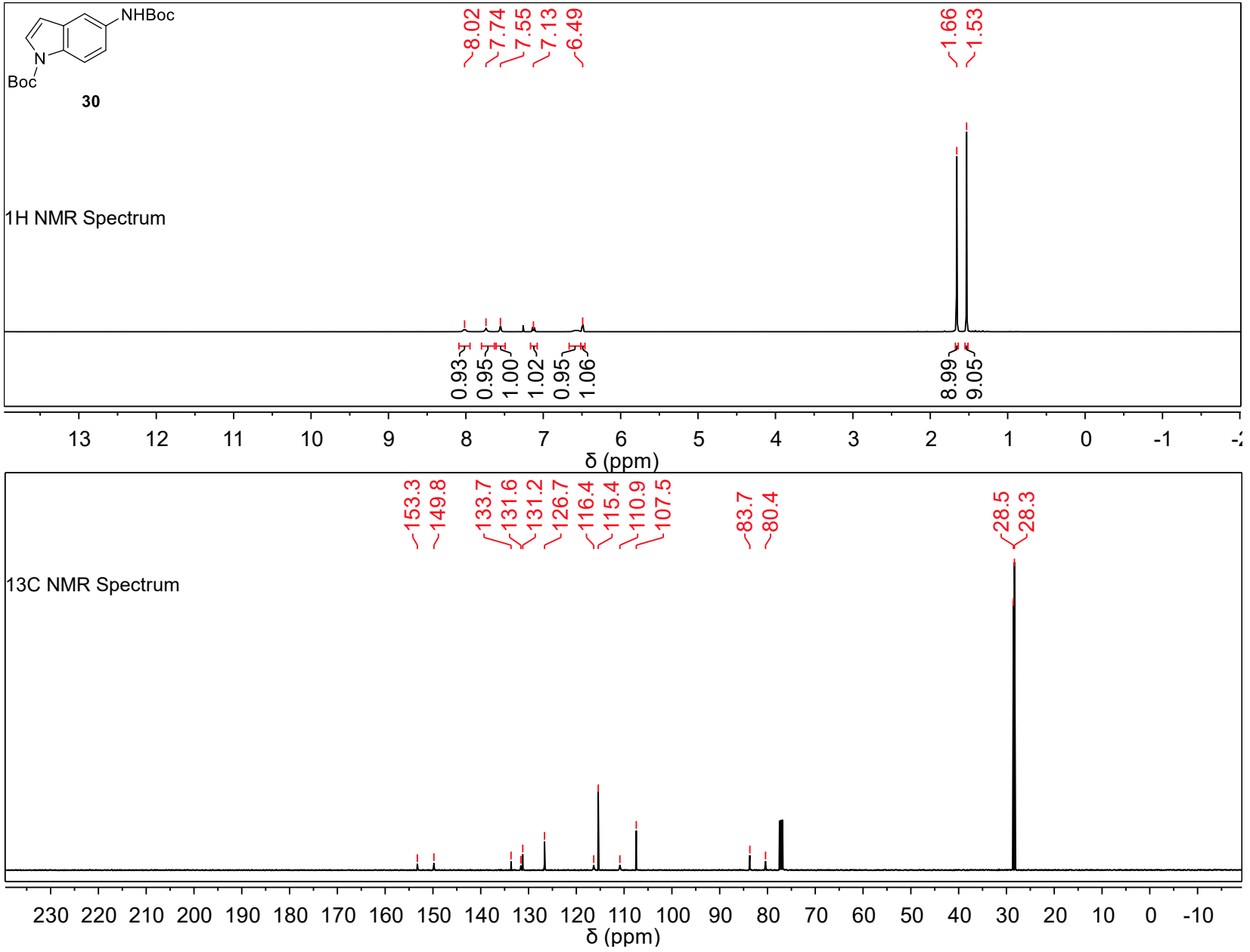
NHBoc
N
Boc
30
8.02
7.74
7.55
7.13
6.49
1.66
1.53
1H NMR Spectrum
0.93
0.95
1.00
1.02
0.95
1.06
8.99
9.05
13 12 11 10 9 8 7 6 5 4 3 2 1 0 -1
δ (ppm)
153.3
149.8
133.7
131.6
131.2
126.7
116.4
115.4
110.9
107.5
83.7
80.4
28.5
28.3
13C NMR Spectrum
230 220 210 200 190 180 170 160 150 140 130 120 110 100 90 80 70 60 50 40 30 20 10 0 -10
δ (ppm)

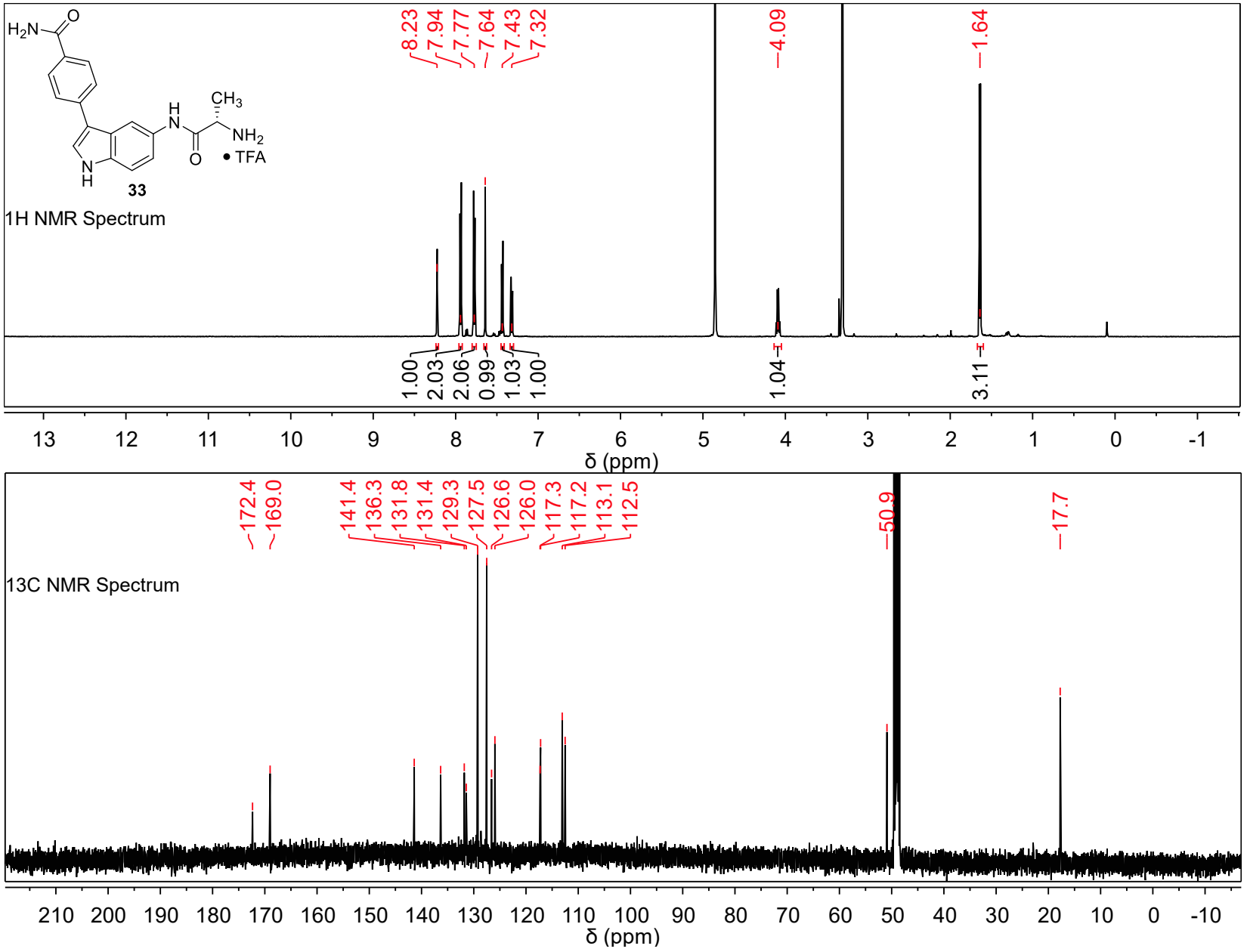
33
1H NMR Spectrum
8.23
7.94
7.77
7.64
7.43
7.32
4.09
1.64
1.00
2.03
2.06
0.99
1.03
1.00
1.04
3.11
δ (ppm)
13C NMR Spectrum
172.4
169.0
141.4
136.3
131.8
131.4
129.3
127.5
126.6
126.0
117.3
117.2
113.1
112.5
50.9
17.7
δ (ppm)

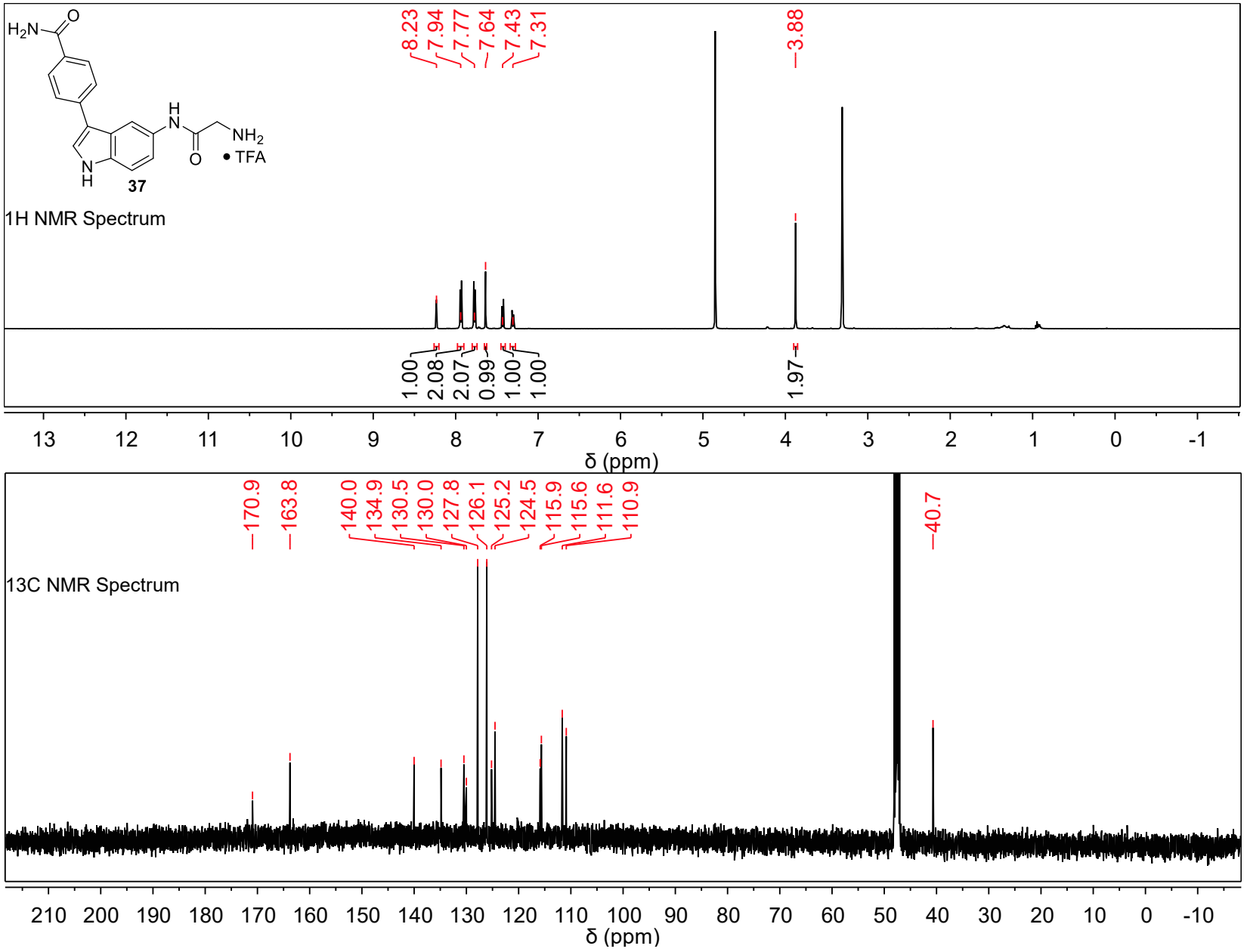
H2N
O
H
N
NH2
O
• TFA
N
H
37
1H NMR Spectrum
8.23
7.94
7.77
7.64
7.43
7.31
3.88
1.00
2.08
2.07
0.99
1.00
1.00
1.97
13 12 11 10 9 8 7 6 5 4 3 2 1 0 -1
δ (ppm)
13C NMR Spectrum
170.9
163.8
140.0
134.9
130.5
130.0
127.8
126.1
125.2
124.5
115.9
115.6
111.6
110.9
40.7
210 200 190 180 170 160 150 140 130 120 110 100 90 80 70 60 50 40 30 20 10 0 -10
δ (ppm)

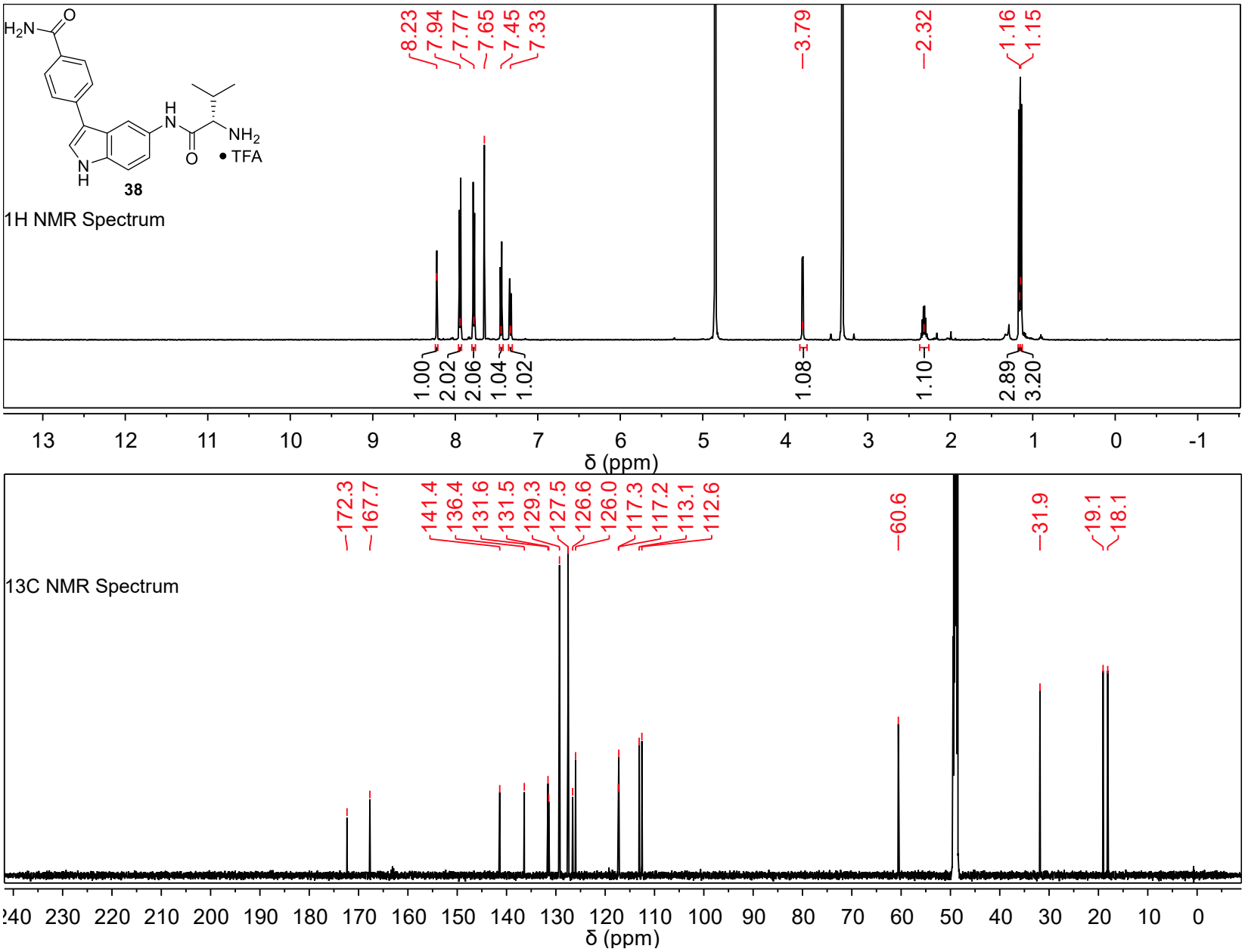
38
1H NMR Spectrum
8.23
7.94
7.77
7.65
7.45
7.33
3.79
2.32
1.16
1.15
1.00
2.02
2.06
1.04
1.02
1.08
1.10
2.89
3.20
δ (ppm)
13C NMR Spectrum
172.3
167.7
141.4
136.4
131.6
131.5
129.3
127.5
126.6
126.0
117.3
117.2
113.1
112.6
60.6
31.9
19.1
18.1
δ (ppm)

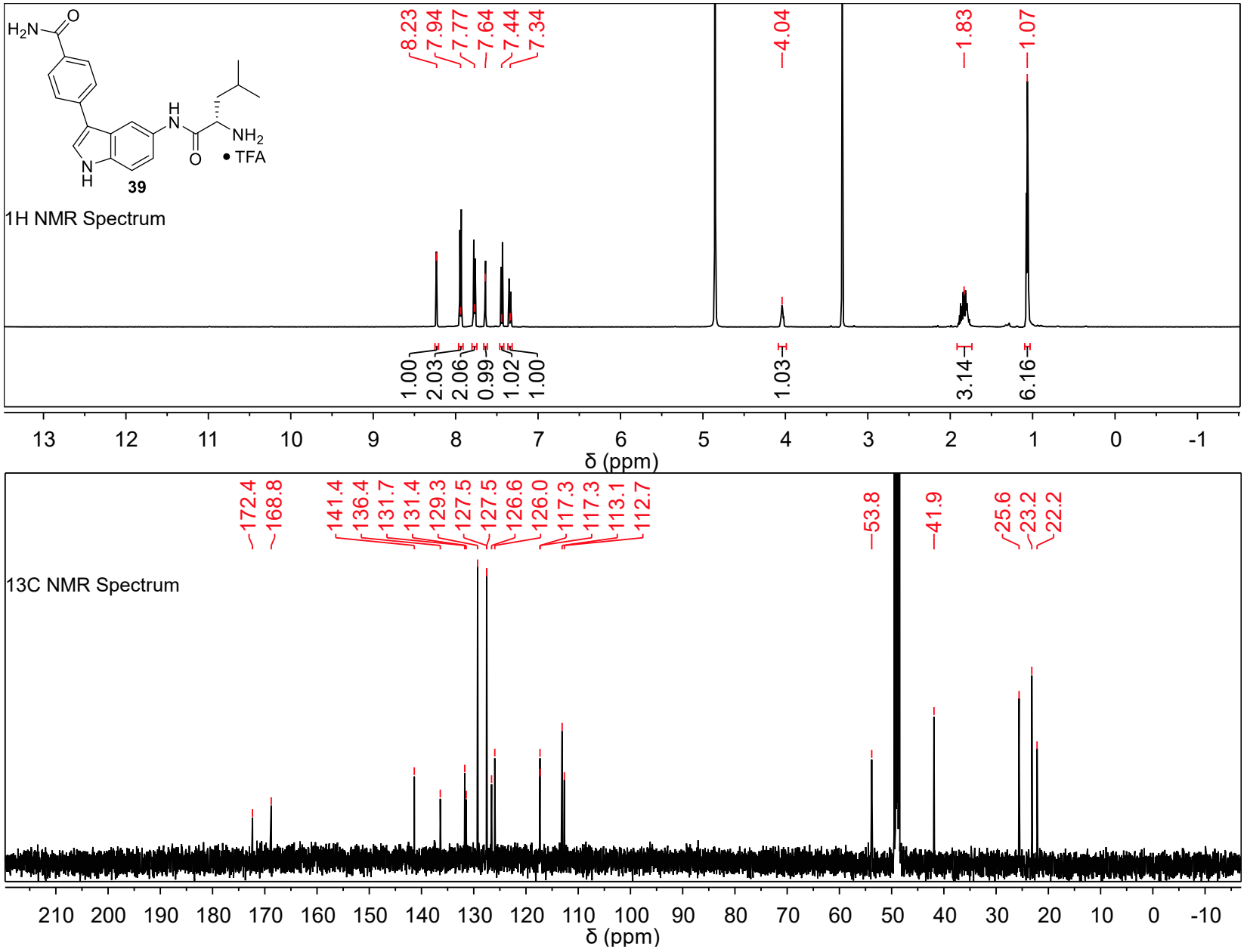
39
1H NMR Spectrum
8.23
7.94
7.77
7.64
7.44
7.34
4.04
1.83
1.07
1.00
2.03
2.06
0.99
1.02
1.00
1.03
3.14
6.16
δ (ppm)
13C NMR Spectrum
172.4
168.8
141.4
136.4
131.7
131.4
129.3
127.5
127.5
126.6
126.0
117.3
117.3
113.1
112.7
53.8
41.9
25.6
23.2
22.2
δ (ppm)

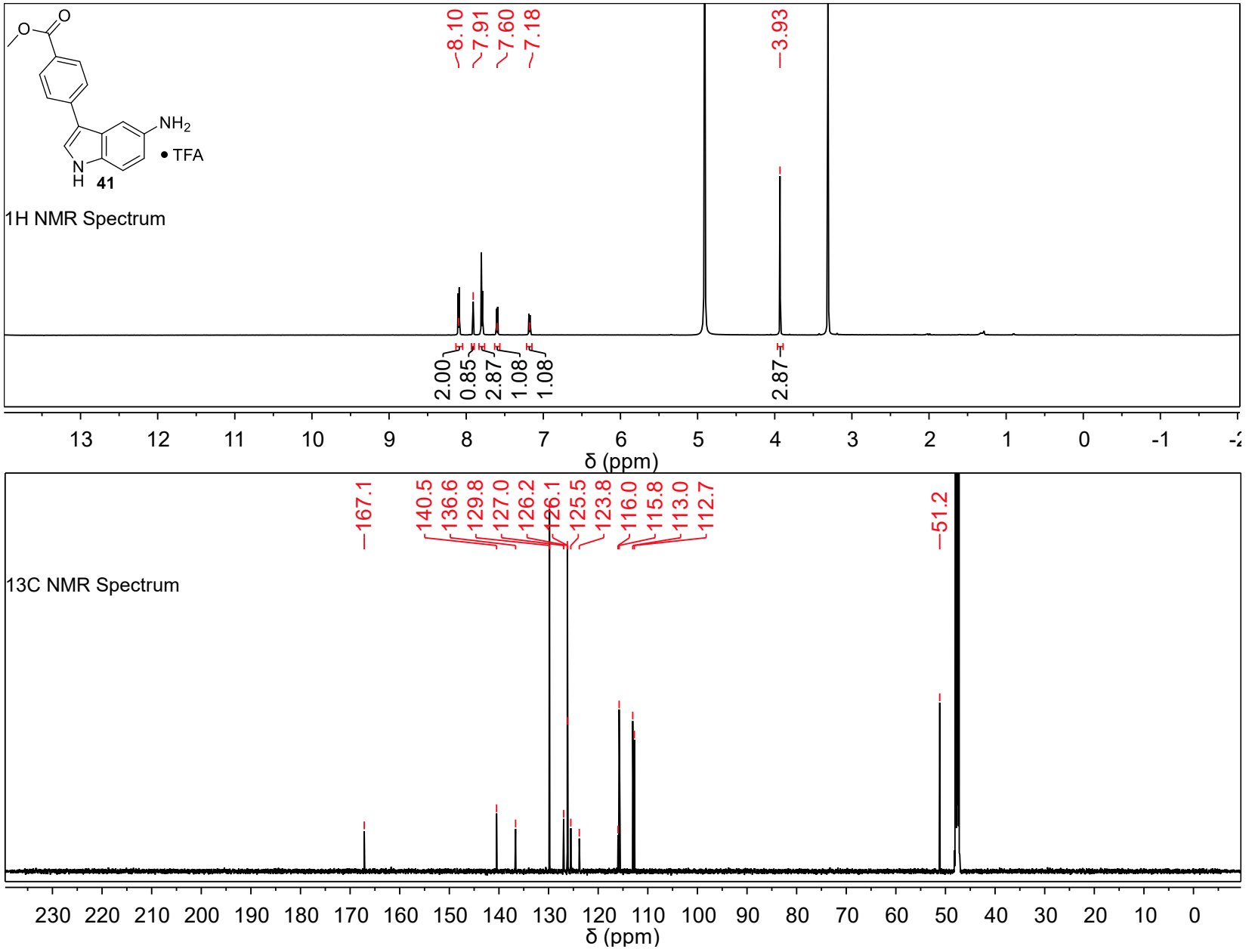
41
1H NMR Spectrum
8.10
7.91
7.60
7.18
3.93
2.00
0.85
2.87
1.08
1.08
2.87
δ (ppm)
13C NMR Spectrum
167.1
140.5
136.6
129.8
127.0
126.2
126.1
125.5
123.8
116.0
115.8
113.0
112.7
51.2
δ (ppm)

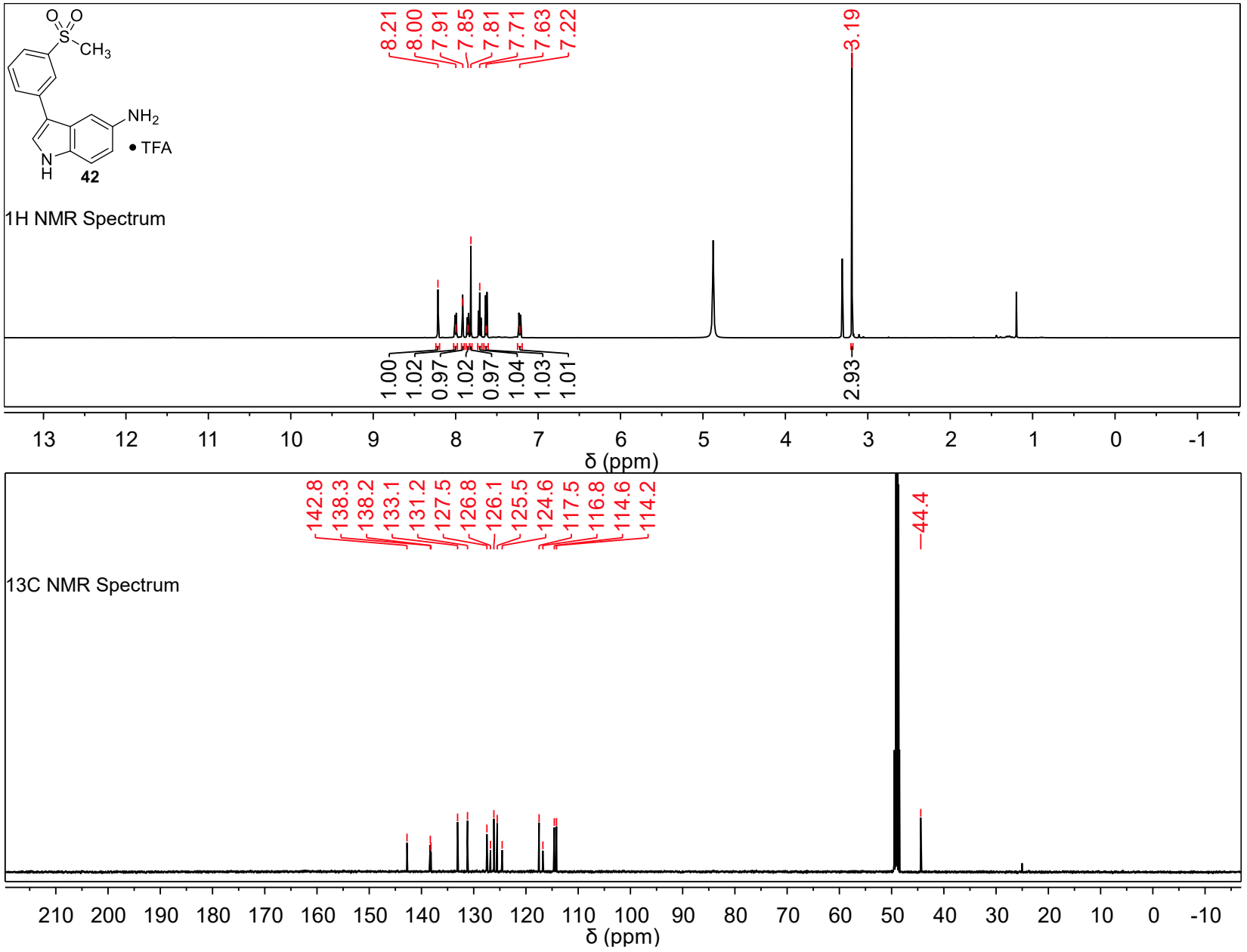
42
1H NMR Spectrum
8.21
8.00
7.91
7.85
7.81
7.71
7.63
7.22
3.19
1.00
1.02
0.97
1.02
0.97
1.04
1.03
1.01
2.93
δ (ppm)
13C NMR Spectrum
142.8
138.3
138.2
133.1
131.2
127.5
126.8
126.1
125.5
124.6
117.5
116.8
114.6
114.2
44.4
δ (ppm)

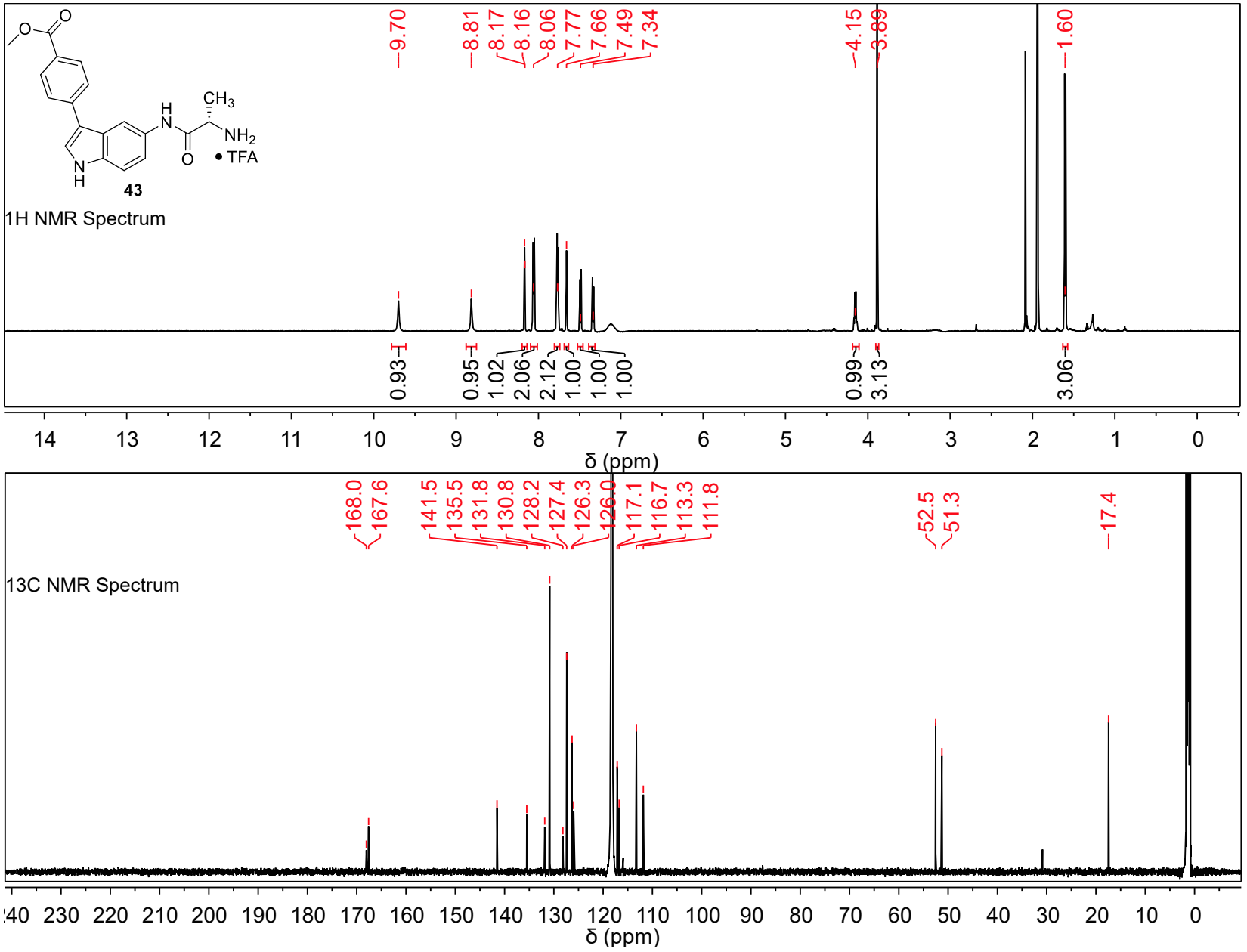
43
1H NMR Spectrum
9.70
8.81
8.17
8.16
8.06
7.77
7.66
7.49
7.34
4.15
3.89
1.60
0.93
0.95
1.02
2.06
2.12
1.00
1.00
1.00
0.99
3.13
3.06
δ (ppm)
13C NMR Spectrum
168.0
167.6
141.5
135.5
131.8
130.8
128.2
127.4
126.3
126.0
117.1
116.7
113.3
111.8
52.5
51.3
17.4
δ (ppm)

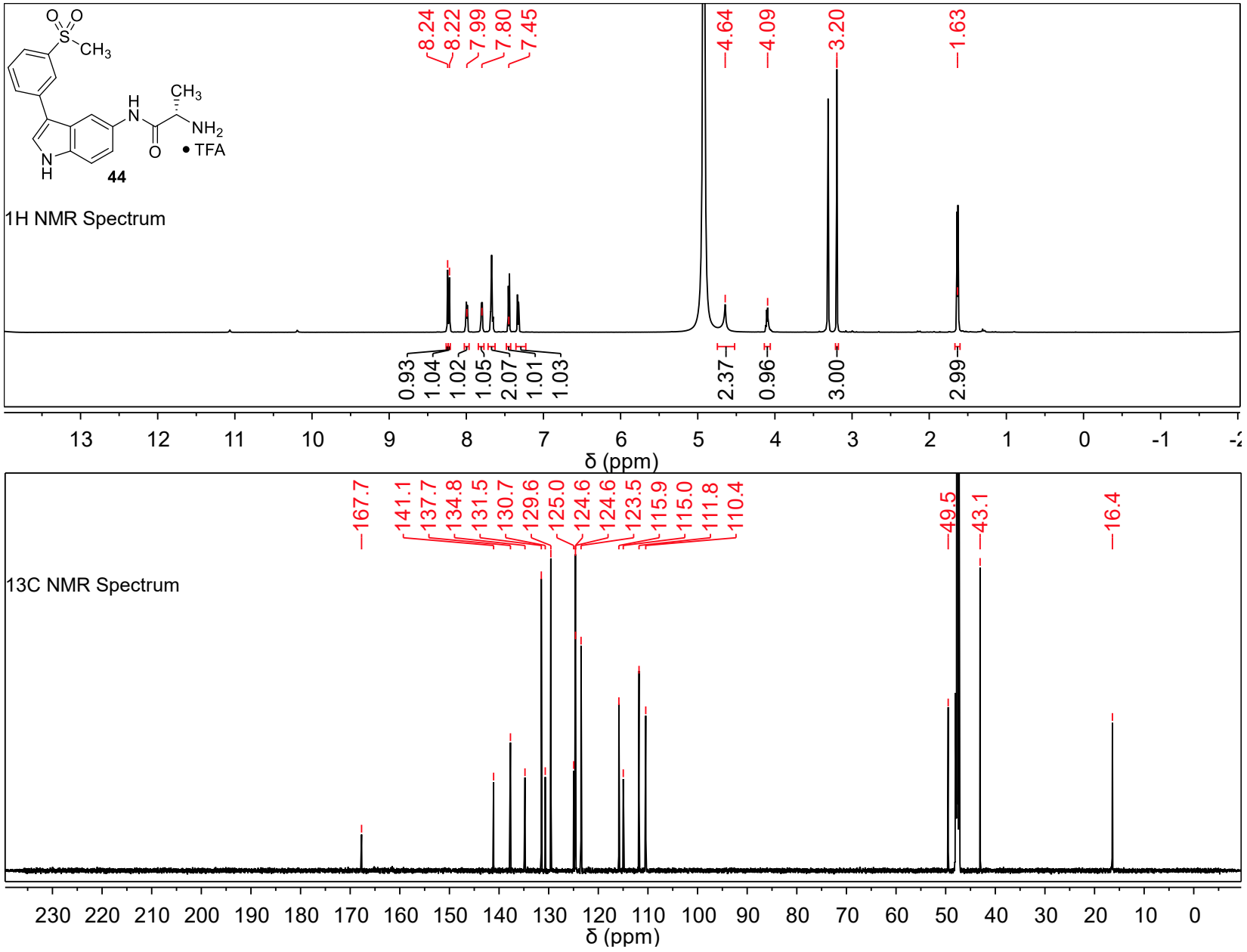
44
1H NMR Spectrum
8.24
8.22
7.99
7.80
7.45
4.64
4.09
3.20
1.63
0.93
1.04
1.02
1.05
2.07
1.01
1.03
2.37
0.96
3.00
2.99
δ (ppm)
13C NMR Spectrum
167.7
141.1
137.7
134.8
131.5
130.7
129.6
125.0
124.6
124.6
123.5
115.9
115.0
111.8
110.4
49.5
43.1
16.4
δ (ppm)

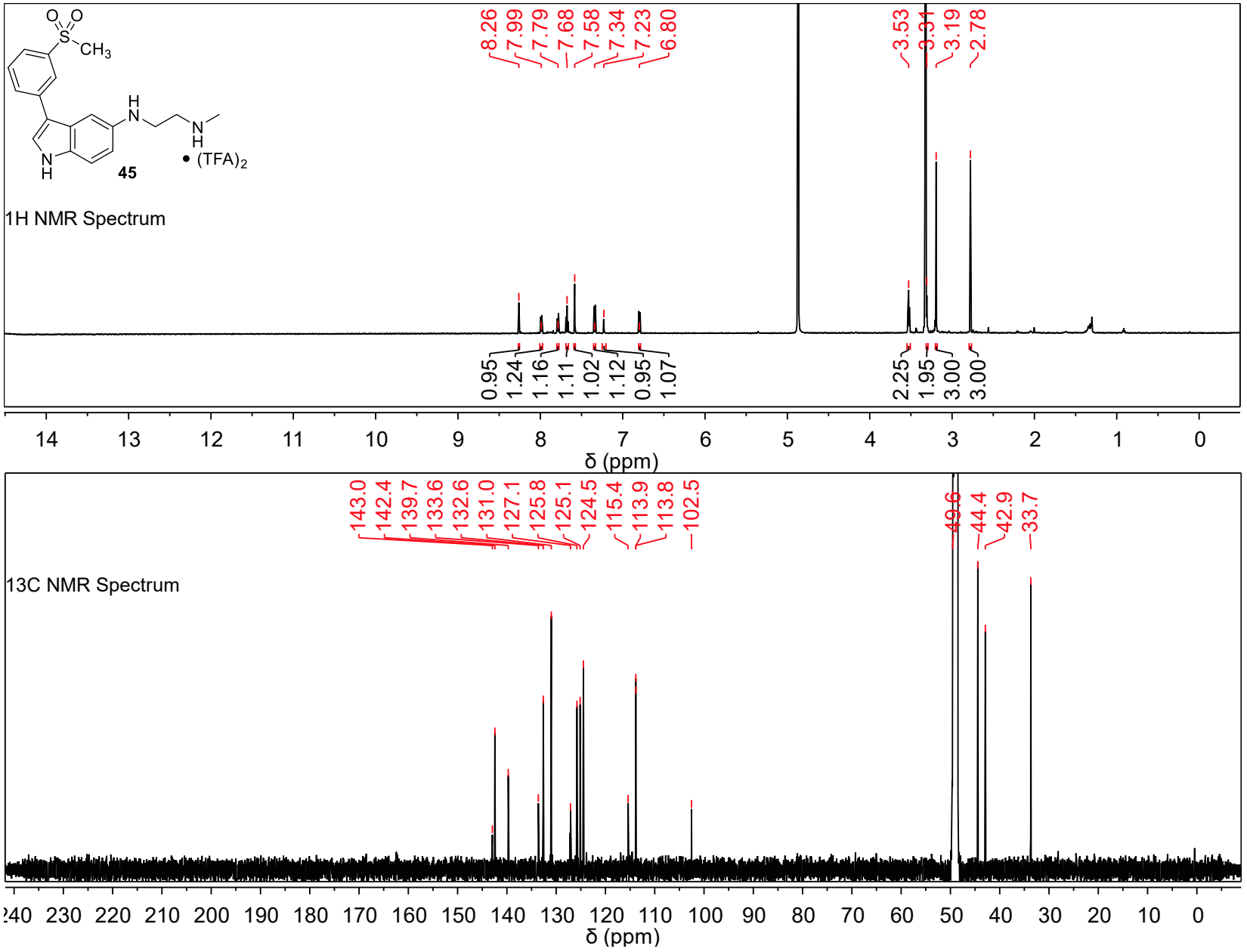
45
• (TFA)2
1H NMR Spectrum
8.26
7.99
7.79
7.68
7.58
7.34
7.23
6.80
3.53
3.34
3.19
2.78
0.95
1.24
1.16
1.11
1.02
1.12
0.95
1.07
2.25
1.95
3.00
3.00
δ (ppm)
13C NMR Spectrum
143.0
142.4
139.7
133.6
132.6
131.0
127.1
125.8
125.1
124.5
115.4
113.9
113.8
102.5
49.6
44.4
42.9
33.7
δ (ppm)

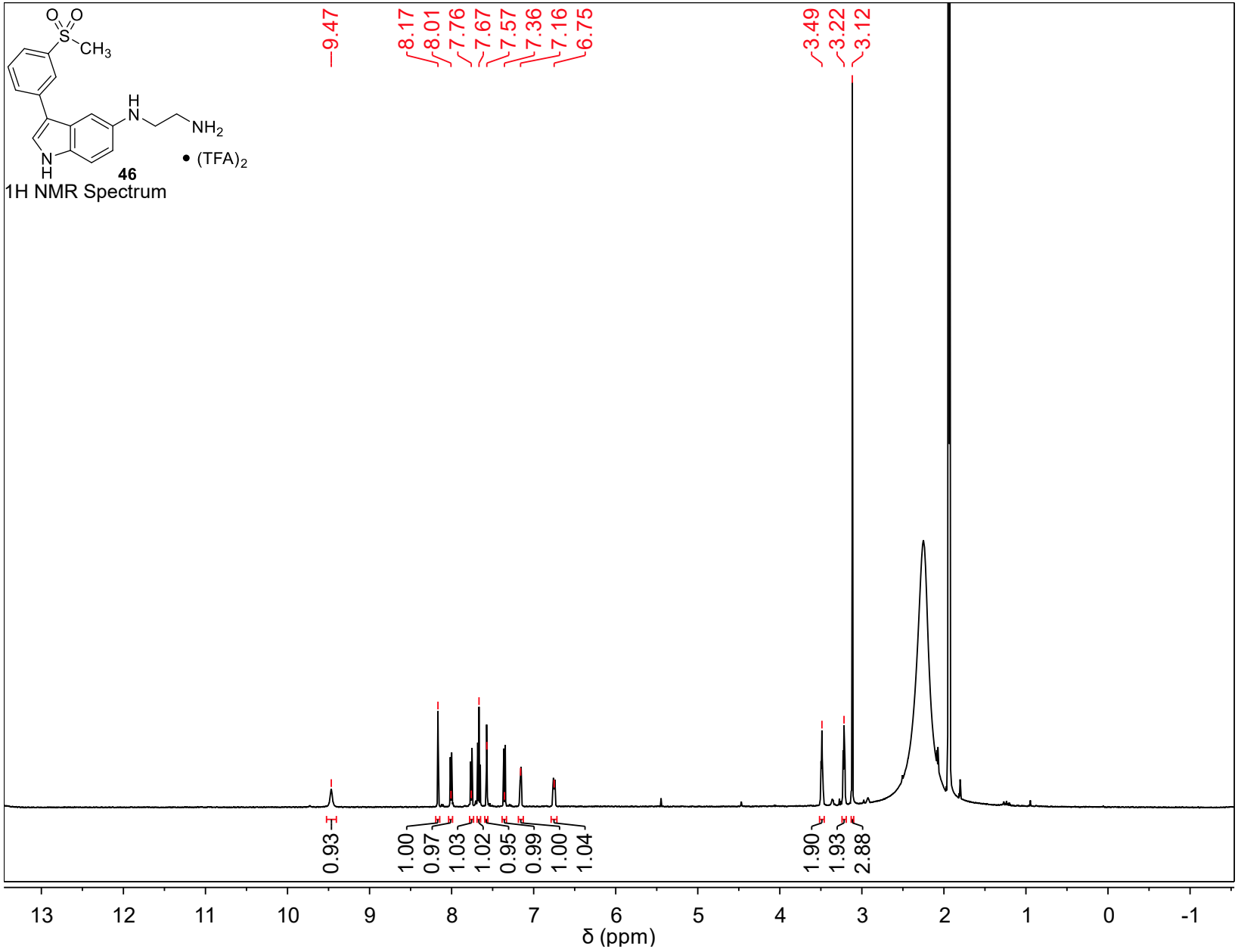

46

1H NMR Spectrum

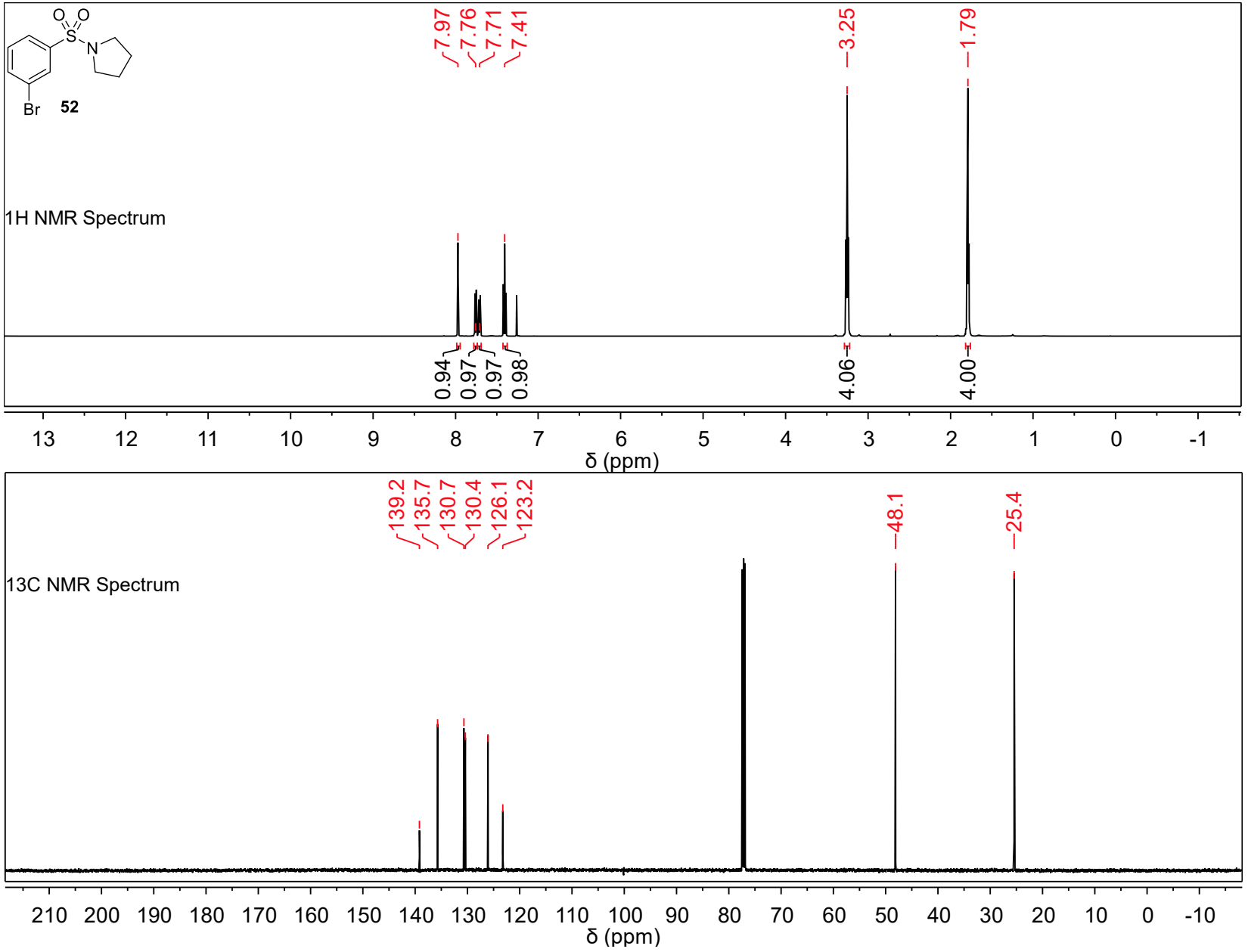
Br
52
1H NMR Spectrum
7.97
7.76
7.71
7.41
3.25
1.79
0.94
0.97
0.97
0.98
4.06
4.00
δ (ppm)
13C NMR Spectrum
139.2
135.7
130.7
130.4
126.1
123.2
48.1
25.4
δ (ppm)

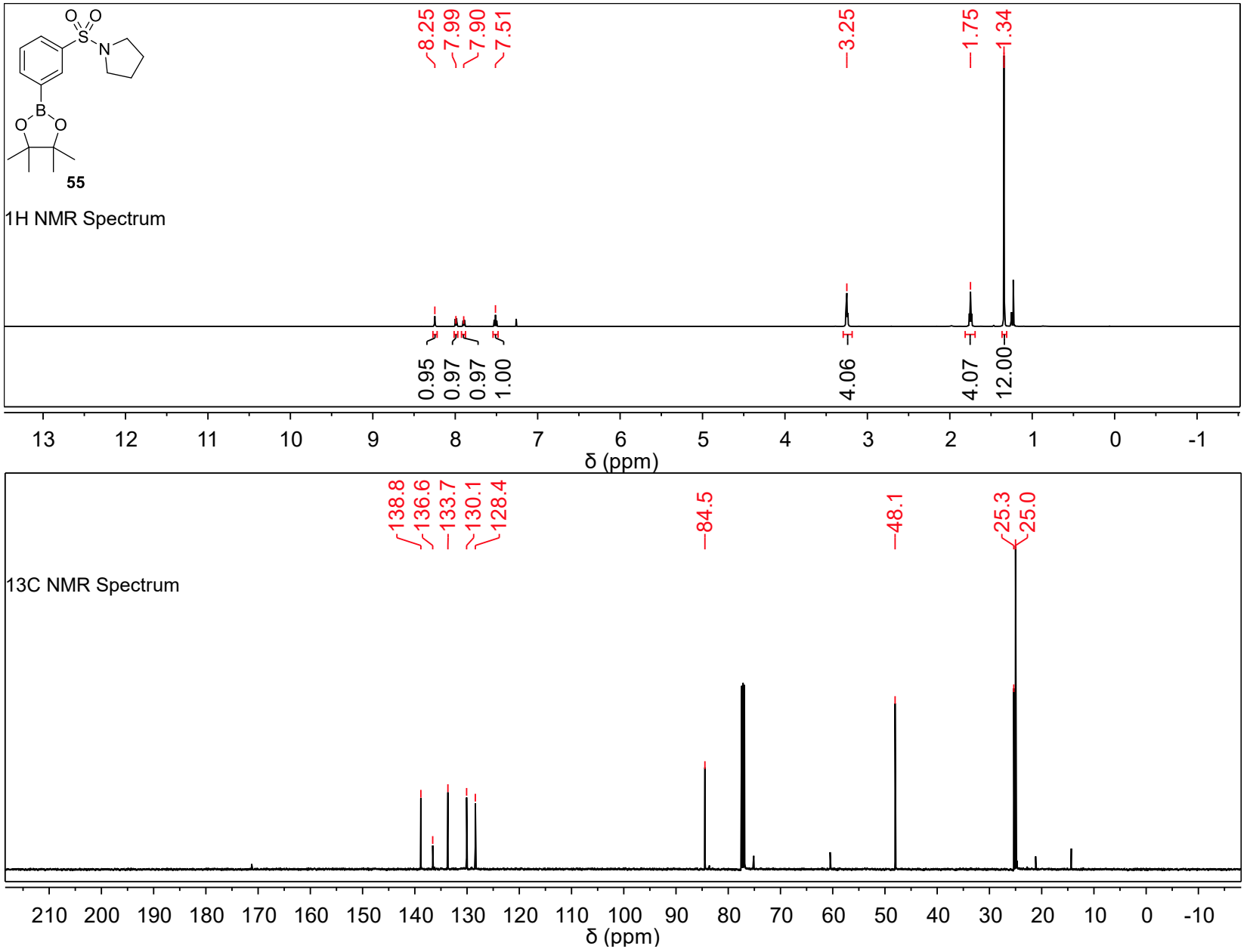
55
1H NMR Spectrum
8.25
7.99
7.90
7.51
3.25
1.75
1.34
0.95
0.97
0.97
1.00
4.06
4.07
12.00
δ (ppm)
13C NMR Spectrum
138.8
136.6
133.7
130.1
128.4
84.5
48.1
25.3
25.0
δ (ppm)

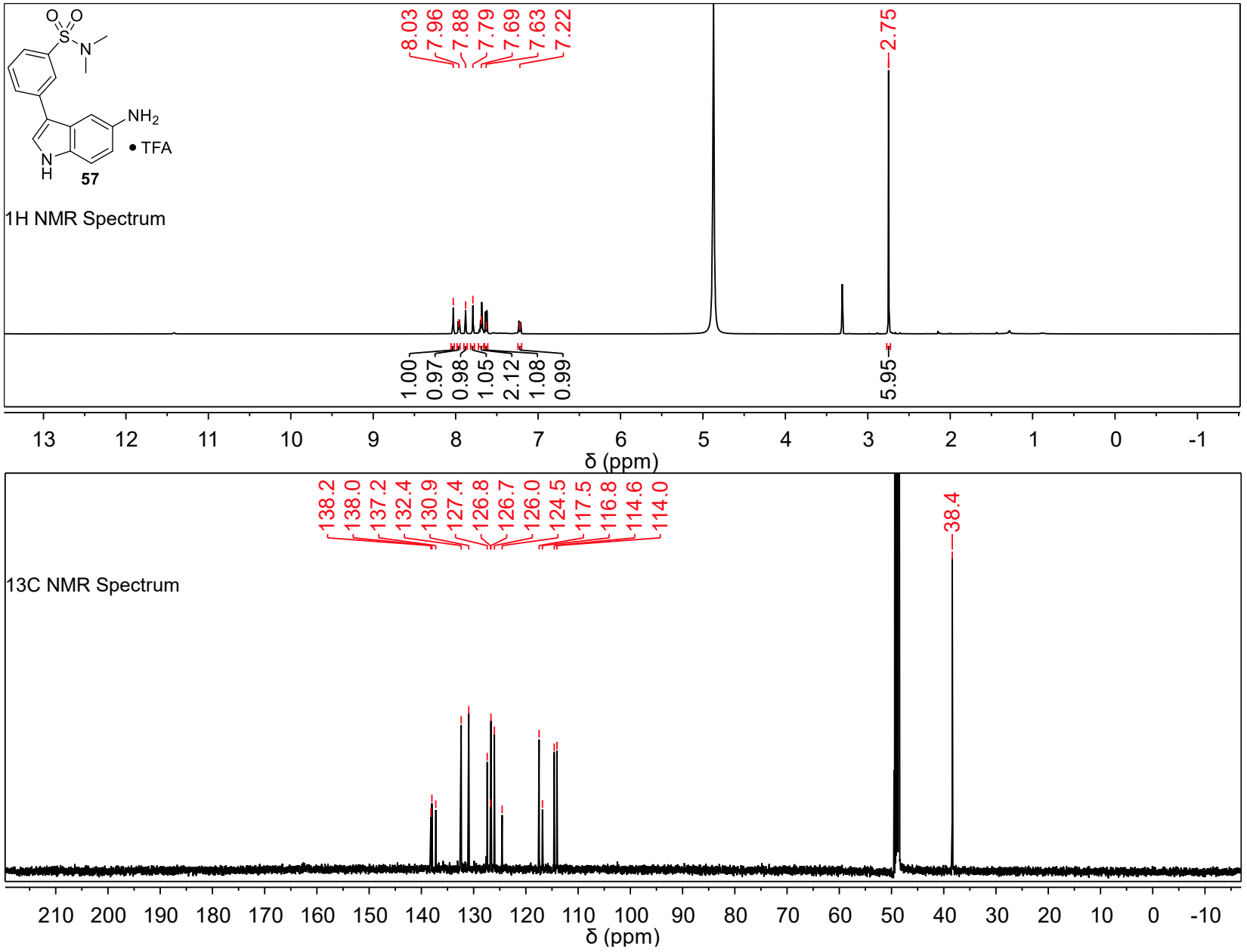
8.03
7.96
7.88
7.79
7.69
7.63
7.22
2.75
1.00
0.97
0.98
1.05
2.12
1.08
0.99
5.95
NH2
• TFA
57
1H NMR Spectrum
δ (ppm)
138.2
138.0
137.2
132.4
130.9
127.4
126.8
126.7
126.0
124.5
117.5
116.8
114.6
114.0
38.4
13C NMR Spectrum
δ (ppm)

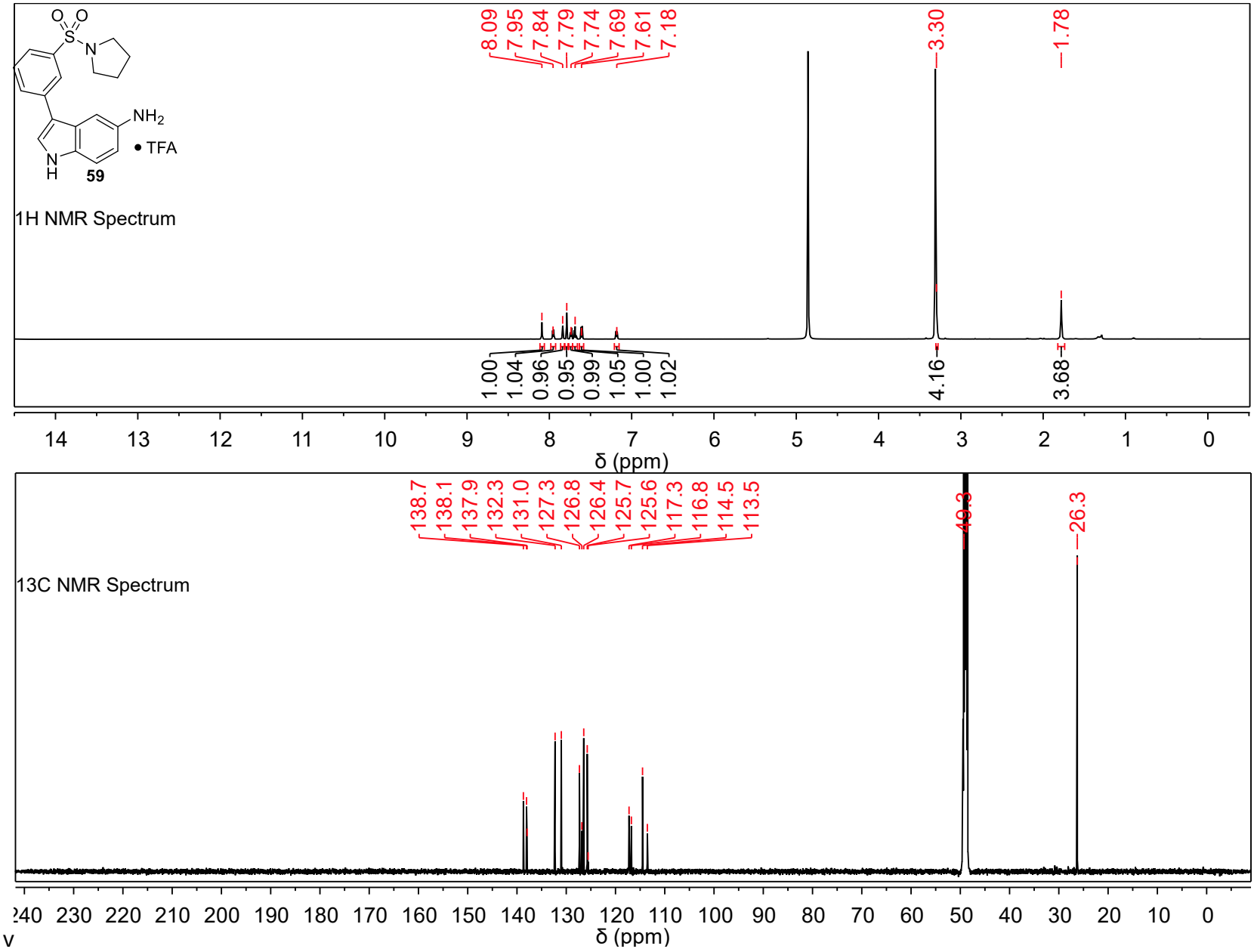
59
• TFA
1H NMR Spectrum
8.09
7.95
7.84
7.79
7.74
7.69
7.61
7.18
3.30
1.78
1.00
1.04
0.96
0.95
0.99
1.05
1.00
1.02
4.16
3.68
δ (ppm)
13C NMR Spectrum
138.7
138.1
137.9
132.3
131.0
127.3
126.8
126.4
125.7
125.6
117.3
116.8
114.5
113.5
49.3
26.3
δ (ppm)

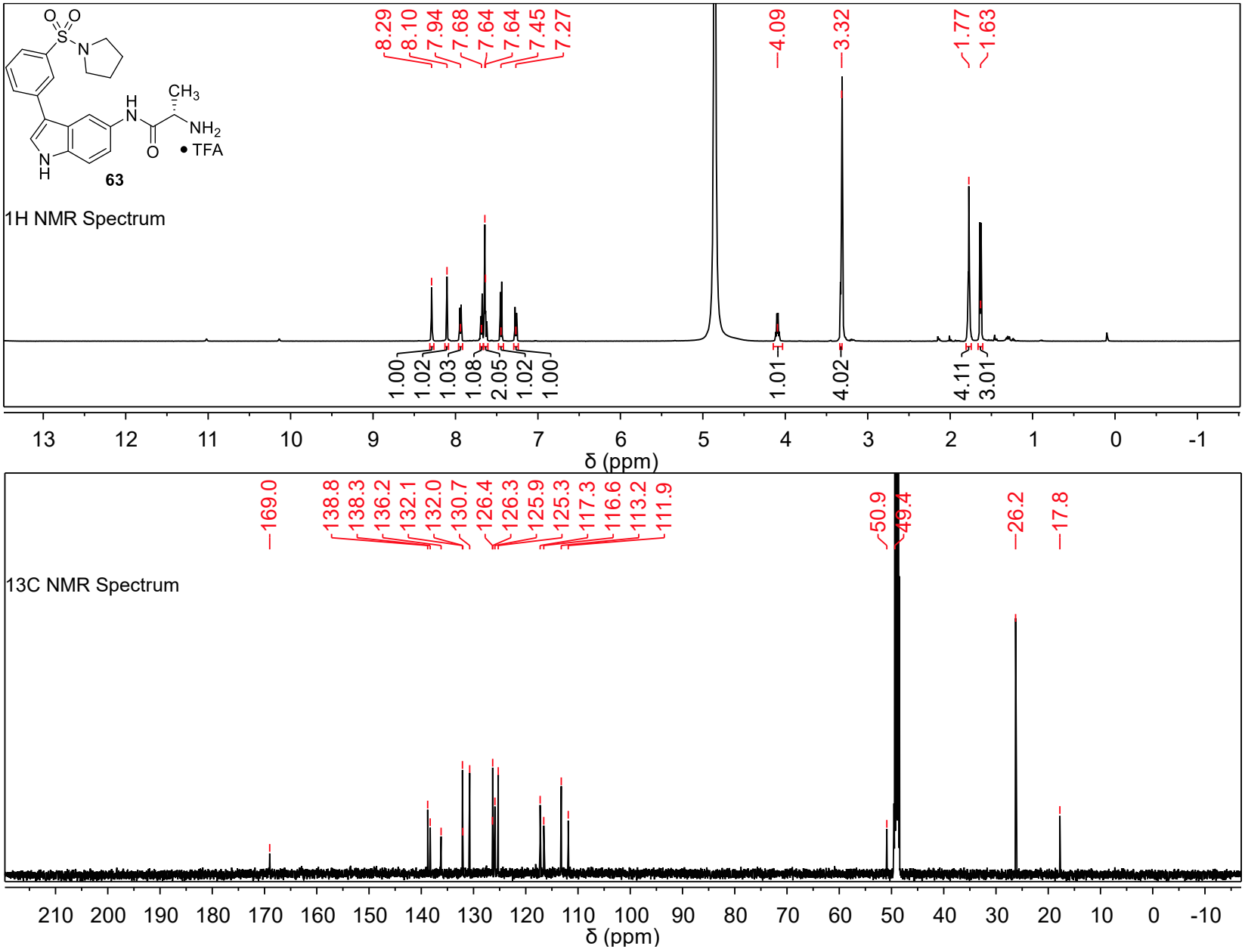
63
1H NMR Spectrum
8.29
8.10
7.94
7.68
7.64
7.64
7.45
7.27
4.09
3.32
1.77
1.63
1.00
1.02
1.03
1.08
2.05
1.02
1.00
1.01
4.02
4.11
3.01
δ (ppm)
13C NMR Spectrum
169.0
138.8
138.3
136.2
132.1
132.0
130.7
126.4
126.3
125.9
125.3
117.3
116.6
113.2
111.9
50.9
49.4
26.2
17.8
δ (ppm)

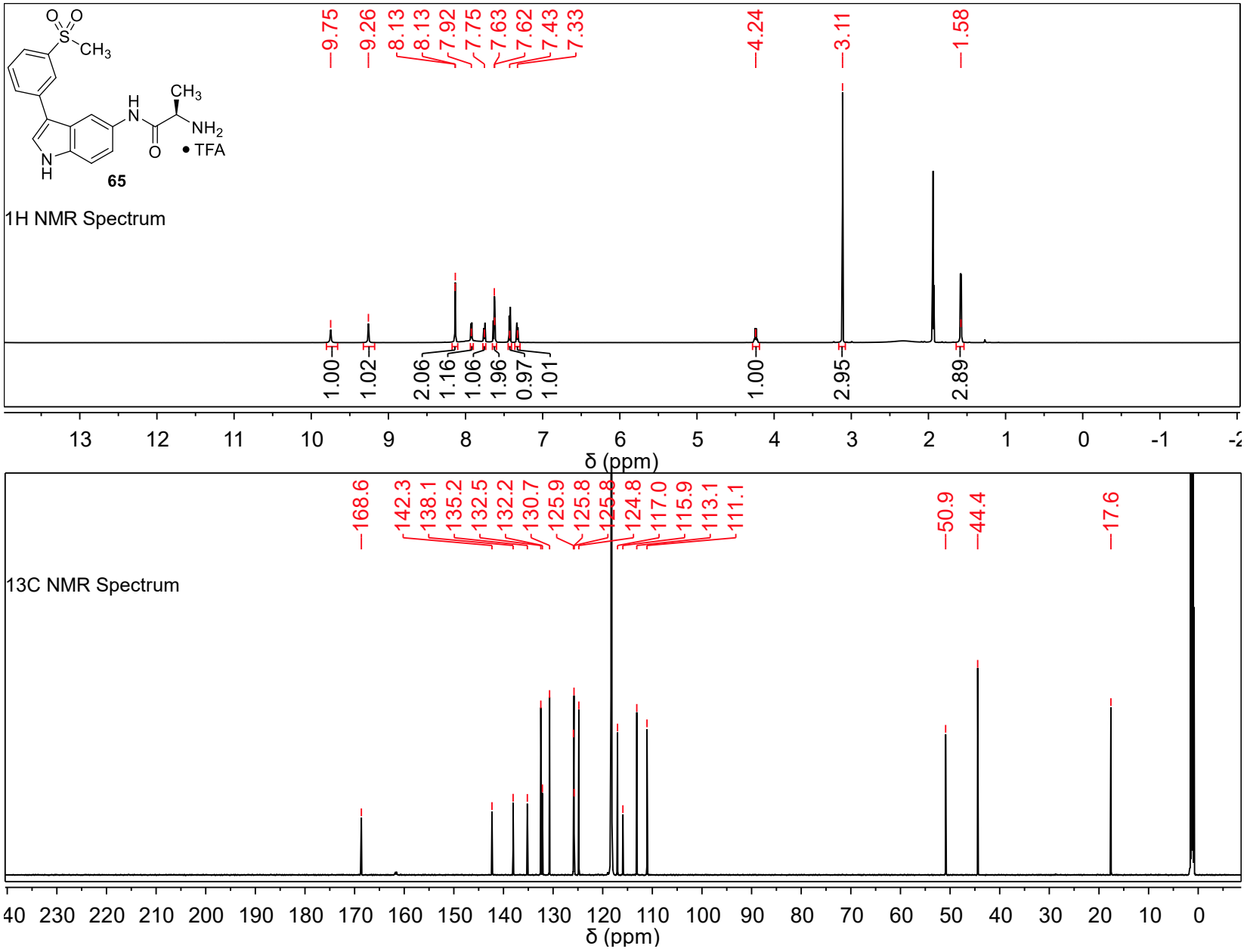
65
1H NMR Spectrum
9.75
9.26
8.13
8.13
7.92
7.75
7.63
7.62
7.43
7.33
4.24
3.11
1.58
1.00
1.02
2.06
1.16
1.06
1.96
0.97
1.01
1.00
2.95
2.89
δ (ppm)
13C NMR Spectrum
168.6
142.3
138.1
135.2
132.5
132.2
130.7
125.9
125.8
125.8
124.8
117.0
115.9
113.1
111.1
50.9
44.4
17.6
δ (ppm)

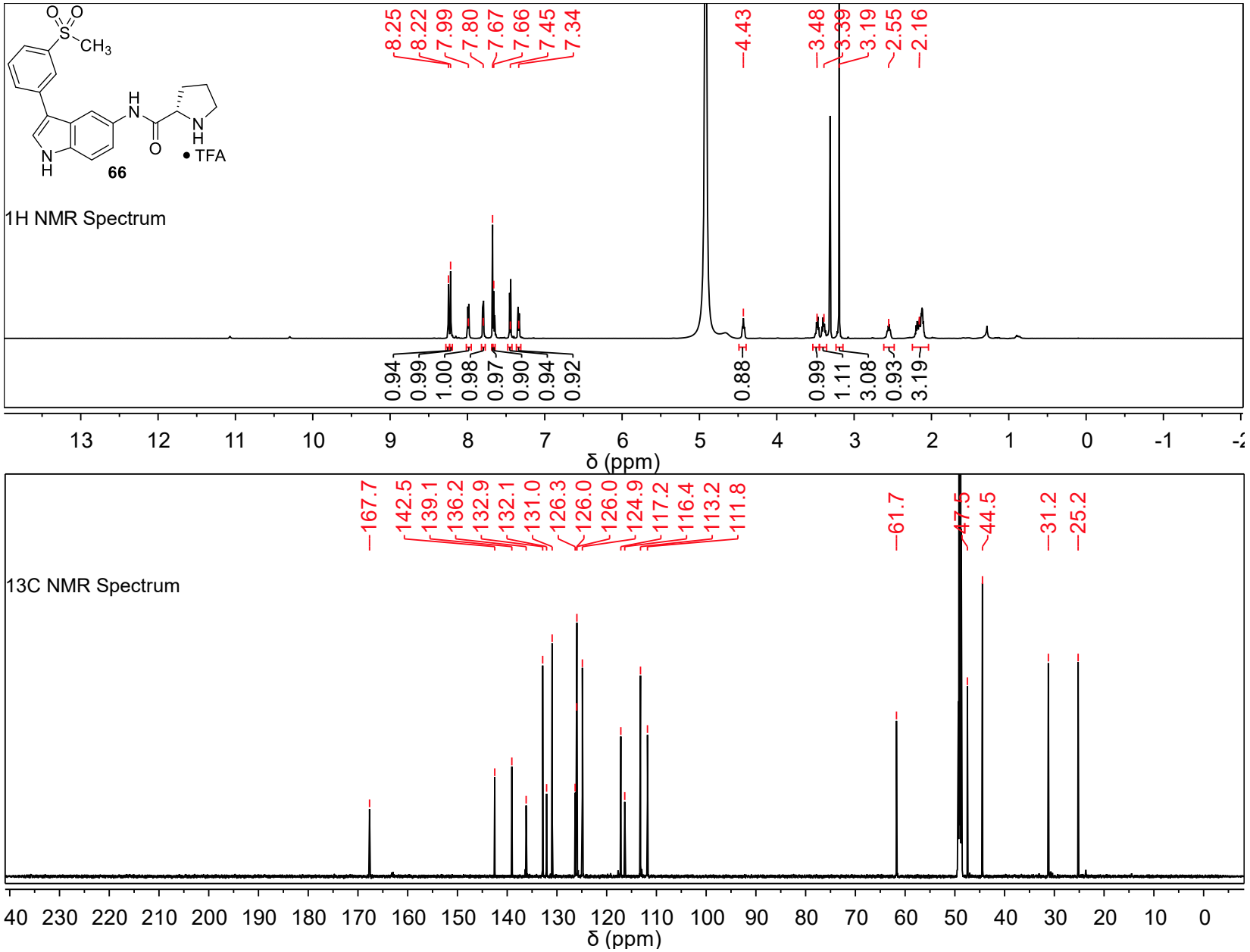
66
• TFA
1H NMR Spectrum
8.25
8.22
7.99
7.80
7.67
7.66
7.45
7.34
4.43
3.48
3.39
3.19
2.55
2.16
0.94
0.99
1.00
0.98
0.97
0.90
0.94
0.92
0.88
0.99
1.11
3.08
0.93
3.19
δ (ppm)
13C NMR Spectrum
167.7
142.5
139.1
136.2
132.9
132.1
131.0
126.3
126.0
126.0
124.9
117.2
116.4
113.2
111.8
61.7
47.5
44.5
31.2
25.2
δ (ppm)

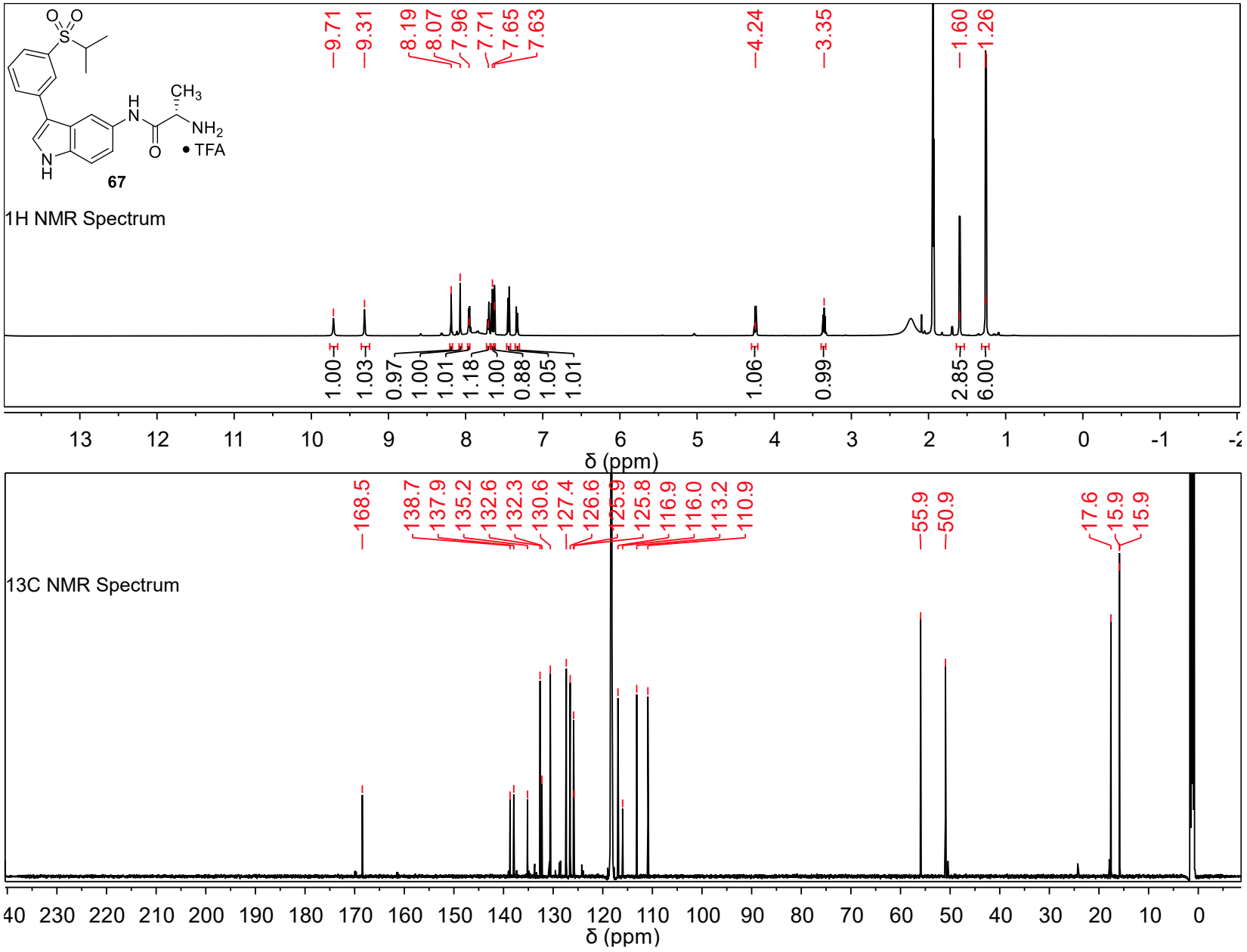
67
1H NMR Spectrum
9.71
9.31
8.19
8.07
7.96
7.71
7.65
7.63
4.24
3.35
1.60
1.26
1.00
1.03
0.97
1.00
1.01
1.18
1.00
0.88
1.05
1.01
1.06
0.99
2.85
6.00
δ (ppm)
13C NMR Spectrum
168.5
138.7
137.9
135.2
132.6
132.3
130.6
127.4
126.6
125.9
125.8
116.9
116.0
113.2
110.9
55.9
50.9
17.6
15.9
15.9
δ (ppm)

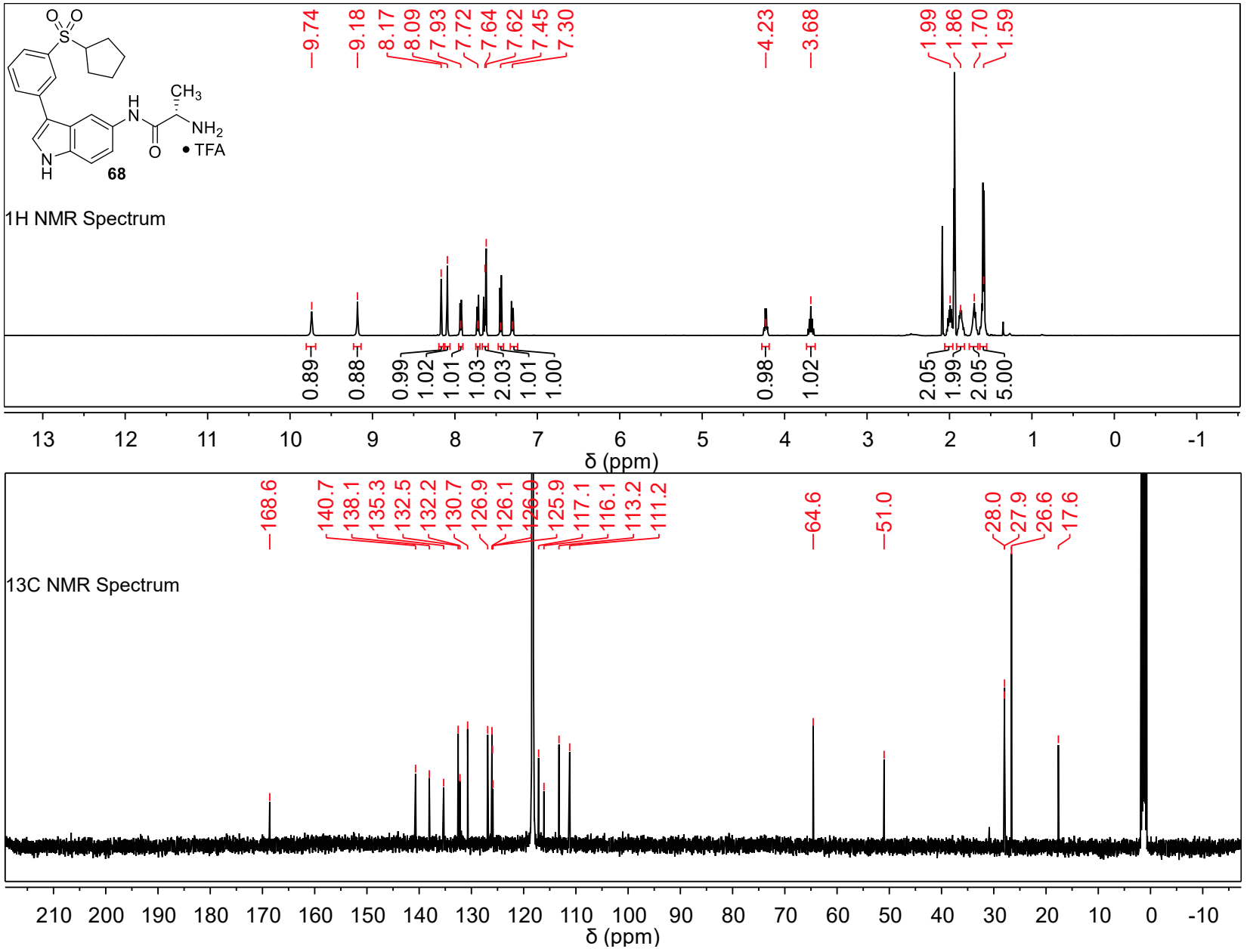
68
1H NMR Spectrum
9.74
9.18
8.17
8.09
7.93
7.72
7.64
7.62
7.45
7.30
4.23
3.68
1.99
1.86
1.70
1.59
0.89
0.88
0.99
1.02
1.01
1.03
2.03
1.01
1.00
0.98
1.02
2.05
1.99
2.05
5.00
δ (ppm)
13C NMR Spectrum
168.6
140.7
138.1
135.3
132.5
132.2
130.7
126.9
126.1
126.0
125.9
117.1
116.1
113.2
111.2
64.6
51.0
28.0
27.9
26.6
17.6
δ (ppm)

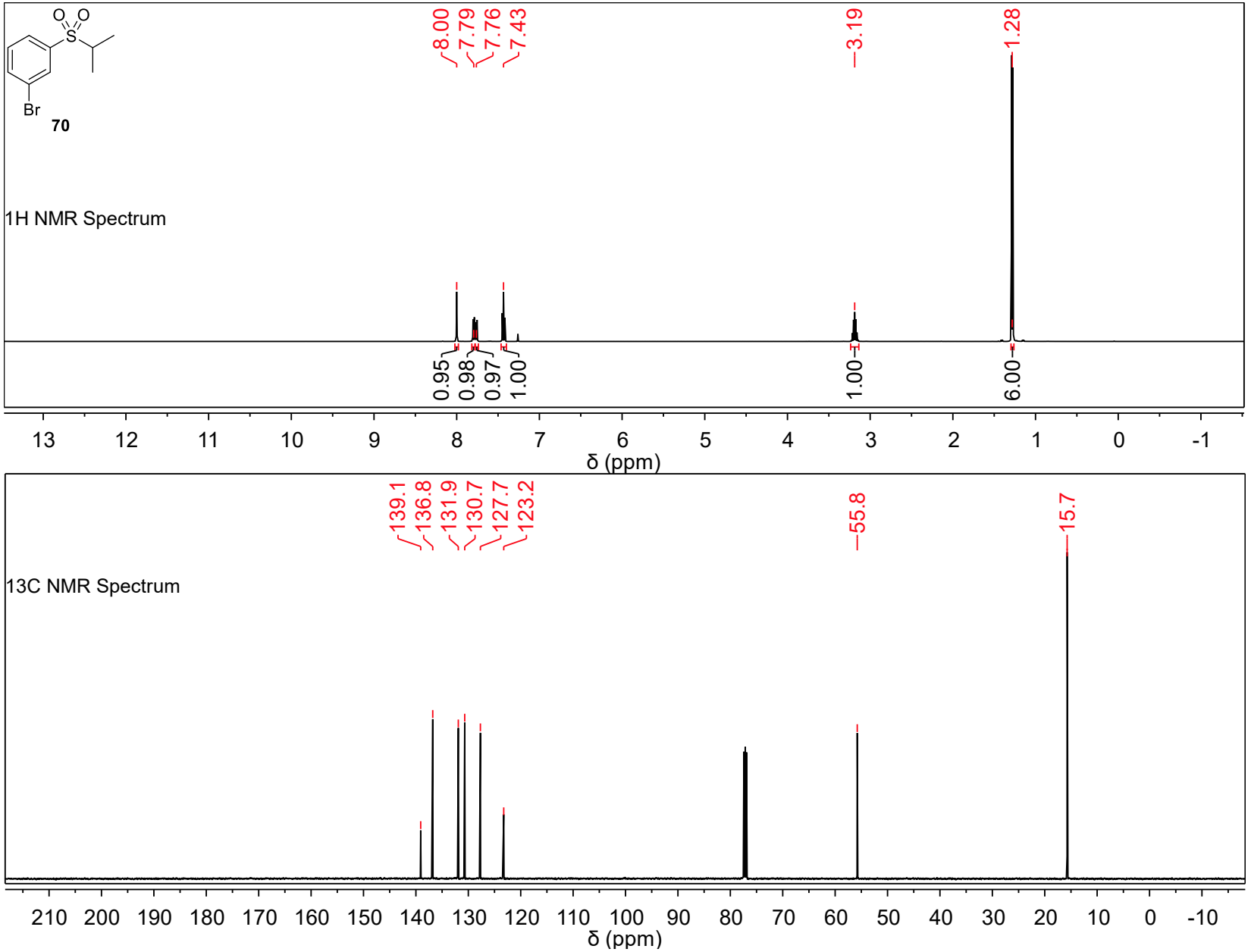
70
1H NMR Spectrum
8.00
7.79
7.76
7.43
3.19
1.28
0.95
0.98
0.97
1.00
1.00
6.00
δ (ppm)
13C NMR Spectrum
139.1
136.8
131.9
130.7
127.7
123.2
55.8
15.7
δ (ppm)

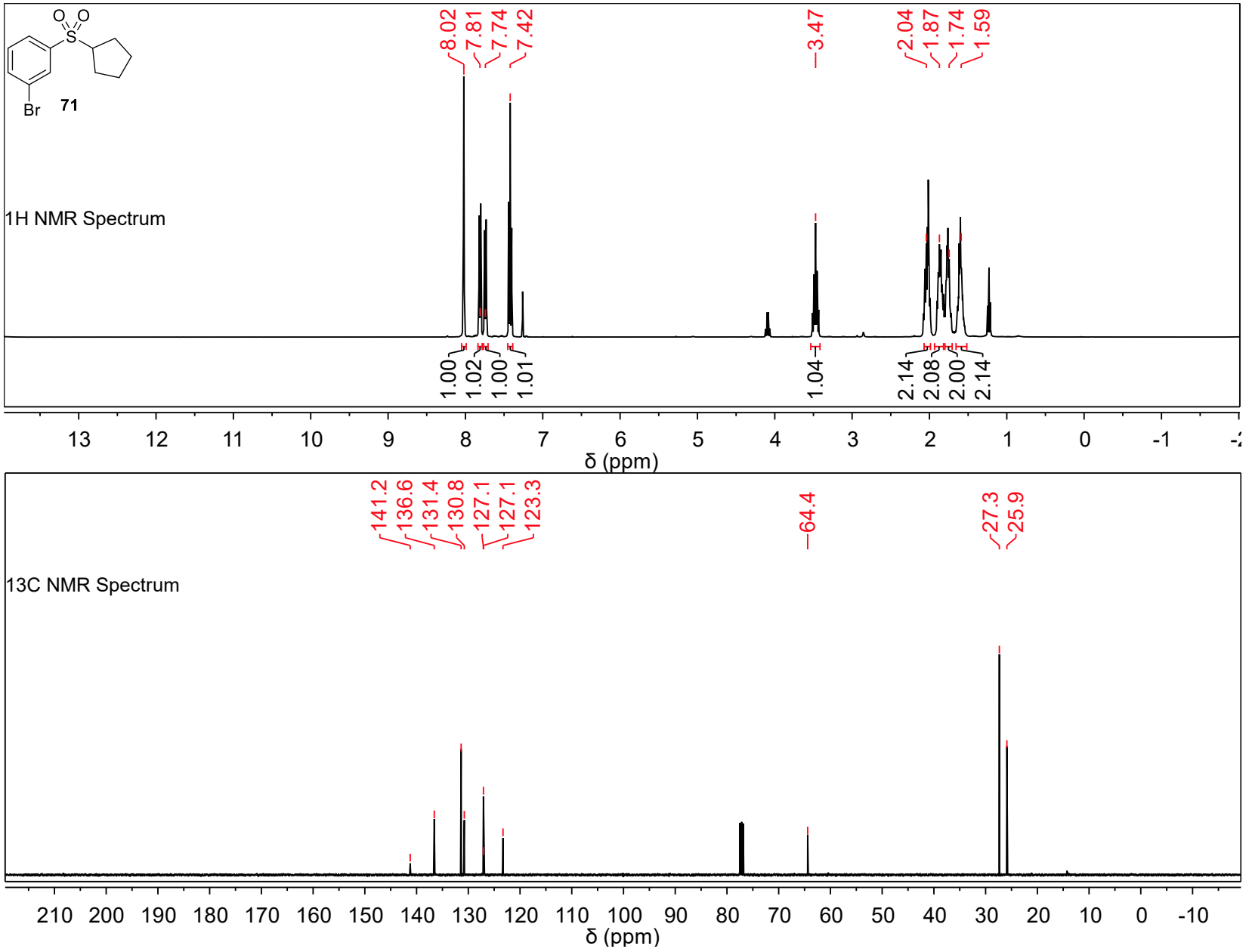
Br
71
1H NMR Spectrum
8.02
7.81
7.74
7.42
3.47
2.04
1.87
1.74
1.59
1.00
1.02
1.00
1.01
1.04
2.14
2.08
2.00
2.14
δ (ppm)
13C NMR Spectrum
141.2
136.6
131.4
130.8
127.1
127.1
123.3
64.4
27.3
25.9
δ (ppm)

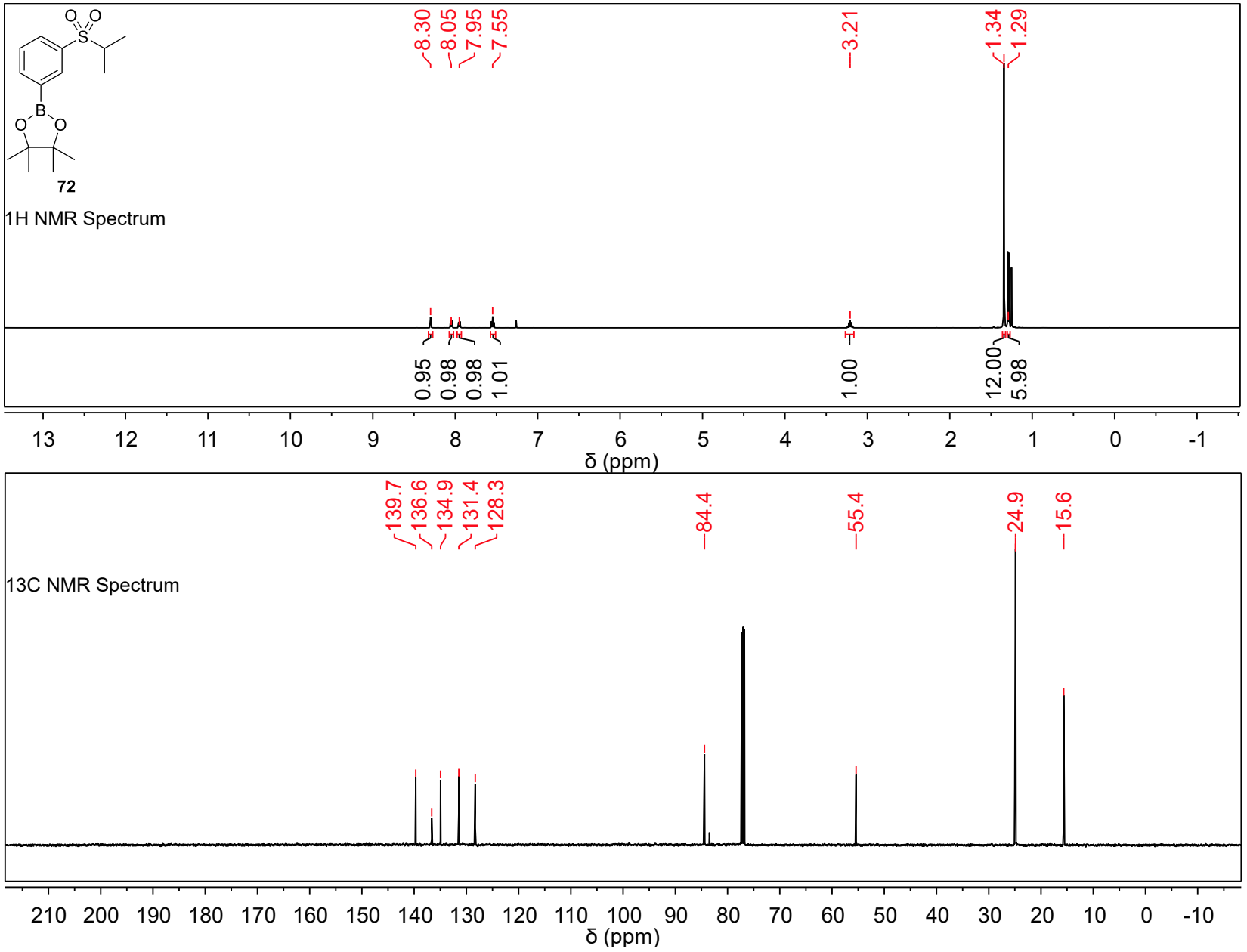
72
1H NMR Spectrum
8.30
8.05
7.95
7.55
3.21
1.34
1.29
0.95
0.98
0.98
1.01
1.00
12.00
5.98
δ (ppm)
13C NMR Spectrum
139.7
136.6
134.9
131.4
128.3
84.4
55.4
24.9
15.6
δ (ppm)

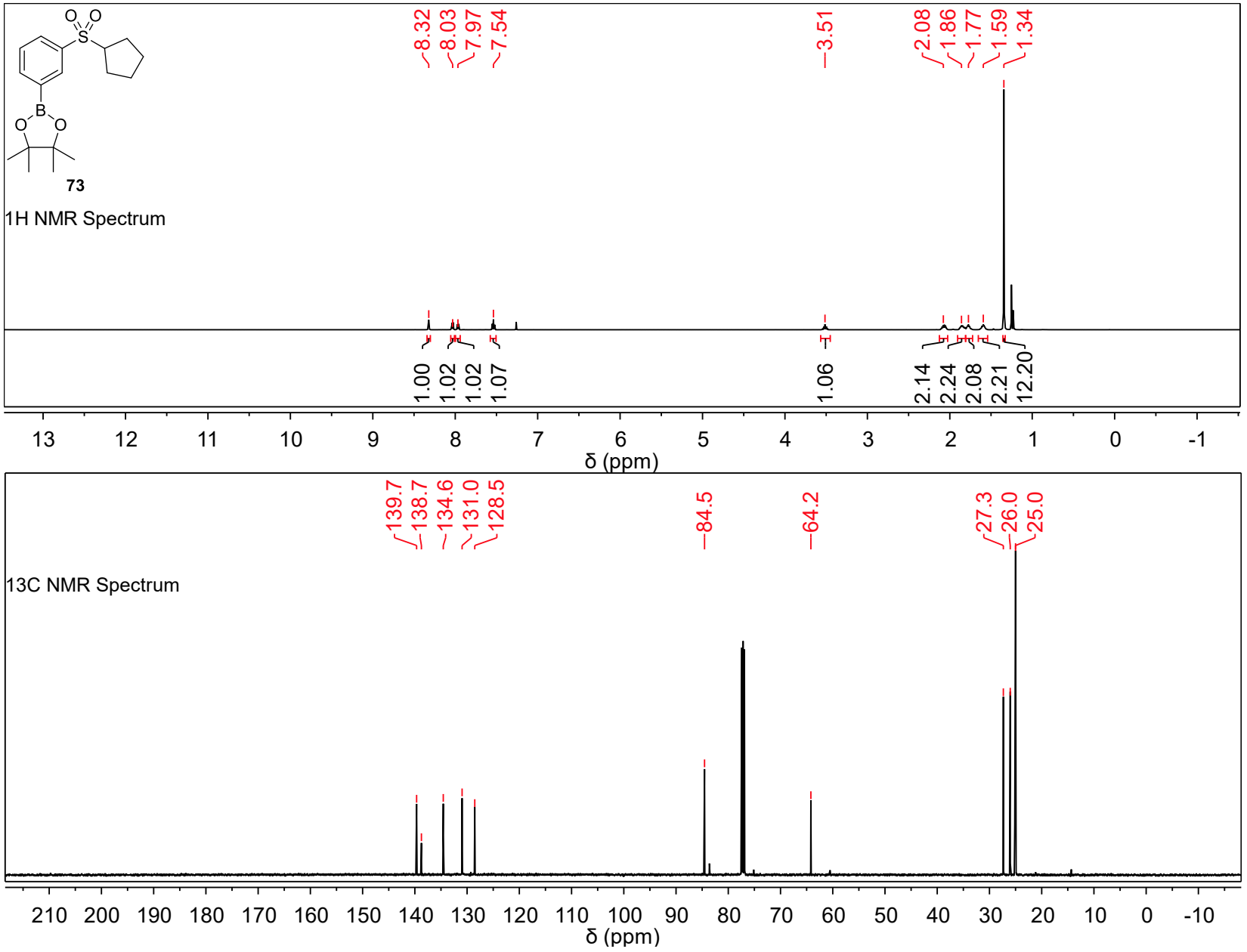
73
1H NMR Spectrum
8.32
8.03
7.97
7.54
3.51
2.08
1.86
1.77
1.59
1.34
1.00
1.02
1.02
1.07
1.06
2.14
2.24
2.08
2.21
12.20
δ (ppm)
13C NMR Spectrum
139.7
138.7
134.6
131.0
128.5
84.5
64.2
27.3
26.0
25.0
δ (ppm)

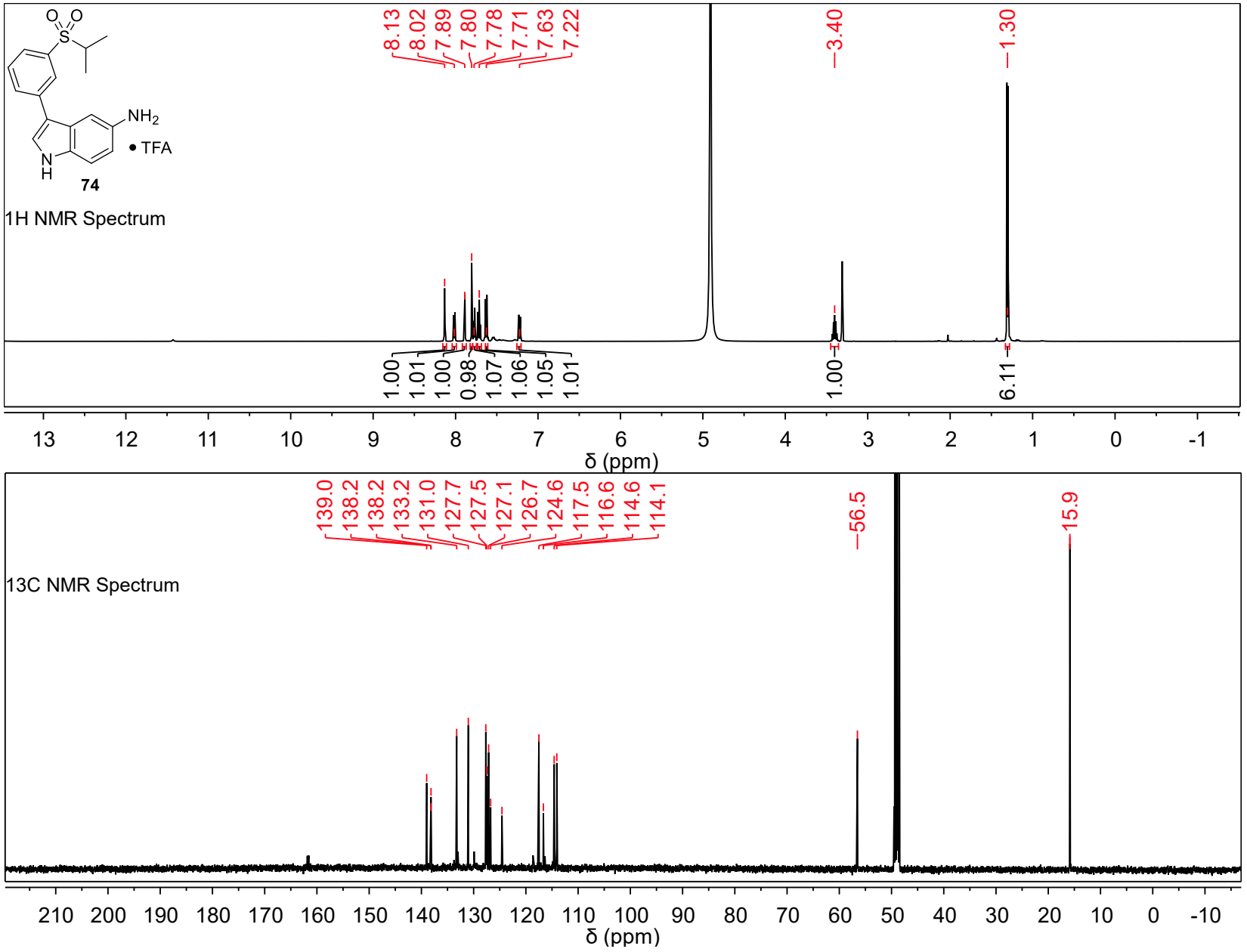
74
1H NMR Spectrum
8.13
8.02
7.89
7.80
7.78
7.71
7.63
7.22
3.40
1.30
1.00
1.01
1.00
0.98
1.07
1.06
1.05
1.01
1.00
6.11
δ (ppm)
13C NMR Spectrum
139.0
138.2
138.2
133.2
131.0
127.7
127.5
127.1
126.7
124.6
117.5
116.6
114.6
114.1
56.5
15.9
δ (ppm)

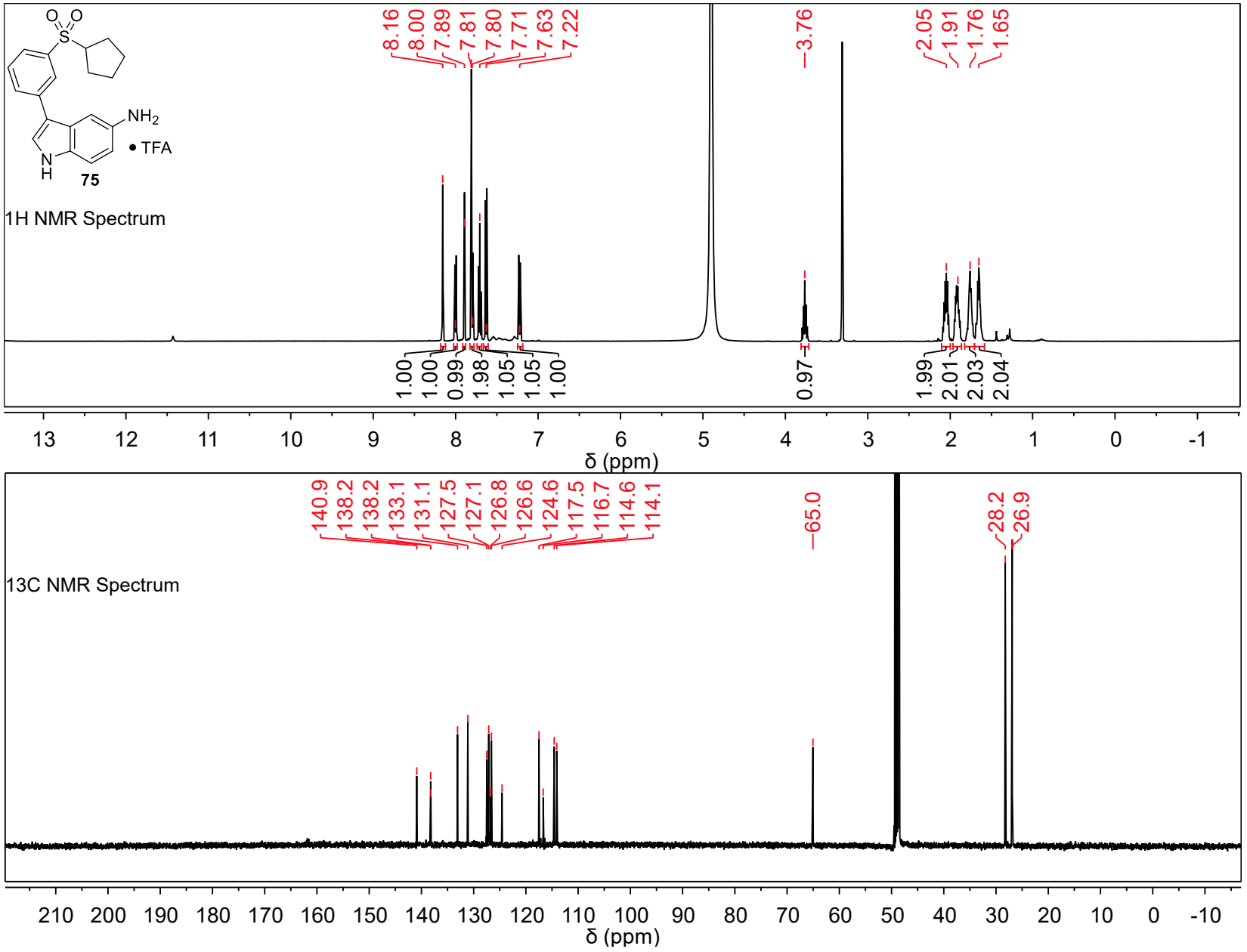
8.16
8.00
7.89
7.81
7.80
7.71
7.63
7.22
3.76
2.05
1.91
1.76
1.65
1.00
1.00
0.99
1.98
1.05
1.05
1.00
0.97
1.99
2.01
2.03
2.04
NH2
• TFA
N
H
75
1H NMR Spectrum
δ (ppm)
140.9
138.2
138.2
133.1
131.1
127.5
127.1
126.8
126.6
124.6
117.5
116.7
114.6
114.1
65.0
28.2
26.9
13C NMR Spectrum
δ (ppm)

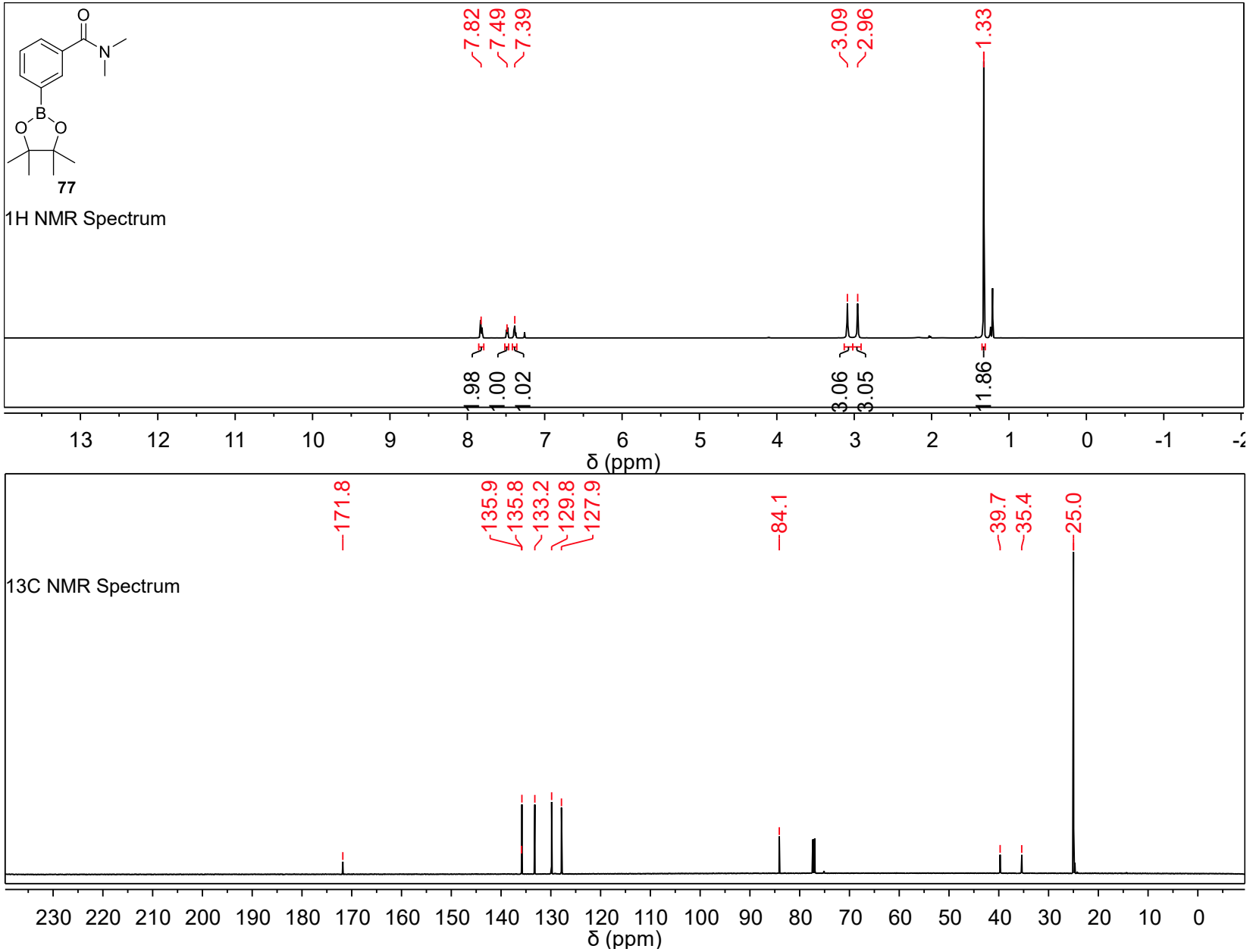
77
1H NMR Spectrum
7.82
7.49
7.39
3.09
2.96
1.33
1.98
1.00
1.02
3.06
3.05
11.86
δ (ppm)
13C NMR Spectrum
171.8
135.9
135.8
133.2
129.8
127.9
84.1
39.7
35.4
25.0
δ (ppm)

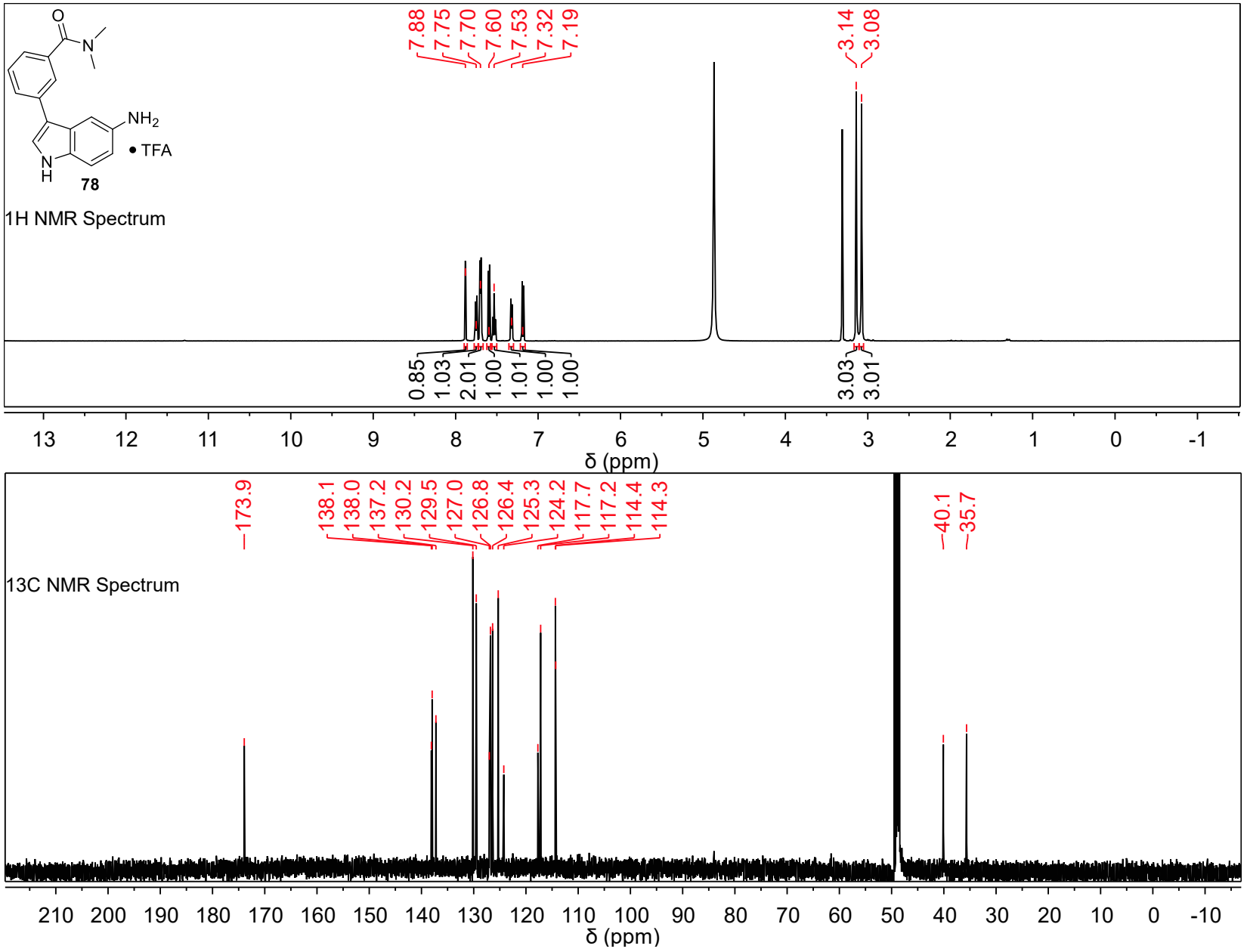
78
1H NMR Spectrum
7.88
7.75
7.70
7.60
7.53
7.32
7.19
3.14
3.08
0.85
1.03
2.01
1.00
1.01
1.00
1.00
3.03
3.01
δ (ppm)
13C NMR Spectrum
173.9
138.1
138.0
137.2
130.2
129.5
127.0
126.8
126.4
125.3
124.2
117.7
117.2
114.4
114.3
40.1
35.7
δ (ppm)

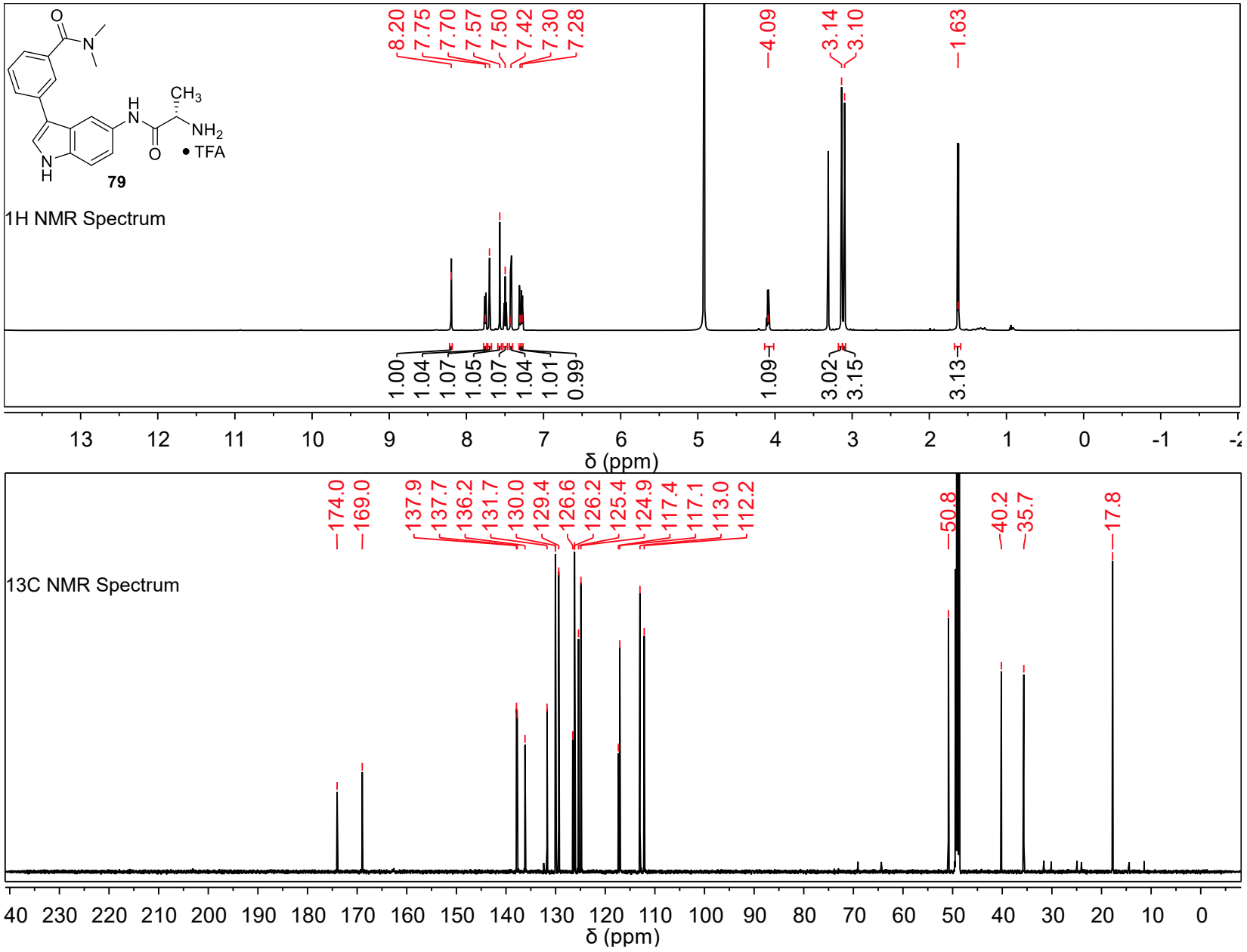
79
1H NMR Spectrum
8.20
7.75
7.70
7.57
7.50
7.42
7.30
7.28
4.09
3.14
3.10
1.63
1.00
1.04
1.07
1.05
1.07
1.04
1.01
0.99
1.09
3.02
3.15
3.13
δ (ppm)
13C NMR Spectrum
174.0
169.0
137.9
137.7
136.2
131.7
130.0
129.4
126.6
126.2
125.4
124.9
117.4
117.1
113.0
112.2
50.8
40.2
35.7
17.8
δ (ppm)

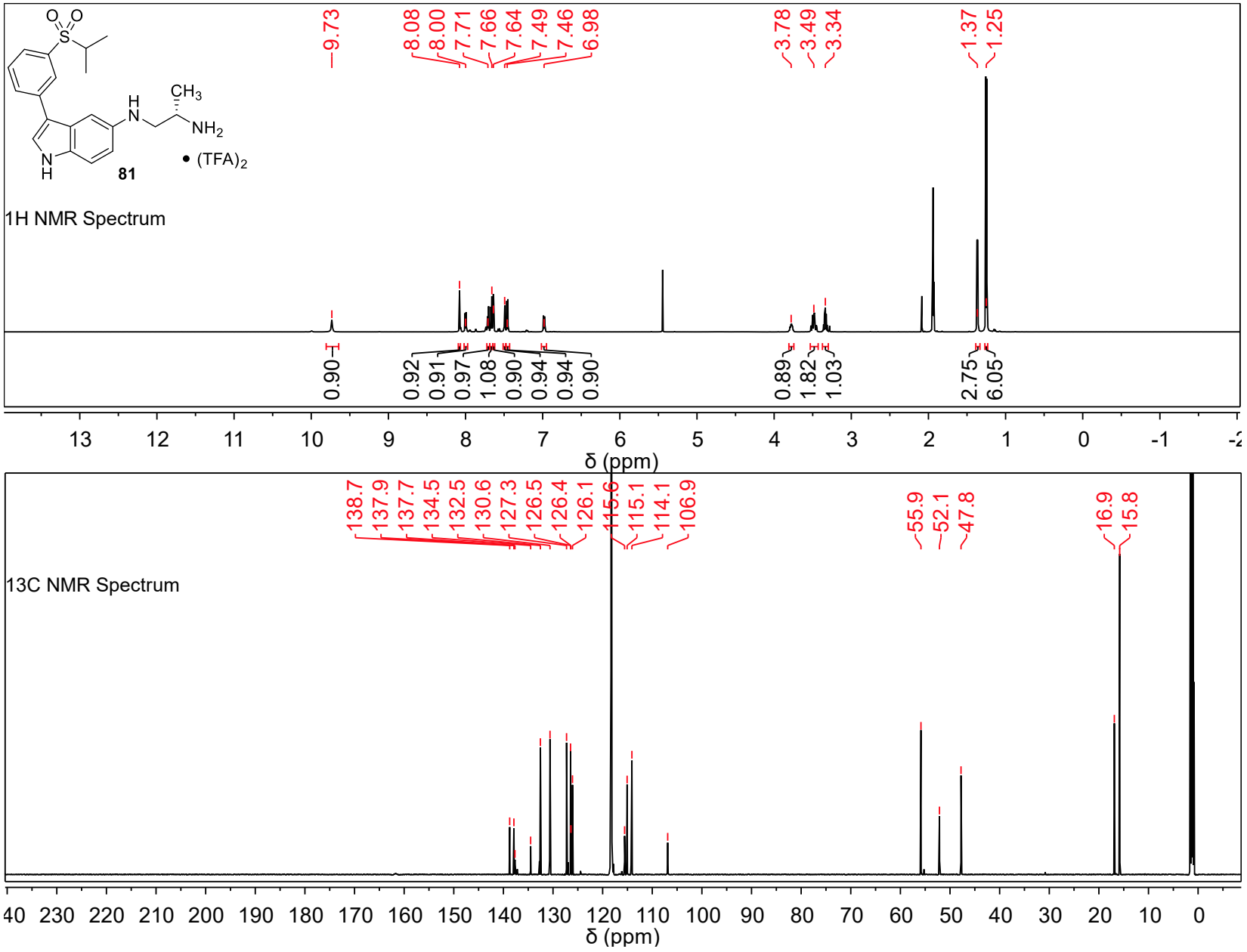
81
• (TFA)2
1H NMR Spectrum
9.73
8.08
8.00
7.71
7.66
7.64
7.49
7.46
6.98
3.78
3.49
3.34
1.37
1.25
0.90
0.92
0.91
0.97
1.08
0.90
0.94
0.94
0.90
0.89
1.82
1.03
2.75
6.05
δ (ppm)
13C NMR Spectrum
138.7
137.9
137.7
134.5
132.5
130.6
127.3
126.5
126.4
126.1
115.6
115.1
114.1
106.9
55.9
52.1
47.8
16.9
15.8
δ (ppm)

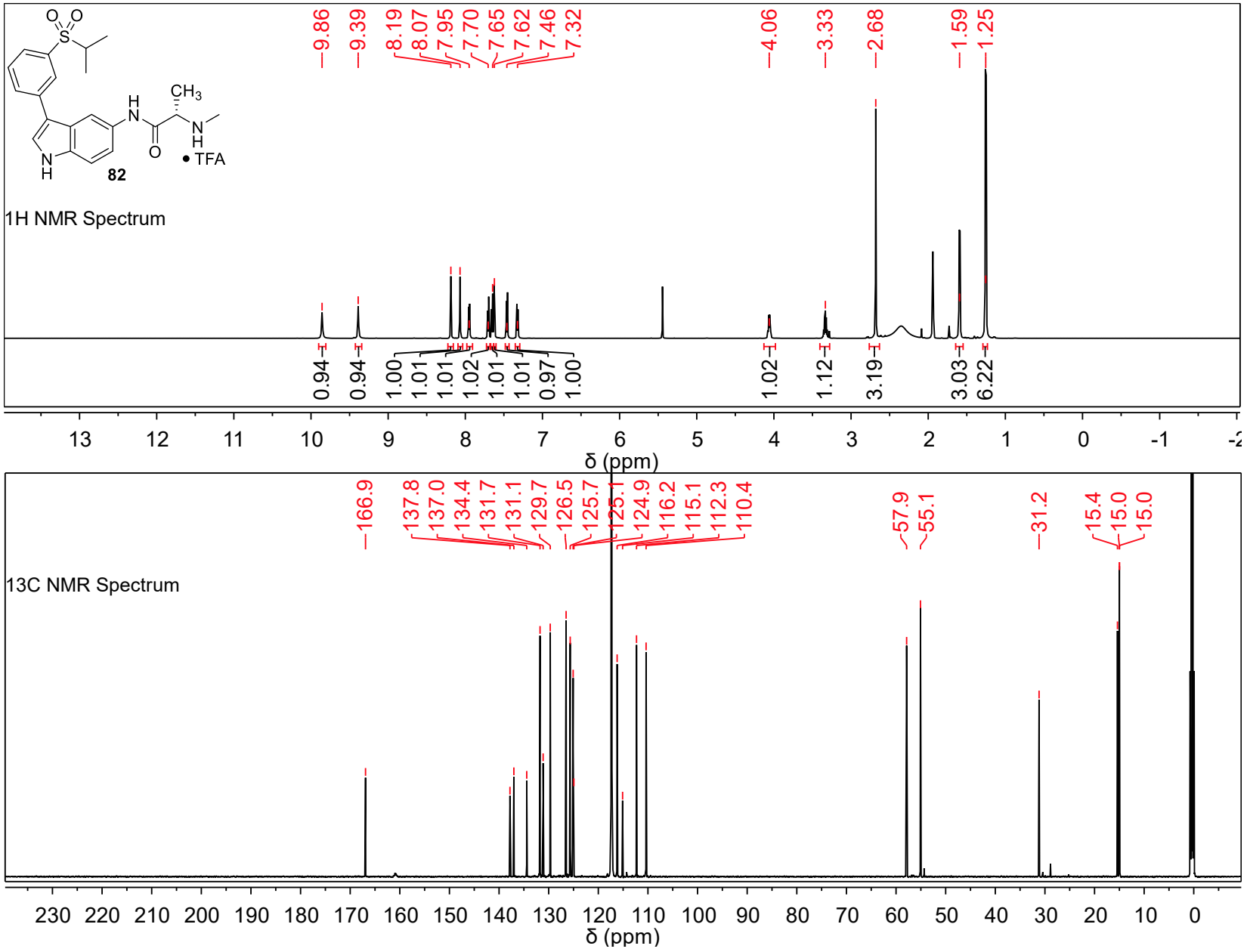
82
• TFA
1H NMR Spectrum
9.86
9.39
8.19
8.07
7.95
7.70
7.65
7.62
7.46
7.32
4.06
3.33
2.68
1.59
1.25
0.94
0.94
1.00
1.01
1.01
1.02
1.01
1.01
0.97
1.00
1.02
1.12
3.19
3.03
6.22
δ (ppm)
13C NMR Spectrum
166.9
137.8
137.0
134.4
131.7
131.1
129.7
126.5
125.7
125.1
124.9
116.2
115.1
112.3
110.4
57.9
55.1
31.2
15.4
15.0
15.0
δ (ppm)

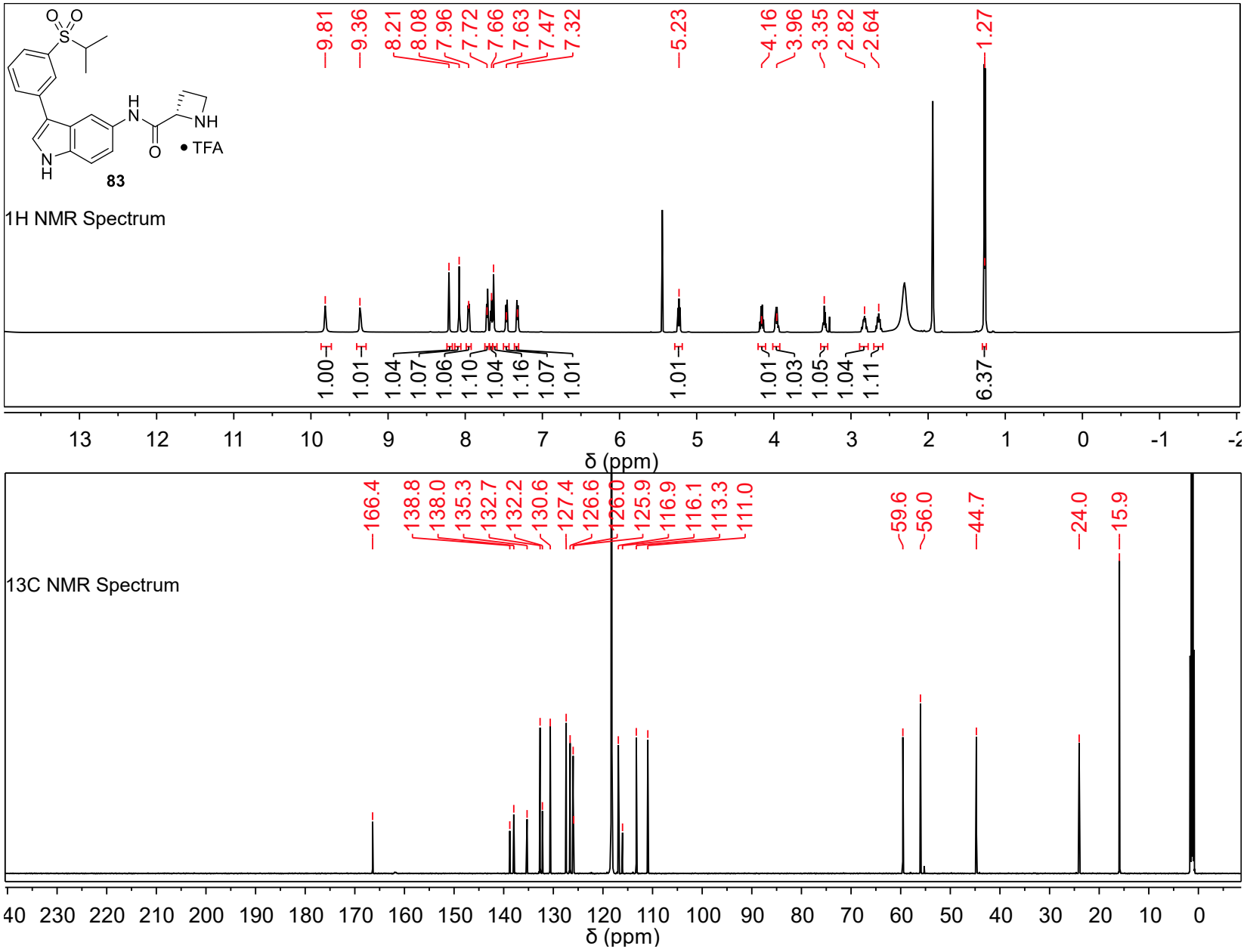
83
• TFA
1H NMR Spectrum
9.81
9.36
8.21
8.08
7.96
7.72
7.66
7.63
7.47
7.32
5.23
4.16
3.96
3.35
2.82
2.64
1.27
1.00
1.01
1.04
1.07
1.06
1.10
1.04
1.16
1.07
1.01
1.01
1.01
1.03
1.05
1.04
1.11
6.37
δ (ppm)
13C NMR Spectrum
166.4
138.8
138.0
135.3
132.7
132.2
130.6
127.4
126.6
126.0
125.9
116.9
116.1
113.3
111.0
59.6
56.0
44.7
24.0
15.9
δ (ppm)

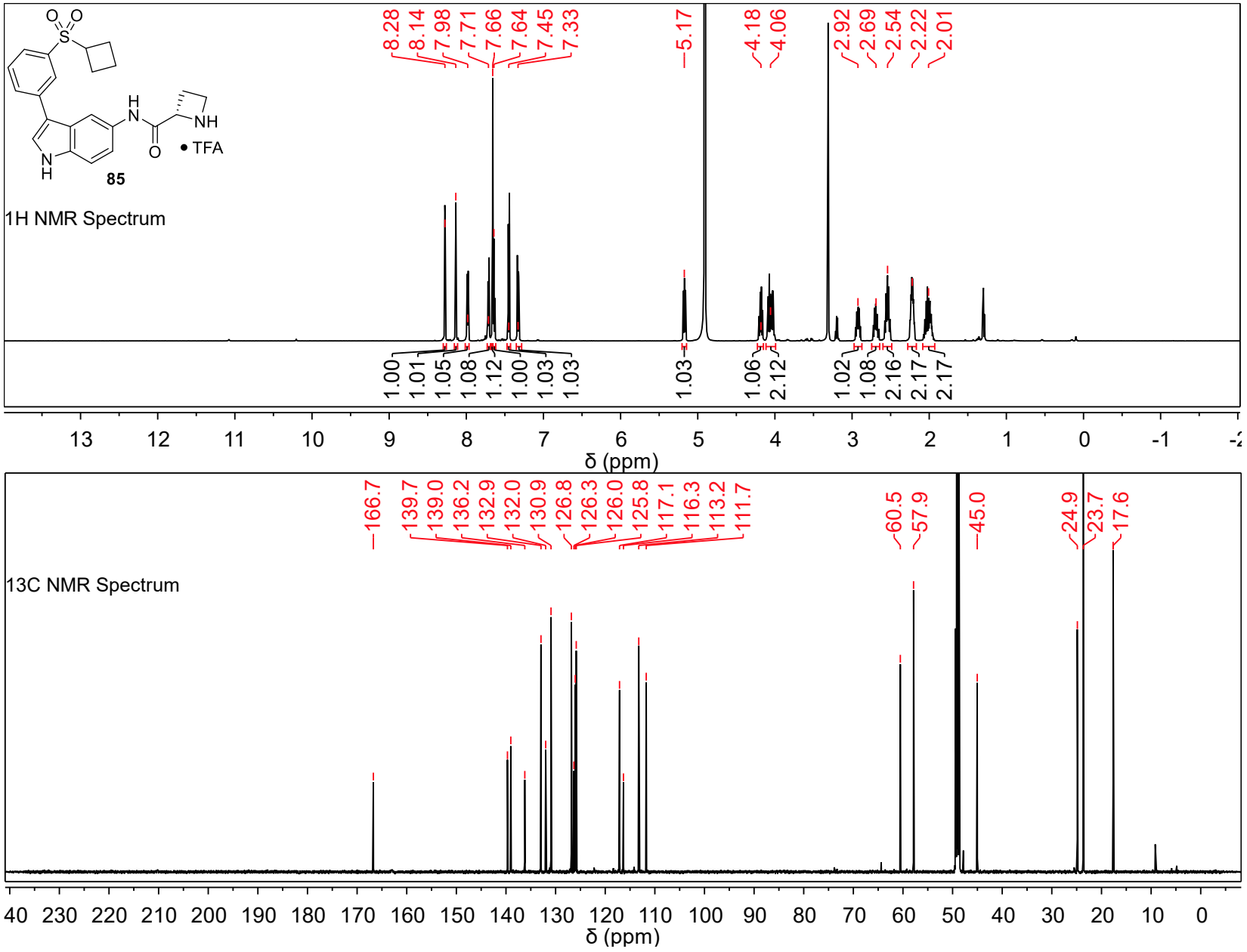
85
• TFA
1H NMR Spectrum
8.28
8.14
7.98
7.71
7.66
7.64
7.45
7.33
5.17
4.18
4.06
2.92
2.69
2.54
2.22
2.01
1.00
1.01
1.05
1.08
1.12
1.00
1.03
1.03
1.03
1.06
2.12
1.02
1.08
2.16
2.17
2.17
δ (ppm)
13C NMR Spectrum
166.7
139.7
139.0
136.2
132.9
132.0
130.9
126.8
126.3
126.0
125.8
117.1
116.3
113.2
111.7
60.5
57.9
45.0
24.9
23.7
17.6
δ (ppm)

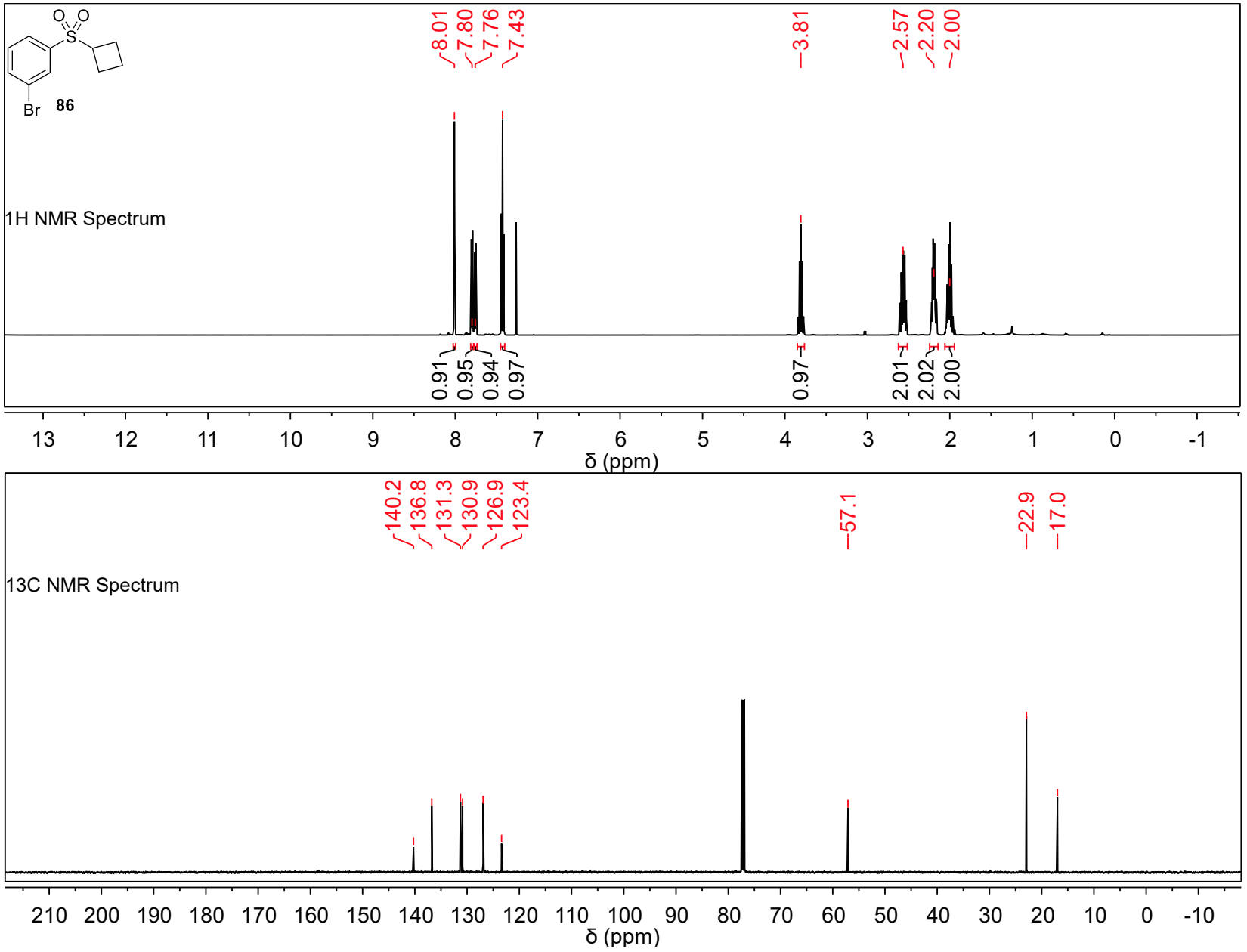
Br 86
1H NMR Spectrum
8.01
7.80
7.76
7.43
3.81
2.57
2.20
2.00
0.91
0.95
0.94
0.97
0.97
2.01
2.02
2.00
δ (ppm)
13C NMR Spectrum
140.2
136.8
131.3
130.9
126.9
123.4
57.1
22.9
17.0
δ (ppm)

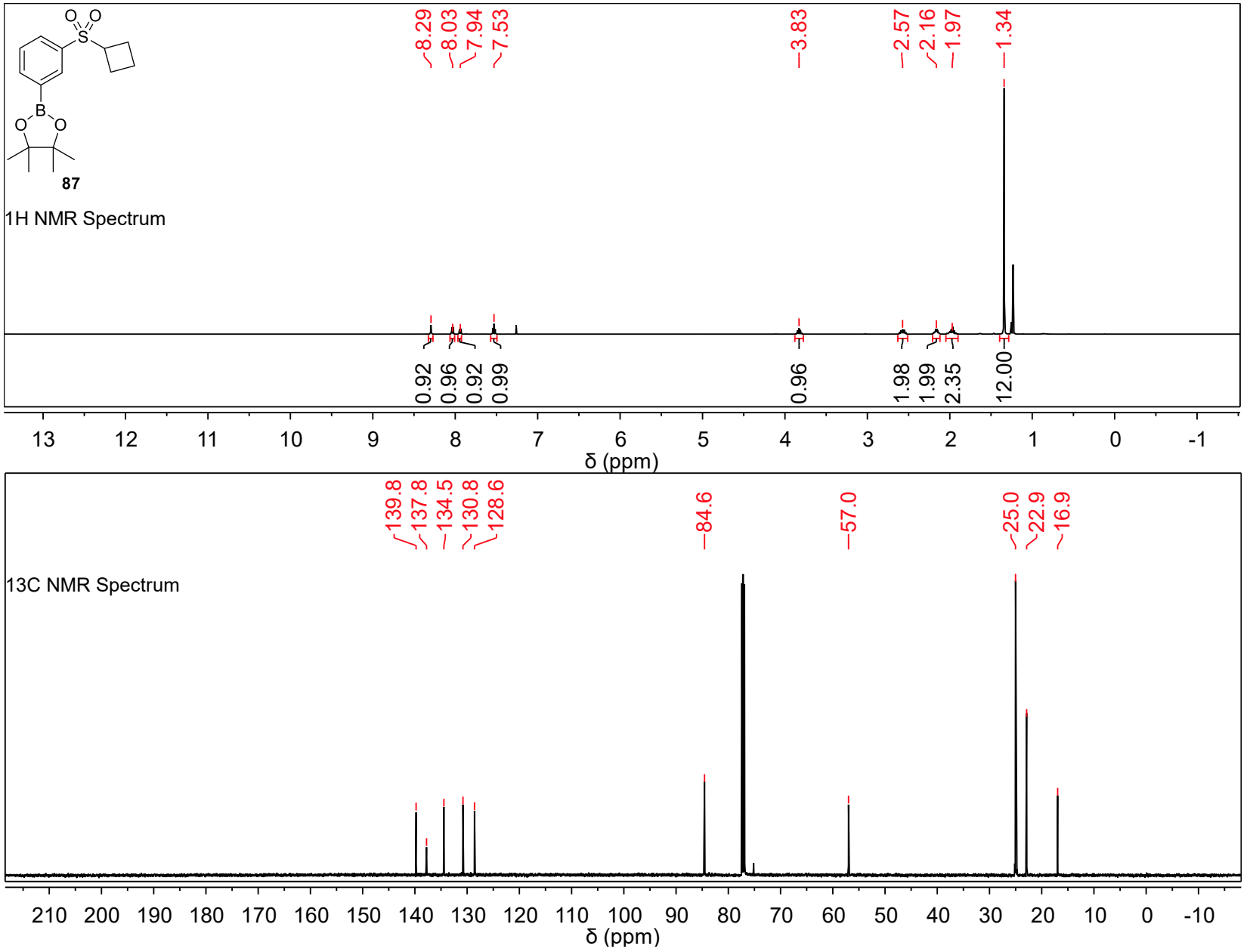
87
1H NMR Spectrum
8.29
8.03
7.94
7.53
3.83
2.57
2.16
1.97
1.34
0.92
0.96
0.92
0.99
0.96
1.98
1.99
2.35
12.00
δ (ppm)
13C NMR Spectrum
139.8
137.8
134.5
130.8
128.6
84.6
57.0
25.0
22.9
16.9
δ (ppm)

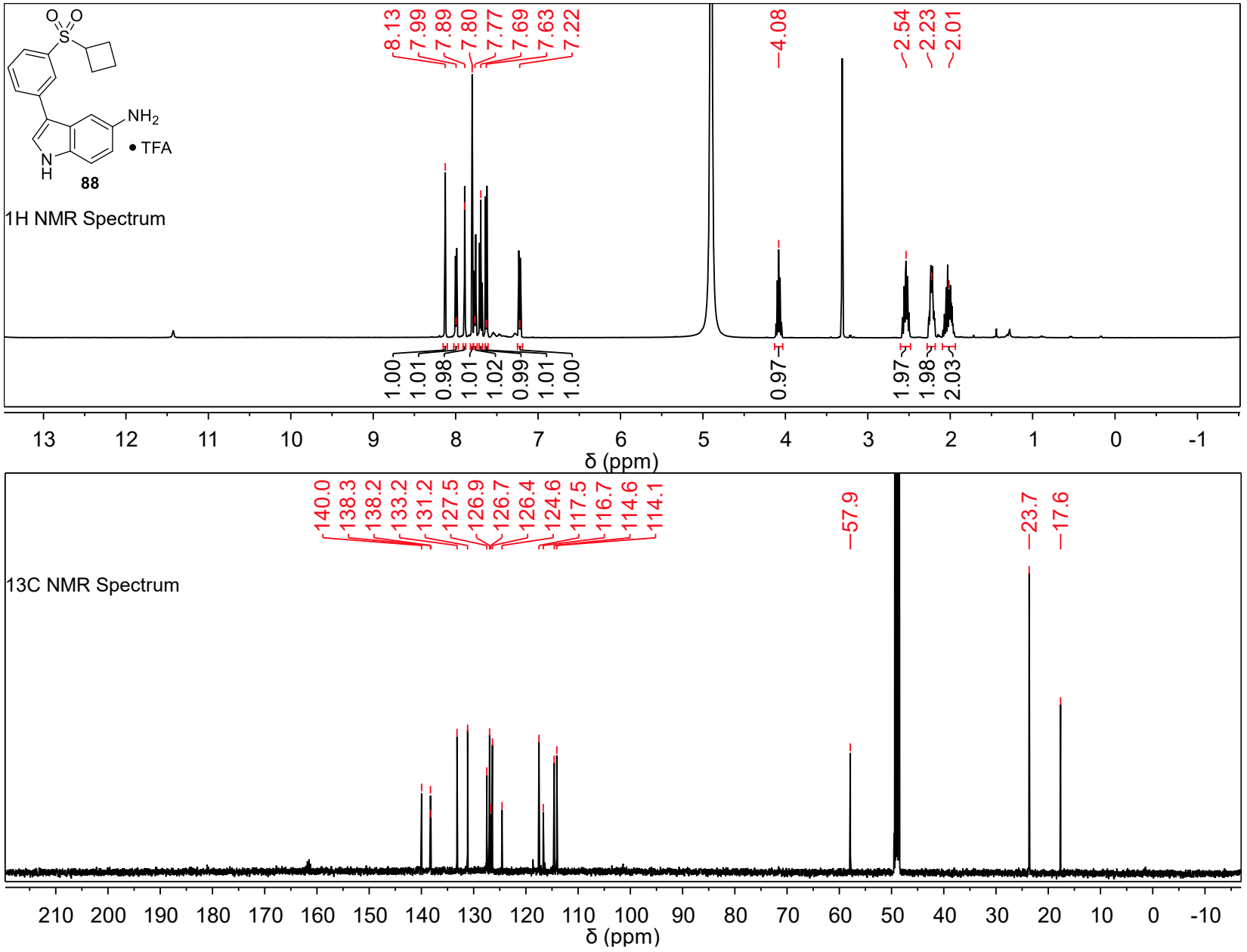
88
1H NMR Spectrum
8.13
7.99
7.89
7.80
7.77
7.69
7.63
7.22
4.08
2.54
2.23
2.01
1.00
1.01
0.98
1.01
1.02
0.99
1.01
1.00
0.97
1.97
1.98
2.03
δ (ppm)
13C NMR Spectrum
140.0
138.3
138.2
133.2
131.2
127.5
126.9
126.7
126.4
124.6
117.5
116.7
114.6
114.1
57.9
23.7
17.6
δ (ppm)

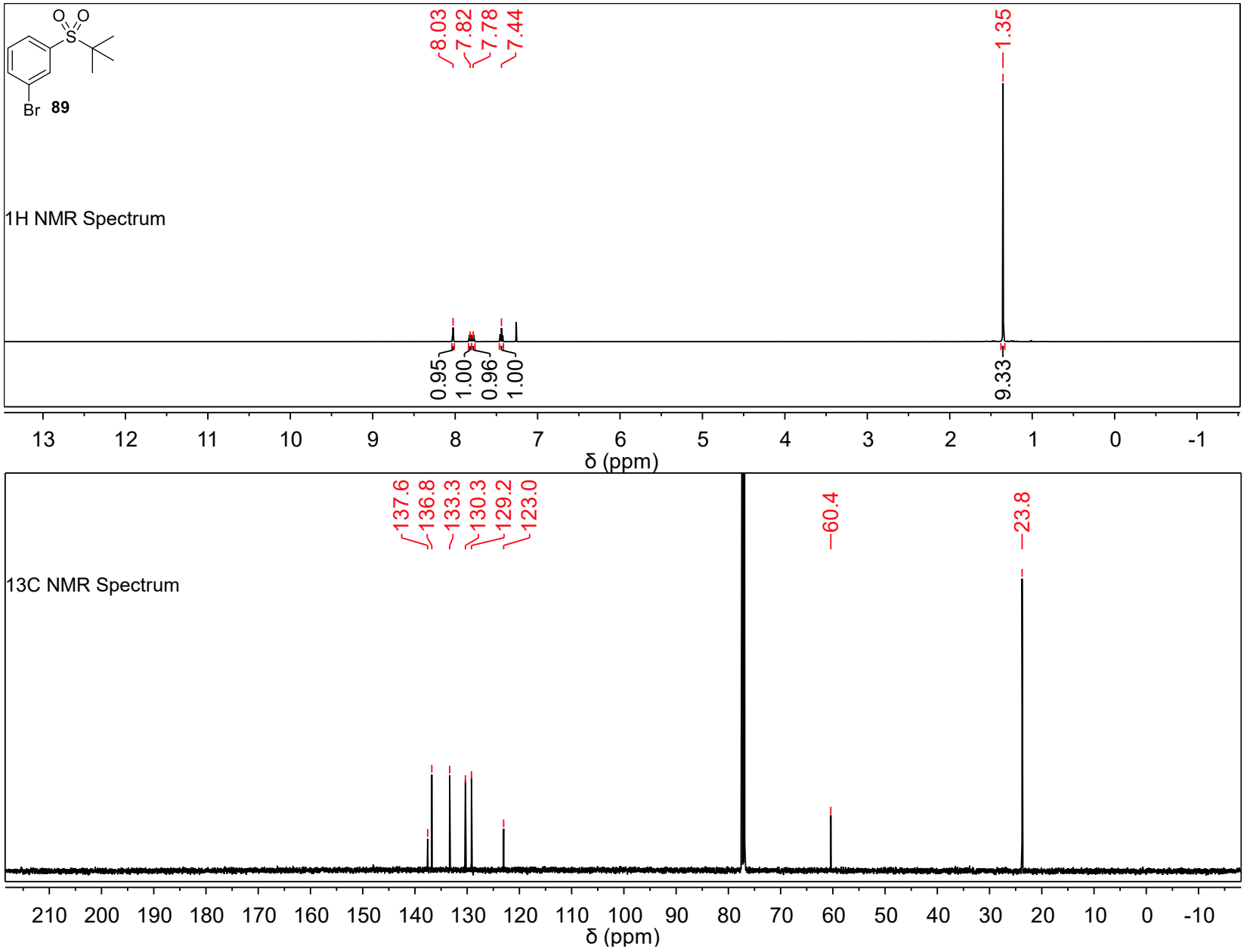
Br 89
8.03
7.82
7.78
7.44
1.35
1H NMR Spectrum
0.95
1.00
0.96
1.00
9.33
13 12 11 10 9 8 7 6 5 4 3 2 1 0 -1
δ (ppm)
137.6
136.8
133.3
130.3
129.2
123.0
60.4
23.8
13C NMR Spectrum
210 200 190 180 170 160 150 140 130 120 110 100 90 80 70 60 50 40 30 20 10 0 -10
δ (ppm)

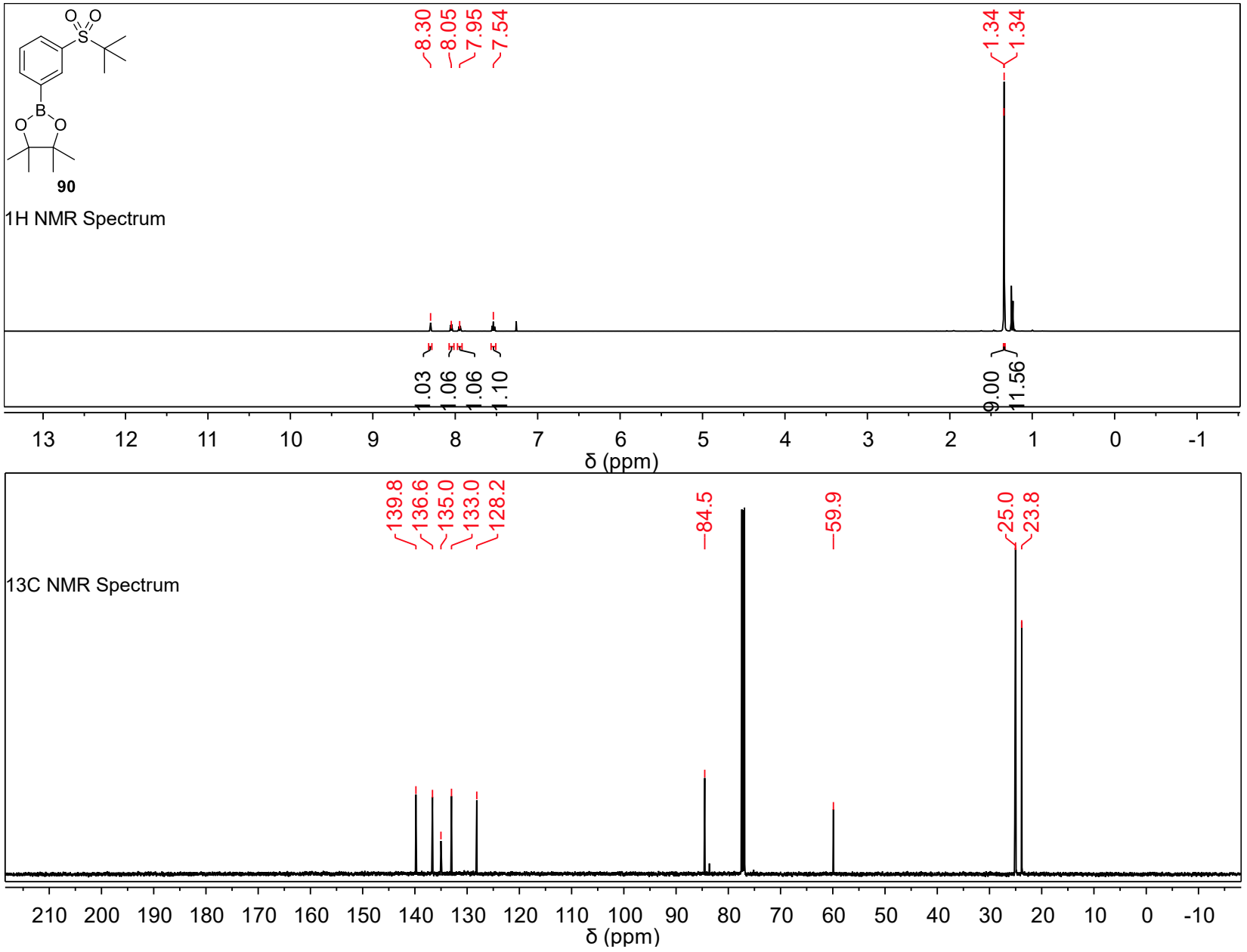
90
1H NMR Spectrum
8.30
8.05
7.95
7.54
1.34
1.34
1.03
1.06
1.06
1.10
9.00
11.56
δ (ppm)
13C NMR Spectrum
139.8
136.6
135.0
133.0
128.2
84.5
59.9
25.0
23.8
δ (ppm)

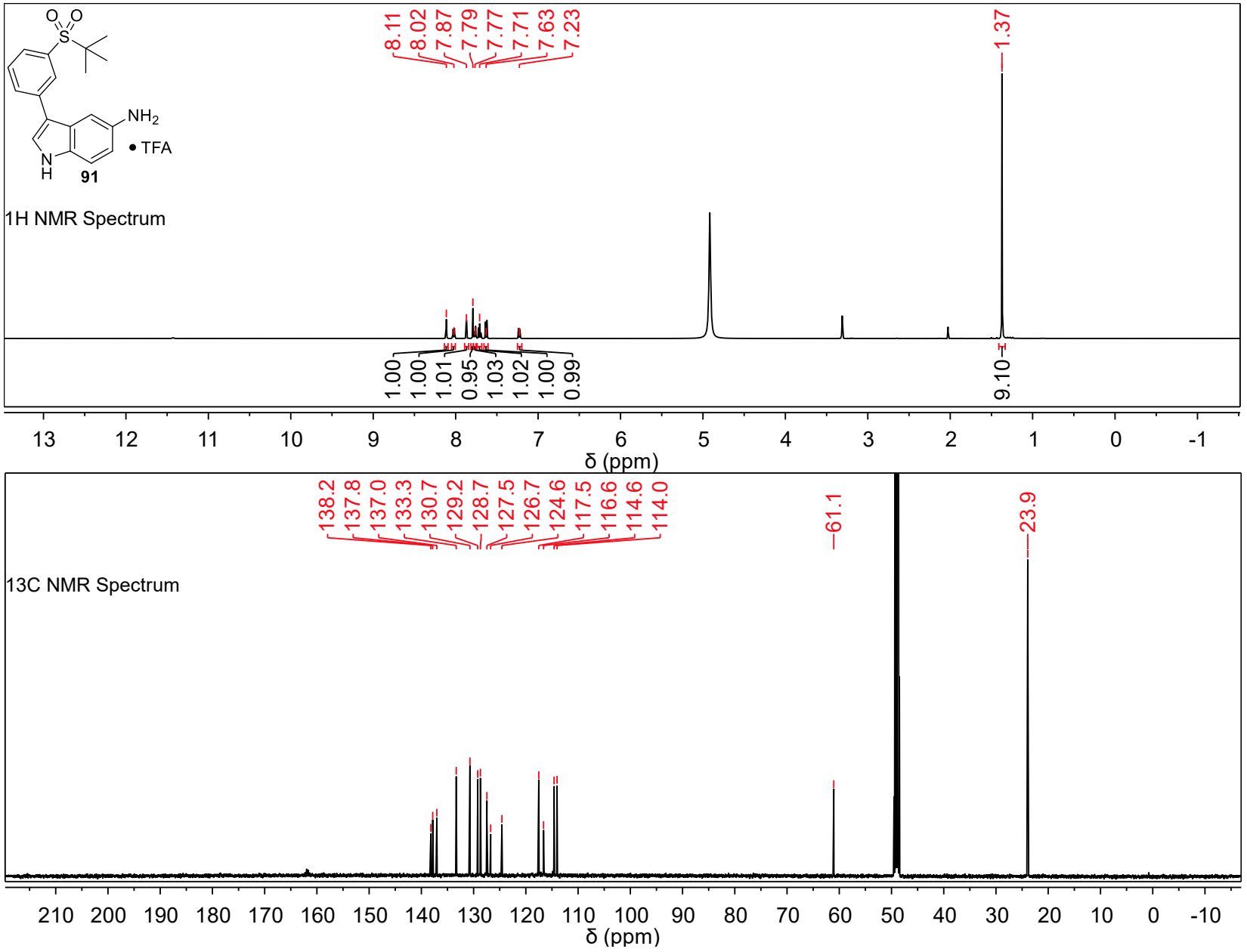
8.11
8.02
7.87
7.79
7.77
7.71
7.63
7.23
1.37
1.00
1.00
1.01
0.95
1.03
1.02
1.00
0.99
9.10
NH2
• TFA
N
H
91
1H NMR Spectrum
δ (ppm)
138.2
137.8
137.0
133.3
130.7
129.2
128.7
127.5
126.7
124.6
117.5
116.6
114.6
114.0
61.1
23.9
13C NMR Spectrum
δ (ppm)

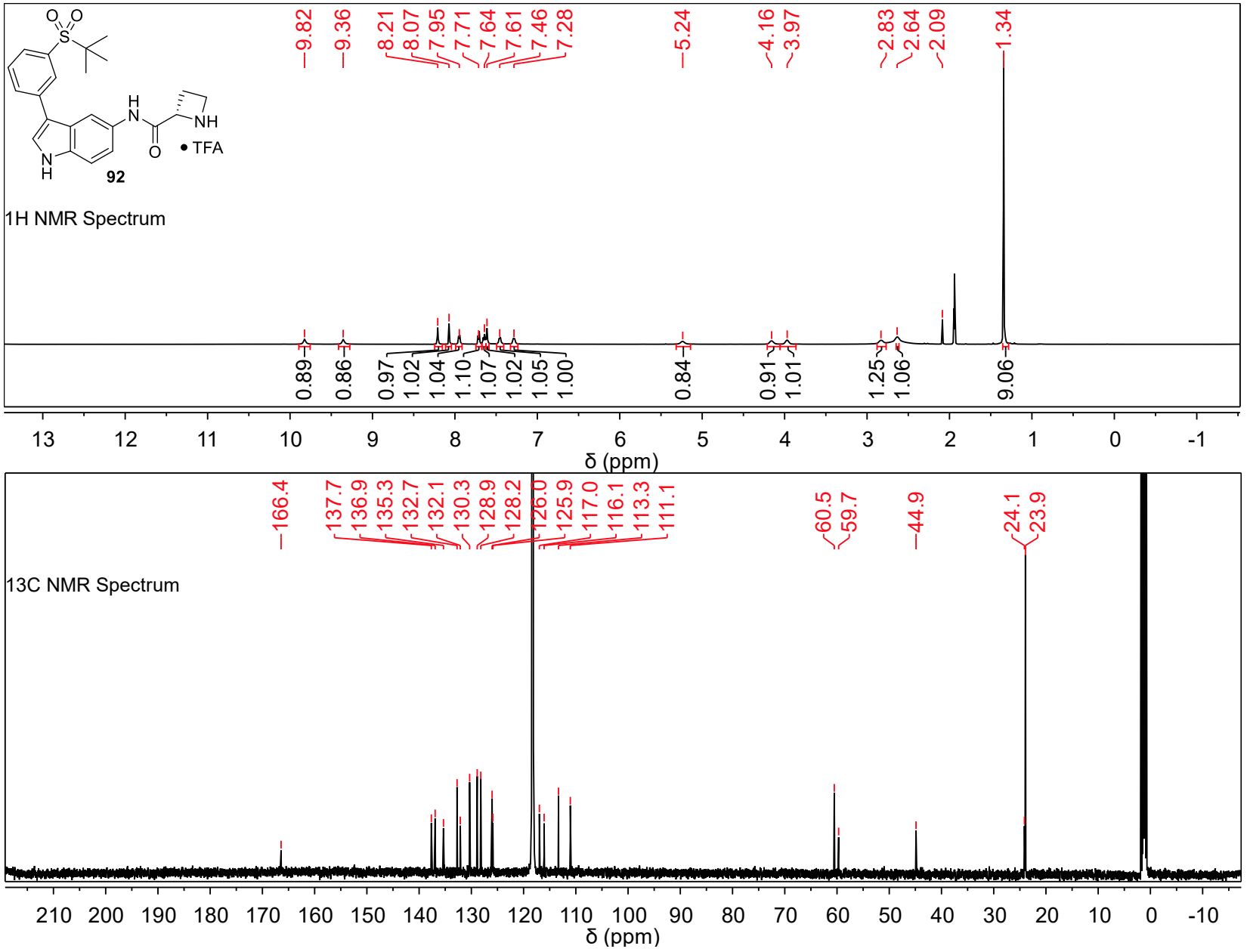
92
• TFA
1H NMR Spectrum
9.82
9.36
8.21
8.07
7.95
7.71
7.64
7.61
7.46
7.28
5.24
4.16
3.97
2.83
2.64
2.09
1.34
0.89
0.86
0.97
1.02
1.04
1.10
1.07
1.02
1.05
1.00
0.84
0.91
1.01
1.25
1.06
9.06
δ (ppm)
13C NMR Spectrum
166.4
137.7
136.9
135.3
132.7
132.1
130.3
128.9
128.2
126.0
125.9
117.0
116.1
113.3
111.1
60.5
59.7
44.9
24.1
23.9
δ (ppm)

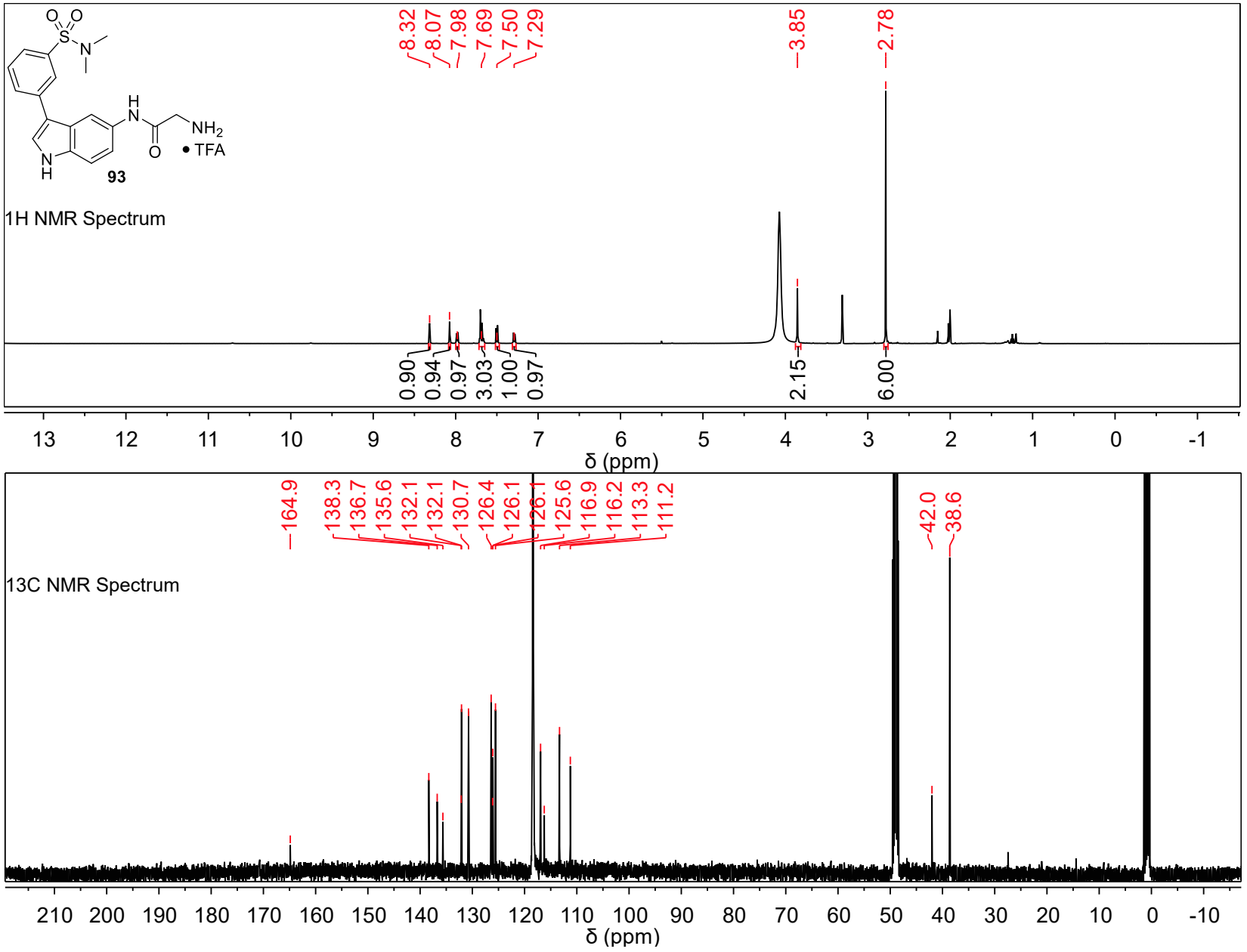
93
1H NMR Spectrum
8.32
8.07
7.98
7.69
7.50
7.29
3.85
2.78
0.90
0.94
0.97
3.03
1.00
0.97
2.15
6.00
δ (ppm)
13C NMR Spectrum
164.9
138.3
136.7
135.6
132.1
132.1
130.7
126.4
126.1
126.1
125.6
116.9
116.2
113.3
111.2
42.0
38.6
δ (ppm)

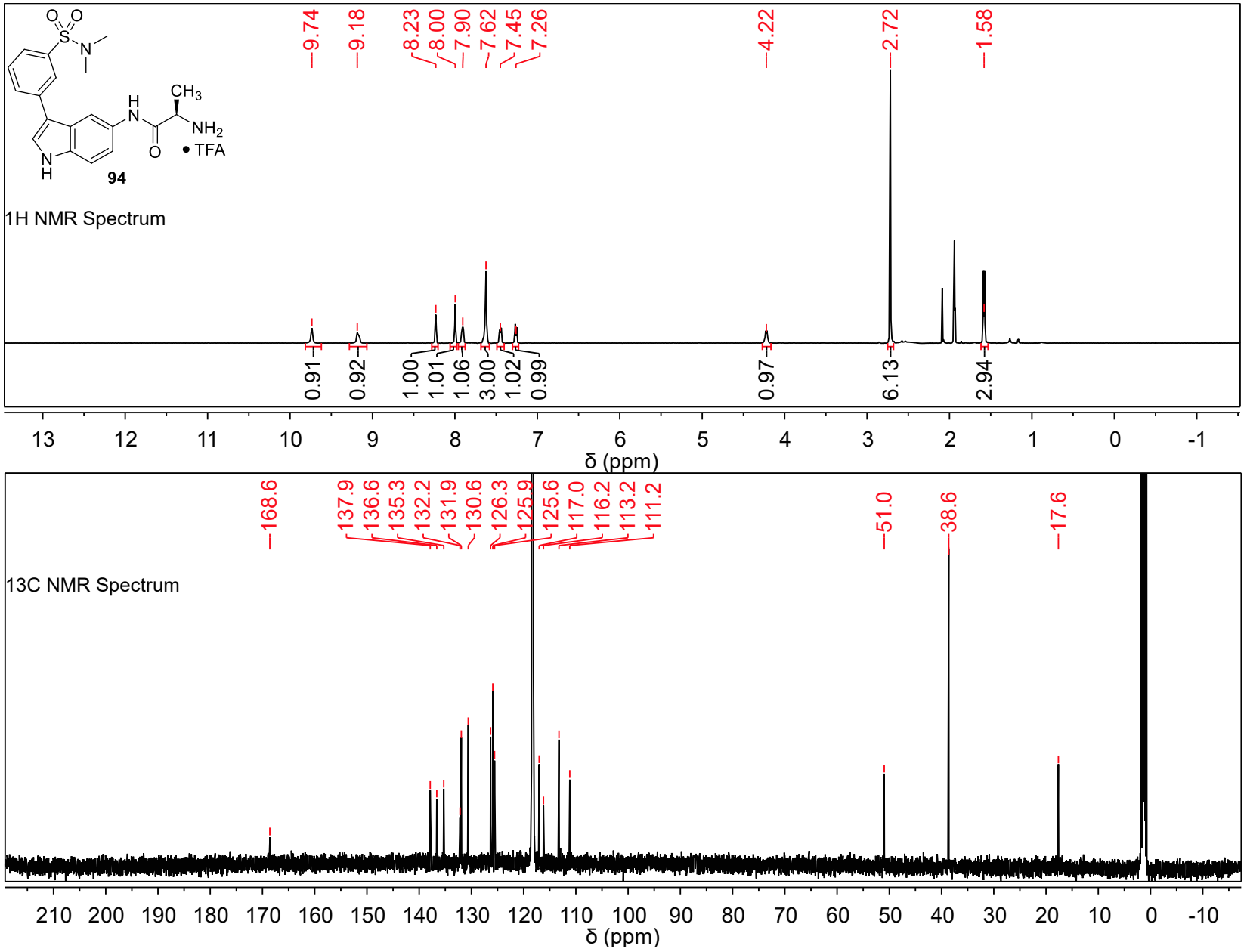
94
1H NMR Spectrum
9.74
9.18
8.23
8.00
7.90
7.62
7.45
7.26
4.22
2.72
1.58
0.91
0.92
1.00
1.01
1.06
3.00
1.02
0.99
0.97
6.13
2.94
δ (ppm)
13C NMR Spectrum
168.6
137.9
136.6
135.3
132.2
131.9
130.6
126.3
125.9
125.6
117.0
116.2
113.2
111.2
51.0
38.6
17.6
δ (ppm)

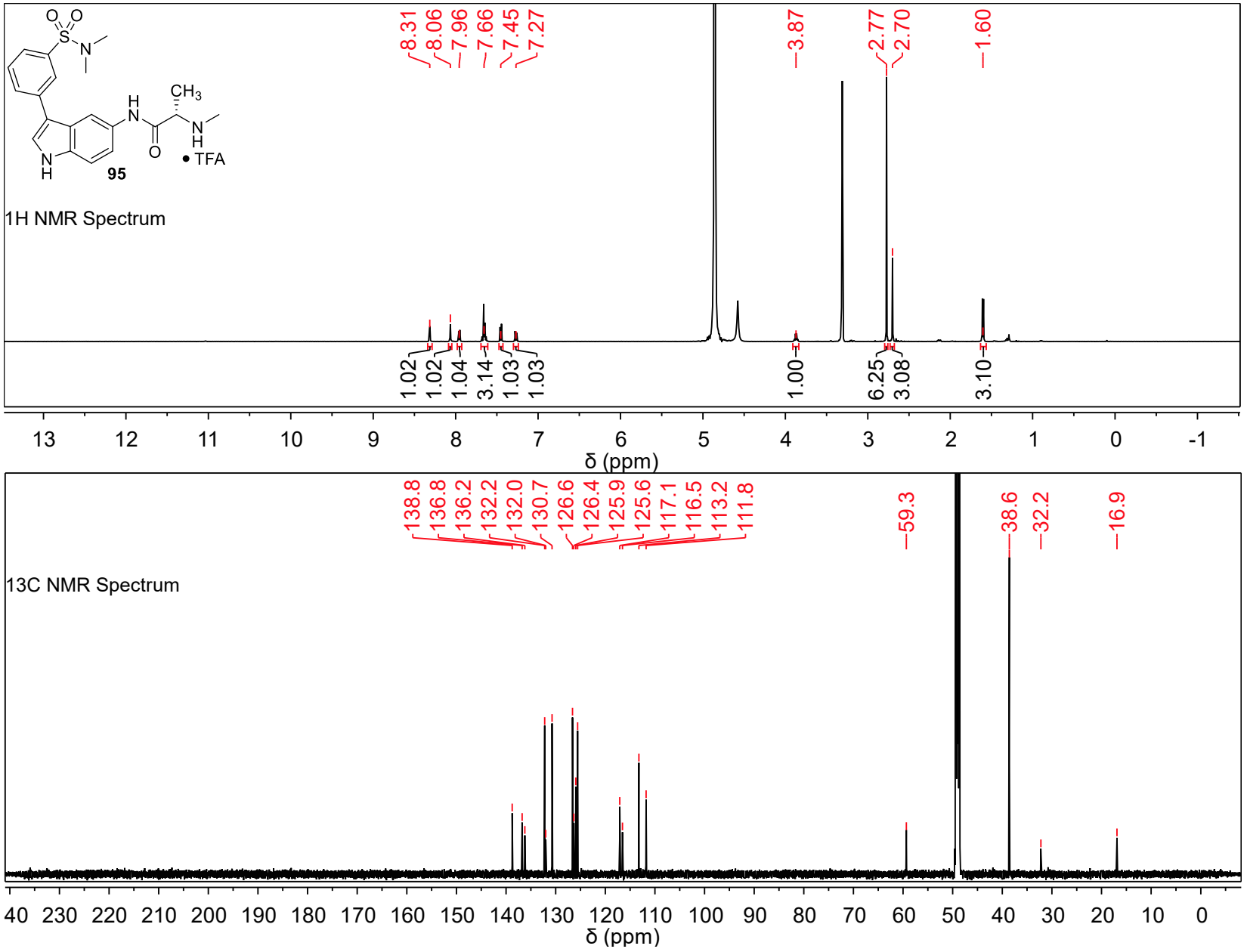
95
• TFA
1H NMR Spectrum
8.31
8.06
7.96
7.66
7.45
7.27
3.87
2.77
2.70
1.60
1.02
1.02
1.04
3.14
1.03
1.03
1.00
6.25
3.08
3.10
δ (ppm)
13C NMR Spectrum
138.8
136.8
136.2
132.2
132.0
130.7
126.6
126.4
125.9
125.6
117.1
116.5
113.2
111.8
59.3
38.6
32.2
16.9
δ (ppm)

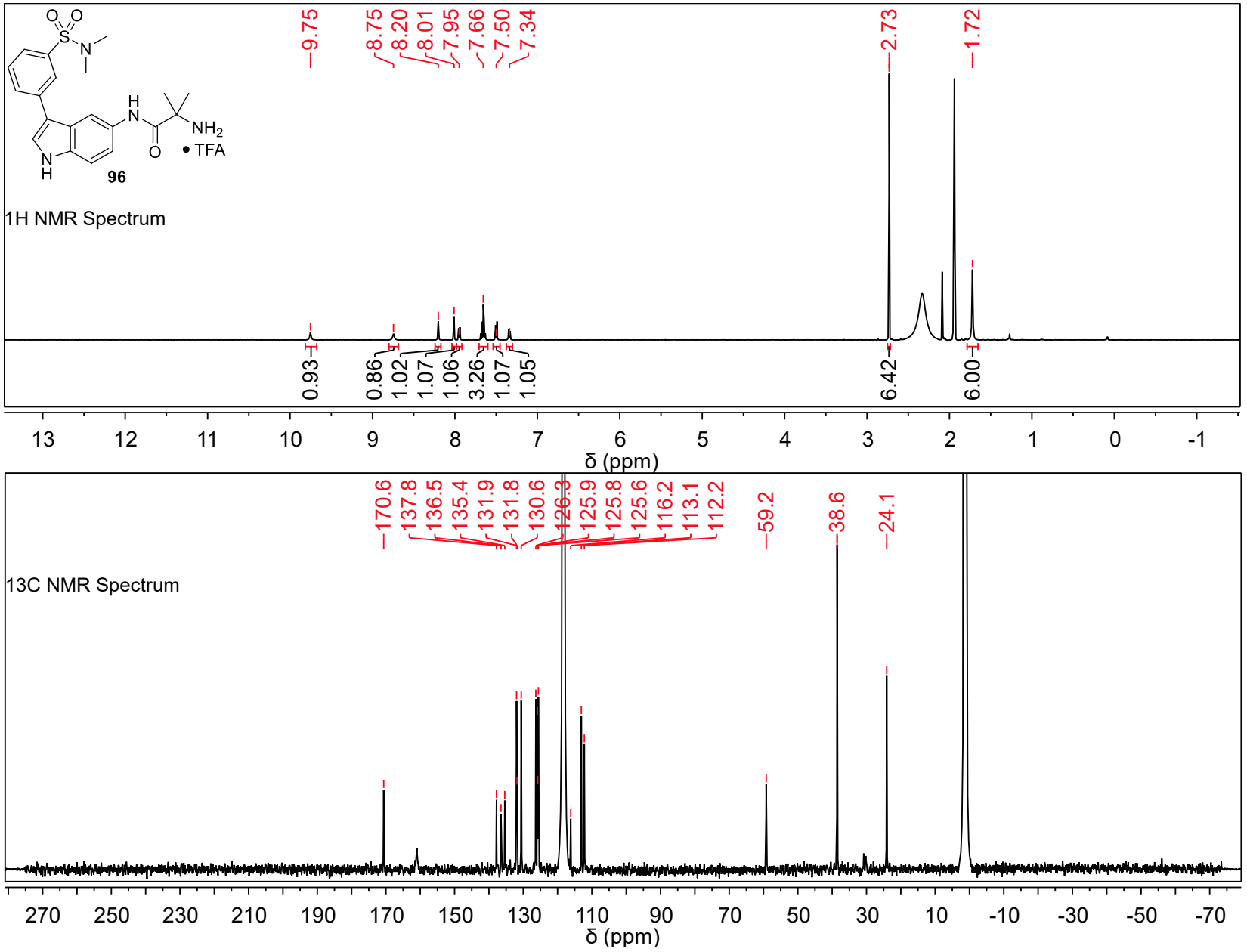
96
• TFA
1H NMR Spectrum
9.75
8.75
8.20
8.01
7.95
7.66
7.50
7.34
2.73
1.72
0.93
0.86
1.02
1.07
1.06
3.26
1.07
1.05
6.42
6.00
δ (ppm)
13C NMR Spectrum
170.6
137.8
136.5
135.4
131.9
131.8
130.6
126.3
125.9
125.8
125.6
116.2
113.1
112.2
59.2
38.6
24.1
δ (ppm)

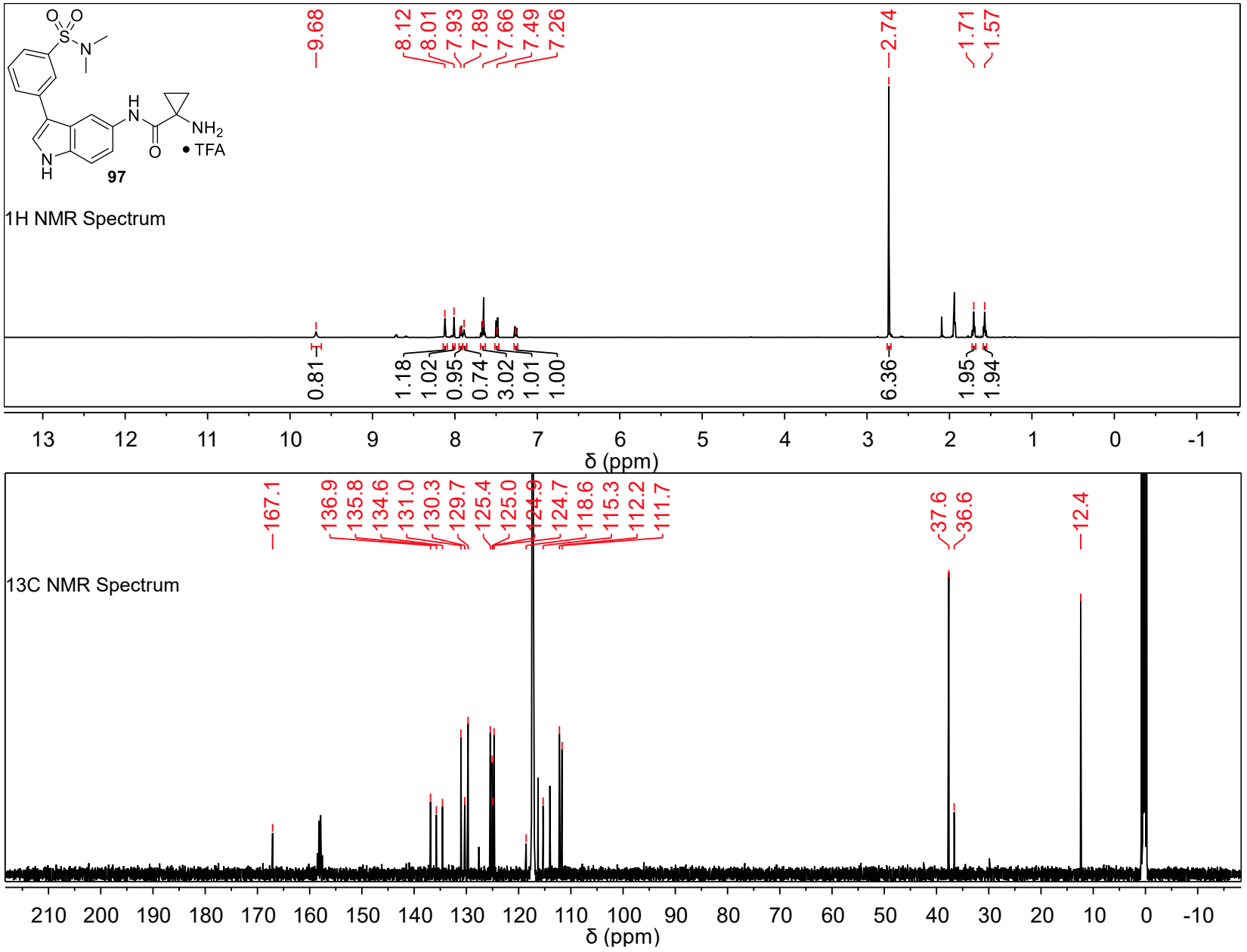
97
• TFA
1H NMR Spectrum
9.68
8.12
8.01
7.93
7.89
7.66
7.49
7.26
2.74
1.71
1.57
0.81
1.18
1.02
0.95
0.74
3.02
1.01
1.00
6.36
1.95
1.94
δ (ppm)
13C NMR Spectrum
167.1
136.9
135.8
134.6
131.0
130.3
129.7
125.4
125.0
124.9
124.7
118.6
115.3
112.2
111.7
37.6
36.6
12.4
δ (ppm)

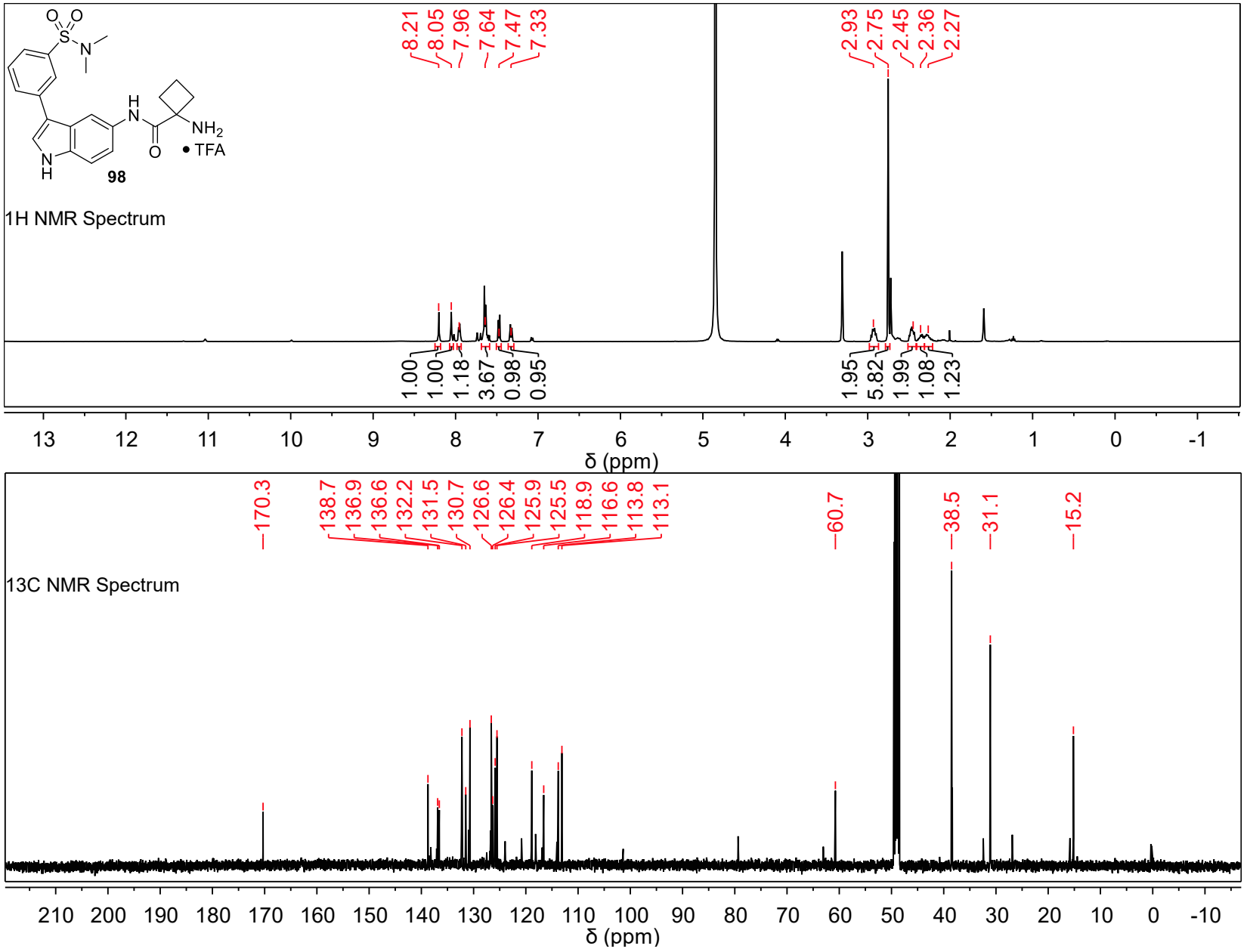
98
• TFA
1H NMR Spectrum
8.21
8.05
7.96
7.64
7.47
7.33
2.93
2.75
2.45
2.36
2.27
1.00
1.00
1.18
3.67
0.98
0.95
1.95
5.82
1.99
1.08
1.23
δ (ppm)
13C NMR Spectrum
170.3
138.7
136.9
136.6
132.2
131.5
130.7
126.6
126.4
125.9
125.5
118.9
116.6
113.8
113.1
60.7
38.5
31.1
15.2
δ (ppm)

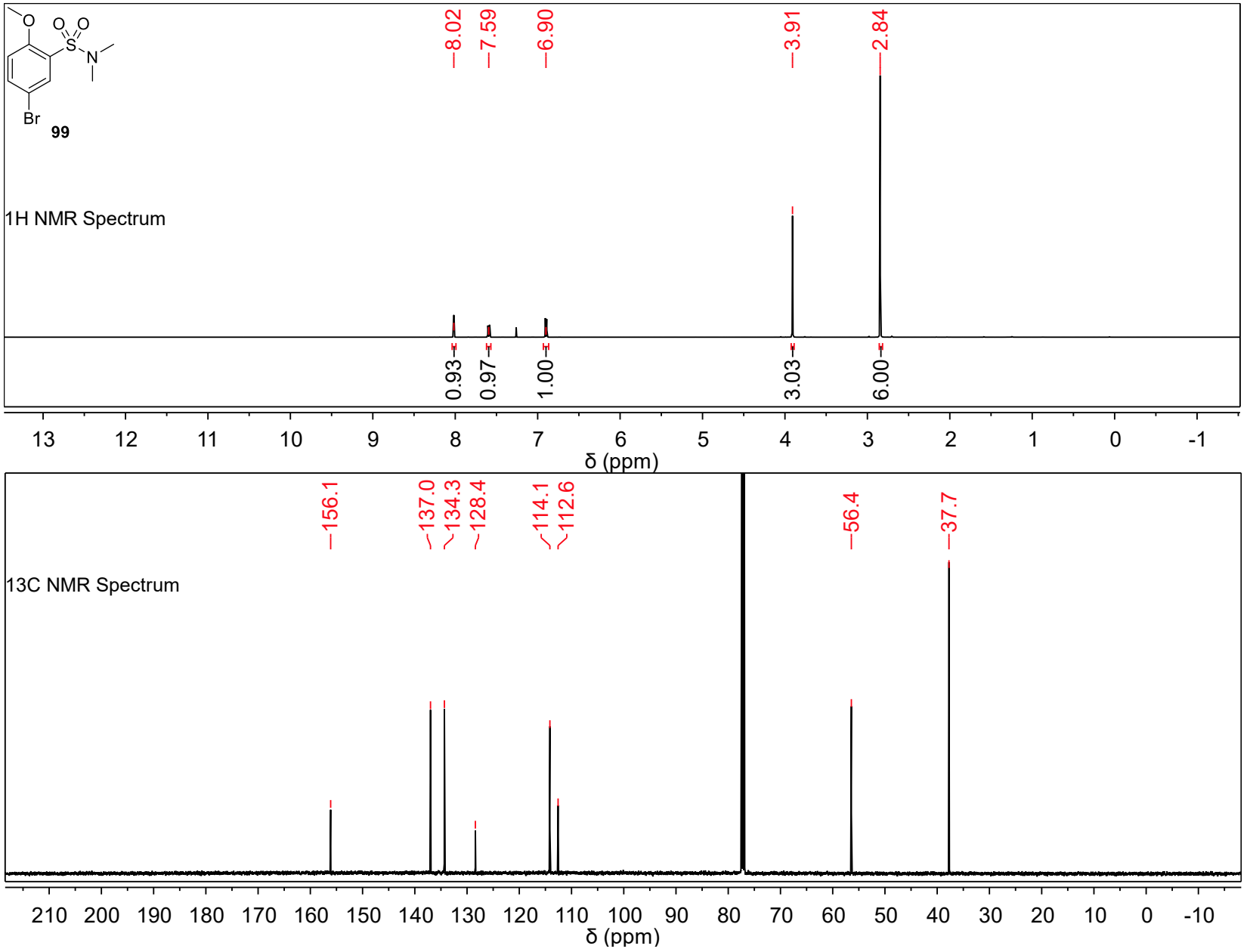
99
1H NMR Spectrum
8.02
7.59
6.90
3.91
2.84
0.93
0.97
1.00
3.03
6.00
δ (ppm)
13C NMR Spectrum
156.1
137.0
134.3
128.4
114.1
112.6
56.4
37.7
δ (ppm)

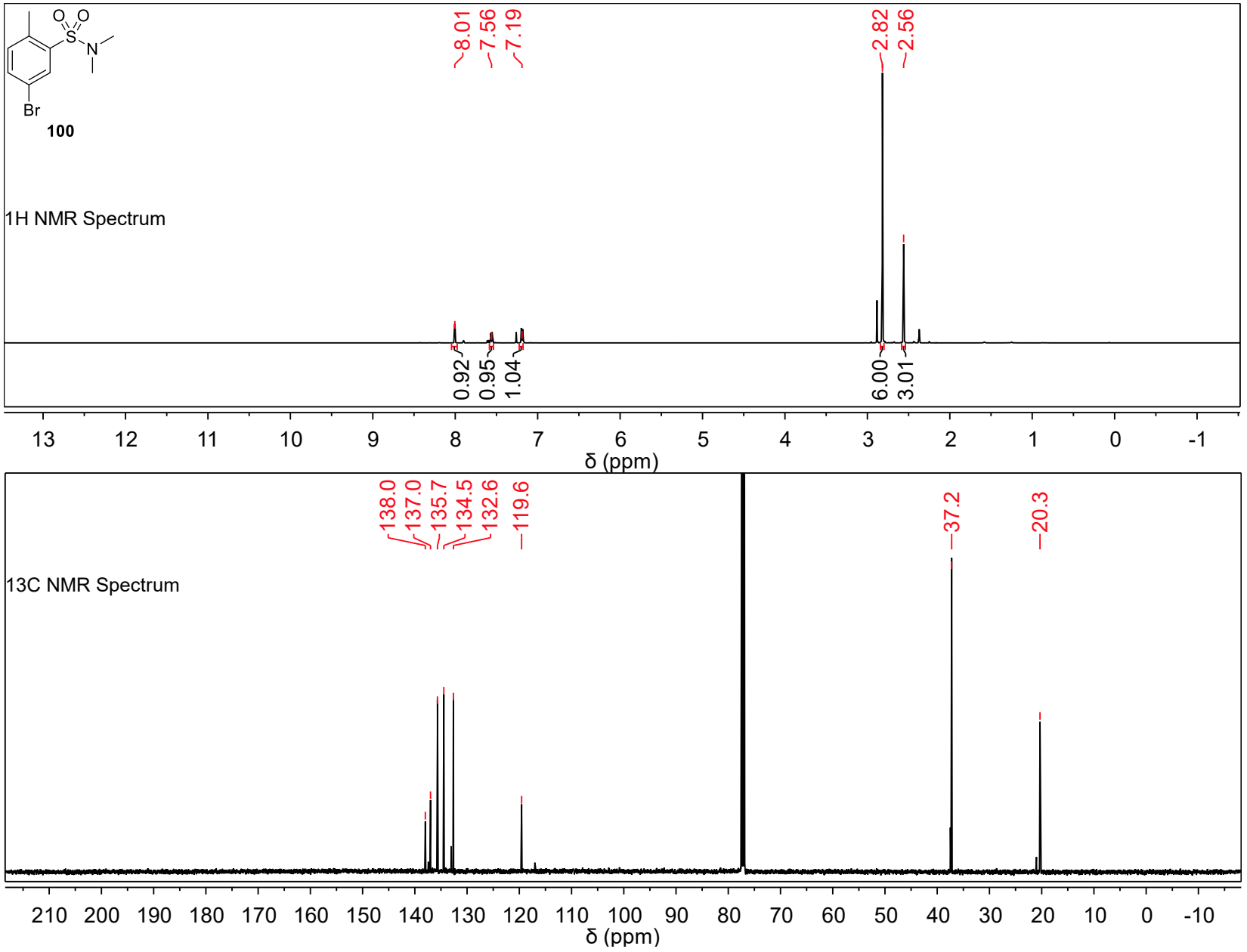
100
1H NMR Spectrum
8.01
7.56
7.19
2.82
2.56
0.92
0.95
1.04
6.00
3.01
δ (ppm)
13C NMR Spectrum
138.0
137.0
135.7
134.5
132.6
119.6
37.2
20.3
δ (ppm)

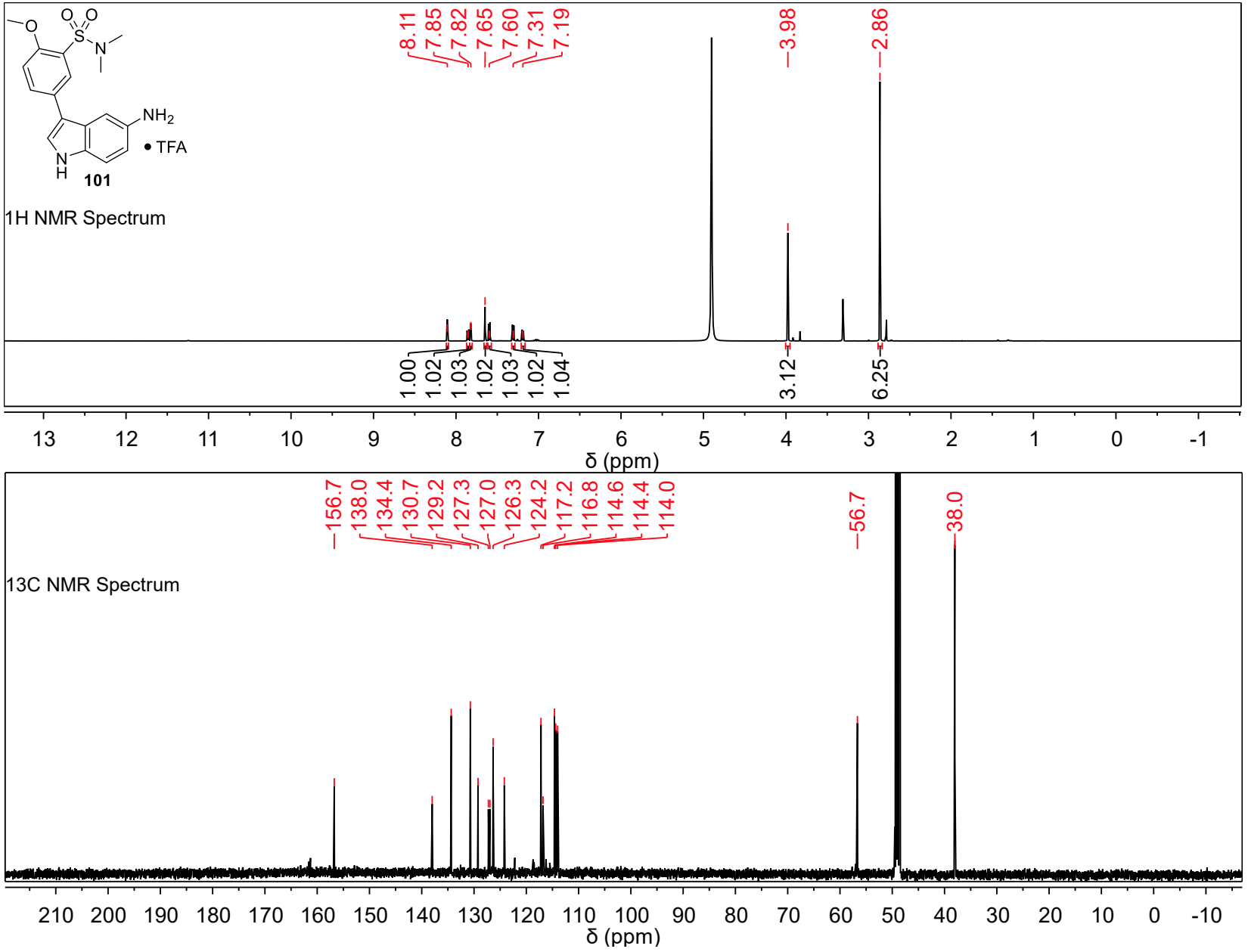
101
1H NMR Spectrum
8.11
7.85
7.82
7.65
7.60
7.31
7.19
3.98
2.86
1.00
1.02
1.03
1.02
1.03
1.02
1.04
3.12
6.25
δ (ppm)
13C NMR Spectrum
156.7
138.0
134.4
130.7
129.2
127.3
127.0
126.3
124.2
117.2
116.8
114.6
114.4
114.0
56.7
38.0
δ (ppm)

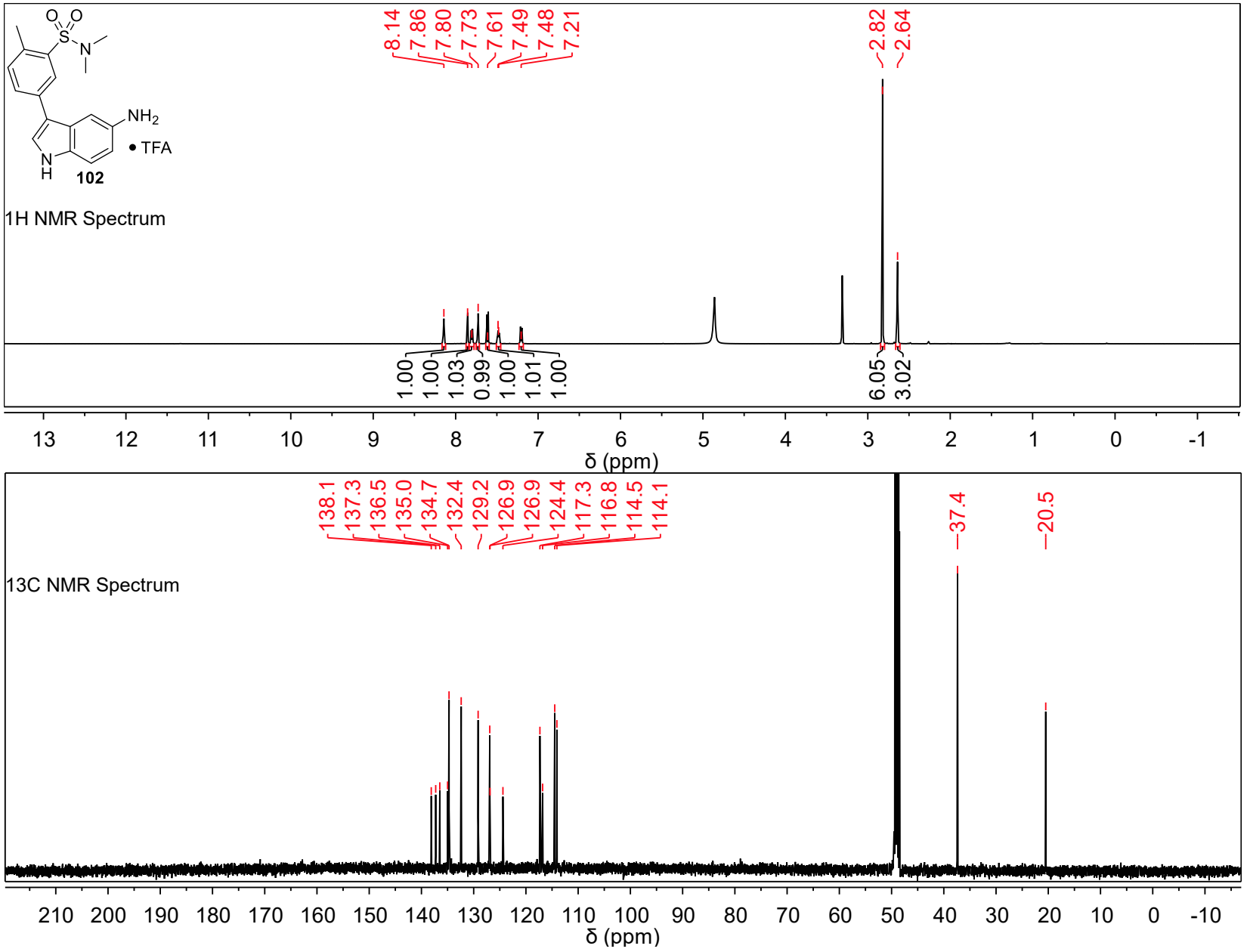
8.14
7.86
7.80
7.73
7.61
7.49
7.48
7.21
2.82
2.64
1.00
1.00
1.03
0.99
1.00
1.01
1.00
6.05
3.02
NH2
• TFA
102
1H NMR Spectrum
δ (ppm)
138.1
137.3
136.5
135.0
134.7
132.4
129.2
126.9
126.9
124.4
117.3
116.8
114.5
114.1
37.4
20.5
13C NMR Spectrum
δ (ppm)

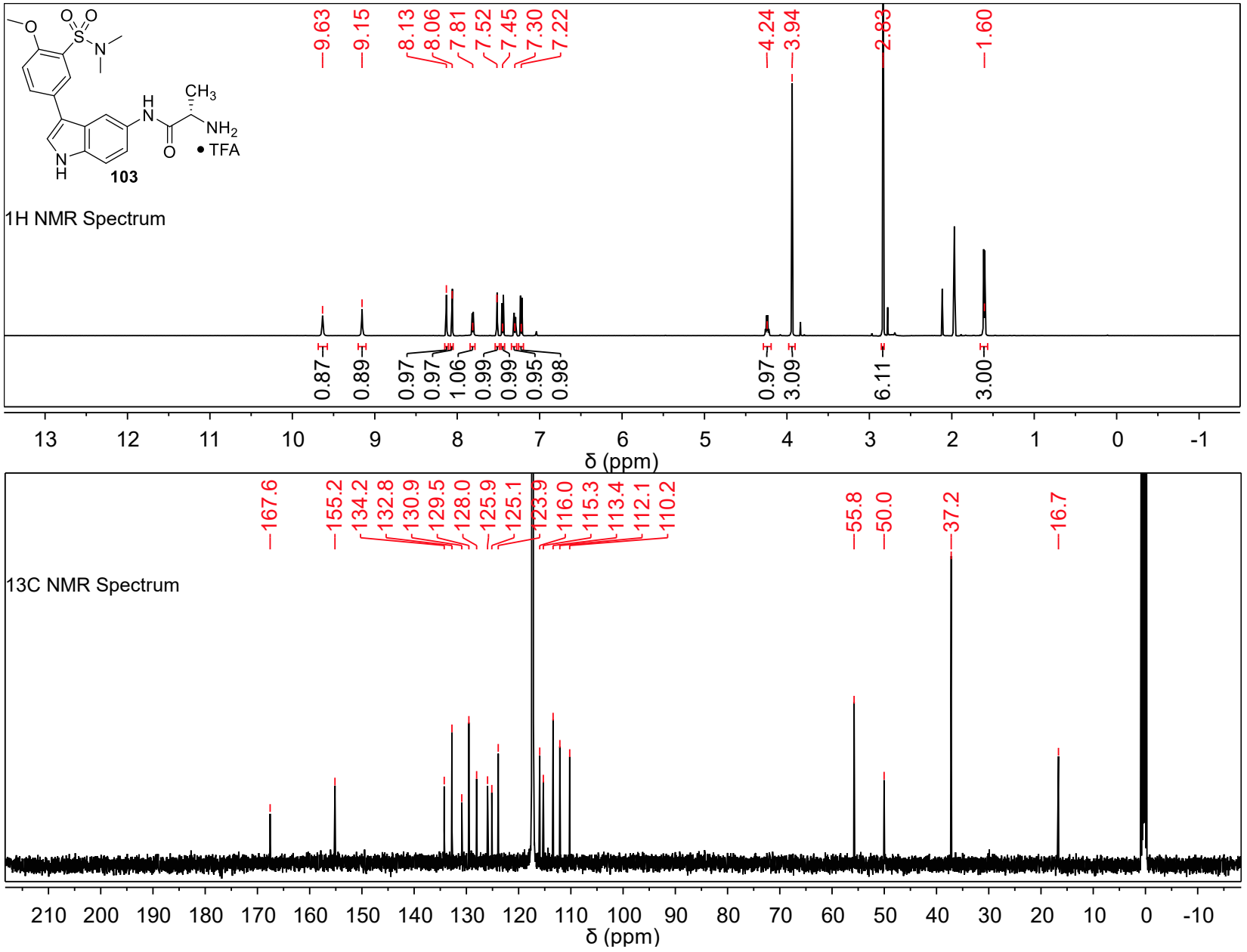
103
• TFA
1H NMR Spectrum
9.63
9.15
8.13
8.06
7.81
7.52
7.45
7.30
7.22
4.24
3.94
2.83
1.60
0.87
0.89
0.97
0.97
1.06
0.99
0.99
0.95
0.98
0.97
3.09
6.11
3.00
δ (ppm)
13C NMR Spectrum
167.6
155.2
134.2
132.8
130.9
129.5
128.0
125.9
125.1
123.9
116.0
115.3
113.4
112.1
110.2
55.8
50.0
37.2
16.7
δ (ppm)

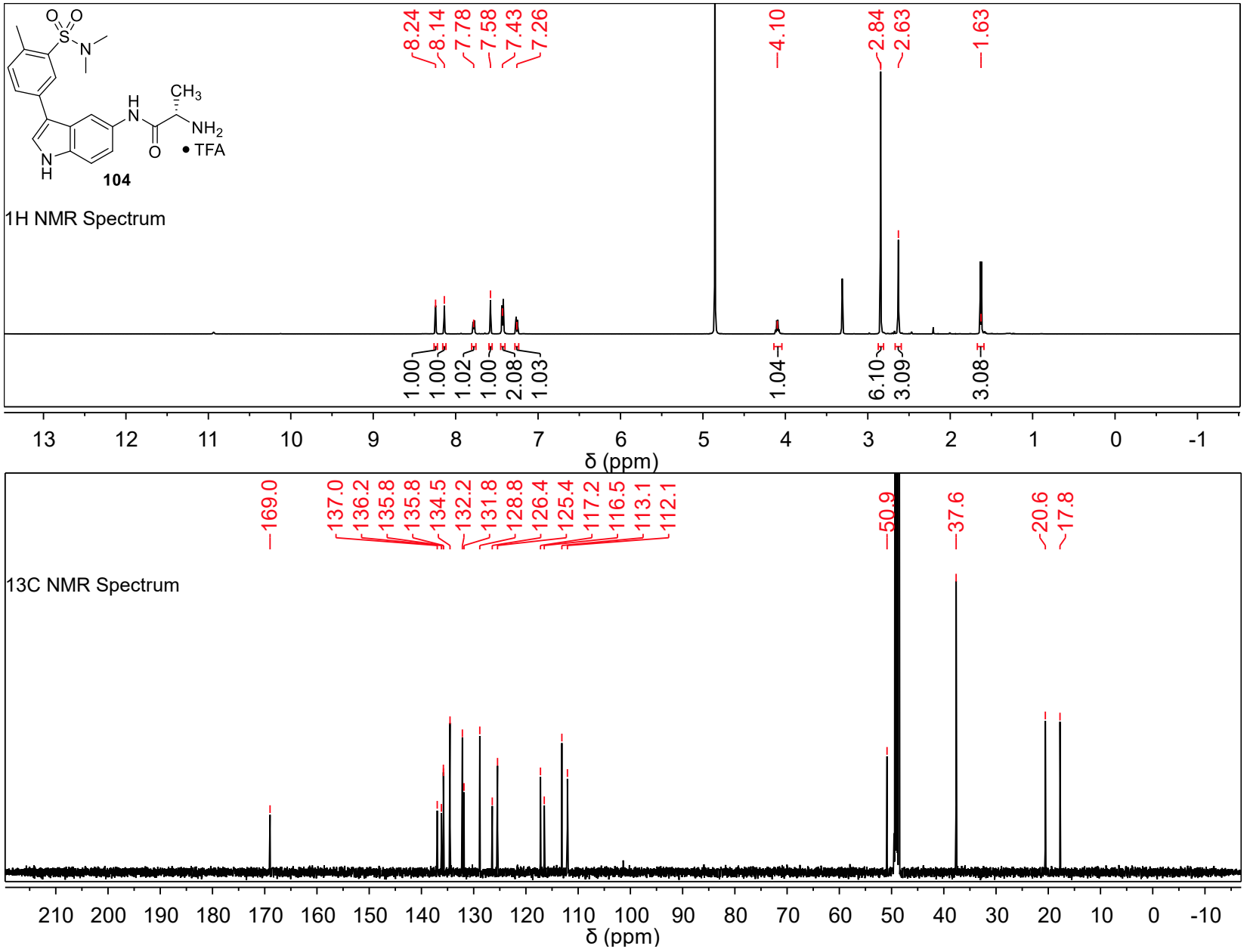
104
1H NMR Spectrum
8.24
8.14
7.78
7.58
7.43
7.26
4.10
2.84
2.63
1.63
1.00
1.00
1.02
1.00
2.08
1.03
1.04
6.10
3.09
3.08
δ (ppm)
13C NMR Spectrum
169.0
137.0
136.2
135.8
135.8
134.5
132.2
131.8
128.8
126.4
125.4
117.2
116.5
113.1
112.1
50.9
37.6
20.6
17.8
δ (ppm)

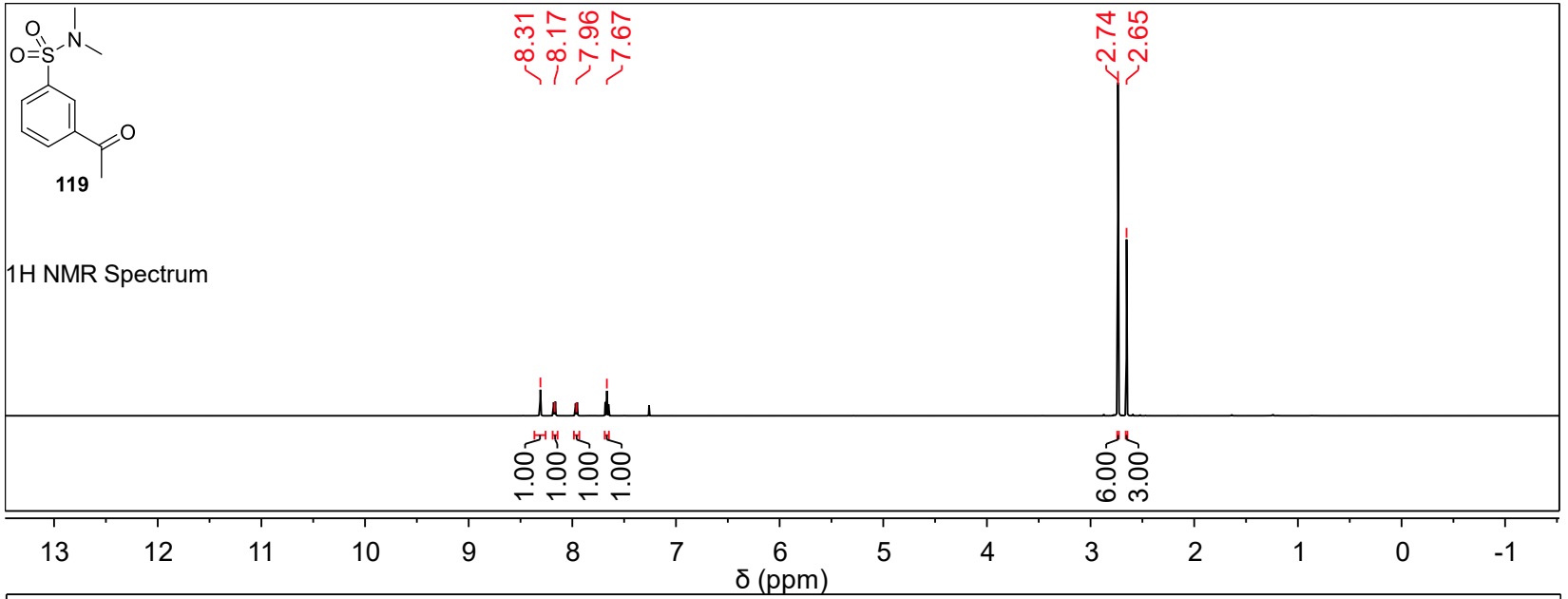
119
1H NMR Spectrum
8.31
8.17
7.96
7.67
2.74
2.65
1.00
1.00
1.00
1.00
6.00
3.00
13 12 11 10 9 8 7 6 5 4 3 2 1 0 -1
δ (ppm)

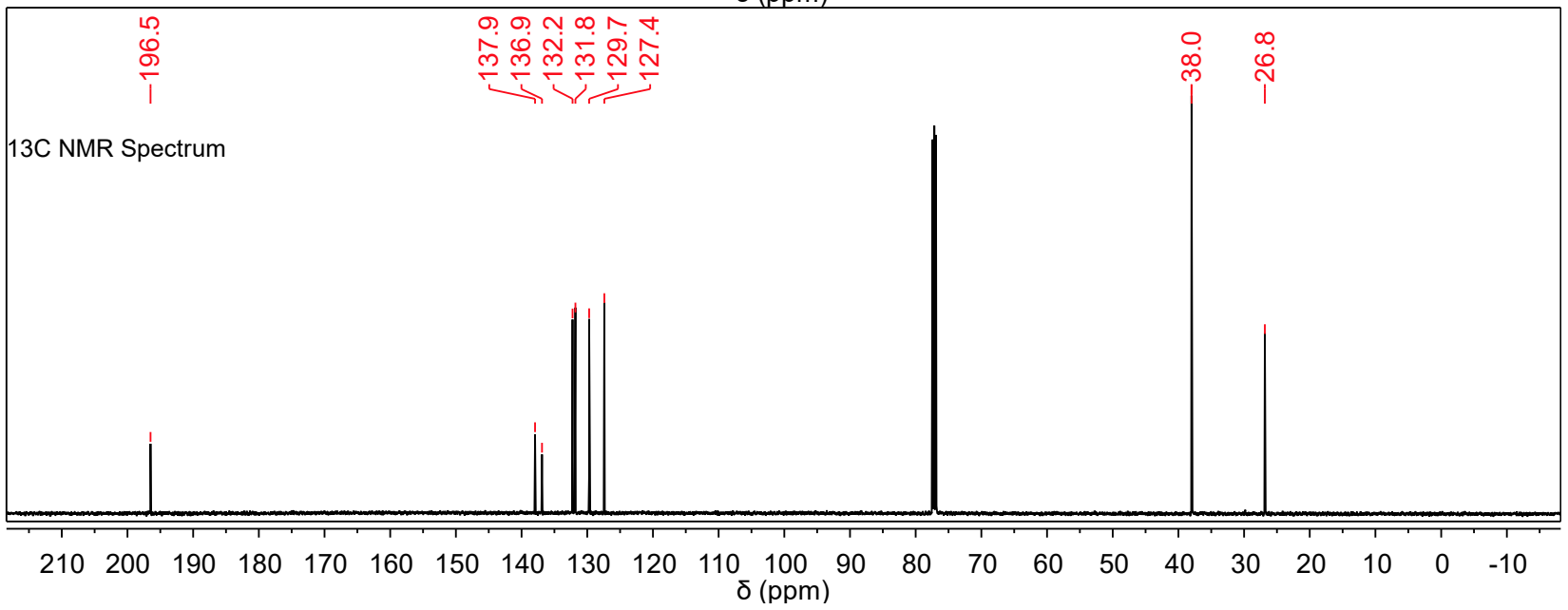
13C NMR Spectrum
196.5
137.9
136.9
132.2
131.8
129.7
127.4
38.0
26.8
210 200 190 180 170 160 150 140 130 120 110 100 90 80 70 60 50 40 30 20 10 0 -10
δ (ppm)

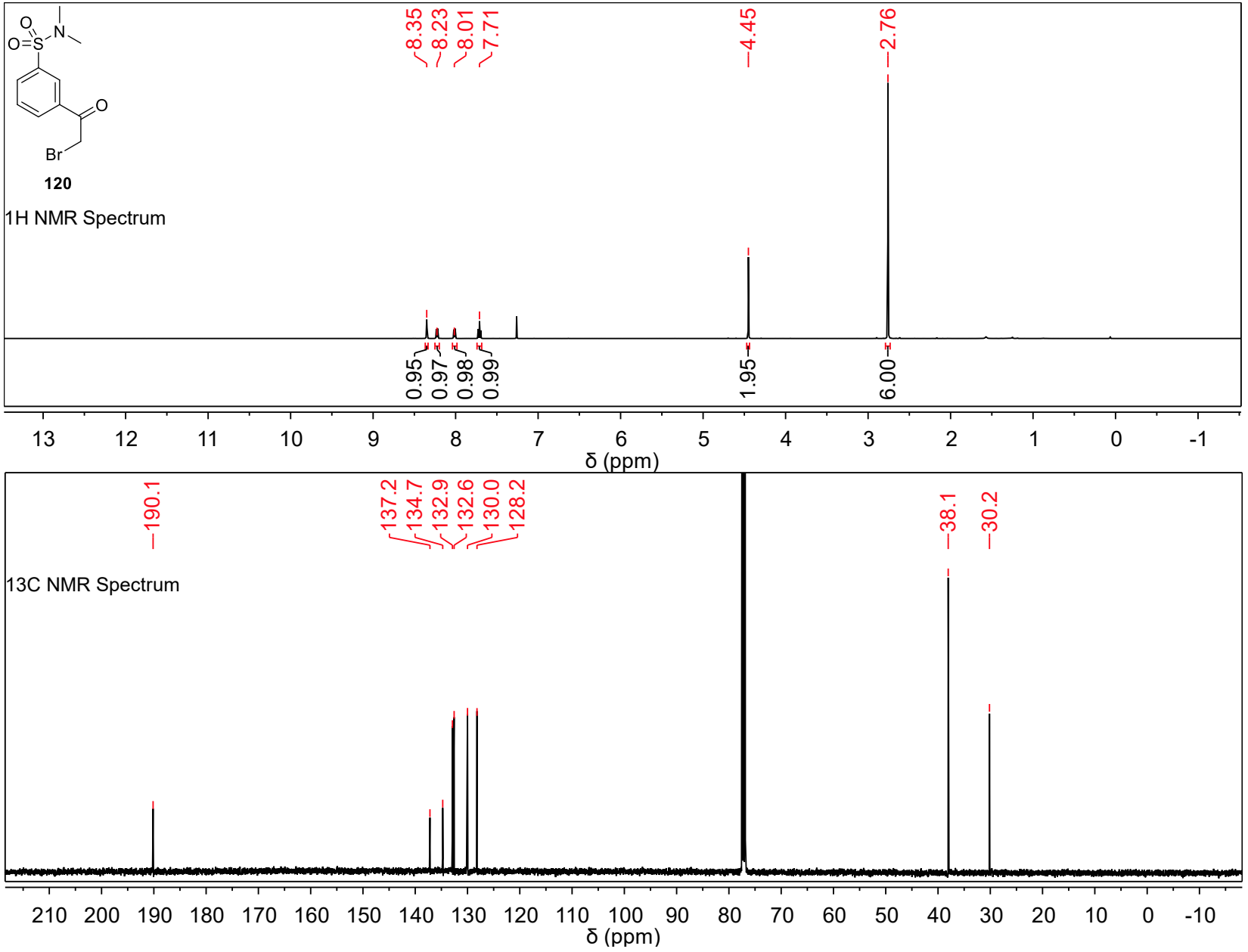
120
1H NMR Spectrum
8.35
8.23
8.01
7.71
4.45
2.76
0.95
0.97
0.98
0.99
1.95
6.00
δ (ppm)
13C NMR Spectrum
190.1
137.2
134.7
132.9
132.6
130.0
128.2
38.1
30.2
δ (ppm)

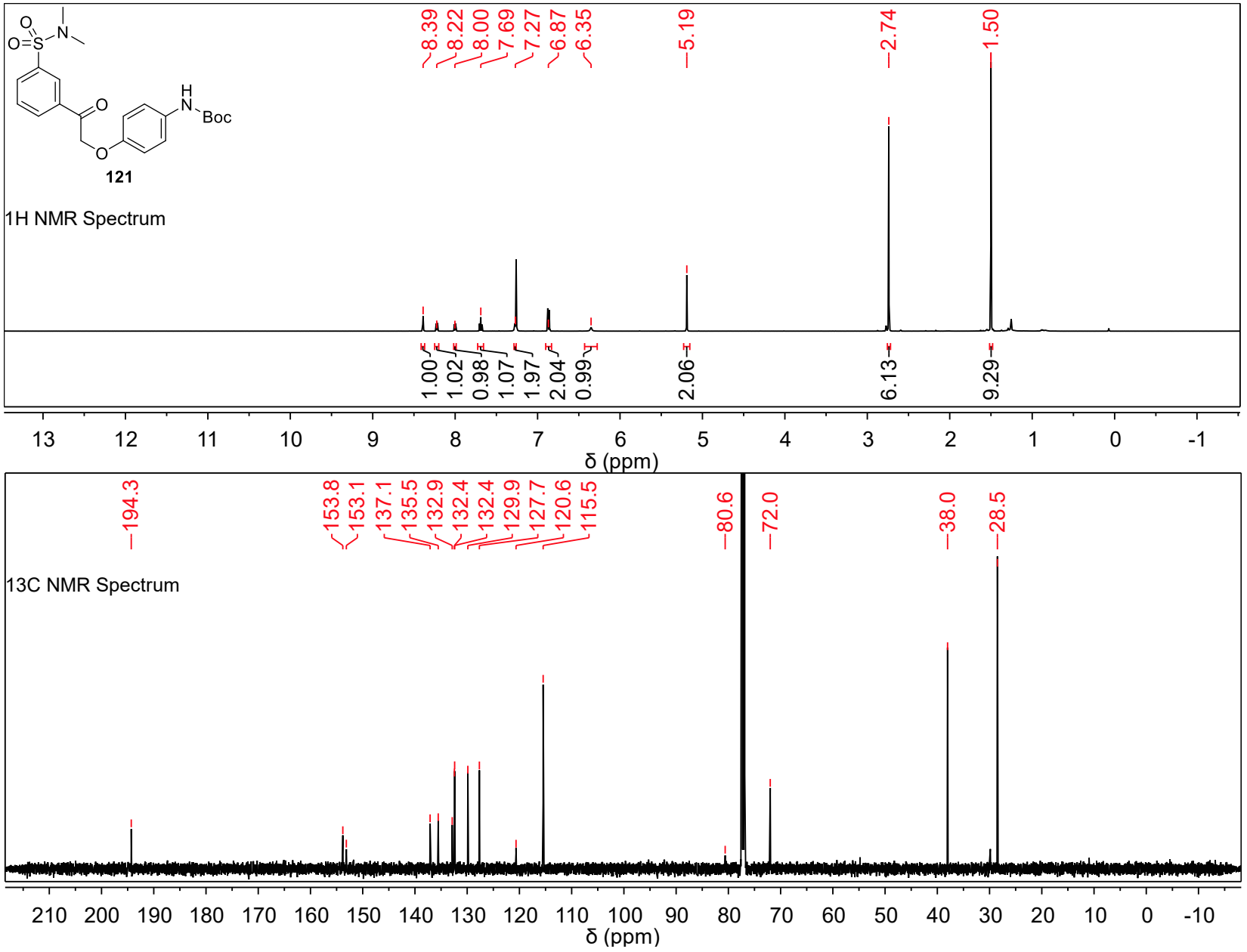
121
1H NMR Spectrum
8.39
8.22
8.00
7.69
7.27
6.87
6.35
5.19
2.74
1.50
1.00
1.02
0.98
1.07
1.97
2.04
0.99
2.06
6.13
9.29
δ (ppm)
13C NMR Spectrum
194.3
153.8
153.1
137.1
135.5
132.9
132.4
132.4
129.9
127.7
120.6
115.5
80.6
72.0
38.0
28.5
δ (ppm)

Appendix B

NMR Spectra of Compounds Synthesized in Chapter 3

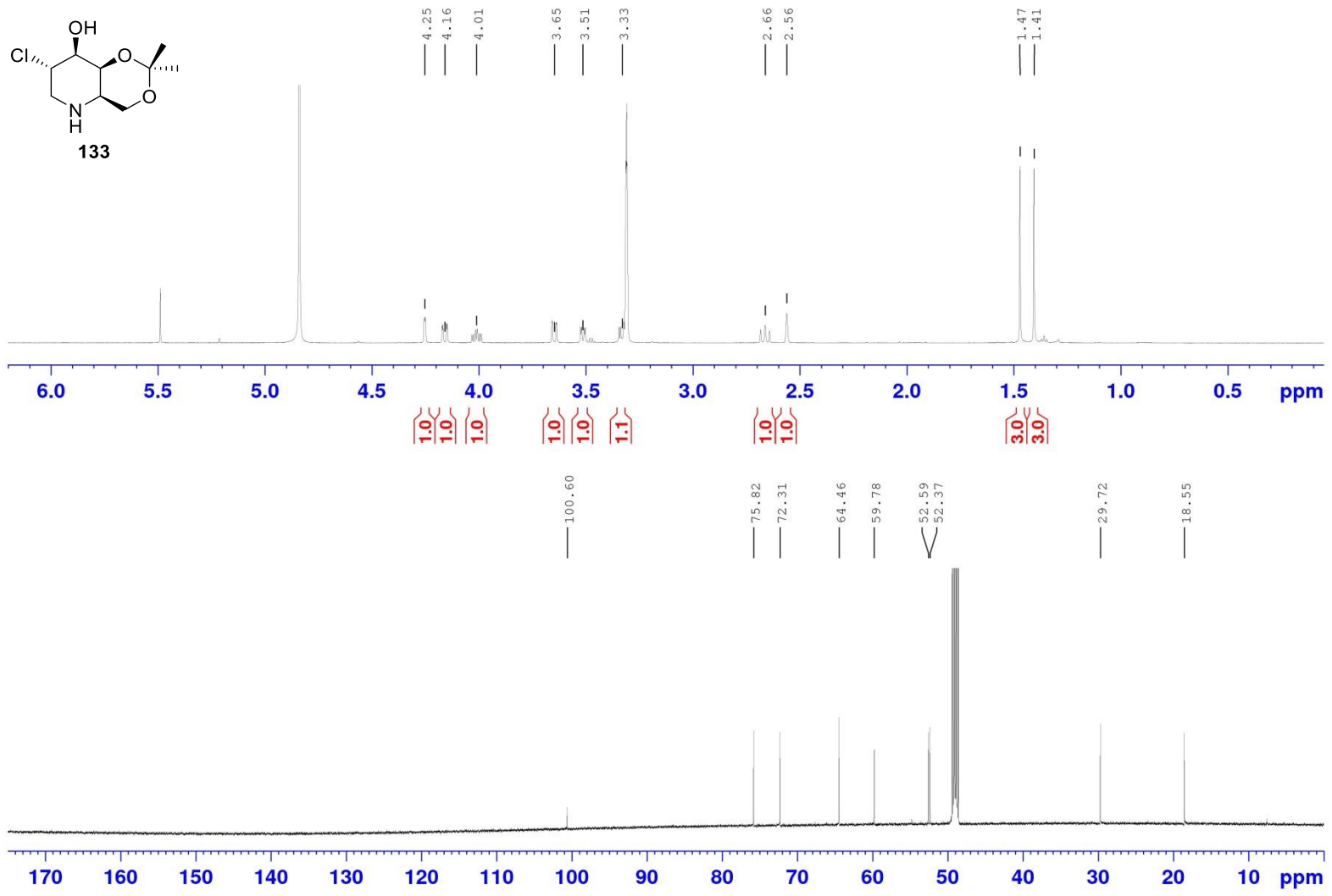
OH
Cl
O
O
N
H
133
4.25
4.16
4.01
3.65
3.51
3.33
2.66
2.56
1.47
1.41
6.0
5.5
5.0
4.5
4.0
3.5
3.0
2.5
2.0
1.5
1.0
0.5
ppm
1.0
1.0
1.0
1.0
1.0
1.1
1.0
1.0
3.0
3.0
100.60
75.82
72.31
64.46
59.78
52.59
52.37
29.72
18.55
170
160
150
140
130
120
110
100
90
80
70
60
50
40
30
20
10
ppm

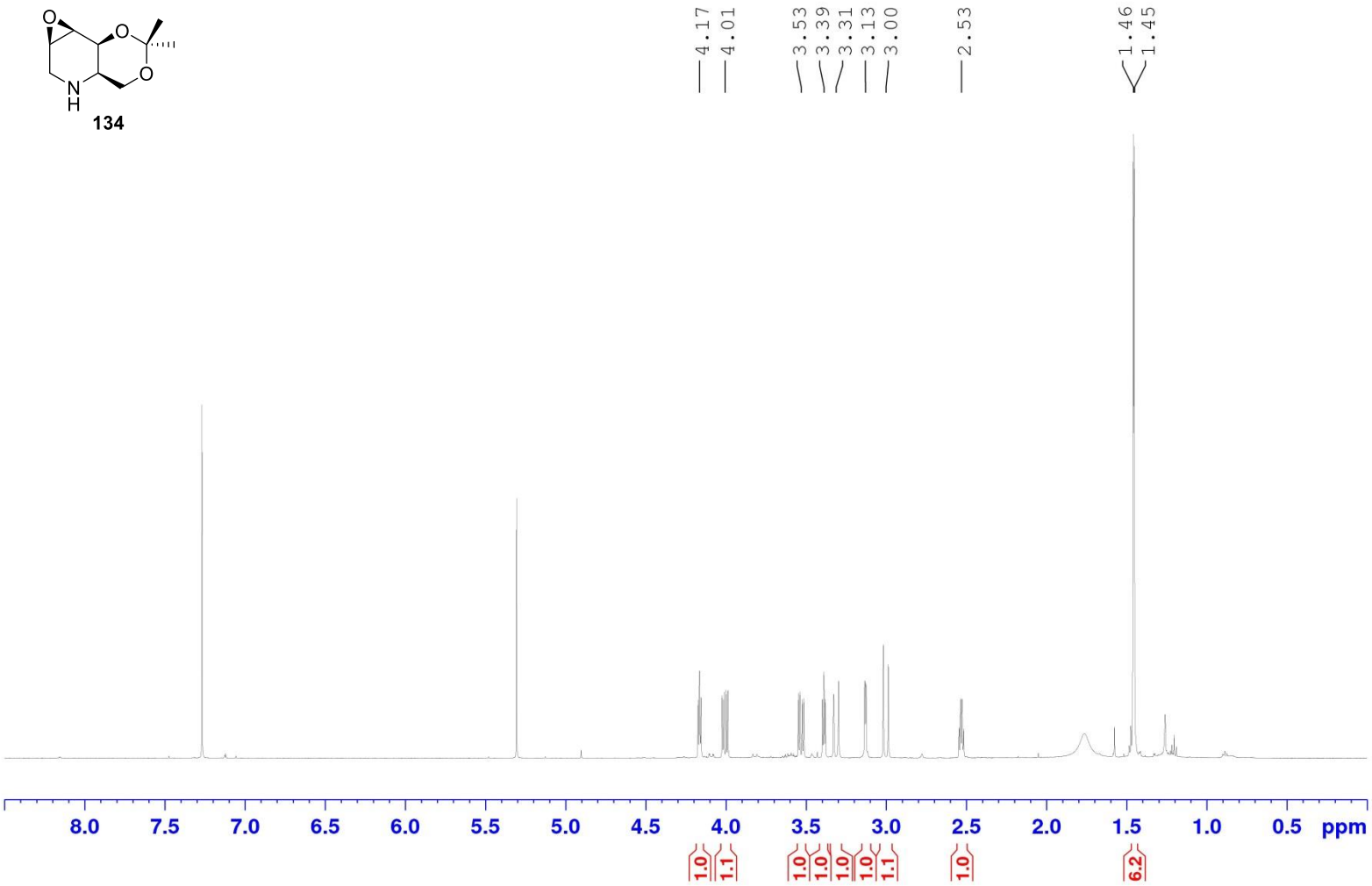
134
4.17
4.01
3.53
3.39
3.31
3.13
3.00
2.53
1.46
1.45
8.0
7.5
7.0
6.5
6.0
5.5
5.0
4.5
4.0
3.5
3.0
2.5
2.0
1.5
1.0
0.5
ppm
1.0
1.1
1.0
1.0
1.0
1.1
1.0
6.2

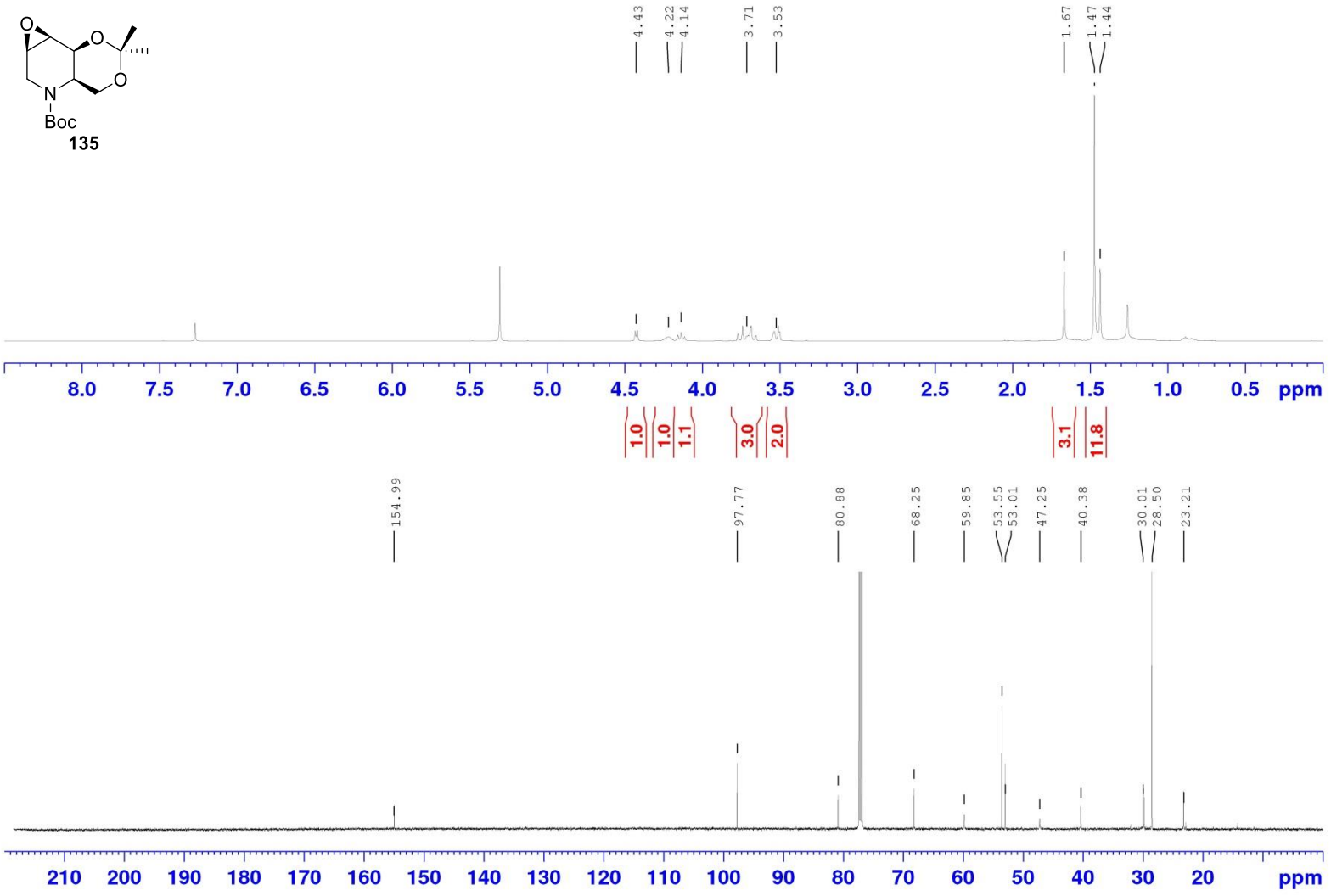
O
O
O
N
Boc
135
4.43
4.22
4.14
3.71
3.53
1.67
1.47
1.44
8.0 7.5 7.0 6.5 6.0 5.5 5.0 4.5 4.0 3.5 3.0 2.5 2.0 1.5 1.0 0.5 ppm
1.0
1.0
1.1
3.0
2.0
3.1
11.8
154.99
97.77
80.88
68.25
59.85
53.55
53.01
47.25
40.38
30.01
28.50
23.21
210 200 190 180 170 160 150 140 130 120 110 100 90 80 70 60 50 40 30 20 ppm

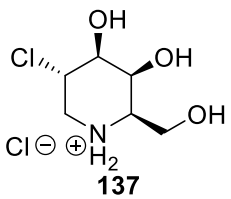
OH
Cl
OH
OH
Cl
N
H2

137

4.25
4.03
3.80
3.66
3.58
3.40
3.18
8.0
7.5
7.0
6.5
6.0
5.5
5.0
4.5
4.0
3.5
3.0
2.5
2.0
1.5
1.0
0.5
ppm
1.0
1.0
1.9
1.1
1.1
1.0
1.0